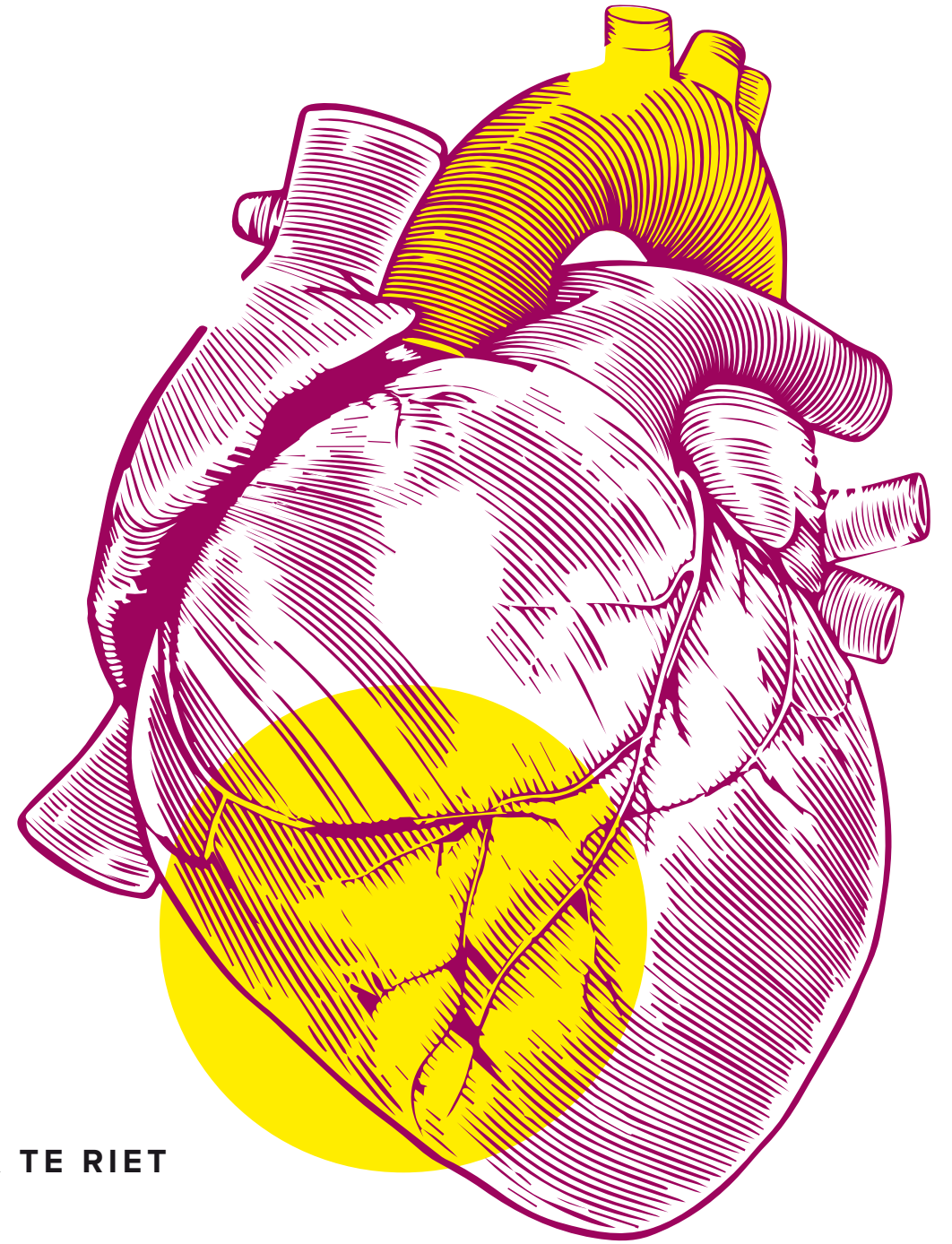


Renin-Angiotensin System and Genetic Factors in Aneurysms

A TRANSLATIONAL APPROACH



LUUK TE RIET

Renin-Angiotensin System and Genetic Factors in Aneurysms

A TRANSLATIONAL APPROACH

LUUK TE RIET

Colofon

L. te Riet

Renin-Angiotensin System and Genetic Factors in Aneurysms: A Translational Approach

ISBN: 978-94-6328-023-5

Cover: Maureen Oude Avenhuis - (maureenoudeavenhuis@hotmail.com)

Lay-out and chapter design: Luuk te Riet and Maureen Oude Avenhuis

Printed by: CPI Koninklijke Wöhrman B.V.

Copyright © Luuk te Riet 2016

All rights reserved. No part of this thesis may be reproduced, stored in a retrieval system of any nature, or transmitted in any form or means, without written permission of the author, or when appropriate, of the publishers of the publications.

Renin-Angiotensin System and Genetic Factors in Aneurysms

A TRANSLATIONAL APPROACH

Renine-angiotensine systeem
en genetische factoren in aneurysmata:
een translationele aanpak

Proefschrift

Ter verkrijging van de graad van doctor aan de
Erasmus Universiteit Rotterdam
op gezag van de rector magnificus

Prof.dr. H.A.P. Pols

en volgens besluit van het College voor Promoties

De openbare verdediging zal plaatsvinden op

dinsdag 5 april 2016 om 15.30 uur

door

Luuk te Riet

Geboren te Oldenzaal

Promotiecommissie

Promotoren: Prof.dr. A.H.J. Danser
Prof.dr. H.J.M. Verhagen

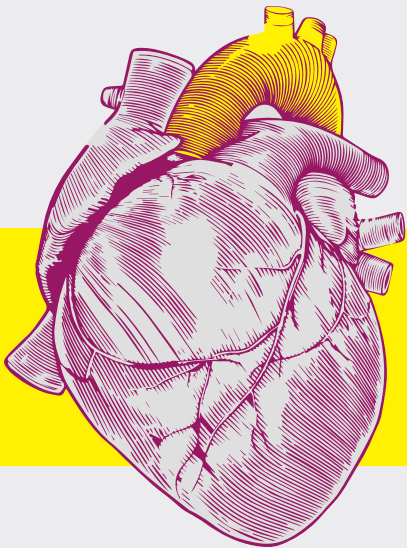
Overige leden: Prof.dr. J.W. Roos-Hesselink
Prof.dr. D.J.G.M. Duncker
Prof.dr. M.C. de Ruiter

Copromotoren: Dr. J. Essers
Dr. E.V. Rouwet

Voor mijn familie

Table of Contents

Part I	
Chapter 1	Introduction: The Renin-Angiotensin Aldosterone Alterations and its Involvement in Vascular Disease
Chapter 2	Scope of this Thesis
Part II	The Role of the Renin-Angiotensin System on Aortic and Cardiac Pathology in Aneurysmatic Fibulin-4 Mice
Chapter 3	Impaired vascular contractility and aortic wall degeneration in fibulin-4 deficient mice: effect of angiotensin II type 1 (AT ₁) receptor blockade
Chapter 4	Reduced Fibulin-4 Expression Causes Myocardial Remodeling and Dysfunction
Chapter 5	AT ₁ Receptor Blockade, but not Renin Inhibition, Reduces Aneurysm Growth and Cardiac Failure in Fibulin-4 Mice
Chapter 6	Fibulin-4 Deficiency Increases TGF β Signaling in Isolated Aortic Smooth Muscle Cells Due to Elevated TGF β 2 Levels
Part III	The Identification of Genetic Factors Involved in Aneurysms
Chapter 7	RNA Expression Profiling of Abdominal Aortic Aneurysm Disease Identifies Signaling Cross-talk Between TGF β and BMP
Chapter 8	Long range polymerase chain reaction amplification of Aortic Aneurysm Genes
Part IV	(Pro)Renin Receptor Inhibition in Diabetic Rats
Chapter 9	Deterioration of Kidney Function by the (Pro)renin Receptor Blocker Handle Region Peptide in Aliskiren-treated Diabetic Transgenic (mRen2)27 Rats
Part V	Summary
Chapter 10	Summary and Discussion Nederlandse samenvatting Curriculum Vitae Publications PhD Portfolio Dankwoord



CHAPTER I

Part I: Introduction

Renin-Angiotensin-Aldosterone System Alterations
and its Involvement in Vascular Disease

ADAPTED FROM

Te Riet L. et al. Hypertension: renin-angiotensin-aldosterone system alterations. *Circulation Research*. 2015 Mar 13; 116(6): 960-975.

Van Thiel BS. et al. The renin-angiotensin system and its involvement in vascular disease. *European Journal of Pharmacology*. 2015 Sep 15; 763(Pt A): 3-14.

**ABSTRACT**

Blockers of the renin-angiotensin-aldosterone system (RAAS), i.e., renin inhibitors, ACE inhibitors, angiotensin (Ang) II type 1 (AT₁) receptor antagonists and mineralocorticoid receptor (MR) antagonists, are a cornerstone in the treatment of hypertension. How exactly they exert their effect, in particular in patients with low circulating RAAS activity, also taking into consideration the so-called Ang II/aldosterone escape that often occurs after initial blockade, is still incompletely understood. Multiple studies have tried to find parameters that predict the response to RAAS blockade, allowing a personalized treatment approach. Consequently, the question should now be answered on what basis (e.g., gender, ethnicity, age, salt intake, baseline renin, ACE or aldosterone, and genetic variance) a RAAS blocker can be chosen to treat an individual patient. Are all blockers equal? Does optimal blockade imply maximum RAAS blockade, e.g., by combining 2 or more RAAS blockers, or by simply increasing the dose of 1 blocker? Exciting recent investigations reveal a range of unanticipated extrarenal effects of aldosterone, as well as a detailed insight in the genetic causes of primary aldosteronism, and MR blockers have now become an important treatment option for resistant hypertension. Finally, apart from the deleterious ACE-Ang II-AT₁ receptor arm, animal studies support the existence of protective aminopeptidase A-Ang III-Ang II type 2 receptor and ACE-2-Ang-(1-7)-Mas receptor arms, paving the way for multiple new treatment options. This review provides an update about all these aspects, critically discussing the many controversies, and allowing the reader to obtain a full understanding of what we currently know about RAAS alterations in hypertension.

INTRODUCTION

Blockers of the renin-angiotensin-aldosterone system (RAAS), i.e., renin inhibitors, ACE inhibitors, angiotensin (Ang) II type 1 (AT_1) receptor antagonists and mineralocorticoid receptor (MR) antagonists, are a cornerstone in the treatment of hypertension. At first sight, their mechanism of action appears simple: they reduce the formation or block the effects of Ang II and/or aldosterone, thereby preventing the deleterious cardiovascular effects of these 2 compounds. Logically, they should then be particularly applied in patients with 'high' RAAS activity, as measured in blood plasma. However, it is now well accepted that they are also effective in patients with medium-to-low RAAS activity. Moreover, after an initial suppression/blockade of Ang II/aldosterone, the plasma levels of these 2 compounds often return to normal, or even rise above pre-treatment levels: the so-called Ang II/aldosterone 'escape'.^{1,2} Yet, remarkably, the RAAS blocker effect remains, at least partially. These puzzling observations have led to the concept of a 'local' RAAS in various organs, i.e., the real site of action of RAAS blockers. According to some investigators, this local RAAS occurs entirely intracellular ('intracrine' RAAS).³ In addition, during RAAS blocker application, an upregulation occurs of multiple angiotensin metabolites, which may exert actions of their own and possibly even contribute to the beneficial effects of RAAS blockade. Examples of these 'protective' (vasodilator) pathways include the angiotensinase A-Ang III-Ang II type 2 (AT_2) receptor pathway and the ACE2-Ang-(1-7)-Mas receptor pathway (Figure 1). Further knowledge in this area might lead to new drugs.

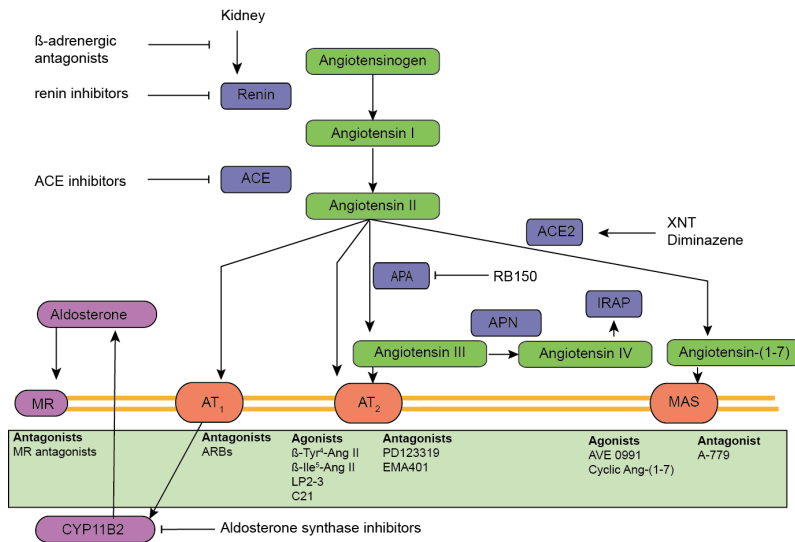


Figure 1

New and existing drugs interfering with the renin-angiotensin system cascade. Classically, interference occurs at the level of renin, ACE, the AT_1 receptor (R) or the mineralocorticoid receptor (MR), with renin inhibitors, ACE inhibitors AT_1 receptor blockers ARBs) or MR antagonists. Novel enzyme inhibitors now target aminopeptidase A (APA), which generates Ang III (=Ang-(2-8)) from Ang II (=Ang-1-8)), or aldosterone synthase (CYP11B2). Activators of ACE2 (XNT and diminazene), which generates Ang-(1-7) from Ang II, were recently found to act equally well in ACE2 KO animals, thus questioning their mechanism of action. Numerous agonists for both the AT_2 receptor and Mas receptor are being developed. Aminopeptidase N (APN) degrades Ang III to Ang IV (=Ang-(3-8)), which may act on the AT_4 receptor, also known as insulin-regulated aminopeptidase (IRAP).

For a long time, it was thought that the more RAAS blockade, the better, also in view of the above described Ang II/aldosterone escape. However, dual RAAS blockade trials have now shown that this is not necessarily the case, and that the consequences of too much RAAS suppression (hyperkalemia, renal dysfunction, hypotension) may overrule the beneficial effects of this approach. A variety of RAAS differences exists between men and women, and between black and white people, with men and white people generally having higher renin levels. This does not necessarily translate into similarly elevated aldosterone levels, and in fact, patients with high aldosterone-to-renin ratios (ARR) can be identified which respond particularly well to MR blockers. A wide range of mutations has recently been identified that gives rise to selective aldosterone rises.

This review will critically discuss all the above aspects. What is a local RAAS? What are the local actions of Ang II in the vessel wall? What are the (genetic) determinants of a solid response to a RAAS blocker? Is there such a thing as 'too much' RAAS blockade? Are all RAAS blockers equally good? Are the gender and ethnicity-related RAAS differences clinically relevant? What about the recent developments in primary hyperaldosteronism, and the extrarenal effects of aldosterone? Finally, can we expect new RAAS drugs?

What is a local RAAS?

Originally, when developing the concept of local RAAS, it was proposed that all components required to generate Ang II and aldosterone locally are synthesized at multiple sites in the body, allowing their generation to occur independently from the classical sites of RAAS component synthesis: the kidney (renin), liver (angiotensinogen) and adrenal (aldosterone). In addition, a wide variety of non-classical enzymes, in particular chymase, was suggested to contribute to Ang II generation as well.⁴ Some, if not all, RAAS components were even detected in cells, leading to the concept of an 'intracrine' RAAS, involving the intracellular generation of Ang II acting on intracellular (nuclear) receptors.³

Finally, the confusing observation that humans have large amounts of prorenin, the inactive precursor of renin, has led to a search for prorenin receptors, that bind and activate prorenin locally, thus offering an explanation of why we have so much prorenin (its concentrations are up to 100 times of renin): it would then function as a regulator of tissue Ang generation. One such candidate, the so-called (pro)renin receptor ((P)RR), which binds both renin and prorenin, has received much attention during the last decade.⁵ Unfortunately, the concentrations of renin/prorenin (together denoted here as (pro)renin) that are required to result in receptor binding are far above the normal (patho)physiological levels, and transgenic rodents overexpressing either the (P)RR or prorenin did not reveal any evidence for (pro)renin-(P)RR interaction *in vivo*, i.e., their Ang II levels were unaltered.⁶ Moreover, (P)RR knockout (KO), unlike renin KO, is lethal.⁷ This may relate to (P)RR's association with vacuolar H⁺-ATPase, a crucial enzyme found in virtually every cell type that is important for the acidification of intracellular compartments. Therefore, (P)RR research is now focusing on its functions beyond the RAAS, as the (P)RR may not be a part of the RAAS after all, except perhaps in organs where (pro)renin is synthesized locally (allowing high local concentrations that result in receptor activation).

Similarly, the view of chymase as a major Ang I-II converting enzyme is most likely an *in vitro* artefact, related to the measurement of Ang II formation in tissue homogenates (particularly from the human heart), where chymase is no longer in its intracellular storage sites.⁴ Careful measurements of Ang II in ACE KO mice did not support the concept that chymase is an Ang I-II converting enzyme *in vivo*.⁸ In fact, renin and angiotensin measurements are hampered by multiple technical difficulties, particularly in tissues, and since many of the original conclusions on tissue RAAS were based on such non-ideal measurements, they need to be viewed with care. For instance, the original observations that renin and Ang II are unaltered after a bilateral nephrectomy turned out not to be true.⁹ Moreover, there is no intracellular Ang II in AT receptor KO mice.¹⁰ Clearly therefore, there is only one renin source in the body (the kidney), angiotensin generation occurs extracellularly (in blood, interstitial fluid and/or on the cell surface), and any Ang II present in cells accumulated there after its internalization following AT receptor binding. Selective KO of renal angiotensinogen revealed that the concept of renal angiotensinogen contributing to renal Ang II production was not true: all renal Ang II generation

depended on hepatic angiotensinogen.¹¹ Although similar conclusions have been reached in the heart,¹² local angiotensinogen synthesis has been claimed in the vessel wall,¹³ and adipocytes are generally believed to generate angiotensinogen.¹⁴ Surprisingly, adipocyte angiotensinogen deficiency did not affect plasma angiotensinogen levels, but greatly reduced circulating Ang II under high fat diet conditions.¹⁴ Additional studies, inducing selective KO of adipocyte angiotensinogen, hepatic angiotensinogen, or both are required to fully understand the contribution of adipocyte angiotensinogen to Ang II production. Also with regard to aldosterone, the original reports on its generation in heart, vessel wall and kidney, were not confirmed upon careful re-examination of the measurements after adrenalectomy and in isolated organs.¹⁵⁻¹⁷

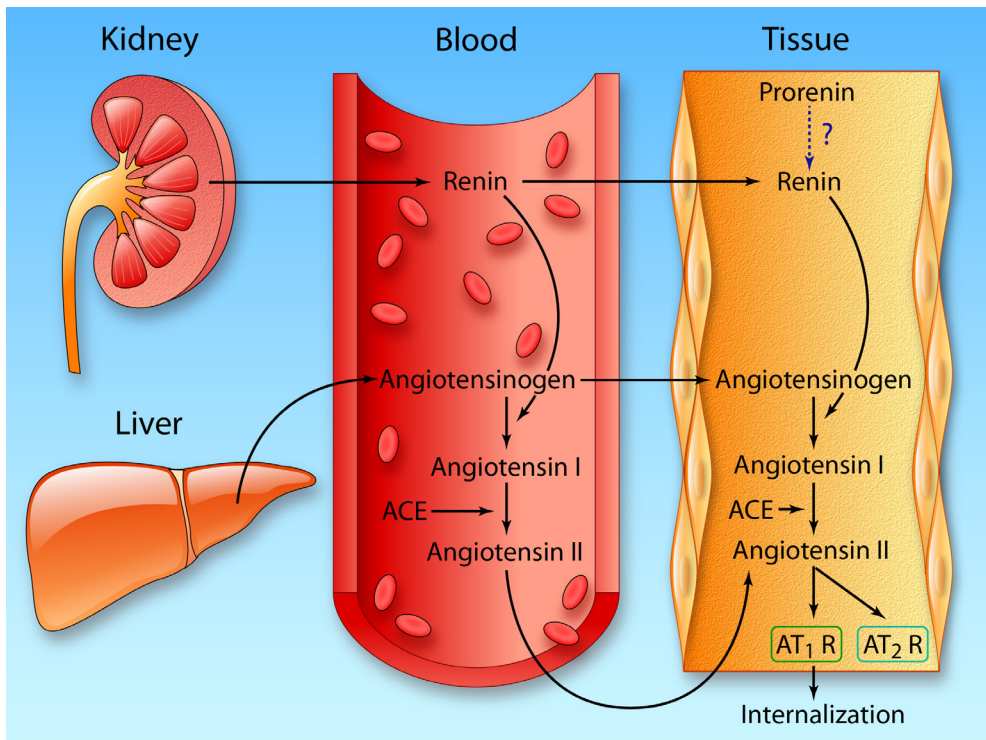


Figure 2

Circulating versus tissue renin-angiotensin system. Circulating renin is kidney-derived, and circulating angiotensinogen originates in the liver. ACE is located on endothelial cells. Ang II generated in the circulation will diffuse to tissues in order to bind to its main receptor (the Ang II type 1 receptor, AT₁R) to exert effects. In addition, circulating renin and angiotensinogen might also diffuse to tissue sites (e.g., the interstitial space) and generate, with the help of tissue ACE, Ang II locally. In a limited number of tissues renin's precursor prorenin is produced locally. To what degree such prorenin, e.g. following its conversion to renin, contributes to local angiotensin production remains unknown. Although local production has also been claimed for angiotensinogen, in particular in the kidney, current evidence does not support a functional role for kidney-derived angiotensinogen, since the renal Ang II levels in renal angiotensinogen KO mice are identical to those in wild-type mice.¹¹ Locally generated Ang II rapidly binds to AT₁ and AT₂ receptors, the former being followed by internalization. This explains the intracellular presence of Ang II, as well as the high tissue levels of Ang II in high AT₁ receptor-density organs like the adrenal. (Illustrated Credit: Ben Smith).

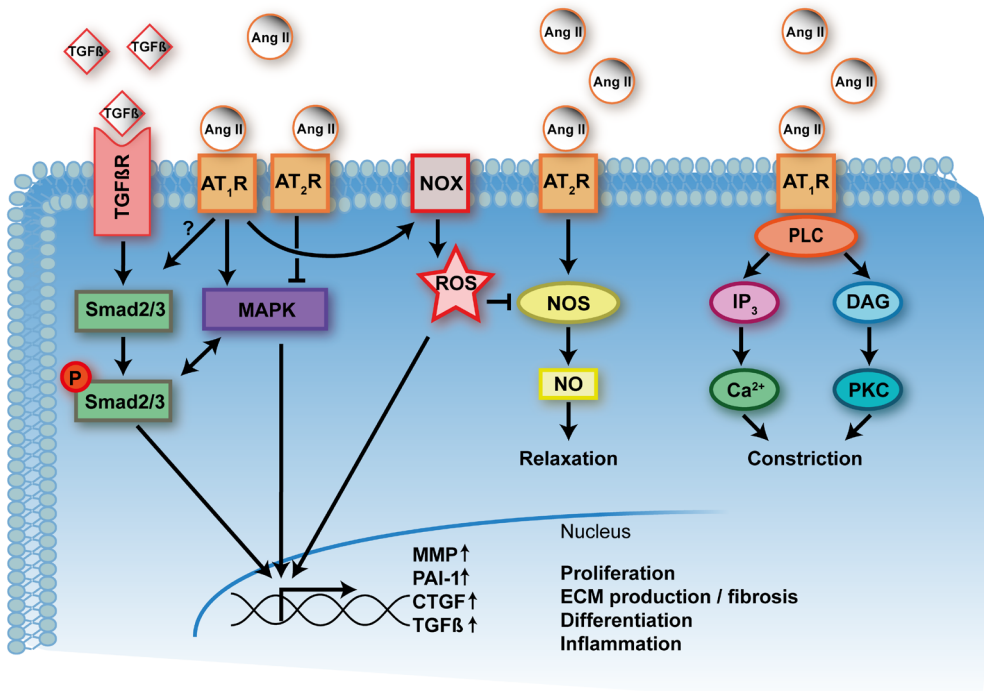


Figure 3

Effects of Ang II, via its AT_1 and AT_2 receptors (AT_1R , AT_2R) on vascular remodeling and constriction/vasodilation. Transforming growth factor- β (TGF- β)-signaling by the TGF- β receptor (via the Smad2/3 pathway) and mitogen-activated protein kinase (MAPK) activation following AT_1 receptor stimulation jointly regulate the transcription of target genes (e.g., matrix metalloproteinase, MMP; plasminogen-activator inhibitor-1, PAI-1; connective tissue growth factor, CTGF) that result in proliferation, extracellular matrix production/fibrosis, differentiation and inflammation. AT_1 receptor stimulation additionally upregulates NAD(P)H oxidase (NOX), thereby increasing reactive oxygen species (ROS) formation, which also regulates the transcription of the above-mentioned target genes. AT_2 receptor stimulation inhibits this pathway by blocking MAPK. AT_2 receptors also induce vasorelaxation by activating NO synthase (NOS). This may counteract the constrictor effects of AT_1 receptor stimulation (mediated by the inositol trisphosphate (IP_3)- Ca^{2+} and diacylglycerol (DAG)-protein kinase C (PKC) pathways). Under pathological condition, ROS uncouple NOS, thereby diminishing NO production, and potentially facilitating ROS formation by NOS.

Summarizing, the current view is that Ang II generation in tissues does occur (in fact, >90% of tissue Ang II is synthesized locally, and not taken up from plasma^{18,19}), but depends on renal renin and largely, if not completely, on hepatic angiotensinogen. Both diffuse into the interstitium, allowing local Ang II generation to take place in that compartment with the help of membrane-bound, ubiquitously present ACE (Figure 2). This Ang II rapidly binds to AT receptors, and such binding is followed by internalization, explaining why tissue Ang II levels are often high and correlate closely with tissue AT receptor density.²⁰ Aldosterone is exclusively adrenal-derived. To what degree prorenin has a role, beyond the (P)RR, remains to be determined.

Local effects of Ang II in the vessel wall

When focusing on the vessel wall, it is well-established that activation of AT₁ receptors induces vasoconstriction, endothelial dysfunction, inflammation, growth and remodeling, while AT₂ receptors are believed to counteract these effects (Figure 3). However, the latter is not a uniform finding, and under certain conditions, e.g., in the spontaneously hypertensive rat (SHR), AT₂ receptors may become AT₁ receptor-like.^{21, 22} The mechanism behind this phenotype change is unclear, but most likely involves a difference in location (endothelial cell (EC) vs. vascular smooth muscle cell (VSMC)) and/or heterodimerization with AT₁ receptors. Therefore, whether upregulation of AT₂ receptors under pathological conditions is always beneficial remains unknown.²³ Similar opposing findings with regard to AT₂ receptor function have been made in the heart.²⁴ Of interest, post-myocardial infarction a moderate cardiac AT₂ receptor overexpression in transgenic mice protected against maladaptive remodeling and dysfunction, whereas a massive, 9-fold overexpression did not yield such positive effects.²⁵ Thus, also the degree of overexpression may determine AT₂ receptor function.

Wide attention has been paid to the fact that increased vascular Ang II levels increase NAD(P)H oxidase activity in EC, adventitial cells, and VSMC, thereby stimulating reactive oxygen species (ROS) formation in the vessel wall.²⁶ ROS products like superoxide and H₂O₂ subsequently activate multiple signaling pathways, involving mitogen-activated protein kinases (MAPK), tyrosine kinases, phosphatases, calcium channels and redox-sensitive transcription factors,^{26, 27} together resulting in cell growth, expression of pro-inflammatory genes (e.g., transforming growth factor- β (TGF- β)), and the production of extracellular matrix (ECM) proteins, like collagen, elastin, fibrillin, fibronectin and proteoglycans. The latter production usually involves a phenotype switch in VSMC, from contractile to proliferative/synthetic. In addition, there is an imbalance between apoptosis and growth.

Extracellular matrix defects and vascular disease

The extracellular matrix is composed of numerous macromolecules, including collagens, elastin and proteoglycans. These extracellular matrix molecules not only provide structural support to cells and tissues, but also exhibit important functional roles that control the behaviour of cells such as adhesion, migration, proliferation and differentiation. Moreover, the extracellular matrix provides mechanical properties required for the functioning of the vasculature.²⁸ Minor alterations in extracellular matrix composition of the vasculature can lead to changes in cellular phenotype and function, which can ultimately lead to development of vascular disease. Diseases that are associated with an extracellular matrix defect include cutis laxa, osteogenesis imperfecta, Ehlers-Danlos and Marfan syndrome.²⁹

The strength and elasticity of our blood vessels is mainly established by the extracellular matrix components elastin and collagen, which originate in the medial layer of the vessel wall. Degeneration of the medial layer of the aorta allows the development of an aneurysm, which is characterized by elastic fibre fragmentation, loss of smooth muscle cells, and accumulation of amorphous extracellular matrix.³⁰ Two main types of aortic aneurysms can be distinguished; abdominal aortic aneurysm and thoracic aortic aneurysm. Abdominal aortic aneurysms are usually caused by multiple environmental factors, such as smoking, high blood pressure and inflammation, while the development of thoracic aortic aneurysms often has a genetic origin. Moreover, it is suggested that alterations towards the breakdown of the extracellular matrix contributes to the progression of atherosclerosis and plaque instability,³¹ and to the formation of aortic aneurysms.^{32, 33}

Involvement of the RAS in atherosclerosis

Atherosclerosis refers to the build-up of fat, cholesterol and other substances in and around the vasculature. Over time this build-up, so-called plaques, causes thickening and stiffening of the vessel wall. Moreover, as these plaques grow larger and larger, they eventually partially or totally block the blood flow through an artery. Numerous cardiovascular diseases are a direct consequence of the atherosclerotic process. Diseases that could develop as a result of this plaque build-up include coronary heart disease, carotid artery disease, peripheral artery disease and chronic kidney disease. Two types of plaques are described in literature; stable and unstable/

vulnerable plaques, the latter having a high risk of rupture.³⁴ Plaque rupture and subsequent thrombus formation are among the main causes of acute cardiovascular events like unstable angina, acute myocardial infarction and sudden cardiac death.³⁵ It is suggested that loss of vascular function together with oxidation and accumulation of low-density lipoprotein and endothelial damage promotes an inflammatory vascular response, which plays an essential role in the development of atherosclerotic plaques. Several risk factors are strongly associated with the onset of plaque build-up such as ageing, smoking, lack of physical activity, unhealthy diet, hypercholesterolemia, hypertension and genetic background. In addition, it is proposed that the RAS, and particularly Ang II, is involved in the initiation and progression of atherosclerotic plaques, since various atherogenic stimuli are mediated by RAS activity.³⁶ Ang II stimulates the atherogenic process not only through its hemodynamic effects but also through various effects on the vessel wall itself.³⁷ In particular, Ang II promotes the generation of oxidative stress in the vasculature, which plays a pivotal role in endothelial dysfunction and lipoprotein oxidation. Furthermore, Ang II induces the expression of cellular adhesion molecules and pro-inflammatory cytokines, which contribute to the induction of the inflammatory process in the vessel wall. Ang II also triggers vascular smooth muscle cells to proliferate and migrate, subsequently leading them to produce growth factors and extracellular matrix components. It was also reported that overexpression of ACE2, which converts Ang II to Ang-(1-7), improves endothelial function and decreases plaque formation in atherosclerotic mice.^{38, 39} Moreover, several studies suggest that Ang II may be involved in the acute complications of atherosclerosis by promoting plaque vulnerability, eventually resulting in plaque rupture.⁴⁰⁻⁴³

Current RAS-related therapeutic interventions for vascular and aneurysm disease

Several studies already demonstrated that ACE inhibitors might inhibit atherosclerosis in animal models independent of blood pressure lowering.⁴⁴⁻⁴⁶ Additionally, renin inhibition and angiotensin receptor blockers reduced atherosclerotic lesion size in cholesterol fed mice susceptible for atherosclerosis.⁴⁷⁻⁵⁰ Moreover, research in aneurysmal mouse models has shown that inhibition of the RAS reduces the formation and progression of aortic aneurysms.

Recent evidence supports a role for the Ang II-TGF- β axis in aneurysm development.^{51, 52} Infusion of Ang II in atherosclerotic apolipoprotein E - or LDL receptor KO mice provides an experimental model for the most common type of aneurysm, the abdominal aortic aneurysm. Thoracic aortic aneurysms (TAAs) are less common, and often have a genetic background, involving mutations in the above-mentioned ECM proteins and TGF- β . A well-known example is Marfan's syndrome. Losartan was shown to be effective in adults with this syndrome,⁵³ and animal data suggest that this effect involves AT₂ receptor stimulation rather than AT₁ receptor blockade.⁵⁴ Both the TGF- β -induced canonical (pSmad2/3) and non-canonical (MAPK) signaling pathways are upregulated in TAA mouse models, and their suppression may underlie the effectiveness of AT₁ receptor blockade in these models.^{54, 55}

Besides, TGF- β -signalling (by TGF- β -neutralizing antibodies) effectively blocks the production of downstream TGF- β and thereby inhibits aortic root dilatation and aneurysm formation.⁵⁶⁻⁵⁸

As a consequence of these exciting new findings, multiple trials now investigate the effectiveness of RAAS blockers in Marfan's syndrome.⁵² An important issue will be to what degree ACE inhibition (which does not result in AT₂ receptor stimulation) differs from AT₁ receptor antagonism. One of these trials was recently published.⁵⁹ Involving 608 Marfan patients (age 6 months-25 years), it did not show superiority of losartan versus the beta-adrenergic antagonist atenolol. Beta-adrenergic antagonists are the current standard therapy in Marfan patients. Here it should be realized that such drugs also suppress renin release. The investigators applied a relatively high dose of atenolol, and a low dose of losartan, and there was no placebo group. Moreover, treatment was started in most cases at an advanced stage of the disease. Thus, on the basis of this study it can be concluded that losartan is a safe alternative for a beta-adrenergic antagonist, but not yet whether (at the appropriate dose and perhaps when given at an earlier stage of development) it might be better.

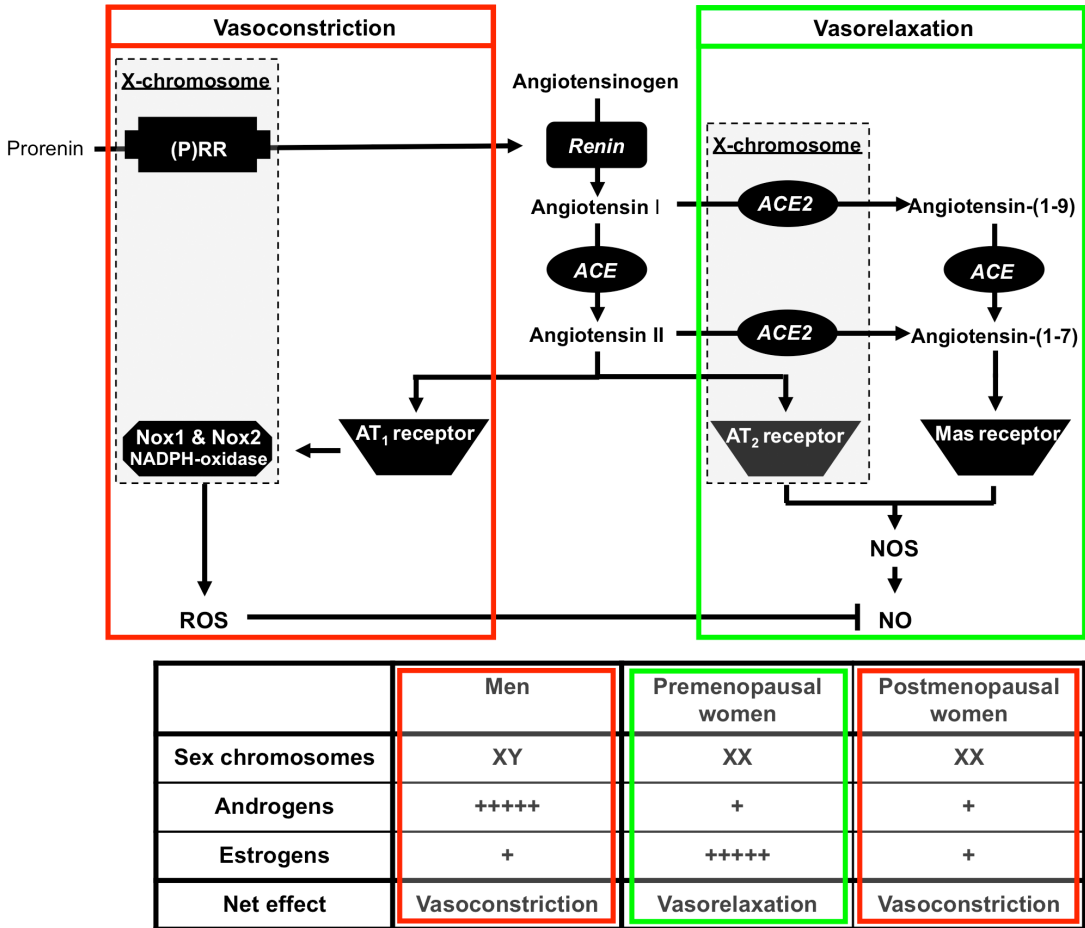


Figure 4

Vasoconstrictor-vasorelaxant balance of the RAAS in relation to sex hormone status in men and pre- and postmenopausal women. The Figure highlights X-chromosome-located RAAS genes, including the (pro) renin receptor ((P)RR) gene. The current view is that its relationship with the RAAS may be limited to (pro) renin-synthesizing organs, where (pro)renin is sufficiently high to result in significant receptor binding.

Gender-related aspects

Physiologically the two major differences between men and women are (1) different levels of sex hormones (testosterone vs. estrogen), and (2) the sex chromosome complement (XY vs. XX). The combination of a different hormonal milieu and different genes located on the sex chromosomes results in a transcriptome with a sex-specific and sex-biased expression. This leads to a marked sexual dimorphism in anatomy, physiology and metabolism, but also extends to sex differences in blood pressure (BP), sensitivity to Ang II, and severity of cardiovascular disease.⁶⁰

Sex hormones

Premenopausal women have a lower BP in comparison to age-matched men (~10 mm Hg for systolic BP and ~5 mm Hg for diastolic BP). Since this sexual dimorphism in BP manifests itself during adolescence and disappears after the menopause, it is logical to assume a role for sex hormones. Testosterone binds to the androgen receptor, whereas estrogen (17 β -estradiol) stimulates the estrogen receptor α and β , as well as the G-protein-coupled estrogen receptor-1 (GPER). These receptors mediate both genomic and non-genomic effects. The former involve interaction of the hormone-receptor complex with nuclear DNA, modulating the transcription of sex hormone-responsive genes (taking hours), while the latter involves signaling cascades resulting in effects within seconds-minutes. In the case of estrogen, this results in endothelium-dependent and -independent dilator effects through nitric oxide (NO), cGMP, cAMP, and/or K⁺-channels.⁶¹ Testosterone is believed to counteract such endothelium-dependent vasorelaxation and to exert direct constrictor effects⁶¹; the BP-lowering effects after castration confirmed this view.⁶²

In addition, sex hormones affect RAAS components and modulate Ang II sensitivity. Indeed, estrogens increase angiotensinogen, ACE2, AT₂ receptor density and endothelial NO synthase (eNOS), while they decrease renin, ACE, AT₁ receptor density, and the NADPH oxidase subunits Nox1 and Nox2 (Figure 4).^{63,64} These alterations are suggestive for an upregulation of ACE2-derived angiotensin-(1-7) formation, enhanced AT₂ receptor stimulation and NO release, combined with reduced ROS formation, in other words they favour the vasodilator arm of the RAAS (see also below). Indeed, low doses of Ang II even decreased BP in female (but not male) rats,⁶⁵ and higher doses exerted larger BP-increasing effects in males than in females, while gonadectomy reversed these effects.⁶⁶ Testosterone increases renin, ACE and AT₁ receptors, and downregulates AT₂ receptors, thereby favouring the constrictor arm. There are no clear differences in aldosterone levels between men and women.⁶⁷ In postmenopausal women the balance will shift towards the vasoconstrictor arm, unless they receive hormone replacement therapy.⁶³

Sex chromosomes

In most mammals, males are heterogametic, possessing one X and one Y chromosome, while females are homogametic with two X chromosomes. This characteristic plays a fundamental role in the sexual dimorphism through variances in gene expression. Evolutionary, sex chromosomes have evolved out of a pair of matched autosomes which eventually lost the ability to recombine due to an accumulation of male-specific functions on one chromosome and degradation of non-recombining regions.⁶⁸ Genes mapped to the Y chromosome play an important role in sex development, testosterone production and fertility.

A limited number of studies suggests that sex chromosomes influence BP and regulate RAAS genes. Introgression of the Y_{SHR} chromosome from the SHR strain on a normotensive WKY background resulted in a ~20 mm Hg BP difference versus rats where the normotensive Y_{WKY} chromosome was introgressed on the SHR background.⁶⁹ The 'four core genotype' mouse model involves the deletion of the sex-determining region Y (Sry) from the Y chromosome and the insertion of the Sry transgene onto an autosome, thereby resulting in XY Sry males.⁷⁰ Crossing these mice to normal XX females will result in four genotypes, XX gonadal males and females, as well as XY gonadal males and females. Interestingly, Ang II induced a larger BP rise in gonadectomized four core genotype mice with an XX genotype than in their XY counterparts independent of prior sex hormone status and gonadal phenotype.⁷¹ It is tempting to speculate that this mechanism underlies the relatively rapid increase in BP observed in postmenopausal women.⁷² The Sry gene family is known to upregulate angiotensinogen, renin and ACE, whereas it downregulates ACE2 in vitro.⁶² In addition, the (P)RR, ACE2, Nox1, Nox2 and the AT₂ receptor are mapped to the X chromosome (Figure 4). Although dosage-compensation takes place in women by an epigenetic mechanism called X-inactivation in order to prevent a lethal dose of X-mapped genes, several genes (15-20%) have been reported to escape X-inactivation⁷³ and contribute to sex differences due to a higher expression in XX than XY cells.⁷⁴ Such escape also applies to the (P)RR,^{75,76} but the physiological relevance of this observation is still unknown.

Consequences for treatment?

It is well-accepted that premenopausal women are protected from the development of cardiovascular disease in comparison to age-matched men.⁷⁷ Obviously, having a higher BP for up to 4-5 decades, even when modest, will have consequences. As discussed above, animal data support a major role for the RAAS in gender-related differences. Yet, there are no sex-specific recommendations for antihypertensive therapy, nor is there currently any evidence that men and women respond differently to RAAS blockers. One retrospective study in patients with heart failure claimed a higher efficacy of ACE inhibitors in males, and of AT₁ receptor blockers in females.⁷⁸ Although this potentially supports the importance of AT₂ receptor stimulation in women, large prospective studies are warranted to confirm such claims.

Determinants of RAAS blocker response and the degree of blockade

Prediction of RAAS blocker response

Although gender, as discussed above, is not an established determinant of RAAS blocker response, multiple attempts have been made to predict the response to a RAAS blocker on the basis of alternative parameters. Genetic variation has been evaluated, usually by studying single nucleotide polymorphisms in RAAS genes in a retrospective manner in large clinical trials.^{79,80} Emphasis has been on the ACE insertion/deletion polymorphism.⁸¹ Unfortunately, the effects were small and difficult to replicate, and, given the non-existence of large prospective studies to further evaluate these findings, at this stage, there is no useful genetic information that can be applied to the individual patient to help choosing a specific RAAS blocker.

Along the same lines, it has been argued that patients with 'high' RAAS activity (like patients with 'bad' RAAS gene variants) should preferably be treated with RAAS blockers. Such patients should then be selected on the basis of their high renin, ACE and/or aldosterone levels. Ang II levels might also be useful, but given the technical difficulties to measure this RAAS component, this is currently not feasible. The background of this concept is that patients with high baseline RAAS activity have a higher risk to develop cardiovascular disease. Indeed, retrospective analyses of patient populations in clinical trials in whom baseline renin measurements were available, support that high renin levels are indicative of future cardiovascular disease and death, particularly in patients with kidney dysfunction and/or hypertension.⁸²⁻⁸⁵ Remarkably, this relationship was not affected by the use of RAAS blockers, which, through interference with the negative feedback loop between Ang II and renin, increase renin release. Obviously, renin measurements, when based on activity, will be disturbed by the use of renin inhibitors, and thus during such treatment only measurements of plasma renin concentration (PRC), and not plasma renin activity (PRA), will give an indication of the true renin levels. In addition, salt intake affects renin secretion, with patients on a low salt diet displaying higher renin levels. Preferably therefore, when considering pre-treatment renin levels as a treatment determinant, salt intake should be taken into account.

Laragh and Sealey distinguish a low renin, sodium-volume dependent form of essential hypertension and a medium-to-high renin form of hypertension.⁸⁶ The former occurs whenever body sodium content increases beyond the point where plasma RAAS activity is turned off, whereas the latter occurs when too much renin is secreted relative to the body sodium content. Antihypertensive treatment should then be aimed at reducing either body salt and volume content (diuretics, calcium antagonists) or RAAS activity (RAAS blockers and β -adrenergic antagonists; the latter suppress renin release). Retrospective analyses of BP trials confirmed this concept.^{87,88} In addition, Gupta et al. observed that African Americans, who on average have lower renin levels compared to Caucasians,⁸⁹ responded less well to atenolol.⁹⁰ Yet, others observed either no role for baseline renin,⁹¹ or at most a weak trend.^{92,93,94} Moreover, the BP decreases for a given baseline renin level (uncorrected for salt intake) varied >40 mm Hg. In addition, a uniform definition of 'high' renin (PRA/PRC) is not available, and clearly complicated by the intake of salt, gender, ethnicity, and the use RAAS-affecting drugs.^{87,91,93} Thus, although in general it is probably true that patients with 'high' renin levels respond better to RAAS blockers (for instance patients pretreated with a diuretic, which activates the RAAS), the variation in renin is such (not even taking into consideration the additional variation at the tissue level!) that it is of limited practical use for the

individual patient. Unfortunately, the same is true for plasma ACE.⁹⁵ The use of aldosterone measurements will be discussed below.

Desired degree of RAAS blockade

Given the Ang II/aldosterone escape during RAAS blocker treatment, usually occurring within days-weeks after drug initiation,⁹⁶ for many years it was argued that the more blockade, the better, to keep the levels of these active components (or their activity) low. Nevertheless, early animal studies in SHR⁹⁷ had already shown that dual RAAS blockade, particularly under low-salt conditions (when the RAAS is most needed) is lethal: it caused a major decrease in BP and severe renal failure which were accompanied by massive rises (up to several 100-fold) in plasma renin and renal renin levels, thereby decreasing the angiotensinogen concentration in plasma. These deleterious effects of dual RAAS blockade were prevented by a high salt diet. Studies in human cardiac tissue, obtained from patients undergoing cardiac transplantation or severe heart failure patients at the time of left ventricular assist device (LVAD) implantation,^{98,99} both being treated with (high) RAAS blocker doses, revealed that also in the human heart renin levels may rise >100-fold, thereby decreasing cardiac angiotensinogen. Interestingly, following LVAD implantation, renin levels dropped 10-fold, and cardiac angiotensinogen levels rose again, thereby allowing a rise in cardiac Ang II levels.⁹⁹ This illustrates the fact that at very high renin levels, angiotensinogen depletion essentially renders Ang II generation impossible.

Taken together, these data illustrate that too much RAAS blockade annihilates the capacity of tissues to acutely generate Ang II when necessary. Particularly in the kidney, this may be crucial to preserve glomerular filtration. Recent data obtained in salt-depleted healthy volunteers exposed to increasing doses of a new renin inhibitor, VTP-27999, provide further evidence for this concept.¹⁰⁰ To fully appreciate these data, it should be mentioned that renin inhibitors selectively accumulate in the kidney, remaining present in renal tissue at high levels, even at days-weeks after stopping treatment, when plasma levels are undetectable.^{101,102} It was observed that at the highest dose of VTP-27999 tested (600 mg), the drug blocks the renal RAAS more effectively than the circulating RAAS. Indeed, when stopping drug intake after 10 days of dosing, the PRC levels at 24-72 hours after the last dose exceeded the capacity of extrarenal VTP-27999 to fully block renin's enzymatic activity (Figure 5). Therefore, even though the intrarenal RAAS is still inhibited at these times, extrarenal RAAS activation now occurred, increasing the circulating concentrations of Ang II and aldosterone. These findings are reminiscent of the nephrocentric view of ACE inhibition noted 25 years ago in patients with congestive heart failure.¹⁰³ It was asked why the kidneys continue to release renin in such patients; the answer being that they do everything possible to preserve renal function and glomerular filtration, apparently at the expense of the hemodynamic burden on the heart. Exactly this happened in the VTP-27999 study, where the kidneys responded to excessive renal RAAS suppression by releasing very large quantities of renin, resulting in elevations of PRA, Ang II and aldosterone. Such elevated Ang II levels were most likely responsible for the (non-significant) increase in heart rate observed in the subjects treated with 600 mg VTP-27999. Clearly therefore, renin inhibition has an upper limit and more is not always better.

The latter also applies to other types of excessive RAAS blockade (e.g. when combining an ACE inhibitor and an AT₁ receptor antagonist): several large dual RAAS blockade studies (ONTARGET, ALTITUDE, NEPHRON-D)¹⁰⁴⁻¹⁰⁶ in a variety of patients all concluded that the adverse effects (hypotension, hyperkalemia and renal dysfunction), all due to (renal) Ang II depletion, outweighed the beneficial effects. In reaching this conclusion, it should be realized that often these patients additionally took β -adrenergic antagonists and MR antagonists, and thus were in reality not exposed to dual but to quadruple RAAS blockade. This led Nussberger and Bohlender to conclude that the goal should not be maximal but optimal RAAS blockade, guided by regularly measuring BP, serum potassium and creatinine.¹⁰⁷

Recent guidelines no longer recommend the combined use of ACE inhibitors, AT₁ receptor blockers and renin inhibitors in hypertension.¹⁰⁸ Most evidence is obviously available for the ACE inhibitors. As explained above, there is still discussion to what degree the AT₂ receptor stimulation during AT₁ receptor blockade is beneficial or harmful. Two recent meta-analyses show that ACE inhibitors reduce all-cause mortality and cardiovascular death

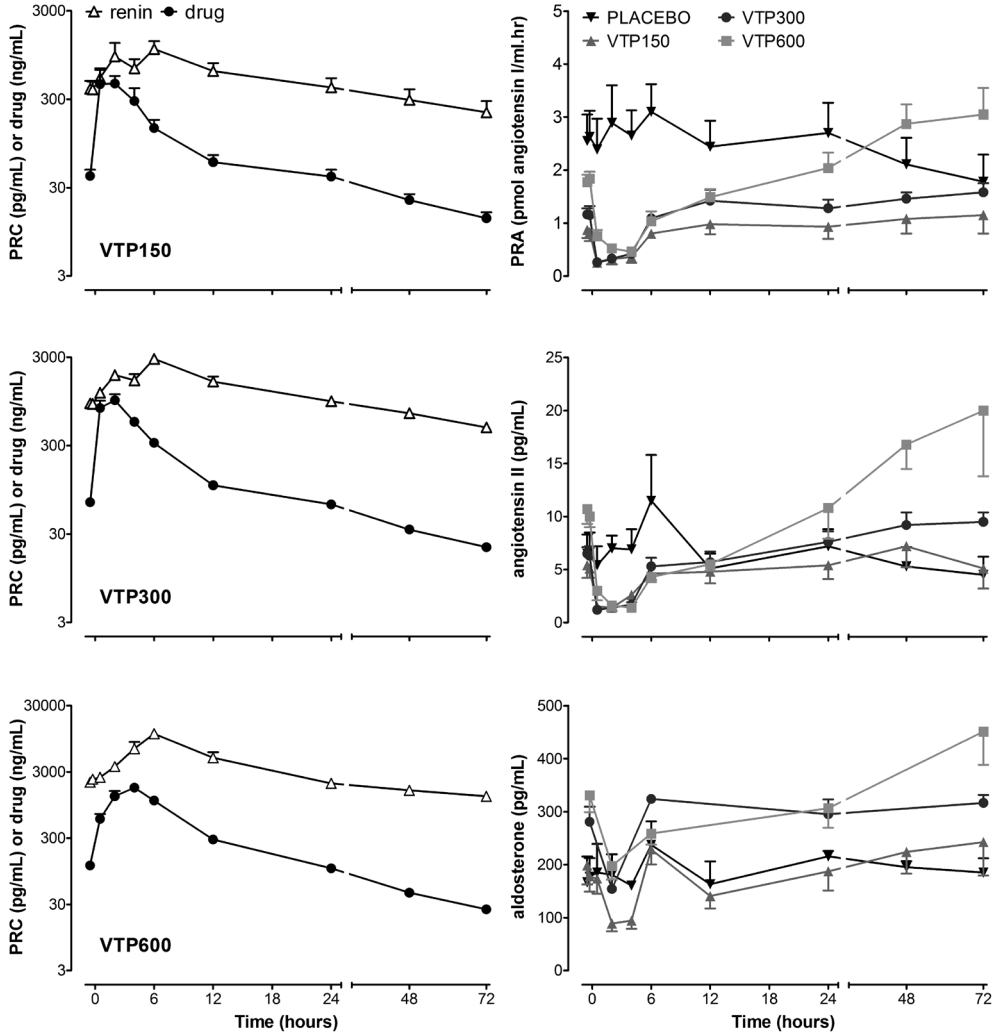


Figure 5

The consequences of too much renin inhibition (with the new renin inhibitor VTP-27999), as observed after stopping treatment. Normally, the decrease in plasma drug level and renin concentration after stopping run in parallel. However, after a high (600 mg) dose of VTP-27999 (which, like aliskiren, is known to accumulate in the kidney¹⁰²), plasma renin suppression lags behind the decline in plasma drug decrease, most likely because the renal RAAS is still suppressed, thus keeping renin release at a (too) high level, which can no longer be suppressed by VTP-27999 in plasma. As a consequence, plasma renin activity, Ang II and aldosterone rise above control levels. In other words, too much renin inhibition, by excessively blocking the renal RAAS, may effectively activate extrarenal RAAS activity. Data are taken from Balcarek et al.¹⁰⁰

in patients with hypertension and diabetes mellitus, whereas AT₁ receptor blockers do not.^{109,110} This may relate to the possibility that AT₂ receptor stimulation affects the incidence of myocardial infarction^{111,112} and induces apoptosis in intestinal epithelial cells, thereby inducing severe gastrointestinal problems.^{113,114} Additionally, AT₂ receptor stimulation activates the bradykinin axis,¹¹⁵ although bradykinin accumulation will also occur after ACE inhibition. The exact contribution of bradykinin to the beneficial effects of RAAS blockade in humans remains to be determined. Nevertheless, based on these findings, it is clear that ACE inhibitors should be considered as first-line agents in patients with hypertension and diabetes mellitus.

Aldosterone

Aldosterone is a steroid hormone produced in the zona glomerulosa of the adrenal gland. Like Ang II, aldosterone is an effector hormone of the RAAS, principally involved in volume and BP regulation. Beyond BP, aldosterone has emerged as a cardiovascular risk factor promoting cardiovascular and renal inflammation, fibrosis and remodeling. Furthermore, in cohort studies of non-hypertensive individuals higher circulating aldosterone levels, but still within the physiological range, are a risk factor for the development of hypertension.¹¹⁶ With regard to hypertension the importance of aldosterone is largely related to primary aldosteronism and treatment-resistant hypertension. The mechanism of action of aldosterone was thought to be restricted to its renal genomic effects, causing sodium and water retention. More recently, evidence has accumulated for effects of aldosterone on EC and VSMC that may or may not be mediated by the MR.¹¹⁷⁻¹¹⁹ In the first part of this section we focus on new insights in the potential vascular effects of aldosterone and the receptors involved. In the second part new developments in the pathogenesis and etiology of primary aldosteronism and the role of aldosterone in resistant hypertension will be reviewed.

Aldosterone, aldosterone receptors and sodium channels

Aldosterone is synthesized from cholesterol in the zona glomerulosa of the adrenal gland by a series of enzymatic reactions. The final steps of aldosterone synthesis are catalyzed by aldosterone synthase encoded by the gene *CYP11B2* located on chromosome 8q21-22. Classic stimulators of aldosterone biosynthesis are Ang II, extracellular potassium concentration and ACTH. Vascular endothelial growth factor has recently emerged as a stimulator of aldosterone production.¹²⁰ Stimulation by these factors results in activation of aldosterone synthase induced by an increase in intracellular calcium concentration.¹²¹

Aldosterone classically works in a genomic way through the induction and modulation of gene transcription with the cytoplasmic/nuclear MR within the renal cortical collecting duct cells as its main target. After binding of aldosterone to the MR, causing dissociation of chaperones and formation of MR dimers, this complex translocates to the nucleus resulting in increased expression of several intracellular kinases, including serum- and glucocorticoid-induced kinase 1, Kirsten Ras GTP-binding protein 2A and WNK4. This process leads to increased expression of the luminal located epithelial sodium channel (ENaC), renal outer medullary K⁺-channels, and the basolaterally located Na⁺/K⁺-ATPase.¹²² Increased renal ENaC activity promotes renal Na⁺ reabsorption, resulting in volume expansion and a rise in BP.

Additionally to its expression in renal collecting duct cells, the MR is also expressed in ECs and VSMCs.^{118,119} Important new insight in the role of the VSMC-MR has been obtained by engineering a mouse with an inducible, selective deletion of VSMC-MR.¹²³ In these KO mice BP at young age is similar as in wild-type control mice, but, despite intact renal MR receptors, the age-related rise in BP is attenuated. Furthermore, aged VSMC-MR-KO mice have a decreased vascular tone, and the aged vessels exhibit decreased contractile responses to thromboxane, Ang II and calcium channel agonists.¹²³ Moreover, these mice have an attenuated increase in BP and superoxide production to Ang II infusion and a decrease in large-artery stiffness after aldosterone salt challenge compared to wild-type mice.¹²⁴

Several new molecular pathways activated by the interaction of aldosterone with the VSMC-MR and contributing to vascular remodeling have been described in the past several years.¹²⁴⁻¹²⁶ These pathways promote vascular inflammation, fibrosis and VSMC hypertrophy and proliferation and may contribute to the development

of large artery stiffness. Although the clinical implication of these pathways requires further research, it has already been shown in patients with familial hyperaldosteronism type I that cardiac and vascular damage may precede the development of hypertension.¹²⁷

In ECs aldosterone increases the expression of endothelial Na channels (EnNaCs) in a MR-dependent way that can be blocked by spironolactone.¹²⁸ Increased EnNaC activity in combination with a high plasma sodium leads to stiffening of the cortex of ECs due to an increase in sodium influx. A direct consequence of this stiffening is a decrease in eNOS-mediated NO release.¹²⁹ Thus high aldosterone in combination with high salt intake may result in endothelial dysfunction, which may contribute to a rise in BP independent of the renal effects of aldosterone.

Besides its genomic effects mediated by stimulation of the MR receptors in the kidney and vasculature, rapid non-genomic effects of aldosterone have also been reported.¹¹⁷ These non-genomic effects of aldosterone may be mediated by GPER.^{117, 130} GPER is a widely distributed receptor, also identified in EC and VSMC.¹³¹ GPER in cultured EC and VSMC can be stimulated by estrogen but also by aldosterone at picomolar concentrations.¹¹⁷ Aldosterone-induced activation of aortic vascular ECs via GPER leads to vasodilation as well as to pro-apoptotic and anti-proliferative effects.¹³⁰ These effects of aldosterone are blocked by the GPER receptor antagonist G15. Whether aldosterone also exerts effects on VSMCs through activation of the GPER is uncertain, as GPER expression is no longer present when aortic VSMCs are cultured.¹¹⁷ GPER seems to play a role in the potentiation of Ang II-induced vasoconstriction by aldosterone, because this potentiation could be blocked by G15, but not by the MR-antagonist eplerenone.¹³²

Sporadic and Familial Primary Aldosteronism

Primary aldosteronism (PA) is characterized by excessive autonomous aldosterone secretion by the adrenal gland. The consequent volume expansion and hypertension leads to renin suppression and accordingly the ARR has been advocated as a screening test for PA.¹³³ Among hypertensive individuals the prevalence of PA is high, ranging from 4.3% in a primary care setting to 9.0% of referred patients, and to 20% of those with therapy-resistant hypertension.¹³⁴ We and others have shown that the sensitivity of the ARR as a screening test for PA is relatively poor, which may relate to the way patients were selected and to overestimation of the true renin concentration by the nowadays commonly used direct renin assay (due to co-detection of prorenin) instead of PRA measurements.^{135, 136}

PA can be divided in frequent sporadic and rare familial forms. Familial hyperaldosteronism (FH) type 1, also known as glucocorticoid-remediable aldosteronism, is an autosomal dominant disease caused by a recombination between the CYP11B2 and CYP11B1 (the latter being responsible for cortisol synthesis) genes, creating a chimeric gene whereby the CYP11B1 promotor and CYP11B2 coding sequences are juxtaposed. In FH-I aldosterone synthesis is regulated by ACTH rather than by Ang II. Administration of glucocorticoids thereby suppressing ACTH reduces aldosterone levels and the lowest dose of glucocorticoids normalizing BP is the treatment of choice. The cause of FH-II has yet to be identified. FH-II is diagnosed if 2 or more members of one family are affected. Adenomas as well as bilateral hyperplasia may underlie FH-II. The first family with FH-III has been described in 2008.¹³⁷ The affected family members presented with severe hypertension and hypokalemia at very young age and in contrast to FH-I aldosterone could not be suppressed by dexamethasone. FH-III appeared to be caused by a mutation in the KCNJ5-gene, encoding for the G-protein-activated inward rectifier potassium channel Kir3.4.¹³⁸ This mutation results in the loss of K⁺-selectivity and increased Na⁺ conductance, leading to membrane depolarization of the zona glomerulosa cell with subsequent opening of voltage-dependent calcium channels and activation of the calcium-signaling pathway (Figure 6). Several other mutations in the KCNJ5 gene causing FH-III, not always accompanied by a severe phenotype as described for the first cases, have been reported.¹³⁹ In addition to the germline mutations causing FH-III, somatic KCNJ5 mutations, resulting in loss of the selectivity filter of Kir3.4 channel, have been identified in surgically removed aldosterone-producing adenomas (APAs). These mutations are present in up to 47% in APAs from Western populations and up to 65% from a Japanese population.¹²¹ In addition, several other less frequently occurring somatic mutations in 2 members

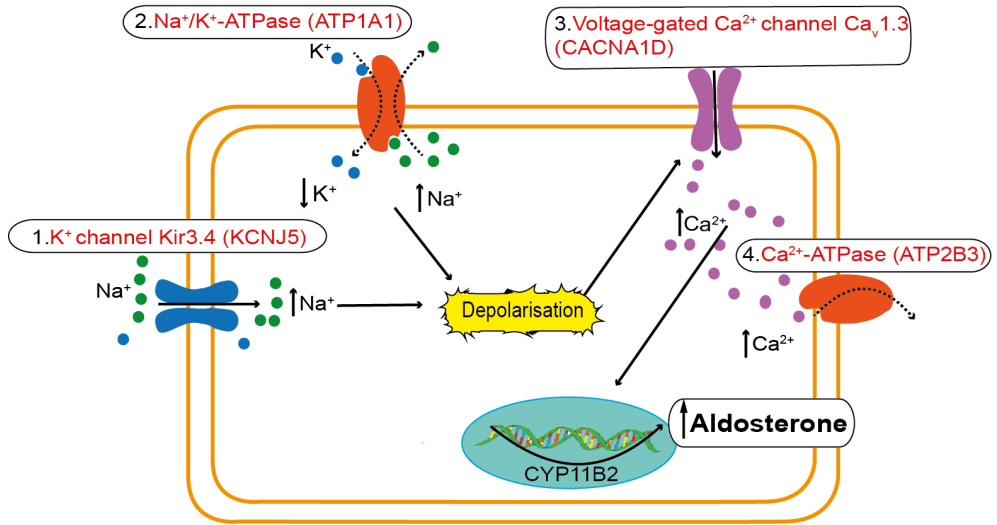


Figure 6

Mutations in ion channels (encoded by the genes KCNJ5, ATP1A1, CACNA1D and ATP2B3) of the adrenal glomerulosa cell that have recently been linked to excessive aldosterone production. Normally, AT₁ receptor activation induces depolarization due to inactivation of the potassium channel Kir3.4 and Na⁺/K⁺-ATPase. Such depolarization triggers Ca²⁺-influx via voltage-gated Ca²⁺ channels (Ca_v1.3), and the resultant rise in intracellular Ca²⁺ activates the aldosterone synthase gene CYP11B2. Ca²⁺-ATPase subsequently removes Ca²⁺ from the cell. KCNJ5 mutations affect the selectivity of the Kir3.4, now also allowing Na⁺ conductance. Similarly, mutations in ATP1A1 result in loss of pump activity and strongly reduced affinity for potassium, thereby increasing intracellular Na⁺. Increased Na⁺ levels cause depolarization, even in the absence of AT₁ receptor stimulation. Mutations in CACNA1D facilitate Ca²⁺ influx, while mutations in ATP2B3 hamper its removal from the cell, thus both elevating intracellular Ca²⁺. This activates CYP11B2 transcription.

of the P-type ATPase gene family (ATP1A1 and ATP2B3) and in CACNA1D (encoding for the voltage-gated Ca²⁺ channel Ca_v1.3) have been identified (Figure 6).^{140,141} In adrenal glomerulosa cells, mutations in ATP1A1 result in inappropriate depolarization, mutations in ATP2B3 in decreased intracellular calcium clearance, and mutations in CACNA1D in increased Ca²⁺ influx. In 308 APAs, negative for KCNJ5 mutations, 5.2% somatic mutations in ATP1A1 and 1.6% mutations in ATP2B3 have been identified.¹²¹ CACNA1D mutations may occur in up to 11% of APAs.¹⁴² Interestingly, KCNJ5 mutations are common in APAs resembling the cortisol-secreting cells of the zona fasciculata, whereas mutations in P-type ATPases and CACNA1D have been found in small zona glomerulosa cell APAs.¹⁴¹ These genotype-phenotype correlations might hopefully be of clinical use in the near future.

Aldosterone and resistant hypertension

Resistant hypertension is defined as uncontrolled hypertension despite therapy with 3 drugs including a diuretic, or BP elevations requiring ≥ 4 drugs for control with an estimated prevalence of 10-15% of hypertensive patients treated.¹⁴³ PA because of its high prevalence, can underlie resistant hypertension, but also in patients without PA BP control was lower in patients with an elevated ARR and higher aldosterone levels.¹⁴⁴ That aldosterone plays a role in resistant hypertension is supported by trials showing that addition of MR blockers

to usual antihypertensive treatment can sometimes produce pronounced BP reductions.¹⁴⁵ In an open-label study addition of spironolactone 25-100 mg per day to 175 patients with true resistant hypertension to existing antihypertensive therapy reduced ambulatory BP by 16/9 mmHg.¹⁴⁶ The mechanism of the BP-lowering effect of MR antagonists in resistant hypertension is incompletely understood, because indices of aldosterone excess such as low renin or high ARR or a low serum potassium do not predict the response to aldosterone receptor blockers.¹⁴⁷ Spironolactone-mediated inhibition of central sympathetic nervous system activity has been proposed as one of the mechanisms.¹⁴⁸ Furthermore, reduction of vascular stiffness and improvement of endothelial function by blockade of vascular MRs may be involved.

The 'protective' arms of the RAAS: can we expect new RAAS drugs?

All current RAAS blockers interfere with the renin-ACE-AT₁ receptor-aldosterone axis. Aldosterone synthase inhibitors are being considered as an alternative for MR antagonists,¹⁴⁹ but such drugs would obviously also interfere with this pathway. Three new RAAS pathways have been discovered in the last 2 decades, which might be of interest for future drug development: (1) AT₂ receptor stimulation, (2) stimulation of ACE2/Ang-(1-7)/Mas receptor signaling, and (3) modulation of angiotensin III and IV signaling. In addition, drugs are being developed which block the RAAS plus an additional hormonal system, e.g., combined AT₁ receptor blockers/nephrilysin inhibitors ('ARNI'), which prevent the degradation of natriuretic peptides (by neprilysin), and combined AT₁ receptor/endothelin-1 receptor antagonists. Their discussion is beyond the scope of this review.

AT₂ receptor stimulation

As discussed before, the AT₂ receptor is generally considered to have effects that are opposite to those of the AT₁ receptor. Its presumed endogenous ligands are Ang II, Ang III, Ang IV and Ang-(1-7), in order of highest to lowest affinity (Figure 1).¹⁵⁰ Ang III appears to be the preferred agonist for AT₂ receptors.¹⁵¹⁻¹⁵³ For reasons that are still unclear, AT₂ receptor-mediated vasodilation is best detected under partial AT₁ receptor blockade, and the same may apply to its natriuretic, antifibrotic, and anti-inflammatory effects in the kidney.^{151, 154-156} AT₂ receptor KO mice display an increased BP, worsened pressure-natriuresis, increased baroreflex sensitivity, increased responsiveness to hypertensive stimuli (NOS inhibition), and decreased cardiac and vascular AT₁ receptor expression.¹⁵⁷⁻¹⁵⁹ AT₂ receptor overexpression shows the opposite.¹⁶⁰ It therefore seemed logical to develop specific AT₂ receptor agonists.

Currently, four candidate drugs for clinical development have been identified, namely the peptidergic agonists β -Tyr⁴-Ang II, β -Ile⁵-Ang II, and LP-2-3, and the non-peptide agonist Compound 21 (C21).^{156, 161} β -Tyr⁴-Ang II and β -Ile⁵-Ang II are Ang II analogues in which the Tyr⁴ and Ile⁵ α -amino acid residues have been replaced by β -amino acids, i.e. amino acids containing an additional methylene group.¹⁵⁶ This results in an almost complete loss of AT₁ receptor affinity, a modest (\times 5-15-fold) decrease in AT₂ receptor affinity, and an increased stability. Both peptide agonists caused weak, AT₂ receptor-mediated, NO-dependent vasorelaxation in the mouse aorta. In addition, β -Ile⁵-Ang II lowered BP in SHR during co-infusion with candesartan.¹⁵⁶

LP2-3 is cyclic Ang-(1-7) (see below) with a D-lysine N-terminal extension.¹⁶¹ Although it inhibits pathological remodeling of lung, cardiac and vascular tissue in a model of hyperoxia-induced neonatal pulmonary dysplasia,¹⁶¹ there is currently no proof of its claimed AT₂ receptor agonistic activity. Much more is known about C21, which is expected to enter the clinical phase of development this year.¹⁶² Confusingly, despite the wealth of data on AT₂ receptor-mediated vasodilation, C21 has either no effect on BP or even increases BP.^{155, 162, 163} The latter may relate to the fact that, for instance in SHR, AT₂ receptors become AT₁ receptor-like (i.e., constrictor), while at exceptionally high doses C21 also activates AT₁ receptors.^{21, 163} In vitro, C21 has a weak vasodilator effect, particularly observed during AT₁ receptor blockade, at concentrations above its K_d.¹⁶⁴ In fact, since such effects were also observed in vessels of AT₂ receptor KO mice, it has been proposed that C21 has pleiotropic effects; its ability to block vasoconstriction to non-angiotensin constrictors further confirmed this view.¹⁶³ In summary, although C21 does not seem to be an appropriate antihypertensive drug, the antifibrotic and anti-inflammatory effects of AT₂ receptor stimulation warrant alternative indications, including Marfan's syndrome.⁵⁴

Since AT_2 receptors also stimulate neurite outgrowth, thereby facilitating pain,¹⁶⁵ a recent clinical trial has investigated to what degree AT_2 receptor antagonists might be applied in neuropathic pain. Indeed, already after 3 weeks, such drugs reduced pain in patients with postherpetic neuralgia.¹⁶⁶ Whether this outcome affects the future application of AT_2 receptor agonists cannot yet be said.

ACE2-Ang-(1-7)-Mas receptor axis

Ang-(1-7), mainly produced from Ang II by ACE2 (Figure 1), opposes AT_1 receptor-mediated effects via its binding to the Mas receptor.¹⁶⁷ Yet, it also binds AT_2 receptors, and at high concentrations even acts as a partial AT_1 receptor agonist.¹⁶⁸ A plethora of beneficial cardiovascular effects has been described for Ang-(1-7) in the past 25 years. These include protection against heart failure, natriuretic, antithrombotic, antihypertrophic, antifibrotic, and anti-arrhythmic effects, attenuation of plaque formation and amelioration of metabolic syndrome-related vascular dysfunction.^{155, 169} It has weak vasodilator effects, which have not uniformly been confirmed. Ang-(1-7) also stimulates the production of endothelial progenitor cells (and tube formation thereof), but simultaneously inhibits tube formation by adult EC.^{155, 169} The circumstances under which the BP-lowering effects of Ang-(1-7) have been investigated varied widely (species, models, co-treatment with RAAS blockers/NOS inhibitors, salt intake) so that even now it cannot be stated with certainty that Ang-(1-7) is an antihypertensive agent. Similarly, although ACE2 overexpression does lower BP, this may be simply due to its capacity to degrade Ang II (rather than its generation of Ang-(1-7)).¹⁷⁰ Even more worryingly, the putative ACE2 activators 1-[(2-dimethylamino)ethylamino]-4-(hydroxymethyl)-7-[(4-methylphenyl) sulfonyl oxy]-9H-xanthene-9-one (XNT) and diminazene were recently shown to act fully independently from either ACE2 or Ang-(1-7), thus questioning whether their in-vivo effects have anything to do with this pathway.¹⁷¹

Despite these controversies, stimulation of the ACE2-Ang-(1-7)-Mas receptor axis might still be an interesting therapeutic option. In view of the rapid breakdown of Ang-(1-7) (as well as its AT_1 receptor agonistic properties at high concentrations), alternative strategies have been developed. These are oligosaccharide (hydroxypropyl β -cyclodextrin)-encapsulated Ang-(1-7), Ang-(1-7) peptide stabilization by thioether bridging (creating so-called cyclic Ang-(1-7)), NorLeu3-Ang-(1-7), the peptide drug CGEN856S, and the non-peptide drug AVE0991.^{155, 172} Cyclodextrin-encapsulated Ang-(1-7), AVE0091 and CGEN856S have shown BP-lowering effects in hypertensive animals, while the other agonists have not been tested yet in such a setting. Clearly, much more work is needed before these drugs can enter the clinic, although NorLeu3-Ang-(1-7) has been used clinically to treat foot ulcers in diabetic patients.¹⁷³

Blockade of Ang III and Ang IV

As discussed above, Ang III is believed to act as an AT_2 receptor agonist, e.g., in the kidney and vessel wall. Yet, in the brain it has been proposed to be the preferred AT_1 receptor agonist, thus causing hypertension.¹⁷⁴ On this basis, aminopeptidase A inhibitors (which block the conversion of Ang II to Ang III) are now being developed, which act exclusively in the brain. Indeed, RB150 (4,4 -dithio[bis(3S)-aminobutyl sulfonic acid]) is a prodrug that, after crossing the blood-brain barrier, is converted to the aminopeptidase A inhibitor EC33 ((3S)-3-amino-4-sulfanyl-butane-1-sulfonic acid).¹⁷⁵ RB150 can be delivered orally, and has already shown antihypertensive and cardioprotective properties in animal models, so that it is now under evaluation in a phase Ib clinical study.¹⁷⁶

To what degree the aminopeptidase N product of Ang III, i.e., Ang IV, has a function in BP regulation remains unclear. At high (micromolar) concentrations, it binds to AT_1 and AT_2 receptors, resulting in both constrictor and relaxant effects, the former possibly involving endothelin-1.^{177, 178} However, the relevance of these observations, given its low (femtomolar) concentrations in vivo, is questionable. Instead, high potency effects of Ang IV may rather involve its binding to insulin-regulated aminopeptidase (IRAP), also known as the AT_4 receptor (please note that AT_3 receptors do not exist, the 4 refers to Ang IV).¹⁷⁹ Unfortunately, even this concept has recently been challenged,¹⁸⁰ leaving as a final option the observation that Ang IV binds with high affinity to AT_1 receptors that are constitutively active, i.e., that already display activity without agonist binding.¹⁸¹ Until today the physiological relevance of this phenomenon is unknown.

CONCLUSIONS

Tissue angiotensin generation depends on kidney-derived renin and hepatic angiotensinogen, occurs extracellular, and is followed by rapid AT receptor binding and internalization. Locally generated Ang II affects the constrictor/relaxant balance, vascular remodeling, and inflammation. Tissue angiotensin generation does not necessarily run in parallel with angiotensin generation in the circulation, and this explains why the beneficial effects of RAAS blockers cannot be simply explained on the basis of changes in the circulating RAAS. Gender, ethnicity, salt intake, genetic variation, and the use of antihypertensive drugs determine the degree of RAAS activity, and although in general 'high' RAAS activity (as evidenced by 'high' plasma renin levels) would be supportive for the application of RAAS blockers, the inter-individual RAAS component variation is such that it is impossible to exactly define 'high' or 'low' renin levels that warrant the choice for a certain RAAS blocker. Too much RAAS blockade yields effects that can be expected when removing Ang II/aldosterone (hypotension, hyperkalemia, renal dysfunction), and thus the goal should be to obtain optimal instead of maximal RAAS blockade, guided by regularly measuring BP, potassium and creatinine. Aldosterone unexpectedly has a wide range of extrarenal effects, among others in EC and VSMC, and these are not necessarily all mediated via the MR. Together with the many mutations that have recently been discovered in genes encoding for proteins that control sodium, potassium and calcium ion homeostasis in adrenal cells (with strong resultant effects on aldosterone synthesis), this explains the revived interest in drugs that block aldosterone, e.g., in resistant hypertension. In addition, the discovery of the relaxant, protective arms of the RAAS, involving AT₂ and Mas receptor stimulation, may yield new drugs that can be applied in the future on top of the existing RAAS blockers in patients with cardiovascular and renal disorders.

REFERENCES

1. Nussberger J, Brunner DB, Waeber B, Brunner HR. Specific measurement of angiotensin metabolites and in vitro generated angiotensin II in plasma. *Hypertension* 1986;8:476-482.
2. van den Meiracker AH, Admiraal PJJ, Janssen JA, Kroodsmas JM, de Ronde WA, Boomsma F, Sissmann J, Blankestijn PJ, Mulder PG, Man In't Veld AJ, Schalekamp MADH. Hemodynamic and biochemical effects of the AT1 receptor antagonist irbesartan in hypertension. *Hypertension* 1995;25:22-29.
3. Danser AHJ. Cardiac angiotensin II: does it have a function? *Am J Physiol Heart Circ Physiol* 2010;299:H1304-1306.
4. Urata H, Healy B, Stewart RW, Bumpus FM, Husain A. Angiotensin II-forming pathways in normal and failing human hearts. *Circ Res* 1990;66:883-890.
5. Batenburg WW, Danser AHJ. (Pro)renin and its receptors: pathophysiological implications. *Clin Sci (Lond)* 2012;123:121-133.
6. Batenburg WW, Lu X, Leijten F, Maschke U, Müller DN, Danser AHJ. Renin- and prorenin-induced effects in rat vascular smooth muscle cells overexpressing the human (pro)renin receptor: does (pro)renin-(pro)renin receptor interaction actually occur? *Hypertension* 2011;58:1111-1119.
7. Kinouchi K, Ichihara A, Sano M, Sun-Wada GH, Wada Y, Kurauchi-Mito A, Bokuda K, Narita T, Oshima Y, Sakoda M, Tamai Y, Sato H, Fukuda K, Itoh H. The (pro)renin receptor/ATP6AP2 is essential for vacuolar H⁺-ATPase assembly in murine cardiomyocytes. *Circ Res* 2010;107:30-34.
8. Alexiou T, Boon WM, Denton DA, Nicolantonio RD, Walker LL, McKinley MJ, Campbell DJ. Angiotensinogen and angiotensin-converting enzyme gene copy number and angiotensin and bradykinin peptide levels in mice. *J Hypertens* 2005;23:945-954.
9. Danser AHJ, van Kats JP, Admiraal PJJ, Derckx FHM, Lamers JMJ, Verdouw PD, Saxena PR, Schalekamp MADH. Cardiac renin and angiotensins. Uptake from plasma versus in situ synthesis. *Hypertension* 1994;24:37-48.
10. van Esch JHM, Gembardt F, Sterner-Kock A, Heringer-Walther S, Le T, Lassner D, Stijnen T, Coffman T, Schultheiss H-P, Danser AHJ, Walther T. Cardiac phenotype and angiotensin II levels in AT1a, AT1b and AT2 receptor single, double and triple knockouts. *Cardiovasc Res* 2010;86:401-409.
11. Matsusaka T, Niimura F, Shimizu A, Pastan I, Saito A, Kobori H, Nishiyama A, Ichikawa I. Liver angiotensinogen is the primary source of renal angiotensin II. *J Am Soc Nephrol* 2012;23:1181-1189.
12. de Lannoy LM, Danser AHJ, van Kats JP, Schoemaker RG, Saxena PR, Schalekamp MADH. Renin-angiotensin system components in the interstitial fluid of the isolated perfused rat heart. Local production of angiotensin I. *Hypertension* 1997;29:1240-1251.
13. Henrion D, Benessiano J, Levy BI. In vitro modulation of a resistance artery diameter by the tissue renin-angiotensin system of a large donor artery. *Circ Res* 1997;80:189-195.
14. Yiannikouris F, Gupte M, Putnam K, Thatcher S, Charnigo R, Rateri DL, Daugherty A, Cassis LA. Adipocyte deficiency of angiotensinogen prevents obesity-induced hypertension in male mice. *Hypertension* 2012;60:1524-1530.
15. Gomez-Sanchez EP, Ahmad N, Romero DG, Gomez-Sanchez CE. Origin of aldosterone in the rat heart. *Endocrinology* 2004;145:4796-4802.
16. Chai W, Garrelts IM, de Vries R, Danser AHJ. Cardioprotective effects of eplerenone in the rat heart: interaction with locally synthesized or blood-derived aldosterone? *Hypertension* 2006;47:665-670.
17. van der Lubbe N, Lim CH, Fenton RA, Meima ME, Danser AHJ, Zietse R, Hoorn EJ. Angiotensin II induces phosphorylation of the thiazide-sensitive sodium chloride cotransporter independent of aldosterone. *Kidney Int* 2011;79:66-76.
18. van Kats JP, Danser AHJ, van Meegen JR, Sassen LM, Verdouw PD, Schalekamp MADH. Angiotensin production by the heart: a quantitative study in pigs with the use of radiolabeled angiotensin infusions. *Circulation* 1998;98:73-81.
19. van Kats JP, Schalekamp MADH, Verdouw PD, Duncker DJ, Danser AHJ. Intrarenal angiotensin II: interstitial and cellular levels and site of production. *Kidney Int* 2001;60:2311-2317.
20. van Kats JP, de Lannoy LM, Danser AHJ, van Meegen JR, Verdouw PD, Schalekamp MADH. Angiotensin II type 1 (AT1) receptor-mediated accumulation of angiotensin II in tissues and its intracellular half-life in vivo. *Hypertension* 1997;30:42-49.
21. Moltzer E, Verkuil AV, van Veghel R, Danser AHJ,

- van Esch JHM. Effects of angiotensin metabolites in the coronary vascular bed of the spontaneously hypertensive rat: loss of angiotensin II type 2 receptor-mediated vasodilation. *Hypertension* 2010;55:516-522.
22. You D, Loufrani L, Baron C, Levy BI, Widdop RE, Henrion D. High blood pressure reduction reverses angiotensin II type 2 receptor-mediated vasoconstriction into vasodilation in spontaneously hypertensive rats. *Circulation* 2005;111:1006-1011.
 23. Busche S, Gallinat S, Bohle RM, Reinecke A, Seebeck J, Franke F, Fink L, Zhu MY, Summers C, Unger T. Expression of angiotensin AT(1) and AT(2) receptors in adult rat cardiomyocytes after myocardial infarction - A single-cell reverse transcriptase-polymerase chain reaction study. *Am J Pathol* 2000;157:605-611.
 24. Ichihara S, Senbonmatsu T, Price E, Ichiki T, Gaffney FA, Inagami T. Angiotensin II type 2 receptor is essential for left ventricular hypertrophy and cardiac fibrosis in chronic angiotensin II-induced hypertension. *Circulation* 2001;104:346-351.
 25. Xu J, Sun Y, Carretero OA, Zhu L, Harding P, Shesely EG, Dai X, Rhaleb NE, Peterson E, Yang XP. Effects of cardiac overexpression of the angiotensin II type 2 receptor on remodeling and dysfunction in mice post-myocardial Infarction. *Hypertension* 2014;63:1251-1259.
 26. Montezano AC, Touyz RM. Reactive Oxygen Species, Vascular Nox, and Hypertension: Focus on Translational and Clinical Research. *Antioxid Redox Sign* 2014;20:164-182.
 27. Virdis A, Neves MF, Amiri F, Touyz RM, Schiffrin EL. Role of NAD(P)H oxidase on vascular alterations in angiotensin II-infused mice. *J Hypertens* 2004;22:535-542.
 28. Wagenseil JE, Mecham RP. Vascular extracellular matrix and arterial mechanics. *Physiological Reviews* 2009;89:957-989.
 29. Bateman JF, Boot-Handford RP, Lamande SR. Genetic diseases of connective tissues: cellular and extracellular effects of ECM mutations. *Nature Reviews Genetics* 2009;10:173-183.
 30. Isselbacher EM. Thoracic and abdominal aortic aneurysms. *Circulation* 2005;111:816-828.
 31. Newby AC. Do metalloproteinases destabilize vulnerable atherosclerotic plaques? *Current Opinion in Lipidology* 2006;17:556-561.
 32. Jeremy RW, Huang H, Hwa J, McCarron H, Hughes CF, Richards JG. Relation between age, arterial distensibility, and aortic dilatation in the Marfan syndrome. *Am J Cardiol* 1994;74:369-373.
 33. Hanada K, Vermeij M, Garinis GA, de Waard MC, Kunen MG, Myers L, Maas A, Duncker DJ, Meijers C, Dietz HC, Kanaar R, Essers J. Perturbations of vascular homeostasis and aortic valve abnormalities in fibulin-4 deficient mice. *Circ Res* 2007;100:738-746.
 34. Virmani R, Burke AP, Farb A, Kolodgie FD. Pathology of the unstable plaque. *Progress in Cardiovascular Diseases* 2002;44:349-356.
 35. Libby P, Theroux P. Pathophysiology of coronary artery disease. *Circulation* 2005;111:3481-3488.
 36. Sata M, Fukuda D. Crucial role of renin-angiotensin system in the pathogenesis of atherosclerosis. *J Med Invest* 2010;57:12-25.
 37. Schmidt-Ott KM, Kagiya S, Phillips MI. The multiple actions of angiotensin II in atherosclerosis. *Regul Peptides* 2000;93:65-77.
 38. Fraga-Silva RA, Costa-Fraga FP, Murca TM, Moraes PL, Lima AM, Lautner RQ, Castro CH, Soares CMA, Borges CL, Nadu AP, Oliveira ML, Shenoy V, Katovich MJ, Santos RAS, Raizada MK, Ferreira AJ. Angiotensin-Converting Enzyme 2 Activation Improves Endothelial Function. *Hypertension* 2013;61:1233-+.
 39. Lovren F, Pan Y, Quan A, Teoh H, Wang GL, Shukla PC, Levitt KS, Oudit GY, Al-Omran M, Stewart DJ, Slutsky AS, Peterson MD, Backx PH, Penninger JM, Verma S. Angiotensin converting enzyme-2 confers endothelial protection and attenuates atherosclerosis. *Am J Physiol-Heart C* 2008;295:H1377-H1384.
 40. Aono J. Deletion of the Angiotensin II Type 1a Receptor Prevents Atherosclerotic Plaque Rupture in Apolipoprotein E-/- Mice (vol 32, pg 1453, 2012). *Arterioscl Throm Vas* 2014;34:E18-E18.
 41. Cheng C, Tempel D, van Haperen R, van Damme L, Algur M, Krams R, de Crom R. Activation of MMP8 and MMP13 by angiotensin II correlates to severe intra-plaque hemorrhages and collagen breakdown in atherosclerotic lesions with a vulnerable phenotype. *Atherosclerosis* 2009;204:26-33.
 42. Mazzolai L, Duchosal MA, Korber M, Bouzourene K, Aubert JF, Hao H, Vallet V, Brunner HR, Nussberger J, Gabbiani G, Hayoz D. Endogenous angiotensin II induces atherosclerotic plaque vulnerability and elicits a Th1 response in ApoE(-/-) mice. *Hypertension*



- 2004;44:277-282.
43. da Cunha V, Martin-McNulty B, Vincelette J, Choy DF, Li WW, Schroeder M, Mahmoudi M, Halks-Miller M, Wilson DW, Vergona R, Sullivan ME, Wang YX. Angiotensin II induces histomorphologic features of unstable plaque in a murine model of accelerated atherosclerosis. *J Vasc Surg* 2006;44:364-371.
 44. Charpiot P, Rolland PH, Friggi A, Piquet P, Scalbert E, Bodard H, Barlatier A, Latrille V, Tranier P, Mercier C, Luccioni R, Calaf R, Garcon D. Ace-Inhibition with Perindopril and Atherogenesis-Induced Structural and Functional-Changes in Minipig Arteries. *Arterioscler Thromb* 1993;13:1125-1138.
 45. Hayek T, Attias J, Coleman R, Brodsky S, Smith J, Breslow JL, Keidar S. The angiotensin-converting enzyme inhibitor, fosinopril, and the angiotensin II receptor antagonist, losartan, inhibit LDL oxidation and attenuate atherosclerosis independent of lowering blood pressure in apolipoprotein E deficient mice. *Cardiovasc Res* 1999;44:579-587.
 46. Kowala MC, Grove RL, Aberg G. Inhibitors of Angiotensin-Converting Enzyme Decrease Early Atherosclerosis in Hyperlipidemic Hamsters - Fosinopril Reduces Plasma-Cholesterol and Captopril Inhibits Macrophage Foam Cell Accumulation Independently of Blood-Pressure and Plasma-Lipids. *Atherosclerosis* 1994;108:61-72.
 47. Daugherty A, Rateri DL, Lu H, Inagami T, Cassis LA. Hyperch olesterolemia stimulates angiotensin peptide synthesis and contributes to atherosclerosis through the AT(1A) receptor. *Circulation* 2004;110:3849-3857.
 48. Lu H, Cassis LA, Daugherty A. Atherosclerosis and arterial blood pressure in mice. *Curr Drug Targets* 2007;8:1181-1189.
 49. Lu H, Rateri DL, Feldman DL, Charnigo RJ, Fukamizu A, Ishida JJ, Oesterling EG, Cassis LA, Daugherty A. Renin inhibition reduces hypercholesterolemia-induced atherosclerosis in mice. *J Clin Invest* 2008;118:984-993.
 50. Nussberger J, Aubert JF, Bouzourene K, Pellegrin M, Hayoz D, Mazzolai L. Renin inhibition by aliskiren prevents atherosclerosis progression - Comparison with irbesartan, atenolol, and amlodipine. *Hypertension* 2008;51:1306-1311.
 51. Lu H, Rateri DL, Bruemmer D, Cassis LA, Daugherty A. Involvement of the renin-angiotensin system in abdominal and thoracic aortic aneurysms. *Clin Sci (Lond)* 2012;123:531-543.
 52. Moltzer E, Essers J, van Esch JHM, Roos-Hesselink JW, Danser AHJ. The role of the renin-angiotensin system in thoracic aortic aneurysms: Clinical implications. *Pharmacol Ther* 2011;131:50-60.
 53. Groenink M, den Hartog AW, Franken R, Radonic T, de Waard V, Timmermans J, Scholte AJ, van den Berg MP, Spijkerboer AM, Marquering HA, Zwinderman AH, Mulder BJ. Losartan reduces aortic dilatation rate in adults with Marfan syndrome: a randomized controlled trial. *Eur Heart J* 2013;34:3491-3500.
 54. Habashi JP, Doyle JJ, Holm TM, Aziz H, Schoenhoff F, Bedja D, Chen Y, Modiri AN, Judge DP, Dietz HC. Angiotensin II type 2 receptor signaling attenuates aortic aneurysm in mice through ERK antagonism. *Science* 2011;332:361-365.
 55. Moltzer E, te Riet L, Swagemakers SM, van Heijningen PM, Vermeij M, van Veghel R, Bouhuizen AM, van Esch JH, Lankhorst S, Ramnath NW, de Waard MC, Duncker DJ, van der Spek PJ, Rouwet EV, Danser AHJ, Essers J. Impaired vascular contractility and aortic wall degeneration in fibulin-4 deficient mice: effect of angiotensin II type 1 (AT1) receptor blockade. *PLoS One* 2011;6:e23411.
 56. Habashi JP, Doyle JJ, Holm TM, Aziz H, Schoenhoff F, Bedja D, Chen YC, Modiri AN, Judge DP, Dietz HC. Angiotensin II Type 2 Receptor Signaling Attenuates Aortic Aneurysm in Mice Through ERK Antagonism. *Science* 2011;332:361-365.
 57. Habashi JP, Judge DP, Holm TM, Cohn RD, Loeys BL, Cooper TK, Myers L, Klein EC, Liu GS, Calvi C, Podowski M, Neptune ER, Halushka MK, Bedja D, Gabrielson K, Rifkin DB, Carta L, Ramirez F, Huso DL, Dietz HC. Losartan, an AT1 antagonist, prevents aortic aneurysm in a mouse model of Marfan syndrome. *Science* 2006;312:117-121.
 58. Moltzer E, Riet LT, Swagemakers SMA, van Heijningen PM, Vermeij M, van Veghel R, Bouhuizen AM, van Esch JHM, Lankhorst S, Ramnath NWM, de Waard MC, Duncker DJ, van der Spek PJ, Rouwet EV, Danser AHJ, Essers J. Impaired Vascular Contractility and Aortic Wall Degeneration in Fibulin-4 Deficient Mice: Effect of Angiotensin II Type 1 (AT1) Receptor Blockade. *PLoS One* 2011;6.
 59. Lacro RV, Dietz HC, Sleeper LA, Yetman AT, Bradley TJ, Colan SD, Pearson GD, Selamet Tierney ES, Levine JC, Atz AM, Benson DW, Braverman AC, Chen S, De Backer J, Gelb BD, Grossfeld PD, Klein GL, Lai WW, Liou A, Loeys BL, Markham LW, Olson AK, Paridon SM, Pemberton VL, Pierpont ME, Pyeritz RE, Radojewski E, Roman MJ, Sharkey AM, Stylianou MP, Wechsler SB, Young LT,

- Mahony L, Pediatric Heart Network I. Atenolol versus losartan in children and young adults with Marfan's syndrome. *N Engl J Med* 2014;371:2061-2071.
60. Jansen R, Batista S, Brooks AI, Tischfield JA, Willemsen G, van Grootheest G, Hottenga JJ, Milaneschi Y, Mbarek H, Madar V, Peyrot W, Vink JM, Verweij CL, de Geus EJ, Smit JH, Wright FA, Sullivan PF, Boomsma DI, Penninx BW. Sex differences in the human peripheral blood transcriptome. *BMC Genomics* 2014;15:33.
 61. Orshal JM, Khalil RA. Gender, sex hormones, and vascular tone. *Am J Physiol Regul Integr Comp Physiol* 2004;286:R233-249.
 62. Sampson AK, Jennings GL, Chin-Dusting JP. Y are males so difficult to understand?: a case where "x" does not mark the spot. *Hypertension* 2012;59:525-531.
 63. Schunkert H, Danser AHJ, Hense HW, Derkx FHM, Kürzinger S, Riegger GAJ. Effects of estrogen replacement therapy on the renin-angiotensin system in postmenopausal women. *Circulation* 1997;95:39-45.
 64. Hilliard LM, Sampson AK, Brown RD, Denton KM. The "his and hers" of the renin-angiotensin system. *Curr Hypertens Rep* 2013;15:71-79.
 65. Sampson AK, Moritz KM, Jones ES, Flower RL, Widdop RE, Denton KM. Enhanced angiotensin II type 2 receptor mechanisms mediate decreases in arterial pressure attributable to chronic low-dose angiotensin II in female rats. *Hypertension* 2008;52:666-671.
 66. Xue B, Pamidimukkala J, Hay M. Sex differences in the development of angiotensin II-induced hypertension in conscious mice. *Am J Physiol Heart Circ Physiol* 2005;288:H2177-2184.
 67. Danser AHJ, Derkx FHM, Schalekamp MADH, Hense HW, Riegger GAJ, Schunkert H. Determinants of interindividual variation of renin and prorenin concentrations: evidence for a sexual dimorphism of (pro)renin levels in humans. *J Hypertens* 1998;16:853-862.
 68. Bellott DW, Hughes JF, Skaletsky H, Brown LG, Pyntikova T, Cho TJ, Koutseva N, Zaghul S, Graves T, Rock S, Kremitzki C, Fulton RS, Dugan S, Ding Y, Morton D, Khan Z, Lewis L, Buhay C, Wang Q, Watt J, Holder M, Lee S, Nazareth L, Rozen S, Muzny DM, Warren WC, Gibbs RA, Wilson RK, Page DC. Mammalian Y chromosomes retain widely expressed dosage-sensitive regulators. *Nature* 2014;508:494-499.
 69. Ely DL, Turner ME. Hypertension in the spontaneously hypertensive rat is linked to the Y chromosome. *Hypertension* 1990;16:277-281.
 70. Arnold AP, Chen X. What does the "four core genotypes" mouse model tell us about sex differences in the brain and other tissues? *Front Neuroendocrinol* 2009;30:1-9.
 71. Ji H, Zheng W, Wu X, Liu J, Ecelbarger CM, Watkins R, Arnold AP, Sandberg K. Sex chromosome effects unmasked in angiotensin II-induced hypertension. *Hypertension* 2010;55:1275-1282.
 72. Staessen JA, Ginocchio G, Thijs L, Fagard R. Conventional and ambulatory blood pressure and menopause in a prospective population study. *J Hum Hypertens* 1997;11:507-514.
 73. Carrel L, Willard HF. X-inactivation profile reveals extensive variability in X-linked gene expression in females. *Nature* 2005;434:400-404.
 74. Xu J, Taya S, Kaibuchi K, Arnold AP. Sexually dimorphic expression of Usp9x is related to sex chromosome complement in adult mouse brain. *Eur J Neurosci* 2005;21:3017-3022.
 75. Zhang Y, Castillo-Morales A, Jiang M, Zhu Y, Hu L, Urrutia AO, Kong X, Hurst LD. Genes that escape X-inactivation in humans have high intraspecific variability in expression, are associated with mental impairment but are not slow evolving. *Mol Biol Evol* 2013;30:2588-2601.
 76. Patrat C, Okamoto I, Diabangouaya P, Vialon V, Le Baccon P, Chow J, Heard E. Dynamic changes in paternal X-chromosome activity during imprinted X-chromosome inactivation in mice. *Proc Natl Acad Sci USA* 2009;106:5198-5203.
 77. van der Schouw YT, van der Graaf Y, Steyerberg EW, Eijkemans JC, Banga JD. Age at menopause as a risk factor for cardiovascular mortality. *Lancet* 1996;347:714-718.
 78. Hudson M, Rahme E, Behloul H, Sheppard R, Pilote L. Sex differences in the effectiveness of angiotensin receptor blockers and angiotensin converting enzyme inhibitors in patients with congestive heart failure--a population study. *Eur J Heart Fail* 2007;9:602-609.
 79. Brugts JJ, Isaacs A, Boersma E, van Duijn CM, Uitterlinden AG, Remme W, Bertrand M, Ninomiya T, Ceconi C, Chalmers J, MacMahon S, Fox K, Ferrari R, Witteman JC, Danser AHJ, Simoons ML, de Maat MP. Genetic determinants of treatment benefit of the angiotensin-converting enzyme-inhibitor perindopril in patients with stable coronary artery disease. *Eur Heart J* 2010;31:1854-1864.
 80. Brugts JJ, Isaacs A, de Maat MP, Boersma E, van Duijn CM, Akkerhuis KM, Uitterlinden AG, Witteman JC, Cambien F, Ceconi C, Remme W, Bertrand M, Ninomiya



- T, Harrap S, Chalmers J, Macmahon S, Fox K, Ferrari R, Simoons ML, Danser AHJ. A pharmacogenetic analysis of determinants of hypertension and blood pressure response to angiotensin-converting enzyme inhibitor therapy in patients with vascular disease and healthy individuals. *J Hypertens* 2011;29:509-519.
81. Harrap SB, Tzourio C, Cambien F, Poirier O, Raoux S, Chalmers J, Chapman N, Colman S, Leguennec S, MacMahon S, Neal B, Ohkubo T, Woodward M. The ACE gene I/D polymorphism is not associated with the blood pressure and cardiovascular benefits of ACE inhibition. *Hypertension* 2003;42:297-303.
 82. Parikh NI, Gona P, Larson MG, Wang TJ, Newton-Cheh C, Levy D, Benjamin EJ, Kannel WB, Vasan RS. Plasma renin and risk of cardiovascular disease and mortality: the Framingham Heart Study. *Eur Heart J* 2007;28:2644-2652.
 83. Alderman MH, Ooi WL, Cohen H, Madhavan S, Sealey JE, Laragh JH. Plasma renin activity: a risk factor for myocardial infarction in hypertensive patients. *Am J Hypertens* 1997;10:1-8.
 84. Szymanski MK, Damman K, van Veldhuisen DJ, van Gilst WH, Hillege HL, de Boer RA. Prognostic value of renin and prorenin in heart failure patients with decreased kidney function. *Am Heart J* 2011;162:487-493.
 85. Danser AHJ. Renin and prorenin as biomarkers in hypertension. *Curr Opin Nephrol Hypertens* 2012;21:508-514.
 86. Laragh JH, Sealey JE. The plasma renin test reveals the contribution of body sodium-volume content (V) and renin-angiotensin (R) vasoconstriction to long-term blood pressure. *Am J Hypertens* 2011;24:1164-1180.
 87. Alderman MH, Cohen HW, Sealey JE, Laragh JH. Pressor responses to antihypertensive drug types. *Am J Hypertens* 2010;23:1031-1037.
 88. Turner ST, Schwartz GL, Chapman AB, Beitelshes AL, Gums JG, Cooper-DeHoff RM, Boerwinkle E, Johnson JA, Bailey KR. Plasma renin activity predicts blood pressure responses to beta-blocker and thiazide diuretic as monotherapy and add-on therapy for hypertension. *Am J Hypertens* 2010;23:1014-1022.
 89. Tu W, Eckert GJ, Pratt JH, Danser AHJ. Plasma levels of prorenin and renin in Blacks and Whites; their relative abundance and associations with plasma aldosterone concentration. *Am J Hypertens* 2012;in press.
 90. Gupta AK, Poulter NR, Dobson J, Eldridge S, Cappuccio FP, Caulfield M, Collier D, Cruickshank JK, Sever PS, Feder G, Ascot. Ethnic differences in blood pressure response to first and second-line antihypertensive therapies in patients randomized in the ASCOT Trial. *Am J Hypertens* 2010;23:1023-1030.
 91. Weintraub HS, Duprez DA, Cushman WC, Zappe DH, Purkayastha D, Samuel R, Izzo JL, Jr. Antihypertensive response to thiazide diuretic or angiotensin receptor blocker in elderly hypertensives is not influenced by pretreatment plasma renin activity. *Cardiovasc Drugs Ther* 2012;26:145-155.
 92. Nussberger J, Gradman AH, Schmieder RE, Lins RL, Chiang Y, Prescott MF. Plasma renin and the antihypertensive effect of the orally active renin inhibitor aliskiren in clinical hypertension. *Int J Clin Pract* 2007;61:1461-1468.
 93. Stanton AV, Dicker P, O'Brien ET. Aliskiren monotherapy results in the greatest and the least blood pressure lowering in patients with high- and low-baseline PRA levels, respectively. *Am J Hypertens* 2009;22:954-957.
 94. Schilders JE, Wu H, Boomsma F, van den Meiracker AH, Danser AHJ. Renin-angiotensin system phenotyping as a guidance toward personalized medicine for ACE inhibitors: can the response to ACE inhibition be predicted on the basis of plasma renin or ACE? *Cardiovasc Drugs Ther* 2014;28:335-345.
 95. Danser AHJ, Batenburg WW, van den Meiracker AH, Danilov SM. ACE phenotyping as a first step toward personalized medicine for ACE inhibitors. Why does ACE genotyping not predict the therapeutic efficacy of ACE inhibition? *Pharmacol Ther* 2007;113:607-618.
 96. van Kats JP, Duncker DJ, Haitsma DB, Schuijt MP, Niebuur R, Stubenitsky R, Boomsma F, Schalekamp MADH, Verdouw PD, Danser AHJ. Angiotensin-converting enzyme inhibition and angiotensin II type 1 receptor blockade prevent cardiac remodeling in pigs after myocardial infarction: role of tissue angiotensin II. *Circulation* 2000;102:1556-1563.
 97. Richer-Giudicelli C, Domergue V, Gonzalez MF, Messadi E, Azizi M, Giudicelli JF, Ménard J. Haemodynamic effects of dual blockade of the renin-angiotensin system in spontaneously hypertensive rats: influence of salt. *J Hypertens* 2004;22:619-627.
 98. Danser AHJ, van Kesteren CAM, Bax WA, Tavenier M, Derckx FHM, Saxena PR, Schalekamp MADH. Prorenin, renin, angiotensinogen, and angiotensin-converting enzyme in normal and failing human hearts. Evidence for renin binding. *Circulation* 1997;96:220-226.
 99. Klotz S, Burkhoff D, Garrelts IM, Boomsma F, Danser AHJ. The impact of left ventricular assist device-

- induced left ventricular unloading on the myocardial renin-angiotensin-aldosterone system: therapeutic consequences? *Eur Heart J* 2009;30:805-812.
100. Balcarek J, Sevã Pessõa B, Bryson C, Azizi M, Ménard J, Garrelts IM, McGeehan G, Reeves RA, Griffith SG, Danser AHJ, Gregg R. Multiple ascending dose study with the new renin inhibitor VTP-27999: nephrocentric consequences of too much renin inhibition. *Hypertension* 2014;63:942-950.
 101. Feldman DL, Jin L, Xuan H, Contrepas A, Zhou Y, Webb RL, Müller DN, Feldt S, Cumin F, Maniara W, Persohn E, Schuetz H, Danser AHJ, Nguyen G. Effects of aliskiren on blood pressure, albuminuria, and (pro)renin receptor expression in diabetic TG(mREN-2)-27 rats. *Hypertension* 2008;52:130-136.
 102. Lange S, Fraune C, Alenina N, Bader M, Danser AHJ, Frenay AR, van Goor H, Stahl R, Nguyen G, Schwedhelm E, Wenzel UO. Aliskiren accumulation in the kidney: no major role for binding to renin or prorenin. *J Hypertens* 2013;31:713-719.
 103. Packer M. Why do the kidneys release renin in patients with congestive heart failure? A nephrocentric view of converting-enzyme inhibition. *Am J Cardiol* 1987;60:179-184.
 104. Parving HH, Brenner BM, McMurray JJ, de Zeeuw D, Haffner SM, Solomon SD, Chaturvedi N, Persson F, Desai AS, Nicolaides M, Richard A, Xiang Z, Brunel P, Pfeffer MA, Investigators A. Cardiorenal end points in a trial of aliskiren for type 2 diabetes. *N Engl J Med* 2012;367:2204-2213.
 105. Fried LF, Emanuele N, Zhang JH, Brophy M, Conner TA, Duckworth W, Leehey DJ, McCullough PA, O'Connor T, Palevsky PM, Reilly RF, Seliger SL, Warren SR, Watnick S, Peduzzi P, Guarino P, Investigators VN-D. Combined angiotensin inhibition for the treatment of diabetic nephropathy. *N Engl J Med* 2013;369:1892-1903.
 106. Yusuf S, Diener HC, Sacco RL, Cotton D, Ounpuu S, Lawton WA, Palesch Y, Martin RH, Albers GW, Bath P, Bornstein N, Chan BP, Chen ST, Cunha L, Dahlof B, De Keyser J, Donnan GA, Estol C, Gorelick P, Gu V, Hermansson K, Hilbrich L, Kaste M, Lu C, Machnig T, Pais P, Roberts R, Skvortsova V, Teal P, Toni D, VanderMaelen C, Voigt T, Weber M, Yoon BW, Group PRS. Telmisartan to prevent recurrent stroke and cardiovascular events. *N Engl J Med* 2008;359:1225-1237.
 107. Nussberger J, Bohlender J. Pharmacotherapy: Optimal blockade of the renin-angiotensin-aldosterone system. *Nat Rev Cardiol* 2013;10:183-184.
 108. James PA, Oparil S, Carter BL, Cushman WC, Dennison-Himmelfarb C, Handler J, Lackland DT, LeFevre ML, MacKenzie TD, Ogedegbe O, Smith SC, Jr., Svetkey LP, Taler SJ, Townsend RR, Wright JT, Jr., Narva AS, Ortiz E. 2014 evidence-based guideline for the management of high blood pressure in adults: report from the panel members appointed to the Eighth Joint National Committee (JNC 8). *JAMA* 2014;311:507-520.
 109. van Vark LC, Bertrand M, Akkerhuis KM, Brugts JJ, Fox K, Mourad JJ, Boersma E. Angiotensin-converting enzyme inhibitors reduce mortality in hypertension: a meta-analysis of randomized clinical trials of renin-angiotensin-aldosterone system inhibitors involving 158,998 patients. *Eur Heart J* 2012;33:2088-2097.
 110. Cheng J, Zhang W, Zhang X, Han F, Li X, He X, Li Q, Chen J. Effect of angiotensin-converting enzyme inhibitors and angiotensin II receptor blockers on all-cause mortality, cardiovascular deaths, and cardiovascular events in patients with diabetes mellitus: a meta-analysis. *JAMA Intern Med* 2014;174:773-785.
 111. Strauss MH, Hall AS. Angiotensin receptor blockers may increase risk of myocardial infarction: unraveling the ARB-MI paradox. *Circulation* 2006;114:838-854.
 112. Bangalore S, Kumar S, Wetterslev J, Messerli FH. Angiotensin receptor blockers and risk of myocardial infarction: meta-analyses and trial sequential analyses of 147 020 patients from randomised trials. *BMJ* 2011;342:d2234.
 113. Sun L, Wang W, Xiao W, Liang H, Yang Y, Yang H. Angiotensin II induces apoptosis in intestinal epithelial cells through the AT2 receptor, GATA-6 and the Bax pathway. *Biochem Biophys Res Commun* 2012;424:663-668.
 114. Koyama N, Nishida Y, Ishii T, Yoshida T, Furukawa Y, Narahara H. Telmisartan induces growth inhibition, DNA double-strand breaks and apoptosis in human endometrial cancer cells. *PLoS One* 2014;9:e93050.
 115. Verdonk K, Danser AHJ, van Esch JHM. Angiotensin II type 2 receptor agonists: where should they be applied? *Expert Opin Investig Drugs* 2012;21:501-513.
 116. Vasan RS, Evans JC, Larson MG, Wilson PW, Meigs JB, Rifai N, Benjamin EJ, Levy D. Serum aldosterone and the incidence of hypertension in nonhypertensive persons. *N Engl J Med* 2004;351:33-41.
 117. Gros R, Ding Q, Sklar LA, Prossnitz EE, Arterburn JB, Chorazyczewski J, Feldman RD. GPR30 expression is required for the mineralocorticoid receptor-independent rapid vascular effects of aldosterone.



- Hypertension* 2011;57:442-451.
118. Koenig JB, Jaffe IZ. Direct role for smooth muscle cell mineralocorticoid receptors in vascular remodeling: novel mechanisms and clinical implications. *Curr Hypertens Rep* 2014;16:427.
 119. Kusche-Vihrog K, Jeggle P, Oberleithner H. The role of ENaC in vascular endothelium. *Pflugers Arch* 2014;466:851-859.
 120. Gennari-Moser C, Khankin EV, Escher G, Burkhard F, Frey BM, Karumanchi SA, Frey FJ, Mohaupt MG. Vascular endothelial growth factor-A and aldosterone: relevance to normal pregnancy and preeclampsia. *Hypertension* 2013;61:1111-1117.
 121. Zennaro MC, Rickard AJ, Boulkroun S. Genetics of mineralocorticoid excess: an update for clinicians. *Eur J Endocrinol* 2013;169:R15-25.
 122. Zhang W, Xia X, Reisenauer MR, Rieg T, Lang F, Kuhl D, Vallon V, Kone BC. Aldosterone-induced Sgk1 relieves Dot1a-Af9-mediated transcriptional repression of epithelial Na⁺ channel alpha. *J Clin Invest* 2007;117:773-783.
 123. McCurley A, Pires PW, Bender SB, Aronovitz M, Zhao MJ, Metzger D, Chambon P, Hill MA, Dorrance AM, Mendelsohn ME, Jaffe IZ. Direct regulation of blood pressure by smooth muscle cell mineralocorticoid receptors. *Nat Med* 2012;18:1429-1433.
 124. Galmiche G, Pizard A, Gueret A, El Moghrabi S, Ouvrard-Pascaud A, Berger S, Challande P, Jaffe IZ, Labat C, Lacolley P, Jaissier F. Smooth muscle cell mineralocorticoid receptors are mandatory for aldosterone-salt to induce vascular stiffness. *Hypertension* 2014;63:520-526.
 125. Montezano AC, Callera GE, Yogi A, He Y, Tostes RC, He G, Schiffrin EL, Touyz RM. Aldosterone and angiotensin II synergistically stimulate migration in vascular smooth muscle cells through c-Src-regulated redox-sensitive RhoA pathways. *Arterioscler Thromb Vasc Biol* 2008;28:1511-1518.
 126. Pruthi D, McCurley A, Aronovitz M, Galayda C, Karumanchi SA, Jaffe IZ. Aldosterone promotes vascular remodeling by direct effects on smooth muscle cell mineralocorticoid receptors. *Arterioscler Thromb Vasc Biol* 2014;34:355-364.
 127. Stowasser M, Sharman J, Leano R, Gordon RD, Ward G, Cowley D, Marwick TH. Evidence for abnormal left ventricular structure and function in normotensive individuals with familial hyperaldosteronism type I. *J Clin Endocrinol Metab* 2005;90:5070-5076.
 128. Kusche-Vihrog K, Sobczak K, Bangel N, Wilhelmi M, Nechyporuk-Zloy V, Schwab A, Schillers H, Oberleithner H. Aldosterone and amiloride alter ENaC abundance in vascular endothelium. *Pflugers Arch* 2008;455:849-857.
 129. Oberleithner H, Riethmuller C, Schillers H, MacGregor GA, de Wardener HE, Hausberg M. Plasma sodium stiffens vascular endothelium and reduces nitric oxide release. *Proc Natl Acad Sci U S A* 2007;104:16281-16286.
 130. Gros R, Ding Q, Liu B, Chorazyczewski J, Feldman RD. Aldosterone mediates its rapid effects in vascular endothelial cells through GPER activation. *Am J Physiol Cell Physiol* 2013;304:C532-540.
 131. Prossnitz ER, Arterburn JB, Smith HO, Oprea TI, Sklar LA, Hathaway HJ. Estrogen signaling through the transmembrane G protein-coupled receptor GPR30. *Annu Rev Physiol* 2008;70:165-190.
 132. Batenburg WW, Jansen PM, van den Bogaerd AJ, Danser AHJ. Angiotensin II-aldosterone interaction in human coronary microarteries involves GPR30, EGFR, and endothelial NO synthase. *Cardiovasc Res* 2012;94:136-143.
 133. Funder JW, Carey RM, Fardella C, Gomez-Sanchez CE, Mantero F, Stowasser M, Young WF, Jr., Montori VM, Endocrine S. Case detection, diagnosis, and treatment of patients with primary aldosteronism: an endocrine society clinical practice guideline. *J Clin Endocrinol Metab* 2008;93:3266-3281.
 134. Jansen PM, Boomsma F, van den Meiracker AH. Aldosterone-to-renin ratio as a screening test for primary aldosteronism—the Dutch ARRAT Study. *Neth J Med* 2008;66:220-228.
 135. Campbell DJ, Nussberger J, Stowasser M, Danser AHJ, Morganti A, Frandsen E, Ménard J. Activity assays and immunoassays for plasma renin and prorenin: information provided and precautions necessary for accurate measurement. *Clin Chem* 2009;55:867-877.
 136. Jansen PM, van den Born BJ, Frenkel WJ, de Bruijne EL, Deinum J, Kerstens MN, Smulders YM, Woittiez AJ, Wijbenga JA, Zietse R, Danser AHJ, van den Meiracker AH. Test characteristics of the aldosterone-to-renin ratio as a screening test for primary aldosteronism. *J Hypertens* 2014;32:115-126.
 137. Geller DS, Zhang J, Wisgerhof MV, Shackleton C, Kashgarian M, Lifton RP. A novel form of human mendelian hypertension featuring nongluocorticoid-remediable aldosteronism. *J Clin Endocrinol Metab* 2008;93:3117-3123.
 138. Choi M, Scholl UI, Yue P, Bjorklund P, Zhao B, Nelson-

- Williams C, Ji W, Cho Y, Patel A, Men CJ, Lolis E, Wisgerhof MV, Geller DS, Mane S, Hellman P, Westin G, Akerstrom G, Wang W, Carling T, Lifton RP. K+ channel mutations in adrenal aldosterone-producing adenomas and hereditary hypertension. *Science* 2011;331:768-772.
139. Scholl UI, Nelson-Williams C, Yue P, Grekin R, Wyatt RJ, Dillon MJ, Couch R, Hammer LK, Harley FL, Farhi A, Wang WH, Lifton RP. Hypertension with or without adrenal hyperplasia due to different inherited mutations in the potassium channel KCNJ5. *Proc Natl Acad Sci U S A* 2012;109:2533-2538.
140. Beuschlein F, Boukroun S, Osswald A, Wieland T, Nielsen HN, Lichtenauer UD, Penton D, Schack VR, Amar L, Fischer E, Walther A, Tauber P, Schwarzmayr T, Diener S, Graf E, Allolio B, Samson-Couterie B, Benecke A, Quinkler M, Fallo F, Plouin PF, Mantero F, Meitinger T, Mulatero P, Jeunemaitre X, Warth R, Vilsen B, Zennaro MC, Strom TM, Reincke M. Somatic mutations in ATP1A1 and ATP2B3 lead to aldosterone-producing adenomas and secondary hypertension. *Nat Genet* 2013;45:440-444.
141. Azizan EA, Poulsen H, Tuluc P, Zhou J, Clausen MV, Lieb A, Maniero C, Garg S, Bochukova EG, Zhao W, Shaikh LH, Brighton CA, Teo AE, Davenport AP, Dekkers T, Tops B, Kusters B, Ceral J, Yeo GS, Neogi SG, McFarlane I, Rosenfeld N, Marass F, Hadfield J, Margas W, Chaggar K, Solar M, Deinum J, Dolphin AC, Farooqi IS, Striessnig J, Nissen P, Brown MJ. Somatic mutations in ATP1A1 and CACNA1D underlie a common subtype of adrenal hypertension. *Nat Genet* 2013;45:1055-1060.
142. Scholl UI, Goh G, Stoltzing G, de Oliveira RC, Choi M, Overton JD, Fonseca AL, Korah R, Starker LF, Kunstman JW, Prasad ML, Hartung EA, Mauras N, Benson MR, Brady T, Shapiro JR, Loring E, Nelson-Williams C, Libutti SK, Mane S, Hellman P, Westin G, Akerstrom G, Bjorklund P, Carling T, Fahlke C, Hidalgo P, Lifton RP. Somatic and germline CACNA1D calcium channel mutations in aldosterone-producing adenomas and primary aldosteronism. *Nat Genet* 2013;45:1050-1054.
143. Calhoun DA. Hyperaldosteronism as a common cause of resistant hypertension. *Annu Rev Med* 2013;64:233-247.
144. Sartori M, Calo LA, Mascagna V, Realdi A, Macchini L, Ciccariello L, De Toni R, Cattelan F, Pessina AC, Semplicini A. Aldosterone and refractory hypertension: a prospective cohort study. *Am J Hypertens* 2006;19:373-379; discussion 380.
145. Jansen PM, Danser AHJ, Imholz BP, van den Meiracker AH. Aldosterone-receptor antagonism in hypertension. *J Hypertens* 2009;27:680-691.
146. de Souza F, Muxfeldt E, Fiszman R, Salles G. Efficacy of spironolactone therapy in patients with true resistant hypertension. *Hypertension* 2010;55:147-152.
147. Jansen PM, Frenkel WJ, van den Born BJ, de Bruijne EL, Deinum J, Kerstens MN, Arnoldus JH, Woittiez AJ, Wijbenga JA, Zietse R, Danser AHJ, van den Meiracker AH. Determinants of blood pressure reduction by eplerenone in uncontrolled hypertension. *J Hypertens* 2013;31:404-413.
148. Raheja P, Price A, Wang Z, Arbiq D, Adams-Huet B, Auchus RJ, Vongpatanasin W. Spironolactone prevents chlorthalidone-induced sympathetic activation and insulin resistance in hypertensive patients. *Hypertension* 2012;60:319-325.
149. Jansen PM, van den Meiracker AH, Danser AHJ. Aldosterone synthase inhibitors: pharmacological and clinical aspects. *Curr Opin Investig Drugs* 2009;10:319-326.
150. Bosnyak S, Jones ES, Christopoulos A, Aguilar MI, Thomas WG, Widdop RE. Relative affinity of angiotensin peptides and novel ligands at AT1 and AT2 receptors. *Clin Sci* 2011;121:297-303.
151. van Esch JHM, Oosterveer CR, Batenburg WW, van Veghel R, Danser AHJ. Effects of angiotensin II and its metabolites in the rat coronary vascular bed: is angiotensin III the preferred ligand of the angiotensin AT2 receptor? *Eur J Pharmacol* 2008;588:286-293.
152. Kemp BA, Bell JF, Rottkamp DM, Howell NL, Shao W, Navar LG, Padia SH, Carey RM. Intrarenal angiotensin III is the predominant agonist for proximal tubule angiotensin type 2 receptors. *Hypertension* 2012.
153. Padia SH, Kemp BA, Howell NL, Siragy HM, Fournie-Zaluski MC, Roques BP, Carey RM. Intrarenal aminopeptidase N inhibition augments natriuretic responses to angiotensin III in angiotensin type 1 receptor-blocked rats. *Hypertension* 2007;49:625-630.
154. van Esch JHM, Schuijt MP, Sayed J, Choudry Y, Walther T, Danser AHJ. AT2 receptor-mediated vasodilation in the mouse heart depends on AT1A receptor activation. *Br J Pharmacol* 2006;148:452-458.
155. Sevá Pessôa B, van der Lubbe N, Verdonk K, Roks AJM, Hoorn EJ, Danser AHJ. Key developments in renin-angiotensin-aldosterone system inhibition. *Nat Rev Nephrol* 2013;9:26-36.
156. Jones ES, Del Borgo MP, Kirsch JF, Clayton D, Bosnyak S, Welungoda I, Hausler N, Unabia S, Perlmutter P,



- Thomas WG, Aguilar MI, Widdop RE. A single beta-amino acid substitution to angiotensin II confers AT2 receptor selectivity and vascular function. *Hypertension* 2011;57:570-576.
157. Gross V, Obst M, Luft FC. Insights into angiotensin II receptor function through AT2 receptor knockout mice. *Acta Physiol Scand* 2004;181:487-494.
 158. Tanaka M, Tsuchida S, Imai T, Fujii N, Miyazaki H, Ichiki T, Naruse M, Inagami T. Vascular response to angiotensin II is exaggerated through an upregulation of AT1 receptor in AT2 knockout mice. *Biochem Biophys Res Commun* 1999;258:194-198.
 159. Gembardt F, Heringer-Walther S, van Esch JHM, Sterner-Kock A, van Veghel R, Le TH, Garrelts IM, Coffman TM, Danser AHJ, Schultheiss HP, Walther T. Cardiovascular phenotype of mice lacking all three subtypes of angiotensin II receptors. *FASEB J* 2008;22:3068-3077.
 160. Tsutsumi Y, Matsubara H, Masaki H, Kurihara H, Murasawa S, Takai S, Miyazaki M, Nozawa Y, Ozono R, Nakagawa K, Miwa T, Kawada N, Mori Y, Shibasaki Y, Tanaka Y, Fujiyama S, Koyama Y, Fujiyama A, Takahashi H, Iwasaka T. Angiotensin II type 2 receptor overexpression activates the vascular kinin system and causes vasodilation. *J Clin Invest* 1999;104:925-935.
 161. Wagenaar GT, Laghmani el H, Fidler M, Sengers RM, de Visser YP, de Vries L, Rink R, Roks AJ, Folkerts G, Walther FJ. Agonists of MAS oncogene and angiotensin II type 2 receptors attenuate cardiopulmonary disease in rats with neonatal hyperoxia-induced lung injury. *Am J Physiol Lung Cell Mol Physiol* 2013;305:L341-351.
 162. Danyel LA, Schmerler P, Paulis L, Unger T, Steckelings UM. Impact of AT2-receptor stimulation on vascular biology, kidney function, and blood pressure. *Integr Blood Press Control* 2013;6:153-161.
 163. Verdonk K, Durik M, Abd-Alla N, Batenburg WW, van den Bogaardt AJ, van Veghel R, Roks AJ, Danser AHJ, van Esch JHM. Compound 21 induces vasorelaxation via an endothelium- and angiotensin II type 2 receptor-independent mechanism. *Hypertension* 2012;60:722-729.
 164. Bosnyak S, Welungoda IK, Hallberg A, Alterman M, Widdop RE, Jones ES. Stimulation of angiotensin AT2 receptors by the non-peptide agonist, Compound 21, evokes vasodepressor effects in conscious spontaneously hypertensive rats. *Br J Pharmacol* 2010;159:709-716.
 165. Anand U, Facer P, Yiangou Y, Sinisi M, Fox M, McCarthy T, Bountra C, Korchev YE, Anand P. Angiotensin II type 2 receptor (AT2 R) localization and antagonist-mediated inhibition of capsaicin responses and neurite outgrowth in human and rat sensory neurons. *Eur J Pain* 2013;17:1012-1026.
 166. Rice AS, Dworkin RH, McCarthy TD, Anand P, Bountra C, McCloud PI, Hill J, Cutter G, Kitson G, Desem N, Raff M, for the EMAsg. EMA401, an orally administered highly selective angiotensin II type 2 receptor antagonist, as a novel treatment for postherpetic neuralgia: a randomised, double-blind, placebo-controlled phase 2 clinical trial. *Lancet* 2014;383:1637-1647.
 167. Santos RAS, Simoes e Silva AC, Maric C, Silva DM, Machado RP, de Buhr I, Heringer-Walther S, Pinheiro SV, Lopes MT, Bader M, Mendes EP, Lemos VS, Campagnole-Santos MJ, Schultheiss HP, Speth R, Walther T. Angiotensin-(1-7) is an endogenous ligand for the G protein-coupled receptor Mas. *Proc Natl Acad Sci U S A* 2003;100:8258-8263.
 168. Iusuf D, Henning RH, van Gilst WH, Roks AJ. Angiotensin-(1-7): pharmacological properties and pharmacotherapeutic perspectives. *Eur J Pharmacol* 2008;585:303-312.
 169. Durik M, Sevã Pessõa B, Roks AJ. The renin-angiotensin system, bone marrow and progenitor cells. *Clin Sci (Lond)* 2012;123:205-223.
 170. Gurley SB, Allred A, Le TH, Griffiths R, Mao L, Philip N, Haystead TA, Donoghue M, Breitbart RE, Acton SL, Rockman HA, Coffman TM. Altered blood pressure responses and normal cardiac phenotype in ACE2-null mice. *J Clin Invest* 2006;116:2218-2225.
 171. Haber PK, Ye M, Wysocki J, Maier C, Haque SK, Battle D. Angiotensin-converting enzyme 2-independent action of presumed angiotensin-converting enzyme 2 activators: studies in vivo, ex vivo, and in vitro. *Hypertension* 2014;63:774-782.
 172. Ferreira AJ, Santos RA, Bradford CN, Mecca AP, Sumners C, Katovich MJ, Raizada MK. Therapeutic implications of the vasoprotective axis of the renin-angiotensin system in cardiovascular diseases. *Hypertension* 2010;55:207-213.
 173. Rodgers K, Verco S, Bolton L, Dizerega G. Accelerated healing of diabetic wounds by NorLeu(3)-angiotensin (1-7). *Expert Opin Investig Drugs* 2011;20:1575-1581.
 174. Wright JW, Tamura-Myers E, Wilson WL, Roques BP, Llorens-Cortes C, Speth RC, Harding JW. Conversion of brain angiotensin II to angiotensin III is critical for pressor response in rats. *Am J Physiol Regul Integr Comp Physiol* 2003;284:R725-R733.

175. Fournie-Zaluski MC, Fassot C, Valentin B, Djordjijevic D, Reaux-Le Goazigo A, Corvol P, Roques BP, Llorens-Cortes C. Brain renin-angiotensin system blockade by systemically active aminopeptidase A inhibitors: a potential treatment of salt-dependent hypertension. *Proc Natl Acad Sci U S A* 2004;101:7775-7780.
176. Gao J, Marc Y, Iturrioz X, Leroux V, Balavoine F, Llorens-Cortes C. A new strategy for treating hypertension by blocking the activity of the brain renin-angiotensin system with aminopeptidase A inhibitors. *Clin Sci* 2014;127:135-148.
177. Faure S, Javellaud J, Achard JM, Oudart N. Vasoconstrictive effect of angiotensin IV in isolated rat basilar artery independent of AT1 and AT2 receptors. *J Vasc Res* 2006;43:19-26.
178. Rowe BP, Dixon B. Angiotensin III depressor action in the conscious rabbit is blocked by losartan but not PD 123319. *Hypertension* 2000;35:130-134.
179. Vanderheyden PM. From angiotensin IV binding site to AT4 receptor. *Mol Cell Endocrinol* 2009;302:159-166.
180. Demaegdt H, De Backer JP, Lukaszuk A, Toth G, Szemenyei E, Tourwe D, Vauquelin G. Angiotensin IV displays only low affinity for native insulin-regulated aminopeptidase (IRAP). *Fundam Clin Pharmacol* 2012;26:194-197.
181. Le MT, Vanderheyden PM, Szaszak M, Hunyady L, Vauquelin G. Angiotensin IV is a potent agonist for constitutive active human AT1 receptors. Distinct roles of the N- and C-terminal residues of angiotensin II during AT1 receptor activation. *J Biol Chem* 2002;277:23107-23110.

CHAPTER 2

Scope of this Thesis



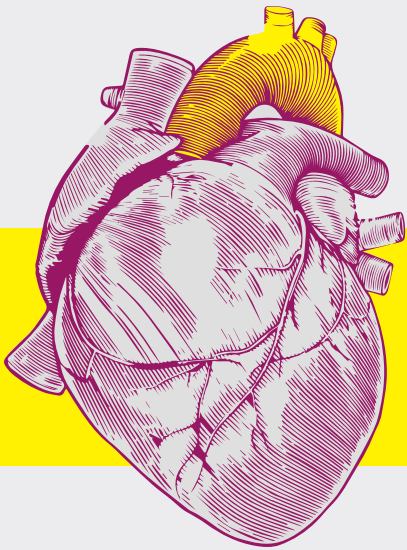
SCOPE OF THIS THESIS

Aortic diseases such as aneurysmal disease and atherosclerosis can be life-threatening conditions and the occurrence of these diseases increase in the elderly as the average age of population rises. Aortic aneurysm disease involves widening of the aorta, and is associated with atherosclerosis. On the other hand atherosclerosis can lead to occlusive arterial disease due to aortic medial wall growth and atherosclerotic plaque formation. These diseases have common risk factors and similarities in the underlying biological processes. In aortic disease, the process of extracellular matrix remodeling is a key component, as deduced from genetic familial aneurysmal disease studies. Additionally, (elevated) blood pressure may affect the aorta. The renin-angiotensin system (RAS) affects aortic pathology locally, as well as via its effect on blood pressure.

In **part II** we investigate the role of the RAS in aneurysmatic Fibulin-4 mice. Aortic aneurysm disease is a degenerative disease of the aortic media, and these mice that express reduced levels of the extracellular matrix protein Fibulin-4 serve as a model organism that can be used to study thoracic aortic aneurysm (TAA) development. In **Chapter 2** we characterize the Fibulin-4 model histologically and functionally through a detailed analysis of the composition of the aortic wall and its contractility. In **Chapter 3** we study the effects of reduced expression of Fibulin-4 on heart function. In **Chapter 2** and **Chapter 4** we investigate the therapeutic potential of RAS blockers, in particular angiotensin II type 1 receptor (AT₁) blockade, on aneurysm progression. In **Chapter 4** the treatment effect on both the aneurysm and the heart failure is described. In **Chapter 5** we analyze the aberrations in TGF β signaling due to Fibulin-4 deficiency in molecular detail in aortic smooth muscle cells.

In **part III**, genetic factors involved in aneurysms are investigated. Aneurysmatic and atherosclerotic arterial diseases have common risk factors and similarities in biological processes, despite the fact that the two diseases have opposite outcomes. In **Chapter 6** we evaluate the genetic factors and molecular pathways that differentiate aneurysmatic from atherosclerotic aortic disease, with the intention to identify new biomarkers. Additionally, since TAA diseases are partly inherited, in **Chapter 7** we have set up a massive parallel sequencing technique to identify pathogenic mutations in the genome of TAA-linked genes.

Finally, in **part IV** we investigate the role of the RAS in rats with hypertension and diabetes, a combination that is well-known to result in (cardio)vascular pathology. Indeed, hypertensive patients with diabetes exhibit an increased risk for cardiovascular complications, like nephropathy, stroke and heart failure. The studies described in **Chapter 8** were aimed to evaluate the therapeutic effect of Handle Region Peptide (HRP), a (pro)renin receptor blocker, on top of renin inhibition in diabetic rats with hypertension.



Part II

The Role of the Renin-Angiotensin System on Aortic and Cardiac Pathology in Aneurysmatic Fibulin-4 Mice

CHAPTER 3

Impaired vascular contractility and aortic wall degeneration in fibulin-4 deficient mice: effect of angiotensin II type 1 (AT₁) receptor blockade

E. Moltzer, L. te Riet, S.M.A. Swagemakers, P.M. van Heijningen, M. Vermeij, R. van Veghel, A. M. Bouhuizen, J. H. M. van Esch, S. Lankhorst, N. W. M. Ramnath, M. C. de Waard, D. J. Duncker, P. J. van der Spek, E. V. Rouwet, A. H. J. Danser, J. Essers

[PloS One 2011;6:e23411](https://doi.org/10.1371/journal.pone.023411)



ABSTRACT

Medial degeneration is a key feature of aneurysm disease and aortic dissection. In a murine aneurysm model we investigated the structural and functional characteristics of aortic wall degeneration in adult fibulin-4 deficient mice and the potential therapeutic role of the angiotensin (Ang) II type 1 (AT₁) receptor antagonist losartan in preventing aortic media degeneration. Adult mice with 2-fold (heterozygous Fibulin-4^{+/-R}) and 4-fold (homozygous Fibulin-4^{RR}) reduced expression of fibulin-4 displayed the histological features of cystic media degeneration as found in patients with aneurysm or dissection, including elastin fiber fragmentation, loss of smooth muscle cells, and deposition of ground substance in the extracellular matrix of the aortic media. The aortic contractile capacity, determined by isometric force measurements, was diminished, and was associated with dysregulation of contractile genes as shown by aortic transcriptome analysis. These structural and functional alterations were accompanied by upregulation of TGF- β signaling in aortas from fibulin-4 deficient mice, as identified by genome-scaled network analysis as well as by immunohistochemical staining for phosphorylated Smad2, an intracellular mediator of TGF- β . Tissue levels of Ang II, a regulator of TGF- β signaling, were increased. Prenatal treatment with the AT₁ receptor antagonist losartan, which blunts TGF- β signaling, prevented elastic fiber fragmentation in the aortic media of newborn Fibulin-4^{RR} mice. Postnatal losartan treatment reduced haemodynamic stress and improved lifespan of homozygous knockdown fibulin-4 animals, but did not affect aortic vessel wall structure. In conclusion, the AT₁ receptor blocker losartan can prevent aortic media degeneration in a non-Marfan syndrome aneurysm mouse model. In established aortic aneurysms, losartan does not affect aortic architecture, but does improve survival. These findings may extend the potential therapeutic application of inhibitors of the renin-angiotensin system to the preventive treatment of aneurysm disease.

INTRODUCTION

Degeneration of the medial layer of the aorta is a key feature of aneurysm disease and aortic dissection¹. Cystic medial degeneration is characterized by elastic fiber fragmentation, loss of smooth muscle cells (SMC), and accumulation of amorphous extracellular matrix (ECM) in the aortic wall. Although media degeneration occurs to some degree with aging, excessive aortic wall degeneration may lead to dilatation of the aorta and aneurysm formation, or, alternatively, aortic dissection^{2,3}. In addition, advanced aortic degeneration may be part of inherited disorders of the connective tissue. One of the most common of these syndromes is Marfan syndrome (MFS), resulting from a mutation in the FBN1 gene which encodes the ECM glycoprotein fibrillin-1⁴. MFS is characterized by elastic fiber fragmentation, loss of elastin content, and accumulation of amorphous matrix components in the aortic wall, resulting in the formation of thoracic aortic aneurysms (TAAs)⁵. Mice with a mutation in the fibrillin-1 gene are widely used to study the pathophysiologic mechanisms underlying MFS and its treatment options⁶.

Several mutations in other genes encoding extracellular matrix proteins have also been identified in patients with TAAs, including mutations in the fibulin-4 gene^{7,8}. Fibulin-4 is one of the seven-member family of ECM proteins that play a role in elastic fiber assembly and function⁹. Fibulin-4 is highly expressed in the medial layers of blood vessel walls, including the aortic media. It has been shown that mutant mice lacking fibulin-4 (Fibulin-4^{-/-}) die perinatally from aortic rupture¹¹. Furthermore, newborn mice with a systemic 4-fold reduced expression of fibulin-4 (Fibulin-4^{R/R}) display elastic fiber fragmentation and develop aneurysms in the ascending thoracic aorta. Interestingly, even a 2-fold reduced expression of fibulin-4 in the heterozygous Fibulin-4^{+R} mice already induces similar, though milder, changes in the aorta¹².

Since aneurysm disease is a condition of the aging population, the present study first focused on the structural and functional characterization of aortic wall degeneration in adult fibulin-4 deficient mice. Recent studies have shown that antagonizing transforming growth factor- β (TGF- β) by either TGF- β neutralizing antibodies or the angiotensin (Ang) II type 1 (AT₁) receptor antagonist losartan can slow the progression rate of aortic root dilatation in an MFS mouse model⁶ and in patients with MFS¹³. Therefore, we next investigated the role of the renin-angiotensin system (RAS) in aneurysm formation in fibulin-4 deficient mice. We show that prenatal treatment with the AT₁ receptor blocker losartan can prevent aortic media degeneration in this non-MFS aneurysm mouse model. Losartan could not attenuate established aortic aneurysms in adult fibulin-4 mice, but largely improved survival of these animals. These findings point towards potential therapeutic application of inhibitors of the RAS to the preventive treatment of aneurysm disease.

METHODS

Experimental animals

We previously generated a fibulin-4 allele with reduced expression by transcriptional interference through placement of a TKneo targeting construct in the downstream Mus81 gene¹². Heterozygous (Fibulin-4^{+/-}) mice in a mixed C57Bl/6j;129Sv background were mated to obtain Fibulin-4^{+/+}, Fibulin-4^{+/-} and Fibulin-4^{-/-} littermates and were housed in the institutional animal facility. All experiments were performed under the regulation and permission of the Animal Care Committee of the Erasmus MC, Rotterdam, The Netherlands (protocol ID 139-08-06). The investigation conforms to the *Guide for the Care and Use of Laboratory Animals* published by the US National Institutes of Health (NIH Publication No. 85-23, revised 1996).

Histology and immunohistochemistry

Mice (age 100 days) were euthanized by an overdose CO₂, fixed by perfusion fixation with 4% formaldehyde, and autopsied according to standard protocols. Perfusion-fixed aortas were isolated and paraffin embedded. Next, 4 μm sections were haematoxylin and eosin stained and stained for elastin (Verhoeff-van Gieson), glycosaminoglycans (Alcian Blue) and SMCs (α-SMA). Immunohistochemistry for phosphorylated Smad2 (pSmad2) was performed as described previously¹⁴ using rabbit antiphospho-smad2 antibodies. The relative SMCs area of the ascending aorta was quantified by calculating the surface area of SMCs divided by the total surface area of the aortic rings (Qwin, Leica, Gleisburg, Switzerland). The relative amount of positive stained pSmad2 cells was calculated as the amount of positive stained pSmad2 cells, divided by the total number of cells.

Hemodynamic measurements

Mice (15-20 weeks old) were sedated with 4% isoflurane and intubated as previously described¹⁵. For measuring systolic and diastolic BP, mice were instrumented with a calibrated high fidelity 1.4 Fr microtip pressure transducer catheter (SPR-671, Millar Instruments), which was inserted into the left carotid artery and advanced into the aortic arch¹². Hemodynamic data were recorded and digitized using an online 4-channel data acquisition program (ATCODAS, Dataq Instruments, Akron, Ohio, USA), for later analysis with a program written in Matlab. Ten consecutive beats were selected for determination of BP.

Mulvany myographs

Male mice (age 120 days) were euthanized with an overdose of pentobarbital i.p. (60 mg/kg). Thoracic aorta, abdominal aorta and iliac artery were isolated and stored overnight in cold, oxygenated Krebs-Henseleit buffer solution. The following day, vessel segments were mounted in 6-mL organ baths (Danish Myograph Technology, Aarhus, Denmark) containing Krebs-Henseleit buffer (NaCl 118, KCl 4.7, CaCl₂ 2.5, MgSO₄ 1.2, KH₂PO₄ 1.2, NaHCO₃ 25 and glucose 8.3; pH 7.4) at 37°C and oxygenated with 95% O₂ and 5% CO₂. The tension was normalized to 90% of the estimated diameter at 100-mm Hg effective transmural pressure.¹⁶ Maximum contractile responses were determined using 100 mmol/L KCl. Concentration response curves (CRCs) were constructed to phenylephrine and Ang II (Sigma); the latter with a 30-minute incubation with the NO synthase inhibitor L-NAME (100 μmol/L; Sigma).

Microarray hybridizations

Standard procedures were used to obtain total RNA (Qiagen) of two Fibulin-4^{+/+}, two Fibulin-4^{+/-} and four Fibulin-4^{-/-} aortas (10 days old). Synthesis and hybridization was performed as described before¹². To examine the quality of the various arrays, several R packages (including affyQCReport) were run starting from the CEL files. All created plots, including the percentage of present calls, noise, background, and ratio of GAPDH 3' to 5' (<1.4) indicated a high quality of all samples and an overall comparability, except for two samples, which were excluded from further analysis. Of the 45101 probe sets, ~55% was called present in all samples. Raw intensities values of all samples were normalized by robust multichip analysis normalization (background correction

and quantile normalization) using Partek version 6.4 (Partek Inc., St. Louis, MO). The normalized data file was transposed and imported into OmniViz version 6.0.1 (Biowisdom, Ltd., Cambridge, UK) for further analysis. For each probe set, the geometric mean of the hybridization intensities of all samples was calculated. The level of expression of each probe set was determined relative to this geometric mean and $^2\log$ transformed. The geometric mean of the hybridization signal of all samples was used to ascribe equal weight to gene expression levels with similar relative distances to the geometric mean. Differentially expressed genes were identified using ANOVA (Partek) and SAM (OmniViz). Cut-offs values for significantly expressed genes were the FDR and a fold change of 1.5. Functional analysis was done using IPA (Ingenuity, Mountain View, CA). Microarray experiments have been previously described and complied with the regulations for Minimum Information of Microarray Experiments (MIAME) and can be retrieved from ArrayExpress, accession code: E-MEXP-840)¹².

Biochemical measurements

Kidneys were excised and blood was collected from the left ventricle and stored in 4 mol/l guanine thiocyanate as described before¹⁷. Both were immediately frozen in liquid nitrogen and stored at -80°C. Ang II was determined using radioimmunoassay, following SepPak extraction and high-performance liquid chromatography separation¹⁸.

Quantitative real-time reverse transcription polymerase chain reaction

Total RNA was isolated from kidneys and aortic arches using RNeasy Fibrous Tissue Mini Kit (Qiagen) and reverse transcribed using the SuperScript VILO cDNA synthesis kit (Invitrogen). The resulting cDNA was amplified in 40 cycles (denaturation at 95°C for 10 min; thermal cycling at 95°C for 15 sec, annealing/extension at 60°C for 1 min) with a Step-One cycler using TaqMan Universal Mastermix and TaqMan probes (Applied Biosystems) of individual genes. Specific primers (Rplp0 Mm01974474_gH, Efemp2 Mm00445429_m1, Agtr1a Mm00616371_m1, Agtr1b Mm02620758_s1 and Agtr2 Mm01341373_m1) were obtained from Applied Biosystems. After PCR cycling, the fluorescence intensities of the reporter (FAM) dyes were quantified. The threshold cycle (Ct), i.e. the cycle number at which the amount of the amplified gene of interest reached a fixed threshold, was determined subsequently. The comparative Ct method ($\Delta\Delta CT$) was used for relative quantification of gene expression¹⁹.

Treatment

Fibulin-4^{+R} mice were bred to produce Fibulin-4^{+/+} and Fibulin-4^{R/R} mice. Pregnant mice received either propranolol (0.5 g/liter, Sigma), losartan (0.6 gram/liter, Sigma) or placebo in their drinking water as described before⁶. Treatment was started at embryonic day (E)14.5 and continued for five days. At E19.5 the pregnant mice were euthanized by an overdose CO₂ and a caesarian section was performed to collect the fetuses. Adult Fibulin-4^{R/R} mice and their wild type littermates were treated during 10-14.5 weeks, starting at the age of 5.5 weeks. Aortas from the fetuses and adult mice were isolated and paraffin embedded. Next, 4- μ m sections were stained for elastin (Verhoeff-van Gieson). Ascending aortic wall thickness is the average of four measurements per quartile using Leica QWin software (Leica, Glattburg, Switzerland).

Data-analysis

Normally distributed data are presented as mean \pm SEM. CRCs were analyzed using Graph Pad Prism 5 (Graph Pad Software Inc., San Diego, California, USA) to determine the maximum effect (E_{max}) as described before.²⁰ Analysis of the differences between CRCs was performed by two-way ANOVA. The one-way ANOVA was considered for the analysis of E_{max} , blood pressures, angiotensin II levels and vessel wall thickness. Both analyses were followed by post hoc evaluation according to Bonferroni. To compare the observed distributions of the genotypes with the expected mendelian distribution, a chi-square test was used. The survival of fibulin-4 mice over time is

presented in a Kaplan-Meier curve for a cohort of mice alive at age 3 weeks and the curves were compared by the Log Rank test. To evaluate the dose-dependent effect of fibulin-4 expression, a linear regression analysis was performed obtain a p for trend. The latter statistical analyses were performed using SPSS 15.0 for Windows (SPSS, Chicago, Ill, USA). All statistical tests were two-sided and a p-value <0.05 was considered statistically significant.

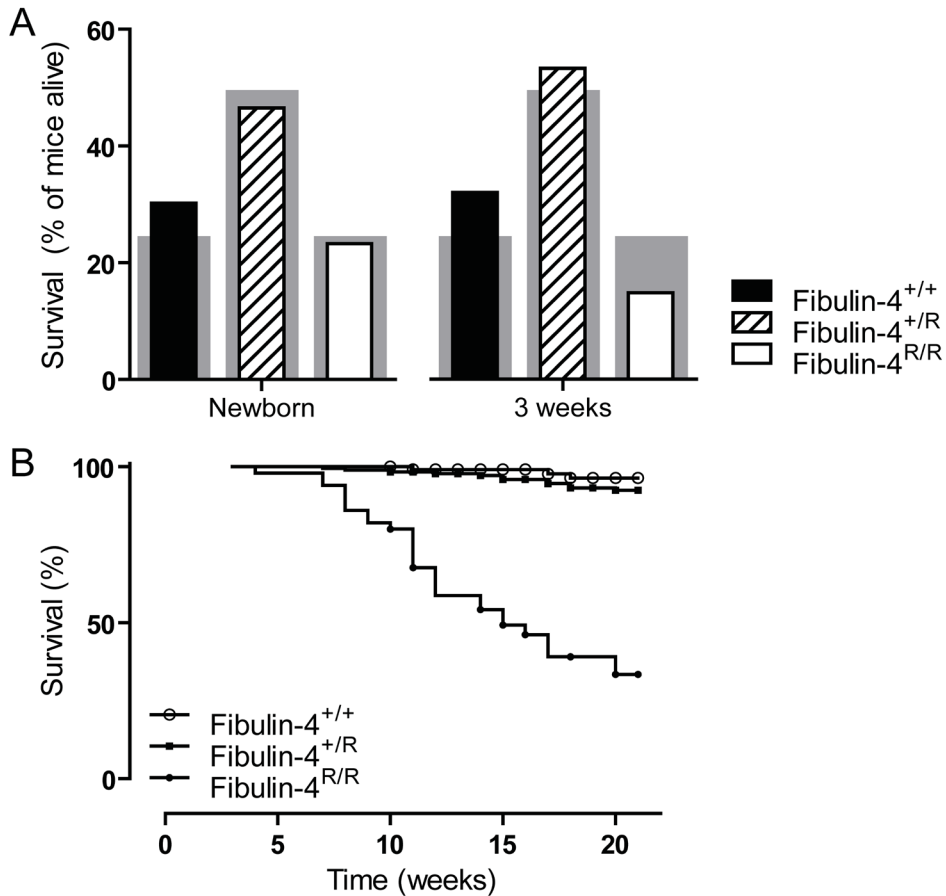


Figure 1

Survival of fibulin-4 mice. (A) Distribution of the three genotypes at 0 and 3 weeks of age. The grey bars show the expected Mendelian distribution and the overlying bars the observed distribution of the different genotypes. Fibulin-4 mice are born in a Mendelian distribution (n=10-20). Already after three weeks, this distribution is lost (n=50-180, p<0.0001). (B) Kaplan-Meier survival curves of Fibulin-4^{+/+}, Fibulin-4^{+/R} and Fibulin-4^{R/R} mice alive at the age of three weeks (n= 50-180). After 21 weeks, 96% of wild type Fibulin-4^{+/+} and 92% of Fibulin-4^{+/R} mice survived. Survival of Fibulin-4^{R/R} mice dramatically decreased to 33% (p<0.0001 vs. wild type). Note that the survival curve starts with all mice alive at the age of three weeks. Symbols indicate censored data.

RESULTS

Adult fibulin-4 deficient mice display aortic wall degeneration

Newborn Fibulin-4^{R/R} mice already showed severe TAAs¹², but only a small number of Fibulin-4^{R/R} mice survived towards adult age. Fig. 1 shows the survival of fibulin-4 deficient mice. Newborn fibulin-4 mice demonstrate a Mendelian distribution of the three genotypes (30.2% Fibulin-4^{+/+}, 46.5% Fibulin-4^{+R} and 23.3% Fibulin-4^{R/R} mice). Due to the high mortality in the first weeks, genotyping takes place at the age of three weeks. At this age, the amount of Fibulin-4^{R/R} mice already dropped to 15% and the Mendelian distribution is lost (Fig. 1A, $p < 0.0001$). To get insight in the mortality rate of these mice, we constructed a Kaplan-Meier curve with all mice alive at the age of three weeks (Fig. 1B). The curves clearly demonstrate a dramatic survival of Fibulin-4^{R/R} mice when compared to their wild type littermates ($p < 0.0001$). The structural alterations resulting from reduced fibulin-4 in adult mice were characterized in 100-days-old mice. All aneurysms of Fibulin-4^{R/R} mice were located in the ascending thoracic aorta. Aortic wall thickness was increased in Fibulin-4^{+R} and Fibulin-4^{R/R} as compared with Fibulin-4^{+/+} mice (Fig. 2A-C). The increase in aortic wall thickness was, at least in part, due to increased deposition of glycosaminoglycans in the ECM, as demonstrated by Alcian blue staining (Fig. 2D-F). Aortas of wild type mice displayed a normal pattern of elastic lamellae forming dense parallel sheets. In contrast, the thickened aortic walls in fibulin-4 deficient mice displayed changes in elastic fiber organization, varying from moderate elastic fiber fragmentation in Fibulin-4^{+R} mice to complete destruction of elastin lamellar organization in Fibulin-4^{R/R} mice (Fig. 2G-I). In addition to changes in elastin structure, aortic walls of Fibulin-4^{+R} and Fibulin-4^{R/R} mice displayed loss of SMCs, as evidenced by α -smooth muscle actin (SMA) staining (Fig. 2J-L) and increased numbers of apoptotic cells (data not shown). Next, to evaluate the reduction of SMCs seen in Fibulin-4^{R/R} aortas, we quantified the amount of SMCs relative to the vessel wall area. Although the absolute amount of SMCs varied among the different genotypes, the relative amount of SMCs was significantly lower in Fibulin-4^{R/R} mice when compared to Fibulin-4^{+/+} and Fibulin-4^{+R} mice (Fig. 2M).

Functional consequences of fibulin-4 deficiency

Increased aortic pulse pressure

Since elastic fiber fragmentation may be associated with loss of elasticity and increased stiffness of the aortic wall, we next determined the *in vivo* aortic blood pressure using a microtip pressure catheter. In Fibulin-4^{R/R} mice a slightly increased systolic blood pressure and decreased diastolic blood pressure was observed compared to wild type animals resulting in a significantly higher aortic pulse pressure in Fibulin-4^{R/R} mice compared to controls (Fig. 3), which is consistent with increased arterial stiffness²¹. Interestingly, we observed a gene dose-dependent decrease (trend) in diastolic blood pressure and increase (trend) in pulse pressure (Fig. 3), while no aortic valve abnormalities are present in Fibulin-4^{+R} mice. We therefore hypothesize that this blood pressure effect is due to primary vessel wall impairment in fibulin-4 deficient mice, while in Fibulin-4^{R/R} mice, this phenotype is aggravated due to aortic valve dysfunction.

Reduced aortic contractility

To evaluate the functional effects of SMC loss, *in vitro* vascular contractility was studied in different segments of the aorta and the iliac arteries. After mounting, the vessel diameter was measured for each segment. Ascending thoracic aortic diameters were 1106 ± 22 , 1086 ± 27 and 2023 ± 88 μm for Fibulin-4^{+/+}, Fibulin-4^{+R} and Fibulin-4^{R/R} mice respectively ($n=14-18$). Descending thoracic aortic diameters were 830 ± 17 , 797 ± 17 and 955 ± 49 μm for Fibulin-4^{+/+}, Fibulin-4^{+R} and Fibulin-4^{R/R} mice respectively ($n=17-22$). Abdominal aortic diameters were 568 ± 12 , 585 ± 15 and 611 ± 30 μm for Fibulin-4^{+/+}, Fibulin-4^{+R} and Fibulin-4^{R/R} mice respectively ($n=18-20$). Iliac arteries were 420 ± 12 , 401 ± 11 and 378 ± 14 μm for Fibulin-4^{+/+}, Fibulin-4^{+R} and Fibulin-4^{R/R} mice respectively ($n=18-19$). The diameter of both the ascending and descending thoracic aorta were significantly larger in Fibulin-4^{R/R} mice when compared to wild type Fibulin-4^{+/+} mice, while the iliac arteries were significantly smaller in diameter. Furthermore, the increase in vessel diameter of the ascending thoracic aorta was accompanied by an

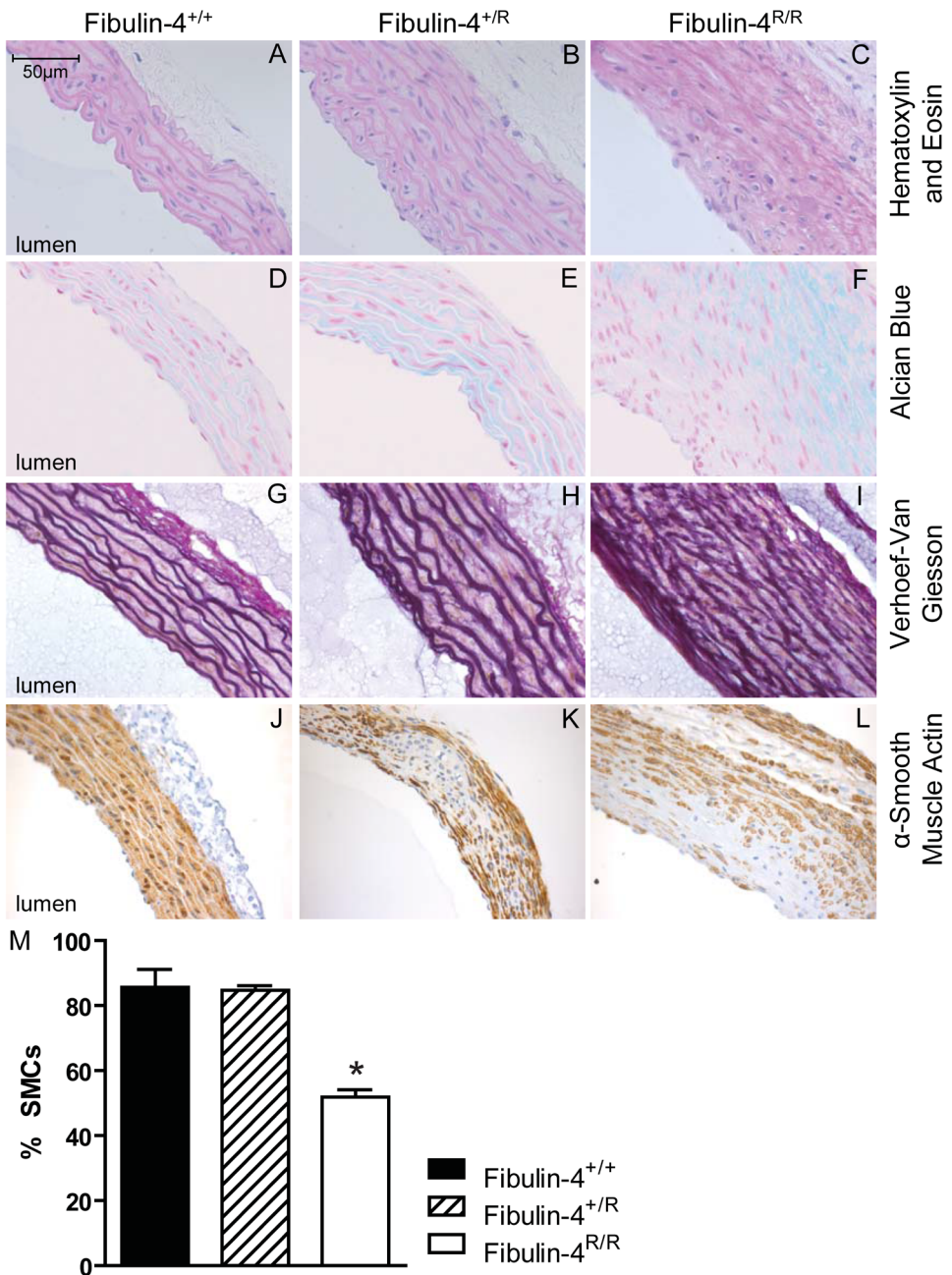


Figure 2

Architecture of ascending thoracic aortas. In adult *Fibulin-4*^{+/*R*} and *Fibulin-4*^{R/R} aortas there is an increase in aortic wall thickness (A-C), glycosaminoglycan depositions (blue areas) (D-F), elastic fiber fragmentation (G-I) and loss of smooth muscle cells in the media (J-L), also quantified (M).

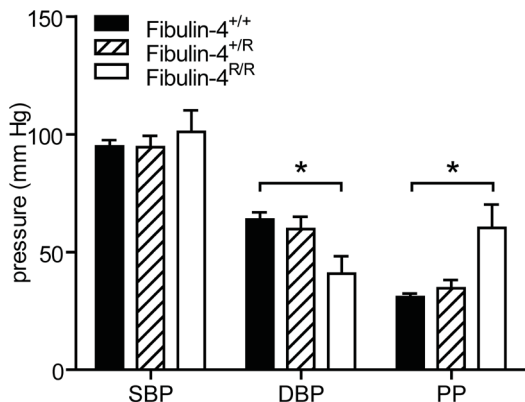


Figure 3

Systolic blood pressure (SBP) and diastolic blood pressure (DBP) measured using an intra-aortic microtip pressure transducer catheter. With decreasing expression of Fibulin-4, DBP decreased and pulse pressure (PP) increased (*p* for trend 0.009 and <0.001 resp.). Data are mean±SEM of 4-17 mice. * *p* <0.05 vs. Fibulin-4^{+/+} and Fibulin-4^{+/R} (two-way ANOVA).

approximately 2-fold elongation of the aortic segment.

In line with the relative reduction of SMCs in the thoracic aorta, the maximum contractility of thoracic aortas in response to KCl (100 mmol/L) was more than 3-fold lower in Fibulin-4^{R/R} mice than in Fibulin-4^{+/+} mice (Fig. 4A). Similarly, receptor-mediated vasoconstriction in response to phenylephrine (100 μmol/L) was significantly lower in thoracic aortic rings of Fibulin-4^{R/R} mice than in Fibulin-4^{+/+} mice (Fig. 4B). The contractile responses of the abdominal aorta and the iliac arteries did not differ between groups (data not shown). Increasing doses of Ang II, following a 30-minute incubation with *N*^G-nitro-L-arginine methyl ester (L-NAME), did not induce vasoconstriction in the thoracic aorta (Fig. 4C-D). The contractile responses of the abdominal aorta and iliac arteries in response to Ang II were not different between fibulin-4 deficient and wild type mice (Fig. 4E-F). This difference probably relates to the lower AT₁ receptor levels in the thoracic aorta than in other large arteries in the mouse^{22,23}.

Disturbed calcium signaling in fibulin-4 deficient mice

Next, genome-scaled network analysis from Fibulin-4^{+/+}, Fibulin-4^{+/R} and Fibulin-4^{R/R} aortas was performed using dedicated microarray statistics with a focus on canonical pathway analysis. Differentially expressed genes were initially identified using statistical analysis of microarrays ANOVA (false discovery rate (FDR) 0.5 and 1.5-fold change up- or downregulation). Transcriptomes of Fibulin-4^{+/+} and Fibulin-4^{+/R} full length aortas were compared and 26 probe sets were identified. With Ingenuity Pathway Analysis (IPA), a list of involved canonical pathways was constructed (Supplemental Table S1). The calcium signaling showed up as the top canonical pathway. Next, an independent SAM analysis was performed (FDR of 0.0032 (falsely called <1) and 1.5-fold change up- or downregulation). This approach identified 279 probe sets, from which a second top list of canonical pathways was constructed (Supplemental Table S2). Again, the calcium signaling pathway was highly significant. Interestingly, very specific genes involved in muscle cell contraction were up- or downregulated (Fig. 5).

Next, differences between transcriptomes of Fibulin-4^{+/+} and Fibulin-4^{R/R} aortas were analyzed. Statistical analysis of microarrays ANOVA was performed with the same selection criteria as for Fibulin-4^{+/+} vs. Fibulin-4^{+/R} aortas. Canonical pathway analysis identified mainly pathways involved in immunological and inflammatory diseases (Supplemental Table S3) and after analysis with SAM (FDR 0.2 and 1.5-fold change up- or downregulation) a table with principally similar pathways was constructed (Supplemental Table S4). These analyses identified a few genes involved in the aforementioned calcium signaling pathway.

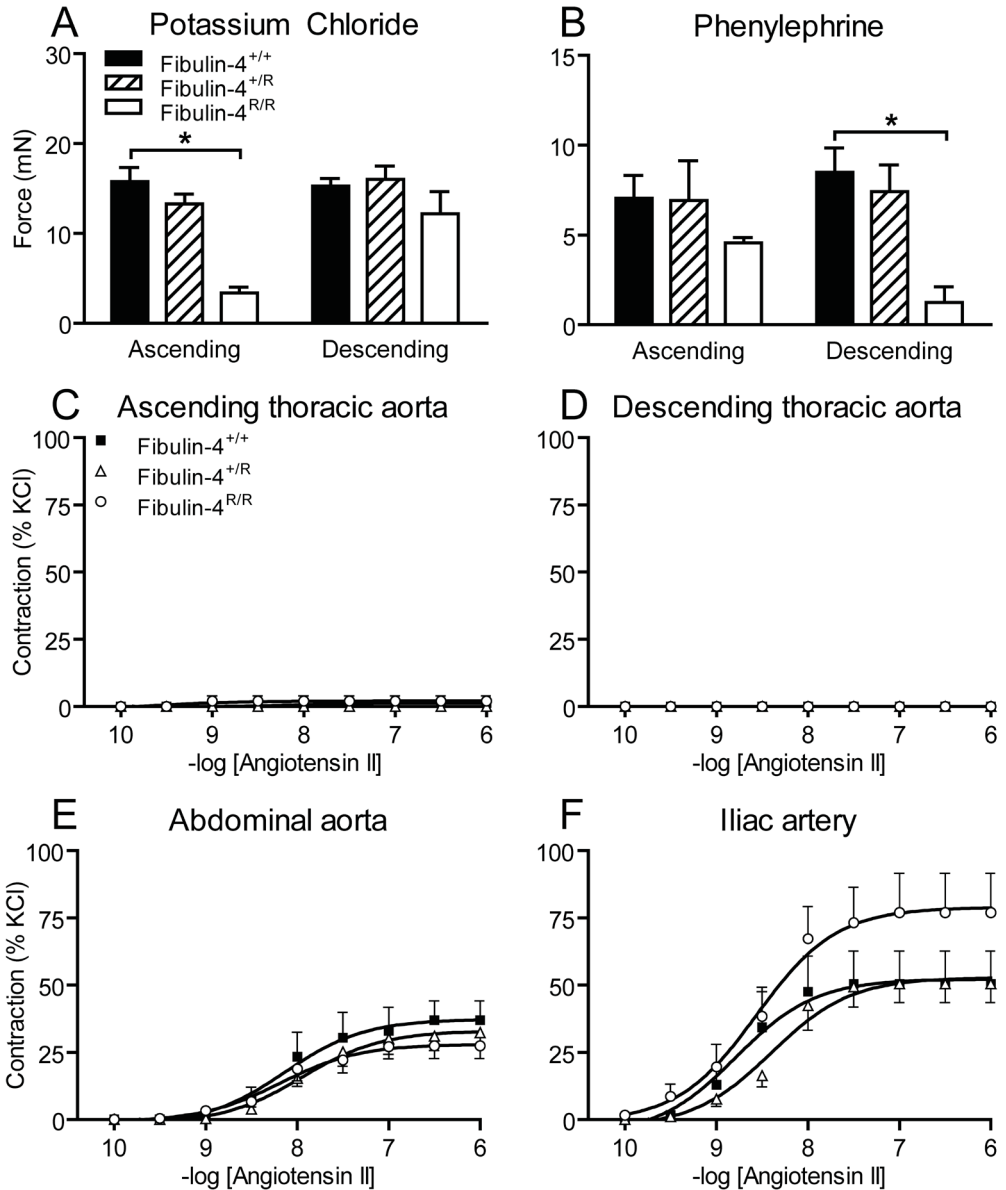


Figure 4

Contractility mediated by KCl, phenylephrine and angiotensin II. (A) In ascending aortas, KCl-induced contractility decreased in a gene dose-dependently in Fibulin-4^{+/R} and Fibulin-4^{R/R} mice (p for trend <0.001). (B) In descending aortas, phenylephrine-induced contractility decreased gene dose-dependently in Fibulin-4^{+/R} and Fibulin-4^{R/R} mice (p for trend 0.004). Data are mean±SEM of 6-18 experiments, *p<0.05 vs. Fibulin-4^{+/+} mice. (C-F) Effect of angiotensin II on (C) ascending thoracic aortas, (D) descending thoracic aortas, (E) abdominal aortas and (F) iliac arteries. Data (mean±SEM of 3-6 experiments) are shown as a percentage of the response to 100 mmol/L KCl.

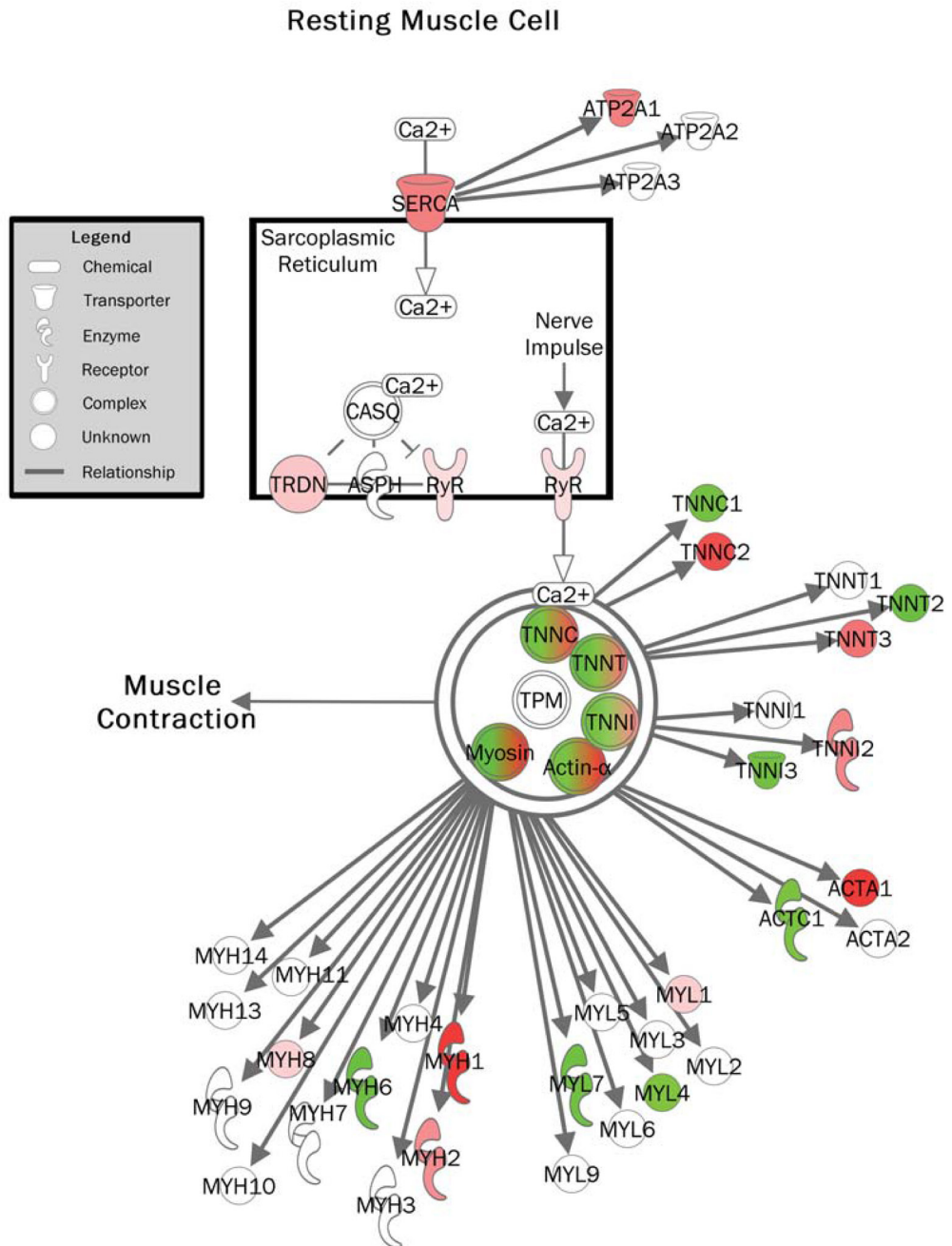


Figure 5
 Calcium signaling pathway in a resting muscle cell (Fibulin-4^{+R} vs. Fibulin-4⁺⁺ aortas). Colors show up- (red) and downregulation (green) of molecules involved in muscle cell contraction.

Fibulin-4 deficient mice show dysregulation of TGF- β signaling and increased tissue angiotensin II

In a mouse model of MFS, it has been demonstrated that dysregulation of TGF- β activation and the RAS play an important role in aneurysm formation^{6,24,25}. Hence, we next investigated the involvement of TGF- β signaling and Ang II in fibulin-4 deficient mice. First, genome-scaled network analysis from Fibulin-4^{+/+}, Fibulin-4^{+R/R} and Fibulin-4^{R/R} aortas identified the upregulation of TGF- β in Fibulin-4^{R/R} mice compared to Fibulin-4^{+/+} mice (Supplemental Table S3 and S4). Next, immunohistochemical staining for phosphorylated Smad2 (pSmad2), an intracellular mediator of the TGF- β signal, in ascending thoracic aortas was performed. A graded increase in the nuclear translocation of pSmad2 in the aortic media of Fibulin-4^{+R/R} and Fibulin-4^{R/R} mice was observed (Fig. 6A), indicating increased TGF- β signaling in adult aneurysmal fibulin-4 deficient mice.

Ang II is important in TGF- β signaling, by stimulating TGF- β 1 mRNA and protein expression, which leads to TGF- β activation. This indicates that TGF- β acts downstream of Ang II signaling²⁶. Therefore, we subsequently measured Ang II levels in blood and in kidney tissue of fibulin-4 deficient mice. Plasma Ang II levels were identical in the three genotypes (Fig. 6B). In contrast, renal tissue Ang II levels displayed a clear gene dose-dependent increase in Fibulin-4^{+R/R} and Fibulin-4^{R/R} mice (Fig. 5b; $p < 0.004$ for gene deletion effect), which may be due to increased AT₁ receptor binding at this site, resulting in increased receptor-bounded Ang II levels²⁷. Subsequent analysis of angiotensin receptor expression indeed demonstrated increased AT_{1b} receptor expression in both the kidneys and aortic arches (Fig. 6C). It is thus reasonable to assume that the Ang II content is also larger in the vasculature of fibulin-4 deficient mice, due to an increased receptor density at this site.

Treatment with AT₁ receptor blocker losartan prevents aortic wall degeneration, but does not attenuate established aortic aneurysms

In genetically engineered MFS mice with abnormal fibrillin-1, blocking TGF- β , either by TGF- β neutralizing antibody or by the AT₁ receptor blocker losartan, has been shown to prevent aortic root dilatation, elastic fiber degeneration, and pSmad2 activation⁶. Since dysregulation of TGF- β signaling and activation of the RAS were also observed in fibulin-4 deficient mice, we next investigated the potential therapeutic effect of losartan. To prevent Fibulin-4^{R/R} mice for premature drop-out due to aortic rupture, mice were treated as early as possible. Thus, mice were prenatally treated with placebo, beta-adrenergic receptor blocker propranolol, or AT₁ receptor blocker losartan. Propranolol, used as standard therapy to slow progression rate of aortic root growth in patients with MFS, served as control agent in an equihypotensive dosage⁶. Cross-sections of ascending aortas collected from Fibulin-4^{+/+} newborn mice, revealed the presence of intact elastic layers (Fig 7A). As expected, placebo-treated Fibulin-4^{R/R} mice showed severe fragmentation and an increased aortic wall thickness in this area (Fig. 7A-B). Treatment of Fibulin-4^{R/R} mice with propranolol did not change elastic fiber fragmentation, but slightly lowered vessel wall thickness. Yet, treatment with losartan improved elastic fiber fragmentation and greatly reduced vessel wall thickness.

Since AT₁ receptor blockade is contraindicated during pregnancy and aortic aneurysms are usually diagnosed in a more advanced state, we performed a postnatal treatment trial with losartan. While only a minority of the Fibulin-4^{R/R} untreated mice reach a lifespan of 120-140 days, losartan-treated Fibulin-4^{R/R} animals could reach a lifespan of at least 160-180 days ($n=3$), after which they were sacrificed for histological analysis. Postnatal treatment of Fibulin-4^{R/R} mice with losartan did not reduce vessel wall thickness, but contrary, led to aortic wall thickening when compared to placebo-treated Fibulin-4^{R/R} mice (Fig. 7D). This might, at least in part, be due to the increase in age of the losartan-treated animals. There were no signs of active remodeling of the aortic wall due to losartan treatment, since no change in elastic fiber architecture (Fig. 7C) or lumen diameter (Fig. 7F) was observed. To address whether losartan was able to reduce TGF- β signaling in these adult animals we performed pSmad2 staining. We found no reduction in pSmad2 positive cells with 99% of all nuclei stained positive for both groups (Fig. 7E). Since losartan reduced systolic blood pressure to approximately 60 mmHg, we therefore attribute the increased lifespan of the losartan-treated animals to the lower blood pressure measured.

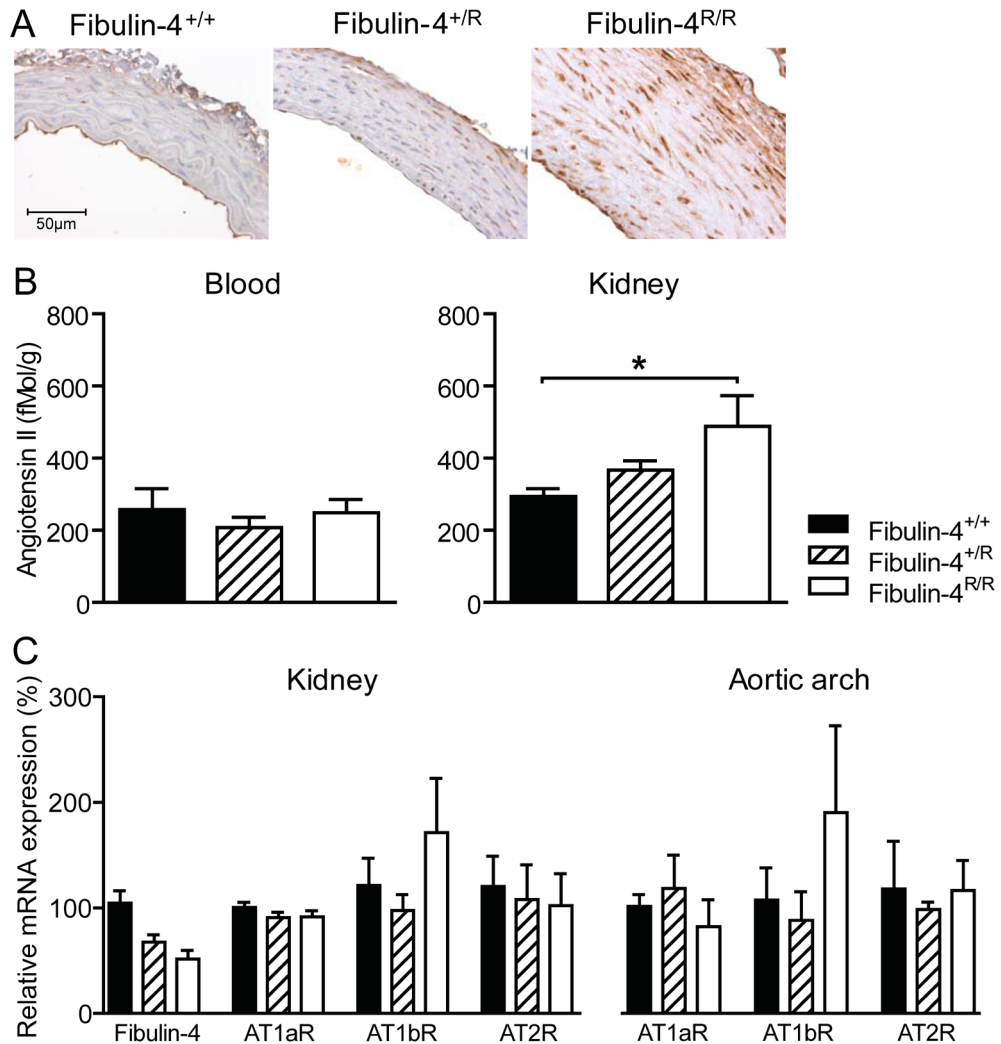


Figure 6

Increased levels of pSmad2 and angiotensin II in fibulin-4 mutant aortas. (A) Immunohistochemistry reveals a graded increase in expression and nuclear translocation of pSmad2 in the aortic media of adult fibulin-4 deficient mice. (B) With reduced fibulin-4 expression, tissue (but not blood) Ang II levels increase (*p* for trend 0.004). Data are shown as mean±SEM of 4–18 experiments. **p*<0.05 vs. Fibulin-4^{+/+}. (C) Relative mRNA expression of Fibulin-4 and Ang II receptors. As published previously, a substantial decrease of fibulin-4 was observed in Fibulin-4^{+/R} and Fibulin-4^{R/R} mice when compared to wild type littermates. Both the renal and aortic arch AT_{1b} receptor content was larger in Fibulin-4^{R/R} mice when compared to Fibulin-4^{+/+} and Fibulin-4^{+/R} mice. No differences in AT_{1a} or AT₂ receptor expression were observed between the different genotypes (n=3-10). AT_{1a}R, angiotensin II type 1a receptor; AT_{1b}R, angiotensin II type 1b receptor; AT₂R, angiotensin II type 2 receptor.

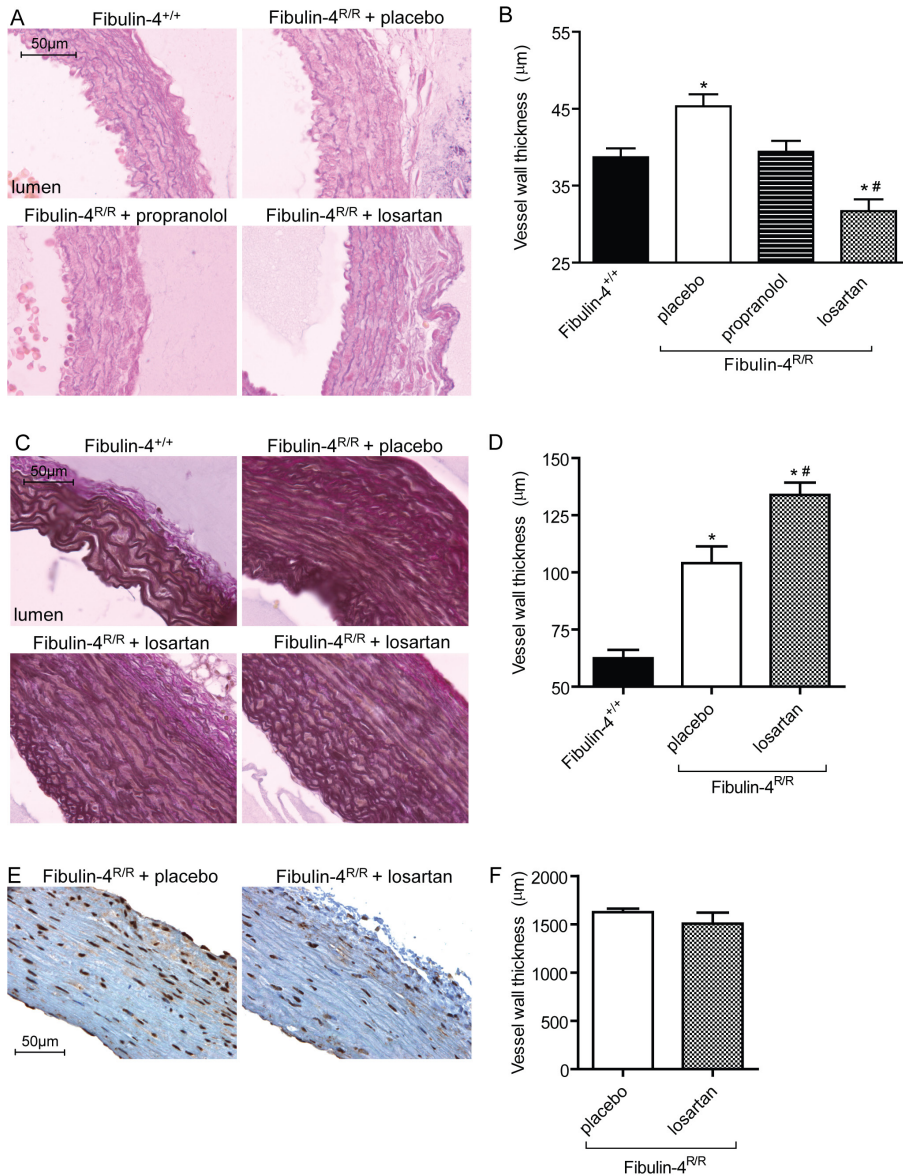


Figure 7

Aortic aneurysm treatment with losartan. (A) Elastic fiber fragmentation in newborn *Fibulin-4^{R/R}* mice could be prevented with losartan, but not with propranolol or placebo. (B) Vessel wall thickness of thoracic aortas from newborn *Fibulin-4^{+/+}* and treated *Fibulin-4^{R/R}* mice. Losartan treatment of *Fibulin-4^{R/R}* mice recovered vessel wall thickness. (C) Losartan treatment of adult *Fibulin-4^{R/R}* mice did not improve elastic fiber fragmentation. (D) Vessel wall thickness increased after postnatal losartan treatment. (E) Postnatal treatment with losartan did not reduce the amount of pSmad2 positive cells, nor did it affect lumen diameter (F). * $p < 0.05$ vs. wild type, # $p < 0.05$ vs. placebo-treated *Fibulin-4^{R/R}* mice, $n = 4-5$.

DISCUSSION

Adult fibulin-4 deficient (Fibulin-4^{+R} and Fibulin-4^{R/R}) mice display gene-dose-dependent elastic fiber fragmentation, dropout of SMCs, and deposition of mucopolysaccharide ground substance in the ECM of the aortic media. The structural changes observed in adult fibulin-4 deficient mice reflect the key histological features of cystic medial degeneration in patients with aortic aneurysm or dissection^{1, 28, 29}. In patients, medial degeneration is histologically characterized by fragmentation and loss of elastin, loss of SMCs, and formation of areas devoid of elastin that are filled with amorphous ECM. Cystic medial degeneration characterizes the final common pathway for various processes that affect the integrity of the aortic media. These findings support the use of the fibulin-4 deficient murine model for the study of aortic degeneration and aneurysm formation and its pharmacotherapeutical intervention.

The ECM provides the structural and functional platform of the aorta. In normal healthy aorta, elastin and collagen account for 50% of the dry weight and provide the aortic wall with non-linear elasticity properties³⁰. One of the critical elements of the ECM are the elastic lamellae. Elastin is incorporated in elastic fibers on a scaffold of microfibrils. The elastic fibers in normal healthy aorta are arranged in concentric elastic lamellae and, together with vascular SMCs, form lamellar units³¹. Deposition of elastin is not uniform in the aorta, with a decrease in the number of elastin lamellar units from the ascending aorta to the abdominal aorta³⁰. The circumferentially aligned collagen and elastin fibers in the aortic media provide tensile strength, permitting the aorta to withstand pulsatile flow and blood pressure delivered by the heart and to limit distal shear stress. The loss of elastic fiber integrity in the aortic wall observed in fibulin-4 deficient mice was associated with an increase in aortic pulse pressure, mainly due to a decline in diastolic blood pressure, reflecting diminished aortic resilience and tensile strength. Similar stiffening of the aortic wall with increased pulse pressure has been found in the well-characterized genetically engineered mouse model of MFS with a mutation in the FBN1 gene (*Fbn1*^{C1039G/+}) and in patients with MFS^{32, 33}. The rise in aortic pulse pressure in conjunction with aortic dilatation will further increase arterial wall stress over the cardiac cycle and thereby extend elastic fiber fragmentation. In MFS patients it has been shown that elevated aortic pulse-wave velocity, as a measure for reduced aortic elasticity, is a predictor for aortic dilatation and dissection³⁴.

The changes in aortic media structure were accompanied by impaired contractile function. Both adrenergic-receptor and receptor-independent vascular contractility were reduced in fibulin-4 deficient aortic rings. The decreased contractile capacity could, at least in part, be explained by the loss of SMCs in fibulin-4 deficient aortas. In addition, loss of fibulin-4 is assumed to disrupt the interaction between elastic fibers and SMCs, leading to alterations in actin cytoskeleton organization³⁵. Third, altered calcium signaling may contribute to disturbed vascular contractile capacity. Using aortic transcriptome analysis, we identified altered expression pattern of genes encoding for proteins involved in calcium signaling in Fibulin-4^{+R} as compared with Fibulin-4^{+/+} aortas. These data indicate that fibulin-4 deletion not only affects aortic media structure, but also affects contractile function, as was also predicted based on fibulin-4 conditional knockout mice³⁵. It has been suggested that aortic contractility contributes to the overall tensile strength and structural integrity of the aortic wall³⁶. The observed disturbances in the biomechanical properties of the aorta are in line with findings in the genetic mouse model of MFS³⁷. The altered load-bearing capacity of the aorta due to disturbances in the synthesis and breakdown of the aortic medial ECM as well as impaired aortic contractility culminates in increased aortic wall stress, which may contribute to dissection and aneurysm formation.

As in the MFS mouse model, the alterations in aortic structure and function were associated with increased TGF- β signaling in adult aneurysmal fibulin-4 deficient mice, as evidenced by a graded increase in the expression of pSmad2, an intracellular mediator of the TGF- β signal, in the aortic media of Fibulin-4^{+R} and Fibulin-4^{R/R} mice. Augmented TGF- β activation is associated with upregulation of matrix metalloproteinases and degradation of the aortic media, as shown in both MFS mice and in newborn fibulin-4 deficient mice³⁷⁻³⁹. Furthermore, altered TGF- β signaling has also been reported in humans with cardiovascular malformations due to fibulin-4 deficiency⁴⁰. The importance of TGF- β signaling in aneurysm formation is further supported by the recent

demonstration of increased circulating TGF- β concentrations in patients and mice with MFS, and the correlation between increased serum TGF- β and aortic root dilatation⁴¹.

It is still unclear how fibulin-4 deficiency correlates with increased TGF- β signaling. Increased TGF- β production may be due to Ang II⁴²⁻⁴⁵. For example, in human vascular SMCs, stimulation with Ang II induced a 6-fold increase in TGF- β production⁴³. The contribution of the RAS in the fibulin-4 mouse model was investigated by measuring circulating and renal tissue Ang II. Changes in renal Ang II content mirror changes in the Ang II content of other tissues, including the aorta^{17, 27}. However, renal Ang II levels are generally much higher than Ang II levels in blood vessel walls, and can thus be measured with much greater accuracy. Therefore, we determined renal tissue Ang II levels as a reflection of changes in aortic Ang II content in adult fibulin-4 deficient mice. While Ang II levels were preserved in plasma, renal Ang II levels increased with decreasing expression of fibulin-4. Parallel increases in renal AT_{1b} receptor content were observed, although these increases were not yet significant at n=3-10. Since tissue Ang II levels are determined largely, if not completely, by AT_{1a} and/or AT_{1b} receptor binding and subsequent internalization of extracellularly generated Ang II^{17, 27}, these data suggest that the increased renal Ang II levels are due to increased renal AT₁ receptor binding. Importantly, qPCR supported an aortic AT receptor upregulation profile in these mice that was identical to the profile in the kidney, i.e., selective AT_{1b} upregulation. Thus, based on these data it seems reasonable to assume that the vascular Ang II levels, like the renal Ang II levels, are increased in fibulin-4 deficient mice due to increased AT₁ receptor binding. Alternatively, upregulated tissue Ang II levels may be due to increased renin uptake at tissue sites⁴⁶, and thus future studies should investigate vascular (pro)renin receptor density. Evidence is accumulating that the RAS plays an important role in the pathogenesis of aneurysm formation^{5, 25, 47-49}. Ang II and AT₂ receptor expression are increased in MFS aortic tissue and have been associated with cystic medial degeneration²⁵. The increased tissue Ang II levels observed in fibulin-4 deficient mice are in line with these findings and support the role for the RAS in this model.

Drugs that interfere with the RAS may reduce aortic media degeneration. In cultured aortic cells from MFS, angiotensin-converting enzyme inhibition and AT₁ receptor antagonism significantly inhibited SMC apoptosis²⁵. Interestingly, blockade of the AT₁ receptor by losartan has been shown to diminish TGF- β signaling, with a reduction in free TGF- β levels, tissue expression of TGF- β -responsive genes, and levels of mediators within the TGF- β signaling cascade, and to prevent aortic aneurysm development in the MFS mouse model⁶. Furthermore, treatment with losartan reduced circulating TGF- β levels and slowed the rate of aortic root dilatation both in MFS mice and in MFS patients^{13, 41}. Based on these findings, we investigated whether aortic media degeneration in the fibulin-4 aneurysm model is associated with increased TGF- β signaling and could be prevented by the TGF- β antagonist losartan. In addition to interfering with TGF- β signaling, AT₁ receptor blockade will indirectly stimulate the AT₂ receptor. Through a negative feedback-mechanism, Ang II levels rise and bind the AT₂ receptor, which can have positive effects on the vascular remodeling. Results obtained in MFS mice further demonstrate that losartan is able to improve phenylephrine-induced contractility⁵⁰.

AT₁ receptor blocker losartan, but not by the β -blocker propranolol, prevented elastic fiber fragmentation and disarray in the aortic media of newborn Fibulin-4^{R/R} mice. Treatment of established aortic aneurysms in adult fibulin-4 mice with these losartan doses (0.6g/L) did not affect elastic fiber architecture. Thus, losartan was only able to prevent aortic wall degeneration in newborn Fibulin-4^{R/R} mice. This is opposite to findings in MFS mice, where postnatal treatment did improve aortic wall degeneration⁶. Clearly, there are differences between the mouse models. All Fibulin-4^{R/R} mice suffer from severe aortic aneurysms from birth that are prone to rupture, resulting in a tremendous reduction in lifespan as compared to their wild type littermates. MFS mice start to develop aortic aneurysms at the age of two months with variable severity of the aneurysm, and have a normal lifespan⁵¹. We hypothesize that aortic damage of Fibulin-4^{R/R} mice at the age of 5.5 weeks is too severe to regress or prevent further aortic growth with losartan treatment. Therefore, no difference in vessel lumen could be observed between placebo- or losartan-treated Fibulin-4^{R/R} mice. Most importantly, lifespan of adult Fibulin-4^{R/R} mice treated with losartan largely improved, accompanied with an increase with vessel wall thickness. Thus, thickening of the aortic wall might prevent aortic rupture. Postnatal losartan treatment of Fibulin-4^{R/R} animals

neither resulted in improved vessel wall structure nor in reduced TGF- β signaling, arguing against an active remodeling of the aorta. Thus, the improved lifespan seem to be a result of a reduced haemodynamic stress, evidenced by a lower blood pressure. Whether results are specific for AT₁ receptor blockers and/or inhibitors of the renin-angiotensin system or whether similar effects can be obtained with other blood pressure lowering agents has to be evaluated.

The present study is the first to show that losartan is effective in the prevention of non-MFS based aortic aneurysms. For established aortic aneurysms, losartan proved to largely improve lifespan, accompanied with a (preventive) thickening of the aortic wall. Together with previous reports, these data suggest that the antihypertensive drug losartan, an AT₁ receptor blocker that blunts TGF- β activation, may be an effective drug in the early secondary prevention of aortic media degeneration and aneurysm formation.

REFERENCES

1. Isselbacher EM. Thoracic and abdominal aortic aneurysms. *Circulation* 2005;**111**:816-828.
2. Kawasaki T, Sasayama S, Yagi S, Asakawa T, Hirai T. Non-invasive assessment of the age related changes in stiffness of major branches of the human arteries. *Cardiovasc Res* 1987;**21**:678-687.
3. Lakatta EG, Levy D. Arterial and cardiac aging: major shareholders in cardiovascular disease enterprises: Part I: aging arteries: a "set up" for vascular disease. *Circulation* 2003;**107**:139-146.
4. Dietz HC, Cutting GR, Pyeritz RE, Maslen CL, Sakai LY, Corson GM, Puffenberger EG, Hamosh A, Nanthakumar EJ, Curristin SM, Stetten G, Meyers DA, Francomano CA. Marfan syndrome caused by a recurrent de novo missense mutation in the fibrillin gene. *Nature* 1991;**352**:337-339.
5. Halme T, Savunen T, Aho H, Vihersaari T, Penttinen R. Elastin and collagen in the aortic wall: changes in the Marfan syndrome and annuloaortic ectasia. *Exp Mol Pathol* 1985;**43**:1-12.
6. Habashi JP, Judge DP, Holm TM, Cohn RD, Loeys BL, Cooper TK, Myers L, Klein EC, Liu G, Calvi C, Podowski M, Neptune ER, Halushka MK, Bedja D, Gabrielson K, Rifkin DB, Carta L, Ramirez F, Huso DL, Dietz HC. Losartan, an AT1 antagonist, prevents aortic aneurysm in a mouse model of Marfan syndrome. *Science* 2006;**312**:117-121.
7. El-Hamamsy I, Yacoub MH. Cellular and molecular mechanisms of thoracic aortic aneurysms. *Nature Reviews in Cardiology* 2009;**6**:771-786.
8. Huchtagowder V, Sausgruber N, Kim KH, Angle B, Marmorstein LY, Urban Z. Fibulin-4: a novel gene for an autosomal recessive cutis laxa syndrome. *Am J Hum Genet* 2006;**78**:1075-1080.
9. Argraves WS, Greene LM, Cooley MA, Gallagher WM. Fibulins: physiological and disease perspectives. *EMBO Reports* 2003;**4**:1127-1131.
10. Giltay R, Timpl R, Kostka G. Sequence, recombinant expression and tissue localization of two novel extracellular matrix proteins, fibulin-3 and fibulin-4. *Matrix Biol* 1999;**18**:469-480.
11. McLaughlin PJ, Chen Q, Horiguchi M, Starcher BC, Stanton JB, Broekelmann TJ, Marmorstein AD, McKay B, Mecham R, Nakamura T, Marmorstein LY. Targeted disruption of fibulin-4 abolishes elastogenesis and causes perinatal lethality in mice. *Mol Cell Biol* 2006;**26**:1700-1709.
12. Hanada K, Vermeij M, Garinis GA, de Waard MC, Kunen MG, Myers L, Maas A, Duncker DJ, Meijers C, Dietz HC, Kanaar R, Essers J. Perturbations of vascular homeostasis and aortic valve abnormalities in fibulin-4 deficient mice. *Circ Res* 2007;**100**:738-746.
13. Brooke BS, Habashi JP, Judge DP, Patel N, Loeys B, Dietz HC, 3rd. Angiotensin II blockade and aortic-root dilation in Marfan's syndrome. *N Engl J Med* 2008;**358**:2787-2795.
14. Hawinkels LJ, Verspaget HW, van der Reijden JJ, van der Zon JM, Verheijen JH, Hommes DW, Lamers CB, Sier CF. Active TGF-beta1 correlates with myofibroblasts and malignancy in the colorectal adenoma-carcinoma sequence. *Cancer science* 2009;**100**:663-670.
15. van den Bos EJ, Mees BM, de Waard MC, de Crom R, Duncker DJ. A novel model of cryoinjury-induced myocardial infarction in the mouse: a comparison with coronary artery ligation. *Am J Physiol Heart Circ Physiol* 2005;**289**:H1291-1300.
16. Mulvany MJ, Halpern W. Contractile properties of small arterial resistance vessels in spontaneously hypertensive and normotensive rats. *Circ Res* 1977;**41**:19-26.
17. van Esch JHM, Gembardt F, Sterner-Kock A, Heringer-Walther S, Le TH, Lassner D, Stijnen T, Coffman TM, Schultheiss HP, Danser AHJ, Walther T. Cardiac phenotype and angiotensin II levels in AT1a, AT1b and AT2 receptor single, double and triple knockouts. *Cardiovasc Res* 2010;**86**:401-409.
18. Danser AHJ, van Kats JP, Admiraal PJJ, Derckx FH, Lamers JMJ, Verdouw PD, Saxena PR, Schalekamp MADH. Cardiac renin and angiotensins. Uptake from plasma versus in situ synthesis. *Hypertension* 1994;**24**:37-48.
19. Livak KJ, Schmittgen TD. Analysis of relative gene expression data using real-time quantitative PCR and the 2(-Delta Delta C(T)) Method. *Methods* 2001;**25**:402-408.
20. DeLean A, Munson PJ, Rodbard D. Simultaneous analysis of families of sigmoidal curves: application to bioassay, radioligand assay, and physiological dose-response curves. *Am J Physiol* 1978;**235**:E97-102.
21. Safar ME, Levy BI, Struijker-Boudier H. Current perspectives on arterial stiffness and pulse pressure in hypertension and cardiovascular diseases. *Circulation* 2003;**107**:2864-2869.
22. Zhou Y, Dirksen WP, Babu GJ, Periasamy M. Differential

- vasoconstrictions induced by angiotensin II: role of AT1 and AT2 receptors in isolated C57BL/6J mouse blood vessels. *Am J Physiol Heart Circ Physiol* 2003;**285**:H2797-2803.
23. Henriques T, Zhang X, Yiannikouris FB, Daugherty A, Cassis LA. Androgen increases AT1a receptor expression in abdominal aortas to promote angiotensin II-induced AAAs in apolipoprotein E-deficient mice. *Arterioscler Thromb Vasc Biol* 2008;**28**:1251-1256.
 24. Daugherty A, Rateri DL, Charo IF, Owens AP, Howatt DA, Cassis LA. Angiotensin II infusion promotes ascending aortic aneurysms: attenuation by CCR2 deficiency in apoE^{-/-} mice. *Clin Sci (Lond)* 2010;**118**:681-689.
 25. Nagashima H, Sakomura Y, Aoka Y, Uto K, Kameyama K, Ogawa M, Aomi S, Koyanagi H, Ishizuka N, Naruse M, Kawana M, Kasanuki H. Angiotensin II type 2 receptor mediates vascular smooth muscle cell apoptosis in cystic medial degeneration associated with Marfan's syndrome. *Circulation* 2001;**104**:I282-287.
 26. Goumans MJ, Liu Z, ten Dijke P. TGF- β signaling in vascular biology and dysfunction. *Cell Res* 2009;**19**:116-127.
 27. van Kats JP, Schalekamp MADH, Verdouw PD, Duncker DJ, Danser AHJ. Intrarenal angiotensin II: interstitial and cellular levels and site of production. *Kidney Int* 2001;**60**:2311-2317.
 28. Nataatmadja M, West M, West J, Summers K, Walker P, Nagata M, Watanabe T. Abnormal extracellular matrix protein transport associated with increased apoptosis of vascular smooth muscle cells in marfan syndrome and bicuspid aortic valve thoracic aortic aneurysm. *Circulation* 2003;**108 Suppl 1**:I329-334.
 29. Lopez-Candales A, Holmes DR, Liao S, Scott MJ, Wickline SA, Thompson RW. Decreased vascular smooth muscle cell density in medial degeneration of human abdominal aortic aneurysms. *Am J Pathol* 1997;**150**:993-1007.
 30. Wolinsky H, Glagov S. Structural Basis for the Static Mechanical Properties of the Aortic Media. *Circ Res* 1964;**14**:400-413.
 31. Faury G. Function-structure relationship of elastic arteries in evolution: from microfibrils to elastin and elastic fibres. *Pathol Biol (Paris)* 2001;**49**:310-325.
 32. Marque V, Kieffer P, Gayraud B, Lartaud-Ijdouadiene I, Ramirez F, Atkinson J. Aortic wall mechanics and composition in a transgenic mouse model of Marfan syndrome. *Arterioscler Thromb Vasc Biol* 2001;**21**:1184-1189.
 33. Jeremy RW, Huang H, Hwa J, McCarron H, Hughes CF, Richards JG. Relation between age, arterial distensibility, and aortic dilatation in the Marfan syndrome. *Am J Cardiol* 1994;**74**:369-373.
 34. Vitarelli A, Conde Y, Cimino E, D'Angeli I, D'Orazio S, Stellato S, Padella V, Caranci F. Aortic wall mechanics in the Marfan syndrome assessed by transesophageal tissue Doppler echocardiography. *Am J Cardiol* 2006;**97**:571-577.
 35. Huang J, Davis EC, Chapman SL, Budatha M, Marmorstein LY, Word RA, Yanagisawa H. Fibulin-4 deficiency results in ascending aortic aneurysms. A potential link between abnormal smooth muscle cell phenotype and aneurysm progression. *Circ Res* 2009;**106**:583-592.
 36. Chew DK, Conte MS, Khalil RA. Matrix metalloproteinase-specific inhibition of Ca²⁺ entry mechanisms of vascular contraction. *J Vasc Surg* 2004;**40**:1001-1010.
 37. Chung AW, Au Yeung K, Sandor GG, Judge DP, Dietz HC, van Breemen C. Loss of elastic fiber integrity and reduction of vascular smooth muscle contraction resulting from the upregulated activities of matrix metalloproteinase-2 and -9 in the thoracic aortic aneurysm in Marfan syndrome. *Circ Res* 2007;**101**:512-522.
 38. Neptune ER, Frischmeyer PA, Arking DE, Myers L, Bunton TE, Gayraud B, Ramirez F, Sakai LY, Dietz HC. Dysregulation of TGF- β activation contributes to pathogenesis in Marfan syndrome. *Nat Genet* 2003;**33**:407-411.
 39. Kaijzel EL, van Heijningen PM, Wielopolski PA, Vermeij M, Koning GA, van Cappellen WA, Que I, Chan A, Dijkstra J, Ramnath NW, Hawinkels LJ, Bernsen MR, Lowik CW, Essers J. Multimodality imaging reveals a gradual increase in matrix metalloproteinase activity at aneurysmal lesions in live fibulin-4 mice. *Circ Cardiovasc Imaging* 2010;**3**:567-577.
 40. Renard M, Holm T, Veith R, Callewaert BL, Ades LC, Baspinar O, Pickart A, Dasouki M, Hoyer J, Rauch A, Trapane P, Earing MG, Coucke PJ, Sakai LY, Dietz HC, De Paepe AM, Loeyls BL. Altered TGF β signaling and cardiovascular manifestations in patients with autosomal recessive cutis laxa type I caused by fibulin-4 deficiency. *Eur J Hum Genet* 2010;**18**:895-901.
 41. Matt P, Schoenhoff F, Habashi J, Holm T, Van Erp C, Loch D, Carlsson OD, Griswold BF, Fu Q, De Backer J, Loeyls

- B, Huso DL, McDonnell NB, Van Eyk JE, Dietz HC, Gen TACC. Circulating transforming growth factor-beta in Marfan syndrome. *Circulation* 2009;**120**:526-532.
42. Gibbons GH, Pratt RE, Dzau VJ. Vascular smooth muscle cell hypertrophy vs. hyperplasia. Autocrine transforming growth factor-beta 1 expression determines growth response to angiotensin II. *J Clin Invest* 1992;**90**:456-461.
 43. Ford CM, Li S, Pickering JG. Angiotensin II stimulates collagen synthesis in human vascular smooth muscle cells. Involvement of the AT(1) receptor, transforming growth factor-beta, and tyrosine phosphorylation. *Arterioscler Thromb Vasc Biol* 1999;**19**:1843-1851.
 44. Kagami S, Border WA, Miller DE, Noble NA. Angiotensin II stimulates extracellular matrix protein synthesis through induction of transforming growth factor-beta expression in rat glomerular mesangial cells. *J Clin Invest* 1994;**93**:2431-2437.
 45. Sun Y, Zhang JQ, Zhang J, Ramires FJ. Angiotensin II, transforming growth factor-beta1 and repair in the infarcted heart. *J Mol Cell Cardiol* 1998;**30**:1559-1569.
 46. Batenburg WW, de Bruin RJ, van Gool JM, Muller DN, Bader M, Nguyen G, Danser AH. Aliskiren-binding increases the half life of renin and prorenin in rat aortic vascular smooth muscle cells. *Arterioscler Thromb Vasc Biol* 2008;**28**:1151-1157.
 47. Lu H, Rateri DL, Cassis LA, Daugherty A. The role of the renin-angiotensin system in aortic aneurysmal diseases. *Current Hypertension Reports* 2008;**10**:99-106.
 48. Pannu H, Tran-Fadulu V, Papke CL, Scherer S, Liu Y, Presley C, Guo D, Estrera AL, Safi HJ, Brasier AR, Vick GW, Marian AJ, Raman CS, Buja LM, Milewicz DM. MYH11 mutations result in a distinct vascular pathology driven by insulin-like growth factor 1 and angiotensin II. *Hum Mol Genet* 2007;**16**:2453-2462.
 49. Moltzer E, Essers J, van Esch JH, Roos-Hesselink JW, Danser AH. The role of the renin-angiotensin system in thoracic aortic aneurysms: Clinical implications. *Pharmacol Ther* 2011;**131**:50-60.
 50. Yang HH, Kim JM, Chum E, van Breemen C, Chung AW. Long-term effects of losartan on structure and function of the thoracic aorta in a mouse model of Marfan syndrome. *Br J Pharmacol* 2009;**158**:1503-1512.
 51. Judge DP, Biery NJ, Keene DR, Geubtner J, Myers L, Huso DL, Sakai LY, Dietz HC. Evidence for a critical contribution of haploinsufficiency in the complex pathogenesis of Marfan syndrome. *J Clin Invest* 2004;**114**:172-181.

CHAPTER 4

Reduced Fibulin-4 Expression Causes Myocardial Remodelling and Dysfunction

E. D. van Deel[#], L. te Riet[#], E. Moltzer, N. van Vliet, J.L. Robertus, N. Boontje, L. R. Fiedler, S. O. Dekker, E. Maifoshie, P. M. van Heijningen, M. Vermeij, I. van der Pluijm, L. Speelman, J. W. Roos-Hesselink, E. V. Rouwet, D. P. Reinhardt, J. van der Velden, A. H. J. Danser, D. J. Duncker, M. D. Schneider, J. Essers

[#]authors contributed equally

(Submitted for publication)



ABSTRACT

Fibulin-4 is a ubiquitously expressed protein essential for elastic fiber formation. Although fibulin-4 is known to be important for aortic wall integrity, little is known about its function in the heart. We therefore examined the role of fibulin-4 in cardiac function and pathology.

Echocardiography and hemodynamic measurements revealed that mice with a 4-fold reduction in fibulin-4 expression (Fibulin-4^{R/R}) spontaneously develop cardiac hypertrophy, dilation and dysfunction as well as aortic aneurysms. This was accompanied by reduced force generating capacity of Fibulin-4^{R/R} cardiomyocytes, and altered transforming growth factor beta signaling. Subsequently, we evaluated the effects of reduced fibulin-4 expression in human induced pluripotent stem cell (iPSC)-derived cardiomyocytes to investigate cell-type specific consequences of reduced elastogenesis. Strikingly, shRNA-mediated knockdown of fibulin-4 expression increased cardiomyocyte size accompanied by increased atrial natriuretic peptide, connective tissue growth factor and plasminogen activator inhibitor-1 mRNA expression. As cardiac hypertrophy might be influenced by aortic regurgitation in homozygous Fibulin-4^{R/R} mice, we additionally studied heterozygous Fibulin-4^{+/R} mice with a 2-fold reduced fibulin-4 expression. While untreated Fibulin-4^{+/R} mice show no apparent cardiovascular or valvular abnormalities, mortality after transverse aortic constriction (TAC) was aggravated in Fibulin-4^{+/R} animals. Moreover, a 2-fold reduced fibulin-4 expression aggravated TAC-induced left ventricular dysfunction and pathological alterations in gene expression, without affecting valvular function.

By using both mouse models with reduced fibulin-4 expression as well as human iPSC-derived cardiomyocytes, we show that cardiac fibulin-4 drives myocardial pathology implying that improper elastogenesis can be a primary cause of cardiac disease.

INTRODUCTION

The extracellular matrix (ECM) not only provides structural support to cells, but its composition and mechanical properties are also essential in cell development, signaling and function.¹ Within the ECM, elastic fibers, determine tissue elasticity.² Accordingly, impaired elastic fiber assembly is the underlying cause of several heritable connective tissue disorders such as Marfan syndrome. These disorders frequently exhibit cardiovascular manifestations including thoracic aortic aneurysm, aortic valve regurgitation and cardiac remodeling and dysfunction^{2,3} accompanied by altered transforming growth factor beta (TGF- β) signaling.⁴ Cardiac dysfunction in patients with improper elastogenesis is predominantly attributed to aortic valve regurgitation. However, primary myocardial impairment has also been postulated in patients with Marfan syndrome.³ A direct link between elastic fibers and cardiac performance indeed seems plausible since elastic fiber components are expressed in the heart,⁵ and mechanical properties of the ECM and its associated components, including TGF- β , highly influence cardiac pathology.⁶ Additionally, studies in rats demonstrate that elevated elastin levels in the infarct zone of a myocardial infarction attenuate cardiac dilation and dysfunction.^{7,8} We therefore hypothesize that improper elastogenesis is a currently unexplored intrinsic cause of cardiac abnormalities in elastin-related ECM disorders.

A crucial factor in elastic fiber assembly and homeostasis is the ECM-protein fibulin-4.^{9,10} Fibulin-4 is expressed in cardiovascular tissues including blood vessels, heart valves, and in the interstitial space surrounding cardiomyocytes.¹¹ In humans, mutations in the fibulin-4 gene cause the cutis laxa syndrome which next to loose skin is characterized by cardiovascular pathology similar to Marfan syndrome¹²⁻¹⁶ We previously demonstrated that mice with a systemic 4-fold reduced fibulin-4 expression (Fibulin-4^{R/R}) share a number of key features with the human disease phenotype, including aortic aneurysm formation, aortic valve disease, increased TGF- β signaling and impaired cardiac function.^{17, 18} Manifestation of fibulin-4 related pathology is dose-dependent since Fibulin-4^{+^R/R} mice, with a milder 2-fold reduction in fibulin-4 expression, develop no apparent cardiovascular abnormalities.^{17, 18}

We investigated the consequence of reduced fibulin-4 expression in the heart of Fibulin-4^{R/R} mice. Because, Fibulin-4^{R/R} mice not only display the cardiac but also the aortic phenotype of human pathology including aortic valve regurgitation and subsequent cardiac volume overload we further evaluate the effects of fibulin-4 knockdown independent of valvular leakage, in human induced pluripotent stem cell (iPSC)-derived cardiomyocytes using lentivirus-mediated short hairpin (sh) RNAmirs. Additionally, we studied the aortic-independent influence of fibulin-4 on cardiac susceptibility to pathology, by subjecting Fibulin-4^{+^R/R} mice, without cardiovascular abnormalities under normal circumstances, to 4 weeks of cardiac pressure-overload. Together these models allow assessment of the novel concept that impaired elastic fiber formation, triggered by fibulin-4 deficiency, drives cardiac pathology.

METHODS

Experimental Animals

We previously generated a fibulin-4 allele with reduced expression by transcriptional interference through placement of a TKneo targeting construct in the downstream *Mus81* gene.¹⁷ Heterozygous Fibulin-4^{+R} mice in a mixed C57Bl/6J;129Sv background were mated to obtain Fibulin-4^{+/+} and Fibulin-4^{R/R} littermates. Systemic fibulin-4 expression is reduced 2-fold in Fibulin-4^{+R} and 4-fold in Fibulin-4^{R/R} mice.¹⁷ Myocardial fibulin-4 protein levels were determined through western blot analysis. All animals received care in compliance with institutional guidelines and the Guide for the Care and Use of Laboratory Animals published by the NIH (Publication No. 85-23, Revised 1996).

Echocardiographic and Hemodynamic Measurements

To evaluate the impact of fibulin-4 on cardiac function and geometry, echocardiographic and hemodynamic measurements were performed in 14-week-old Fibulin-4^{+/+} (n=16) and Fibulin-4^{R/R} mice (n=6). All mice were ventilated and anesthetized with 2.5% isoflurane and echocardiography of the ascending aorta and left ventricle (LV) was performed using a Vevo2100 (VisualSonics Inc., Toronto, Canada). LV lumen diameters and ejection fraction (EF) were obtained from M-Mode images and pulse wave Doppler was used to visualize aortic regurgitation. Subsequently, aortic and LV pressure (LVP) were measured. The maximum rate of rise (LV dP/dt_{max}) and fall (LV dP/dt_{min}) of LVP, as well as the rate of LVP-rise at a pressure of 40 mmHg (LV dP/dt_{p40}) and the time constant of LVP decay (tau) were calculated as previously described.¹⁹ At the end of each experiment LV, right ventricle (RV) and lung weights as well as tibia lengths (TL) were determined and LV tissue samples (not containing aorta or aortic valve tissue) were stored for histological and molecular analysis.

Isometric Force Measurements

The force generating capacity of single membrane-permeabilized cardiomyocytes from Fibulin-4^{+/+} and Fibulin-4^{R/R} mice was assessed as described previously.¹⁹ In short, myocytes from 3 LV sections per group (2–4 cells per section) were isolated and all membranes removed. Isometric force measurements were performed in activation solutions with different calcium concentrations to determine maximal force (F_{max}), myofilament calcium-sensitivity (pCa₅₀) and passive force (F_{pass}).

Cardiac Histology

Paraffin embedded LV tissue was serially sectioned into 5- μ m slices and stained with Gomori's silver staining for determination of cardiomyocyte cross-sectional area. Picrosirius Red and Resorcin Fuchsin dyes were used to determine collagen and elastic fibre content, respectively.

Mouse LV mRNA Analysis

mRNA expression analyses of LV samples (n=5 per group) was performed using real-time fluorescence assessment of SYBR Green Primer sets for atrial natriuretic peptide (ANP), brain natriuretic peptide (BNP), α -skeletal muscle actin (α -SKA), sarcoplasmic reticulum Ca²⁺ ATPase (SERCA2a) and connective tissue growth factor (CTGF) (Integrated DNA Technologies, Coralville, USA) (Suppl. Table 1). mRNA levels were corrected for the housekeeping gene β -actin and normalized to sham Fibulin-4^{+/+}.

Western Blotting

LV tissue samples (n=4-5 per group) were used for immunoblotting of extracellular signal-regulated kinases (ERK1/2), phosphorylated ERK1/2 (pERK1/2), Smad, phosphorylated Smad2 (pSmad2) and fibulin-4 (Cell Signaling Technology, Danvers, MA, USA; Abcam, Cambridge, UK). Ratios of phosphorylated protein levels to total protein levels and ratios of fibulin-4 to loading control β -actin and coomassie staining were calculated.

Cell Culture and Knockdown of Fibulin-4 by Lentivirus-Mediated shRNA

Two lentiviral vectors containing shRNAmirs against Fibulin-4 as well as a non-silencing control shRNAmirs (Thermo Scientific, Huntsville, USA) were used to generate lentivirus.

To inhibit endogenous fibulin-4, human iPSC-derived cardiomyocytes (iCell cardiomyocytes, CDI, Madison, WI, USA) were infected with the lentiviral shRNAmir constructs, achieving an infection rate of ~90%. Four days after infection, cells were harvested or fixed and stained with fluorescently-conjugated antibodies to α -myosin heavy chain (α -MHC) (clone MF20, R&D) and a polyclonal fibulin-4 antibody that was characterized previously.²⁰ Additionally, the purity of iPSC-derived cardiomyocyte cultures was determined as the percentage of α -MHC stained cells. At the time of collection, the cultures contained ~98% α -MHC positive cells demonstrating that only 2% of the total cell population consisted of non-cardiomyocytes.

Gene Expression Analysis in Human iPSC-Derived Cardiomyocytes

Levels of human iPSC-derived cardiomyocyte mRNA were analyzed by real-time PCR using Taqman primers against fibulin-4, ANP, CTGF and plasminogen activator inhibitor type 1 (PAI-1) (Applied Biosystems, Foster City, CA, USA) (Suppl. Table 2) and corrected for the housekeeping gene Large Ribosomal Protein.

Induction of TAC and In Vivo Measurements

To explore the role of fibulin-4 in cardiac pathology, 14-weeks old male Fibulin-4^{+/+} and Fibulin-4^{+R} mice, were subjected to severe TAC (sTAC) (Fibulin-4^{+/+} n=5, Fibulin-4^{+R} n=5), mild TAC (mTAC) (Fibulin-4^{+/+} n=11, Fibulin-4^{+R} n=17) using a 27G or 25G needle respectively or a sham operation (Fibulin-4^{+/+} n=11, Fibulin-4^{+R} n=10) as previously described.¹⁹ Echocardiography and hemodynamic measurements were performed 4 weeks after surgery. LVP and aortic pressure proximal and distal to the stenosis were measured. The systolic pressure gradient over the stenosis was used as a measure for stenosis severity. Subsequently, LV, RV, lung weights as well as TL were determined and LV tissue samples were stored for histological and molecular analysis.

Statistical Analysis

One-way ANOVA was applied to compare Fibulin-4^{+/+} with Fibulin-4^{R/R} mice and evaluate results from iPSC-derived cardiomyocytes. Statistical comparison of Fibulin-4^{+/+} and Fibulin-4^{+R} with or without mTAC was performed using a two-way ANOVA. One-way and two-way ANOVA were followed by a post hoc Dunnett test when appropriate. A p-value <0.05 (two-tailed) was considered statistically significant. Data are presented as means \pm SEM.

RESULTS

A 4-fold Reduced Fibulin-4 Expression Causes Cardiac Remodeling and Dysfunction

As previously shown for the aorta,¹⁷ western blot analysis demonstrated 2-fold and 4-fold reduced myocardial fibulin-4 protein levels in the hearts of 14-week old Fibulin-4^{+/-} and Fibulin-4^{R/R} mice compared to wildtype Fibulin-4^{+/+} littermates (Suppl. Figure 1). This 4-fold reduction in fibulin-4 expression produced marked cardiac hypertrophy and dilation in all Fibulin-4^{R/R} mice, (Figure 1A-D). Additionally, all Fibulin-4^{R/R} mice suffered from aortic valve regurgitation demonstrated by aortic backflow during diastole (Figure 1E). LV remodeling was reflected in an approximate doubling of LV weight/TL and end diastolic LV lumen diameter (LVEDD) in Fibulin-4^{R/R} mice compared to Fibulin-4^{+/+} littermates (Figure 1F). This was associated with marked cardiac dysfunction evidenced by a reduced EF and LVP-derived parameters for cardiac contractility, maximal rise of LVP (dp/dt_{max}) (Table 1) and the less afterload-sensitive rate of LVP increase at a pressure of 40mmHg (dp/dt_{p40}) (Figure 1F). Likewise, Fibulin-4^{R/R} mice showed marked cardiac diastolic dysfunction evident from a decrease in the rate of diastolic LVP decline (dp/dt_{min}) and elevated end diastolic pressure (LVEDP) (Figure 1F). In addition, the LV relaxation constant *tau* tended to be higher in Fibulin-4^{R/R} animals indicating impaired relaxation. Accordingly, lung and RV weight were increased in Fibulin-4^{R/R} mice, indicating right-sided heart failure, (Figure 1F, Table 1). Altogether these data show that Fibulin-4^{R/R} mice develop clear pathological cardiac remodelling and dysfunction.

To assess the effect of reduced fibulin-4 expression on cardiomyocyte function we measured isometric force characteristics of cardiomyocytes from Fibulin-4^{+/+} and Fibulin-4^{R/R} mice. Similar to LV function, a 4-fold reduced fibulin-4 expression decreased F_{max} of single cardiomyocytes by 20% (Figure 1G). However, no changes in F_{pas} or pCa_{50} were observed (Figure 1G). This indicates that force generation is impaired in cardiomyocytes of Fibulin-4^{R/R} mice.

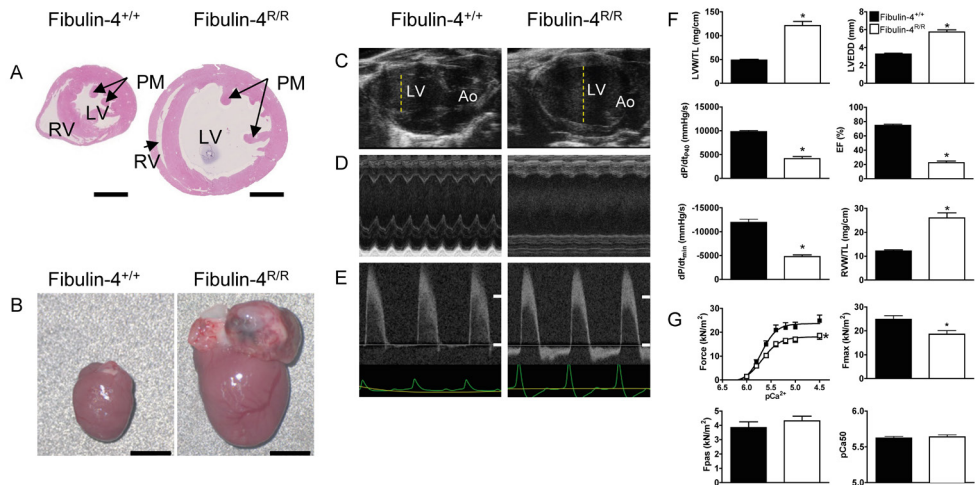


Figure 1 (A) Cross sections (black bars represent 2 mm), (B) whole hearts (bars represent 4 mm), (C) echocardiographic LV long axis B-Mode and (D) M-Mode images, (E) aortic flow patterns (bars represent a flow rate of 0 and 1000 mm/s), (F) parameters of LV function and dimension (Fibulin-4^{+/-} (n=16), Fibulin-4^{R/R} (n=6)) and (G) isometric force characteristics of single cardiomyocytes (3 LVs per group (2-4 cells per LV)). LV, left ventricle; LVW, LV weight; LVEDD, LV end-diastolic diameter; maximal force, F_{max} ; Ca^{2+} -sensitivity, pCa_{50} ; passive force, F_{pas} . * $P < 0.05$ vs Fibulin-4^{+/-}.

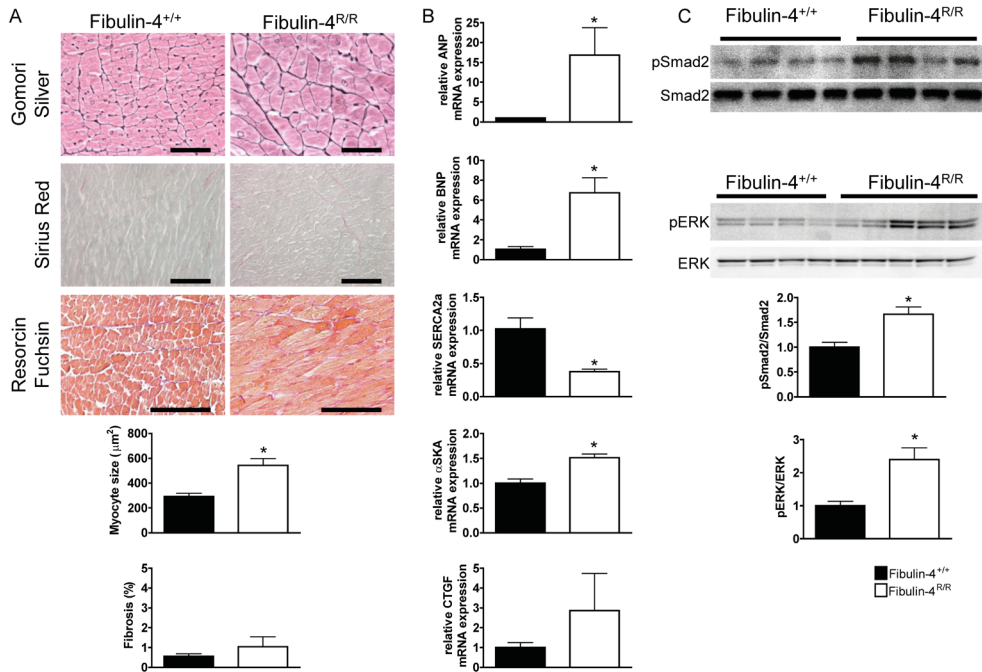


Figure 2

(A) Cardiomyocyte size, fibrosis and elastin content in Fibulin-4^{+/+} (n=7) and Fibulin-4^{R/R} (n=5-6) hearts (bars represent 200 µm). (B) mRNA expression of atrial natriuretic peptide (ANP), brain natriuretic peptide (BNP), α -skeletal muscle actin (α -SKA), sarcoplasmic reticulum Ca²⁺-ATPase (SERCA2a) and connective tissue growth factor (CTGF) in Fibulin-4^{+/+} (n=3-7) and Fibulin-4^{R/R} mice (n=3-4). (C) Enhanced pSmad2 and pERK protein levels in Fibulin-4^{R/R} (n=4-6) versus Fibulin-4^{+/+} hearts (n=4). *P<0.05 vs Fibulin-4^{+/+}

Fibulin-4^{R/R} Mice Develop Cardiomyocyte Hypertrophy and Disturbed TGF- β Signaling

LV hypertrophy in Fibulin-4^{R/R} mice was associated with a 2-fold increase in cardiomyocyte cross sectional area (Figure 2A), but not by cardiac fibrosis (Figure 2A). Additionally, in 4 out of 6 Fibulin-4^{R/R} hearts, elastin content was reduced compared to Fibulin-4^{+/+} hearts (Figure 2A).

Additionally, a 4-fold reduced expression of fibulin-4, elevated expression of genetic markers for cardiac hypertrophy ANP, BNP and α -SKA (Figure 2B) and reduced mRNA levels of the Ca²⁺ pump SERCA2a (Figure 2B), which is indicative for cardiac dysfunction. Additionally mRNA expression of CTGF, associated with ECM deposition, showed a non-significant increase in Fibulin-4^{R/R} animals (Figure 2B).

Since Fibulin-4 deficiency increases TGF- β signalling in aortas of Fibulin-4^{R/R} mice,¹⁷ we explored TGF- β signaling in heart tissue of Fibulin-4^{R/R} animals by measuring relative protein levels of the canonical mediator of TGF- β signaling, pSmad2 and of pERK1/2, which represents non-canonical TGF- β signaling in elastic fibre diseases such as Marfan syndrome.²¹ Reduced fibulin-4 expression increased relative pSmad2 and pERK levels,

indicating increased cardiac TGF- β signaling (Figure 2C). In summary, cellular adaptations, including increased cell size, elevated expression of markers for cardiac hypertrophy and increased TGF- β signaling, are associated with the observed cardiac dysfunction and pathological remodeling in Fibulin-4^{R/R} mice.

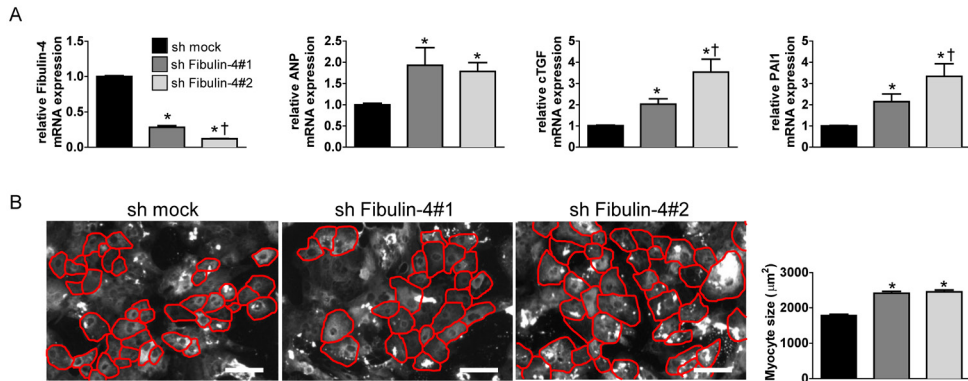


Figure 3

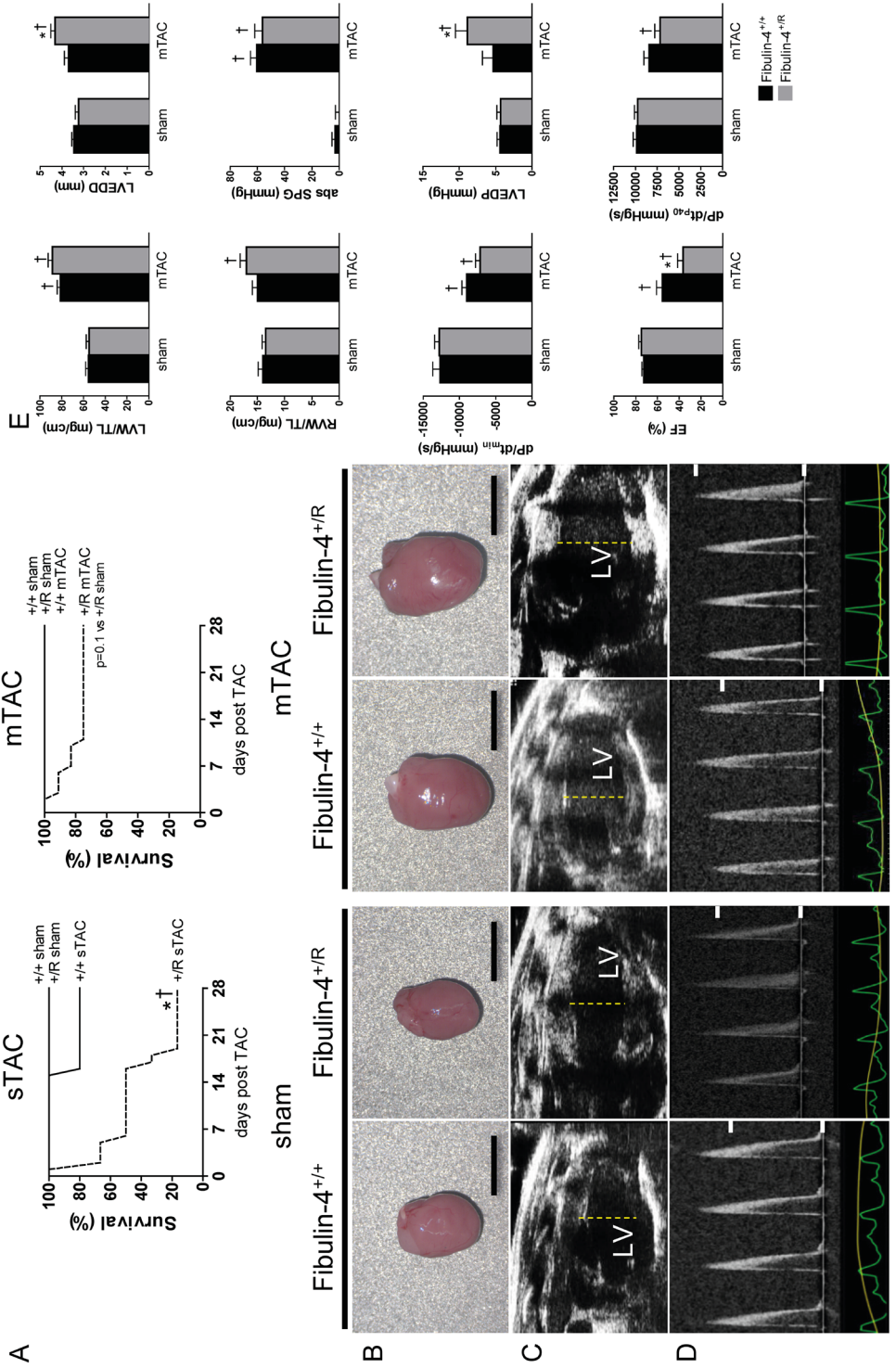
(A) Effects of fibulin-4 knock down in human iPSC-derived cardiomyocytes. mRNA expression of fibulin-4, atrial natriuretic peptide (ANP), connective tissue growth factor (CTGF) and plasminogen activator inhibitor-1 (PAI-1). (B) Cardiomyocyte size, showing one representative field of view of each group (bars represent 100 μm). In a total of 40-46 fields of view per group 1515 shRNA mock, 1082 shRNA Fibulin-4#1 and 831 shRNA Fibulin-4#2 transfected cells of which the borders could be well defined were analysed. * $P < 0.05$ vs sh mock, † $P < 0.05$ vs sh Fibulin-4#1.

Figure 4 (next page)

Reduced fibulin-4 expression aggravates TAC-induced pathology. (A) Survival ratio following sham, mild TAC (mTAC) and severe TAC surgery (sTAC). (B) Representative whole hearts (black bars represent 4 mm), (C) LV long axis B-Mode images, (D) aortic flow patterns (bars represent a flow rate of 0 and 1000 mm/s) and (E) geometrical and functional cardiac parameters of sham (Fibulin-4^{+/+} n=9, Fibulin-4^{+/R} n=8) and mTAC mice (Fibulin-4^{+/+} n=9, Fibulin-4^{+/R} n=10). LV, left ventricle; LVW, LV weight; TL, tibia length; LVEDD, LV end-diastolic diameter; RVW, right ventricular weight; EF, Ejection Fraction; SPG, systolic pressure gradient; LVEDP, LV end-diastolic pressure. * $P < 0.05$ vs corresponding Fibulin-4^{+/+}, † $P < 0.05$ vs corresponding sham.

Knockdown of Fibulin-4 Affects Cardiac Gene Expression and Cellular Dimensions Human iPSC-Derived Cardiomyocytes

Since aortic valve regurgitation contributes to cardiac pathology in Fibulin-4^{R/R} mice, we subsequently studied cardiomyocyte-autonomous effects of fibulin-4, independent of aortic valve abnormalities, using human iPSC-derived cardiomyocytes. In the iPSC-derived cardiomyocyte cultures, fibulin-4 is endogenously expressed and, similar to the vasculature, fibulin-4 is predominately located in the ECM (Suppl. Figure 2). Fibulin-4 knockdown by lentivirus-mediated transfer of two shRNAmirs directed against human fibulin-4, reduced fibulin-4 mRNA levels by 72% and 88% respectively (Figure 3A). Downregulation of fibulin-4 increased mRNA expression of the cardiac stress related gene ANP and the TGF- β activated genes CTGF and PAI1 (Figure 3A). Additionally, analogous



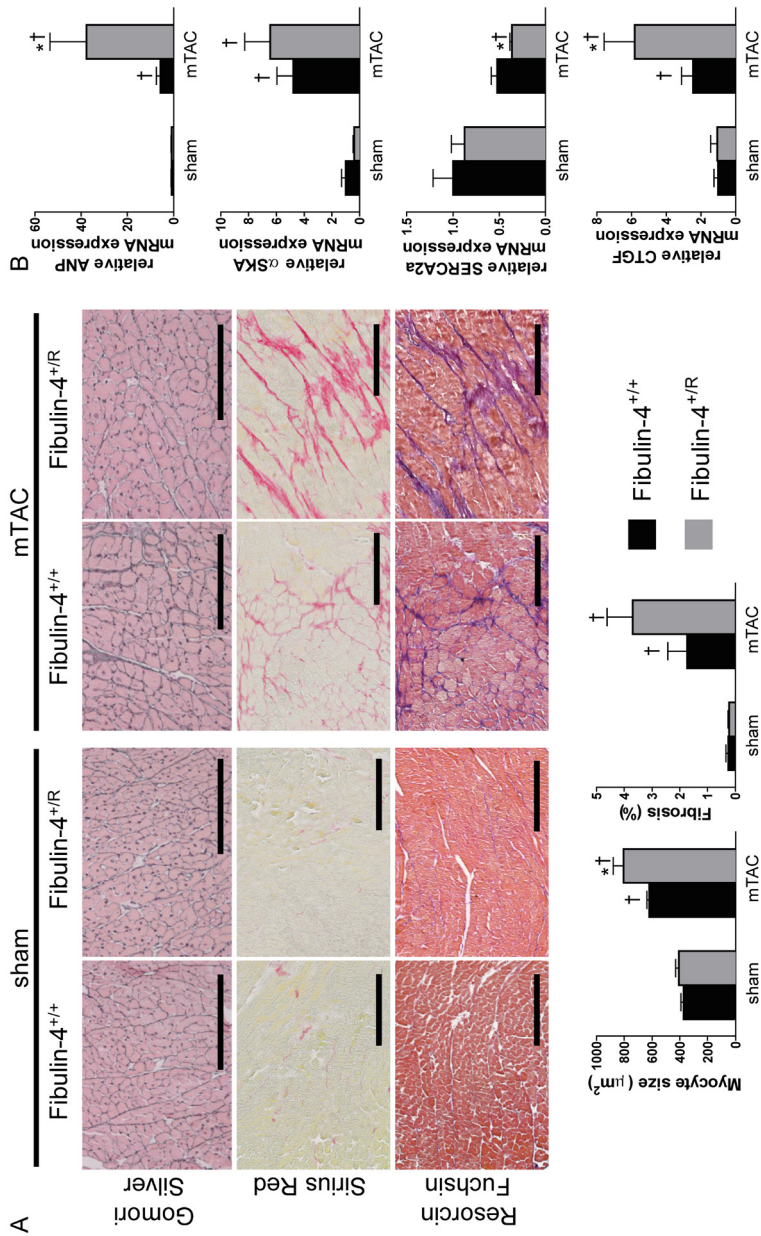


Figure 5

Effects of reduced fibulin-4 levels on mTAC-induced histological and mRNA alterations. (A) Cardiomyocyte size, fibrosis and elastin deposition (bars represent 200 μm, n=6 in all groups). (B) mRNA expression of atrial natriuretic peptide (ANP), α-skeletal muscle actin (αSKA), sarcoplasmic reticulum Ca²⁺-ATPase (SERCA2a) and connective tissue growth factor C (CTGF) in sham (Fibulin-4^{+/+} n=7-8, Fibulin-4^{+/R} n=5-6) and mTAC mice (Fibulin-4^{+/+} n=5-6, Fibulin-4^{+/R} n=4-6). *P<0.05 vs corresponding Fibulin-4^{+/+}, †P<0.05 vs corresponding sham.

to the observed cardiomyocyte hypertrophy in Fibulin-4^{R/R} hearts, knockdown of fibulin-4 by both shRNAmirs increased cardiomyocyte surface area by approximately 1.5-fold (Figure 3B). Even though we cannot completely exclude the possibility that the few present cardiac fibroblasts (<2% of the total cell population) contributed minorly to the fibulin-4 induced effects in our iPSC-derived cells, these results clearly demonstrate that loss of cardiac fibulin-4 induces cardiomyocyte pathology, independent of concomitant aorta-related factors.

Reduced Fibulin-4 Expression Increases Cardiac Susceptibility to Pressure-Overload

We subsequently evaluated fibulin-4-mediated cardiac defects *in vivo* independent of aortic abnormalities in 14-weeks old Fibulin-4^{+R} mice. Fibulin-4^{+R} animals have only a 2-fold reduction in fibulin-4 expression and demonstrate no cardiac or aortic valve dysfunction under normal conditions.¹⁷ To challenge the hearts of Fibulin-4^{+R} mice we induced cardiac pressure-overload through sTAC or mTAC in these animals. Reduced fibulin-4 expression markedly aggravated sTAC-induced mortality from 20% in Fibulin-4^{+/+} mice to 83% in Fibulin-4^{+R} littermates (Figure 4A). Similarly, 4 weeks of mTAC resulted in 27% mortality in Fibulin-4^{+R} mice without affecting survival in Fibulin-4^{+/+} animals (Figure 4A). Accordingly, a 2-fold reduction in fibulin-4 expression by itself did not affect heart size (Figure 4B), LV end diastolic lumen diameter (Figure 4C) or aortic valve function (Figure 4D) in sham mice while mTAC-induced cardiac hypertrophy and remodeling was aggravated in surviving Fibulin-4^{+R} mice (Figure 4B, C, E), without inducing aortic valve regurgitation in either genotype (Figure 4D). This was reflected in a trend towards increased relative LV weight and a significant increase in LV end diastolic lumen diameter (Figure 4E). Additionally, mTAC-induced cardiac dysfunction (EF) was markedly aggravated by reduced fibulin-4 expression and mTAC only affected LV dp/dt_{p40} and LV dp/dt_{max} in Fibulin-4^{+R} animals but not in Fibulin-4^{+/+} littermates. Similarly, only in Fibulin-4^{+R} mice, mTAC aggravated diastolic dysfunction (dPdt_{min}, tau and LVEDP) (Figure 4E and Table 2) and increased relative RV weight indicative for right-sided heart failure (Figure 4E). Thus, a 2-fold reduction in fibulin-4 levels does not produce cardiovascular adaptations under normal circumstances but, independent of aortic valve function, markedly aggravates mortality and LV remodeling and dysfunction following cardiac pressure-overload.

Pressure-Overload-Induced Myocyte Hypertrophy and Altered Gene Expression is Aggravated in Fibulin-4^{+R} Mice

Consistent with the trend towards increased heart weight, TAC increased cardiomyocyte size more in Fibulin-4^{+R} mice than in Fibulin-4^{+/+} animals (Figure 5A). Additionally, reduced fibulin-4 expression tended to aggravate mTAC-induced cardiac fibrosis (Figure 5A). Elastin deposition, which co-localized with fibrotic tissue, was elevated in 3 out of 6 Fibulin-4^{+/+} and 6 out of 6 Fibulin-4^{+R} animals, compared to sham-operated mice (Figure 5A). Additionally, TAC-induced re-expression of the LV hypertrophy-associated gene ANP was exacerbated in Fibulin-4^{+R} mice (Figure 5B). A similar trend was observed in α -SKA mRNA expression. Likewise, reduced fibulin-4 levels exacerbated the TAC-induced reduction of mRNA expression of the Ca²⁺ pump SERCA2a and the increase in TGF- β activated CTGF mRNA. In conclusion, reduced fibulin-4 expression aggravated TAC-induced cardiomyocyte hypertrophy and pathological alterations in expression of genes involved in hypertrophy, cardiac function and TGF- β signaling.

DISCUSSION

Here we identify fibulin-4 as an intrinsic contributor to cardiac pathology irrespective of extrinsic vascular or valve abnormalities. *In vivo*, a 4-fold reduction in fibulin-4 expression increased LV diameter and mass, induced severe cardiac dysfunction, elevated TGF- β signaling and altered mRNA levels of the heart failure associated genes ANP, BNP, α -SKA and SERCA2a. Even though cardiac pathology in Fibulin-4^{R/R} mice is aggravated by aortic valve disease, the development of cardiac remodeling and dysfunction was more pronounced in Fibulin-4^{R/R} mice than in other genetic^{22,23} or mechanically induced^{24,25} models for aortic regurgitation. This suggests that at least part of the cardiac disease in Fibulin-4^{R/R} mice is related to cardiac fibulin-4. To further evaluate this concept we used cardiomyocytes from human pluripotent stem cells that are not affected by aortic disease. Lentiviral knockdown of fibulin-4 in these human iPSC-derived cardiomyocytes similarly demonstrated the importance of cardiac fibulin-4 in heart disease.

Reduction of fibulin-4 expression in these cardiomyocytes not only increased the expression of the cardiac stress-related gene ANP and the TGF- β activated genes CTGF and PAI1, but additionally increased cell area by 40%. Although our iPSC-derived cell population almost exclusively contained cardiomyocytes (98%) we cannot completely exclude the possibility that the few present cardiac fibroblasts contributed to some extent to the fibulin-4 induced effects we found in the cardiomyocytes. Still, these data clearly demonstrate cardiomyocyte pathology as a result of reduced cardiac fibulin-4 levels (produced by cardiomyocytes and/or cardiac fibroblast). This was further confirmed by increased susceptibility to cardiac pathology in Fibulin-4^{+R/R} mice that have normal aortic valve function. In these animals reduced fibulin-4 expression increased mortality and aggravated TAC-induced cardiac hypertrophy and dysfunction as well as expression of heart failure-associated genes.

Enhanced myocardial stiffness in Fibulin-4^{R/R} mice, evidenced by elevation of LV end diastolic pressure, was not explained by cardiac fibrosis, but is most likely related to reduced myocardial ECM elasticity resulting from impaired elastogenesis. Although elastic fibres are predominantly produced during development and early after birth,⁷ previous observations suggest a potential role for elastin in cardiac pathology. For example, in rats with a myocardial infarction, implantation of cells overexpressing elastin into the infarct⁷, and transplantation of a myoblast sheet secreting elastin onto the infarct,⁸ enhanced the amount of elastic fibers in the scar tissue, improved cardiac function and prevented ventricular remodeling. However, a potential role for elastin in other forms of cardiac disease has not been proven to date. It has been suggested that cardiac ECM stiffness does not depend on collagen content but on the elastin/collagen ratio.²⁶ Accordingly, increased myocardial stiffness (indicated by elevated LV end diastolic pressure) was accompanied by less elastin deposition in LV tissue of Fibulin-4^{R/R} mice. Additionally, in Fibulin-4^{+R/R} animals with only a 2-fold reduction in fibulin-4 expression, increased elastin deposition in the ECM, which might be induced in an effort to compensate for TAC induced fibrosis, does not result in sufficient elastic fibres to counterbalance the TAC-induced cardiac stiffening.

In addition to improper elastic fibre assembly, an intrinsic cardiomyocyte defect may underlie cardiac dysfunction in fibulin-4 deficient hearts but this remains the subject of future investigation.

In individuals with impaired elastic fiber assembly, including those with Marfan syndrome and cutis laxa, cardiac failure is generally explained as a consequence of aortic valve disease and thoracic aneurysms. Like fibulin-4, the defective gene in Marfan syndrome, fibrillin-1 is essential for proper elastogenesis. Both fibrillin-1²⁷ and fibulin-4 (evidenced by our western blot analysis, and previously shown¹¹ are present in the myocardium, suggesting the possibility of vascular and valve independent cardiomyopathy in elastic fibre disease. Indeed one quarter of Marfan syndrome patients without significant aortic regurgitation had reduced LV ejection fraction, supporting the concept of primary cardiomyopathy.³

In conclusion, we identified fibulin-4 as a novel direct contributor to cardiac pathology. Severe reduction in fibulin-4 expression results in cardiac remodeling and dysfunction, while fibulin-4 directly affects cardiomyocyte signaling and cell size in human cardiomyocytes. Moreover, a mildly decreased fibulin-4 expression elevates cardiac susceptibility to pathology, irrespective of extrinsic vascular or aortic valve pathology. These findings have important implications for the prevention and attenuation of cardiac disease in patients with elastic fiber

disorders. Due to improvements in medical and surgical treatment of aortic valvular pathology, life expectancy among patients with connective tissue disorders has risen substantially over the past decades.²⁸ Analogous to Fibulin-4^{+/-R} mice, hearts of patients with connective tissue disorders may be unaffected under normal conditions but more susceptible to pathological stimuli. Currently, pharmacological treatment of patients with impaired elastic fiber assembly and causative thoracic aortic disease like in Marfan and cutis laxa syndrome is primarily aimed at reducing aortic growth.^{29,30} Our data suggest that besides prevention of aortic root expansion, medical care of patients with elastic fiber disorders should additionally focus on the heart, to prevent future cardiac pathology. Further studies should therefore also address the mechanisms of matrix-related cardiomyopathy and pharmacological targets to attenuate the progression of heart disease in these patients.

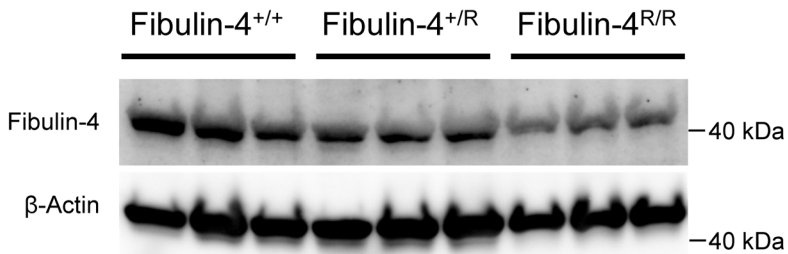
FUNDING

This work was supported by the “UNESCO-L’Oréal for Woman in Science Fellowship” (to EDvD), Natural Sciences and Engineering Research Council of Canada (to DPR), the British Heart Foundation Centre of Research Excellence and British Heart Foundation Simon Marks Chair in Regenerative Cardiology (to MDS) and the “Lijf en Leven”-grant (2008): “Early detection and diagnosis of aneurysms and heart valve abnormalities” (to JE).

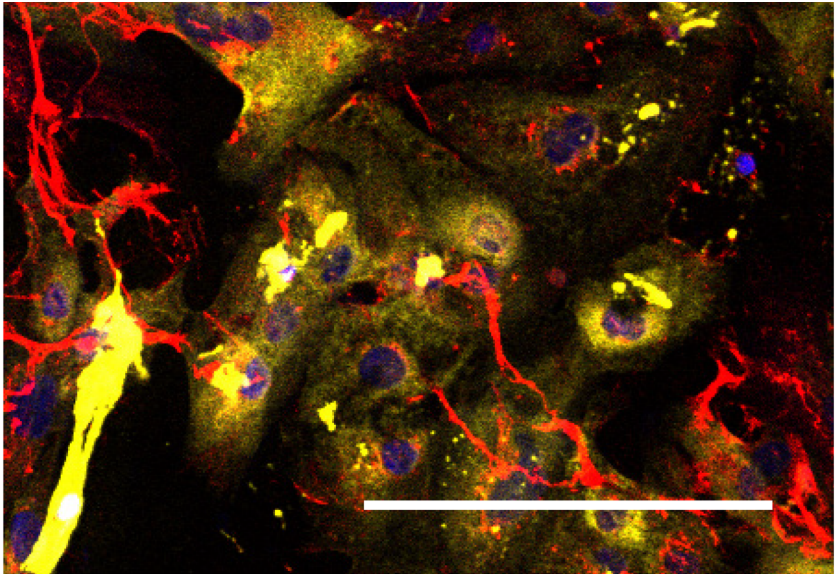
REFERENCES

1. Hynes RO. The extracellular matrix: not just pretty fibrils. *Science* 2009;**326**:1216-1219.
2. Kielty CM, Sherratt MJ, Shuttleworth CA. Elastic fibres. *J Cell Sci* 2002;**115**:2817-2828.
3. Alpendurada F, Wong J, Kiotsekoglou A, Banya W, Child A, Prasad SK, Pennell DJ, Mohiaddin RH. Evidence for Marfan cardiomyopathy. *Eur J Heart Fail* 2010;**12**:1085-1091.
4. Doyle JJ, Gerber EE, Dietz HC. Matrix-dependent perturbation of TGFbeta signaling and disease. *FEBS Lett* 2012;**586**:2003-2015.
5. Mao S, Wang Y, Zhang M, Hinek A. Phytoestrogen, tanshinone IIA diminishes collagen deposition and stimulates new elastogenesis in cultures of human cardiac fibroblasts. *Exp Cell Res*;**323**:189-197.
6. Kim HE, Dalal SS, Young E, Legato MJ, Weisfeldt ML, D'Armiento J. Disruption of the myocardial extracellular matrix leads to cardiac dysfunction. *The Journal of clinical investigation* 2000;**106**:857-866.
7. Mizuno T, Yau TM, Weisel RD, Kiani CG, Li RK. Elastin stabilizes an infarct and preserves ventricular function. *Circulation* 2005;**112**:181-88.
8. Uchinaka A, Kawaguchi N, Hamada Y, Miyagawa S, Saito A, Mori S, Sawa Y, Matsuura N. Transplantation of elastin-secreting myoblast sheets improves cardiac function in infarcted rat heart. *Mol Cell Biochem* 2012;**368**:203-214.
9. Horiguchi M, Inoue T, Ohbayashi T, Hirai M, Noda K, Marmorstein LY, Yabe D, Takagi K, Akama TO, Kita T, Kimura T, Nakamura T. Fibulin-4 conducts proper elastogenesis via interaction with cross-linking enzyme lysyl oxidase. *Proc Natl Acad Sci U S A* 2009;**106**:19029-19034.
10. Papke CL, Yanagisawa H. Fibulin-4 and fibulin-5 in elastogenesis and beyond: Insights from mouse and human studies. *Matrix Biol* 2014.
11. Giltay R, Timpl R, Kostka G. Sequence, recombinant expression and tissue localization of two novel extracellular matrix proteins, fibulin-3 and fibulin-4. *Matrix Biol* 1999;**18**:469-480.
12. Dasouki M, Markova D, Garola R, Sasaki T, Charbonneau NL, Sakai LY, Chu ML. Compound heterozygous mutations in fibulin-4 causing neonatal lethal pulmonary artery occlusion, aortic aneurysm, arachnodactyly, and mild cutis laxa. *Am J Med Genet A* 2007;**143A**:2635-2641.
13. Hoyer J, Kraus C, Hammersen G, Geppert JP, Rauch A. Lethal cutis laxa with contractural arachnodactyly, overgrowth and soft tissue bleeding due to a novel homozygous fibulin-4 gene mutation. *Clin Genet* 2009;**76**:276-281.
14. Huchtagowder V, Sausgruber N, Kim KH, Angle B, Marmorstein LY, Urban Z. Fibulin-4: a novel gene for an autosomal recessive cutis laxa syndrome. *Am J Hum Genet* 2006;**78**:1075-1080.
15. Renard M, Holm T, Veith R, Callewaert BL, Ades LC, Baspinar O, Pickart A, Dasouki M, Hoyer J, Rauch A, Trapane P, Earing MG, Coucke PJ, Sakai LY, Dietz HC, De Paepe AM, Loeyes BL. Altered TGFbeta signaling and cardiovascular manifestations in patients with autosomal recessive cutis laxa type I caused by fibulin-4 deficiency. *Eur J Hum Genet* 2010;**18**:895-901.
16. Roussin I, Sheppard MN, Rubens M, Kaddoura S, Pepper J, Mohiaddin RH. Cardiovascular complications of cutis laxa syndrome: successful diagnosis and surgical management. *Circulation* 2011;**124**:100-102.
17. Hanada K, Vermeij M, Garinis GA, de Waard MC, Kunen MG, Myers L, Maas A, Duncker DJ, Meijers C, Dietz HC, Kanaar R, Essers J. Perturbations of vascular homeostasis and aortic valve abnormalities in fibulin-4 deficient mice. *Circ Res* 2007;**100**:738-746.
18. Moltzer E, te Riet L, Swagemakers SM, van Heijningen PM, Vermeij M, van Veghel R, Bouhuizen AM, van Esch JH, Lankhorst S, Ramnath NW, de Waard MC, Duncker DJ, van der Spek PJ, Rouwet EV, Danser AH, Essers J. Impaired vascular contractility and aortic wall degeneration in fibulin-4 deficient mice: effect of angiotensin II type 1 (AT1) receptor blockade. *PLoS One* 2011;**6**:e23411.
19. van Deel ED, de Boer M, Kuster DW, Boontje NM, Holemans P, Sipido KR, van der Velden J, Duncker DJ. Exercise training does not improve cardiac function in compensated or decompensated left ventricular hypertrophy induced by aortic stenosis. *J Mol Cell Cardiol* 2011;**50**:1017-1025.
20. El-Hallous E, Sasaki T, Hubmacher D, Getie M, Tiedemann K, Brinckmann J, Batge B, Davis EC, Reinhardt DP. Fibrillin-1 interactions with fibulins depend on the first hybrid domain and provide an adaptor function to tropoelastin. *J Biol Chem* 2007;**282**:8935-8946.
21. Habashi JP, Judge DP, Holm TM, Cohn RD, Loeyes BL, Cooper TK, Myers L, Klein EC, Liu G, Calvi C, Podowski M, Neptune ER, Halushka MK, Bedja D, Gabrielson K, Rifkin DB, Carta L, Ramirez F, Huso DL, Dietz HC. Losartan, an AT1 antagonist, prevents aortic aneurysm in a mouse

- model of Marfan syndrome. *Science* 2006;**312**:117-121.
22. Berry CJ, Miller JD, McGroary K, Thedens DR, Young SG, Heistad DD, Weiss RM. Biventricular adaptation to volume overload in mice with aortic regurgitation. *J Cardiovasc Magn Reson* 2009;**11**:27.
 23. Stypmann J, Glaser K, Roth W, Tobin DJ, Petermann I, Matthias R, Monnig G, Haverkamp W, Breithardt G, Schmahl W, Peters C, Reinheckel T. Dilated cardiomyopathy in mice deficient for the lysosomal cysteine peptidase cathepsin L. *Proc Natl Acad Sci U S A* 2002;**99**:6234-6239.
 24. Nakanishi M, Harada M, Kishimoto I, Kuwahara K, Kawakami R, Nakagawa Y, Yasuno S, Usami S, Kinoshita H, Adachi Y, Fukamizu A, Saito Y, Nakao K. Genetic disruption of angiotensin II type 1a receptor improves long-term survival of mice with chronic severe aortic regurgitation. *Circ J* 2007;**71**:1310-1316.
 25. Zhou YQ, Zhu SN, Foster FS, Cybulsky MI, Henkelman RM. Aortic regurgitation dramatically alters the distribution of atherosclerotic lesions and enhances atherogenesis in mice. *Arterioscler Thromb Vasc Biol*; **30**:1181-1188.
 26. Mujumdar VS, Tyagi SC. Temporal regulation of extracellular matrix components in transition from compensatory hypertrophy to decompensatory heart failure. *Journal of hypertension* 1999;**17**:261-270.
 27. Vracko R, Thorning D, Frederickson RG. Spatial arrangements of microfibrils in myocardial scars: application of antibody to fibrillin. *J Mol Cell Cardiol* 1990;**22**:749-757.
 28. Keane MG, Pyeritz RE. Medical management of Marfan syndrome. *Circulation* 2008;**117**:2802-2813.
 29. Hartog AW, Franken R, Zwinderman AH, Groenink M, Mulder BJ. Current and future pharmacological treatment strategies with regard to aortic disease in Marfan syndrome. *Expert Opin Pharmacother* 2012;**13**:647-662.
 30. Thakur V, Rankin KN, Hartling L, Mackie AS. A systematic review of the pharmacological management of aortic root dilation in Marfan syndrome. *Cardiol Young* 2013;**23**:568-581.



Supplemental Figure 1. Fibulin-4 protein expression is reduced in left ventricles of Fibulin-4^{+/R} and Fibulin-4^{R/R} mice. Compared to Fibulin-4^{+/+} animals, fibulin-4 levels were 42% and 55% reduced in Fibulin-4^{+/R} mice corrected for loading control β -actin and coomassie staining respectively and 48% reduced corrected for β -actin and 62% when corrected for coomassie staining in Fibulin-4^{R/R} animals, n=3 in all groups.



Supplemental Figure 2. Fibulin-4 in the extracellular matrix of iPSC-derived cardiomyocytes in culture. Cultured human iPSC-derived cardiomyocytes stained for fibulin-4 protein (Red) and the cardiomyocyte marker, α -myosin heavy chain (yellow). Nuclei are counter-stained with DAPI (blue) (White bar represent 200 μ m).



Table 1

Anatomical and functional data of Fibulin-4^{+/+} and Fibulin-4^{R/R} mice

	Fibulin-4 ^{+/+}	Fibulin-4 ^{R/R}
Anatomical data		
Body weight (g)	24,7 ± 0.8	23.8 ± 1.0
Tibia length (cm)	1.82 ± 0.01	1.80 ± 0.01
LV weight (mg)	89 ± 3	218 ± 16*
RV weight (mg)	22 ± 1	47 ± 4*
Lung weight (mg)	131 ± 2	162 ± 4*
Heart weight / body weight (mg/g)	4.5 ± 0.1	9.8 ± 0.7*
Functional data		
Heart Rate (bpm)	575 ± 5	555 ± 13
MAP (mmHg)	91 ± 2	69 ± 5*
LV dp/dt _{max} (mmHg·s ⁻¹)	10770 ± 300	4650 ± 330*
LVEDP (mmHg)	3.4 ± 0.4	12.1 ± 2.0*
tau (ms)	9.5 ± 0.8	13.4 ± 2.7

Fibulin-4^{+/+} (n=16), Fibulin-4^{R/R} (n=6), *P<0.05 vs Fibulin-4^{+/+}. LV, left ventricle; RV, right ventricle; MAP, mean arterial pressure; LVEDP, LV end diastolic pressure.

Table 2 (next page)

Anatomical and functional data of Fibulin-4^{+/+} and Fibulin-4^{+R} mice

		Fibulin-4 ^{+/+}	Fibulin-4 ^{+/R}
Anatomical data			
Body weight (g)	sham	29.4 ± 0.6	29.6 ± 0.5
	mTAC	28.7 ± 1.1	28.9 ± 0.7
Tibia length (cm)	sham	1.85 ± 0.01	1.83 ± 0.02
	mTAC	1.85 ± 0.01	1.84 ± 0.01
LV weight (mg)	sham	102 ± 4	101 ± 5
	mTAC	150 ± 5†	164 ± 7†
RV weight (mg)	sham	26 ± 2†	25 ± 1†
	mTAC	28 ± 2†	31 ± 2†
Lung weight (mg)	sham	139 ± 3	141 ± 3
	mTAC	165 ± 15†	187 ± 16†
Heart weight / body weight (mg/g)	sham	4.3 ± 0.1	4.3 ± 0.2
	mTAC	6.0 ± 0.2*	6.7 ± 0.3*†
Functional data			
Heart Rate (bpm)	sham	580 ± 9	572 ± 9
	mTAC	555 ± 15	550 ± 11
MAP prox (mmHg)	sham	90 ± 3	83 ± 5
	mTAC	84 ± 5	79 ± 4
ΔSPG (%)	sham	1 ± 2	-1 ± 4
	mTAC	81 ± 7†	89 ± 8†
LV dp/dt _{max} (mmHg·s ⁻¹)	sham	10940 ± 480	10630 ± 500
	mTAC	8880 ± 590†	7620 ± 630†
tau (ms)	sham	9.8 ± 1.4	6.8 ± 0.2
	mTAC	9.8 ± 1.0	13.6 ± 1.6*†

CHAPTER 5

AT₁ Receptor Blockade, but not Renin Inhibition, Reduces Aneurysm Growth and Cardiac Failure in Fibulin-4 Mice

L. te Riet, E. D. van Deel, B. S. van Thiel, E. Moltzer, N. van Vliet, R. Y. Ridwan, R. van Veghel, P. M. van Heijningen, J. L. Robertus, I. M. Garrelds, M. Vermeij, I. van der Pluijm, A. H. J. Danser, J. Essers

(Journal of Hypertension 2016 Jan 29)

ABSTRACT

Aims: Increasing evidence supports a role for the angiotensin (Ang) II-AT₁ receptor axis in aneurysm development. Here we studied whether counteracting this axis via stimulation of AT₂ receptors is beneficial. Such stimulation occurs naturally during AT₁ receptor blockade with losartan, but not during renin inhibition with aliskiren.

Methods and Results: Aneurysmal homozygous Fibulin-4^{R/R} mice, displaying a 4-fold reduced fibulin-4 expression, were treated with placebo, losartan, aliskiren, or the β -blocker propranolol from day 35-100. Their phenotype includes cystic media degeneration, aortic regurgitation, left ventricular (LV) dilation, reduced ejection fraction, and fractional shortening. While losartan and aliskiren reduced hemodynamic stress and increased renin similarly, only losartan increased survival. Propranolol had no effect. No drug rescued elastic fiber fragmentation in established aneurysms, although losartan did reduce aneurysm size. Losartan also increased ejection fraction, decreased LV diameter, and reduced cardiac pSmad2 signaling. None of these effects were seen with aliskiren or propranolol. Longitudinal microCT measurements, a novel method in which each mouse serves as its own control, revealed that losartan reduced LV growth more than aneurysm growth, presumably because the heart profits both from the local (cardiac) effects of losartan and its effects on aortic root remodeling.

Conclusions: Losartan, but not aliskiren or propranolol, improved survival in Fibulin-4^{R/R} mice. This most likely relates to its capacity to improve structure and function of both aorta and heart. The absence of this effect during aliskiren treatment, despite a similar degree of blood pressure reduction and renin-angiotensin system blockade, suggests that it might be due to AT₂ receptor stimulation.

CONDENSED ABSTRACT

Treatment of thoracic aortic aneurysms (TAAs) is aimed at lowering hemodynamic stress. Increasing evidence supports a role for renin-angiotensin system blockade in TAA treatment. To what degree this is related to suppression of the angiotensin II-angiotensin II type 1 receptor (AT₁R) axis, or stimulation of angiotensin II type 2 receptors (AT₂R) is controversial. By comparing the effects of the AT₁R blocker losartan (allowing selective AT₂R stimulation) and the renin inhibitor aliskiren (preventing AT₁R and AT₂R stimulation) in a TAA mouse model, this study supports the latter. Indeed, only losartan improved survival, by stabilizing aortic growth, reducing aortic distensibility, and improving cardiac function and structure, independently of its effect on blood pressure.

INTRODUCTION

Thoracic aorta aneurysms (TAA) show degeneration of the medial layer of the aortic wall, characterized by elastic fiber fragmentation, loss of smooth muscle cells, and the accumulation of amorphous extracellular matrix¹. Such aortic wall degeneration is often a consequence of inherited connective tissue disorders. The most common inherited TAA disease, Marfan syndrome (MFS), is due to a mutation in the *FBN1* gene, which encodes the extracellular matrix (ECM) glycoprotein fibrillin-1. *FBN1* mutations result in a disorganized ECM assembly in the aortic wall², leading to all above described key features of TAA in MFS patients. Mice heterozygous for a cysteine substitution in an epidermal growth factor-like domain of fibrillin-1 (*Fbn1*^{C1039G/+} mice), i.e., a mutation which is prototypical for the *FBN1* mutations in humans, similarly develop TAA³.

Another factor in the elastic fiber assembly of the vessel wall, heart valves and myocardial interstitium, is the ECM protein fibulin-4, encoded by the *FBLN4* gene^{4,5}. In humans, a mutation in this gene causes cutis laxa syndrome, that besides cutis laxa (loose skin), bone fragility and lung emphysema is characterized by vascular tortuosity and aneurysms similar to those observed in MFS⁶⁻¹¹. Moreover, mice with a systemic 4-fold reduced fibulin-4 expression (Fibulin-4^{R/R}) share similar key features as seen in MFS and cutis laxa syndrome, i.e., cystic media degeneration, aortic regurgitation, and impaired cardiac morphology and function^{12,13}, while complete fibulin-4 gene knock-out mice (Fibulin-4^{-/-}) die perinatally from aortic rupture¹⁴.

Recent studies have shown that transforming growth factor (TGF) β signaling is upregulated in TAAs of MFS^{13,15,16}. While direct regulators of TGF β signaling include TGF β and bone morphogenetic protein ligands, indirect stimulation of TGF β signaling is accomplished by angiotensin (Ang) II, via its type 1 receptor (AT₁R). In support of this concept, both TGF β -neutralizing antibodies and the AT₁R blocker losartan exerted beneficial effects in rodent TAA models, including Fibulin-4^{R/R} mice when treated prenatally^{13,15}. Yet, clinical studies with losartan in MFS did not yield uniformly positive results^{17,18}. Blocking AT₁R results in a counterregulatory rise in renin, thereby increasing Ang II levels. This Ang II cannot stimulate the blocked AT₁R, but it may still bind to the unoccupied Ang II type 2 receptors (AT₂R), which antagonizes AT₁R-mediated effects^{19,20}. Such AT₂R stimulation is potentially beneficial in TAA²⁰, and will not occur during other forms of renin-angiotensin system (RAS) blockade, i.e., inhibition of the enzymes that generate Ang I (renin) or Ang II (ACE).

In the present study, we hypothesized that losartan outperforms the renin inhibitor aliskiren in the treatment of Fibulin-4^{R/R} mice, given its additional AT₂R-stimulating effects. Both drugs were compared with placebo and the β -blocker propranolol, a MFS drug that is often used in the clinic because it is expected to reduce heart rate, blood pressure and dP/dt. ACE inhibitors were not included, since such drugs, in addition to suppressing Ang II, also increase bradykinin, thus introducing interference with yet another hormonal system. Treatment started postnatally at a clinically relevant age: day 35, when the aneurysm is already present, and lasted up to 100 days. Moreover, we used a novel in-vivo μ CT-technique allowing longitudinal measurement that monitors the therapeutic treatment effects on both aneurysm progression as well as cardiac growth in time simultaneously. Our data show that losartan, but not aliskiren or propranolol, independently of its blood pressure-lowering effect, improved survival in Fibulin-4^{R/R} mice. The absence of this effect during aliskiren treatment suggests that it might involve AT₂R stimulation.

METHODS

Experimental animals

Generation of Fibulin-4^{R/R} mice has been described previously¹². Heterozygous (Fibulin-4^{+R}) mice in a mixed C57Bl/6x129 background were mated to obtain Fibulin-4^{+/+} (wild-type) and Fibulin-4^{R/R} littermates. Animals were housed in the institutional animal facility. Both males and females were included in the study, and since no apparent sex-related differences were observed, data from both sexes were pooled. All experiments were performed under the regulation and permission of the Animal Care Committee of the Erasmus MC, Rotterdam, The Netherlands (protocol number 139-11-09 and 139-13-11). The investigation conforms to the *Guide for the Care and Use of Laboratory Animals* published by the US National Institutes of Health (NIH Publication, revised 2011).

Treatment

Fibulin-4^{R/R} mice and wild-type mice were treated postnatally from the age of 35 days up to 100 days with placebo, losartan (60 mg/kg p.o. per day; a kind gift of MSD, Haarlem, The Netherlands), aliskiren (62.5 mg/kg p.o. per day; a kind gift of Novartis Pharmaceuticals, Basel, Switzerland), or propranolol (50 mg/kg p.o. per day; Sigma, St. Louis, USA) in drinking water, as described before^{13, 15, 21, 22}.

Histology

Mice (age 100 days) were weighed, euthanized by an overdose of CO₂, and necropsied according to standard protocols. Perfusion-fixed aortas and hearts were isolated and paraffin-embedded. Next, 4 µm-aorta sections were haematoxylin and eosin (HE)-stained, stained for elastin (Verhoeff van Gieson), glycosaminoglycans (Alcian Blue) or vascular smooth muscle cells (VSMCs, α-smooth muscle actin). Immunohistochemistry for phosphorylated Smad2 (pSmad2) was performed as described previously²³, using rabbit antiphospho-smad2 antibodies (Cell Signaling Technology, Danvers, USA). Positively stained pSmad2 nuclei were divided by the total number of nuclei to obtain relative amounts. HE-stained aorta slides were scanned with a nanozoomer (Hamamatsu, Almere, The Netherlands), and subsequently aortic wall diameter and aortic wall area were analyzed with NanoZoomer Digital Pathology view (Hamamatsu). Finally, 5-µm heart sections were stained with Gomori's silver staining to visualize individual cardiomyocytes of the left ventricle (LV)²⁴. Only transversally cut cells showing a nucleus were used to determine the cardiomyocyte area.

Biochemical measurements

RAS components were measured in kidneys (Ang II) and blood plasma (renin). Blood was collected from the left ventricle immediately prior to euthanization in heparin-coated tubes, centrifuged at 5500 RPM, and plasma was stored at -80°C. Kidneys were removed after the animals had been euthanized, frozen in liquid nitrogen, and stored at -80°C. Tissue Ang II was measured by radioimmunoassay, after SepPak extraction and reversed-phase HPLC separation as previously described^{25, 26}. Plasma renin concentration (PRC) was determined by enzyme-kinetic assay in the presence of excess angiotensinogen as described before²⁶. Additionally, B-type natriuretic peptide-45 (BNP-45) was measured in plasma, making use of a commercially available enzyme immuno-assay (Phoenix Pharmaceuticals Inc., Karlsruhe, Germany).

Ultrasound and hemodynamic measurements

To evaluate the treatment of the different compounds on aneurysm formation and cardiac function, cardiac geometry, echocardiographic and hemodynamic measurements were performed in 100-days old Fibulin-4^{+/+} (wild type) and Fibulin-4^{R/R} mice. Mice were anesthetized with 2.5% isoflurane and ventilated with 35% O₂. Anesthesia did not affect heart rate (data not shown). Echocardiography of the ascending aorta and LV was performed using a Vevo2100 (VisualSonics Inc., Toronto, Canada). Ascending aorta and LV lumen diameter, aortic

distensibility, ejection fraction and fractional shortening were obtained from M-Mode images. Ejection fraction and fractional shortening were defined as the relative differences between end-diastolic and end-systolic volumes and diameter, respectively¹³. Subsequently, a 1.4-Fr microtipped manometer (Millar Instruments, Houston, USA) was inserted into the right carotid artery to measure aortic pressure²⁷. Hemodynamic data were recorded and digitized using an online 4-channel data acquisition program (ATCODAS, Dataq Instruments, Akron, USA), analysis was performed with a program written in Matlab²⁸. Ten consecutive beats were selected for determination of systolic and diastolic blood pressure, subsequent mean arterial pressures (MAP) were calculated.

Western blot

LV tissue samples were used for immunoblotting of extracellular signal-regulated kinases (ERK1/2), phosphorylated ERK1/2 (pERK1/2), Smad2 and pSmad2 (Cell Signaling Technology). Ratios of phosphorylated protein levels to loading control β -actin were calculated and corrected for the ratios in wild-type mice.

Quantitative real-time reverse transcription polymerase chain reaction

Expression of angiotensin II type 1a, type 1b and type 2 receptors (AT_{1a}R, AT_{1b}R and AT₂R) was analyzed in LV tissue. Total RNA was isolated using RNeasy Fibrous Tissue Mini Kit (Qiagen, Hilden, Germany) and reverse transcribed using iScript cDNA Synthesis Kit (Bio-Rad, Veenendaal, The Netherlands). cDNA samples were subjected to 40 cycles real-time PCR analysis using SYBR Green qPCR Master Mix 2x (Bio-Rad) and primers; β -actin 5'-AGCCATGTACGTAGCCATCCA-3'; 5'-TCTCCGGAGTCCATCACAATG-3'; β_2 -microglobulin 5'-CTCACACTGAATTCACCCCA-3'; 5'-GTCTCGATCCCAGTAGACGGT-3'; AT_{1a}R 5'-CCCACGTGTCCTGTACTAC-3'; 5'-TTTGGGGACAGTACAGTTTC-3'; AT_{1b}R 5'-CTGTGAAATTGCGGACGTAGT-3'; 5'-AAGCCATAAAACAGAGGGTTCAG-3'; AT₂R 5'-TACCCGTGACCAAGTCTGA-3'; 5'-TACCCATCCAGGTCAGAGCA-3'. Gene expression was calculated using β -actin and β_2 -microglobulin as housekeeping genes and the comparative Ct method ($\Delta\Delta$ Ct) was used for relative quantification of gene expression.

FMT-CT Imaging

We used vascular Computed Tomography (CT) and fluorescent mediated tomography (FMT)-CT imaging with near-infrared fluorescent protease activatable probes as previously described²⁹. In short, mice subjected to FMT-CT were shaved and depilated to remove all hair that otherwise would absorb light and interfere with optical imaging. Mice subjected to vascular CT and FMT-CT mice received 5 mL/kg body weight Exia 160 contrast agent (Binitio Biomedical Inc., Ottawa, Canada) through injection in the tail vein for subsequent CT analysis. Mice only subjected to vascular CT imaging were anesthetized (2.5% isoflurane) and scanned directly with the micro-CT scanner (Quantum FX system, Perkin Elmer Inc., Akron, USA). The thoracic aorta diameter, thoracic aortic volume and left ventricular volume were analyzed with a rendering program 'microCT Tools by Analyze 11.0 software' (AnalyzeDirect Inc., Overland Park, USA). Fibulin-4 mice which were also subjected to FMT imaging, were scanned with an FMT 2500 system (Perkin Elmer Inc.) at 680 nm excitation and emission wavelengths, at 24 hours after tail vein injection of 5 nmol of MMPsense 680 (Perkin Elmer Inc.). Mice were anesthetized (2.5% isoflurane) and fixed into the portable animal imaging cassette that lightly compressed the anesthetized mouse between optically translucent windows, thereby preventing motion during FMT and CT imaging. After FMT imaging, anesthetized mice were scanned with the micro-CT scanner to identify heart and aortic root region of the animals. After FMT-CT imaging, complete aortas were harvested and fluorescence was quantified using the FMT 2500 and Odyssey imaging systems (LI-COR Inc.). Near infrared images were obtained in the 680 nm channel.

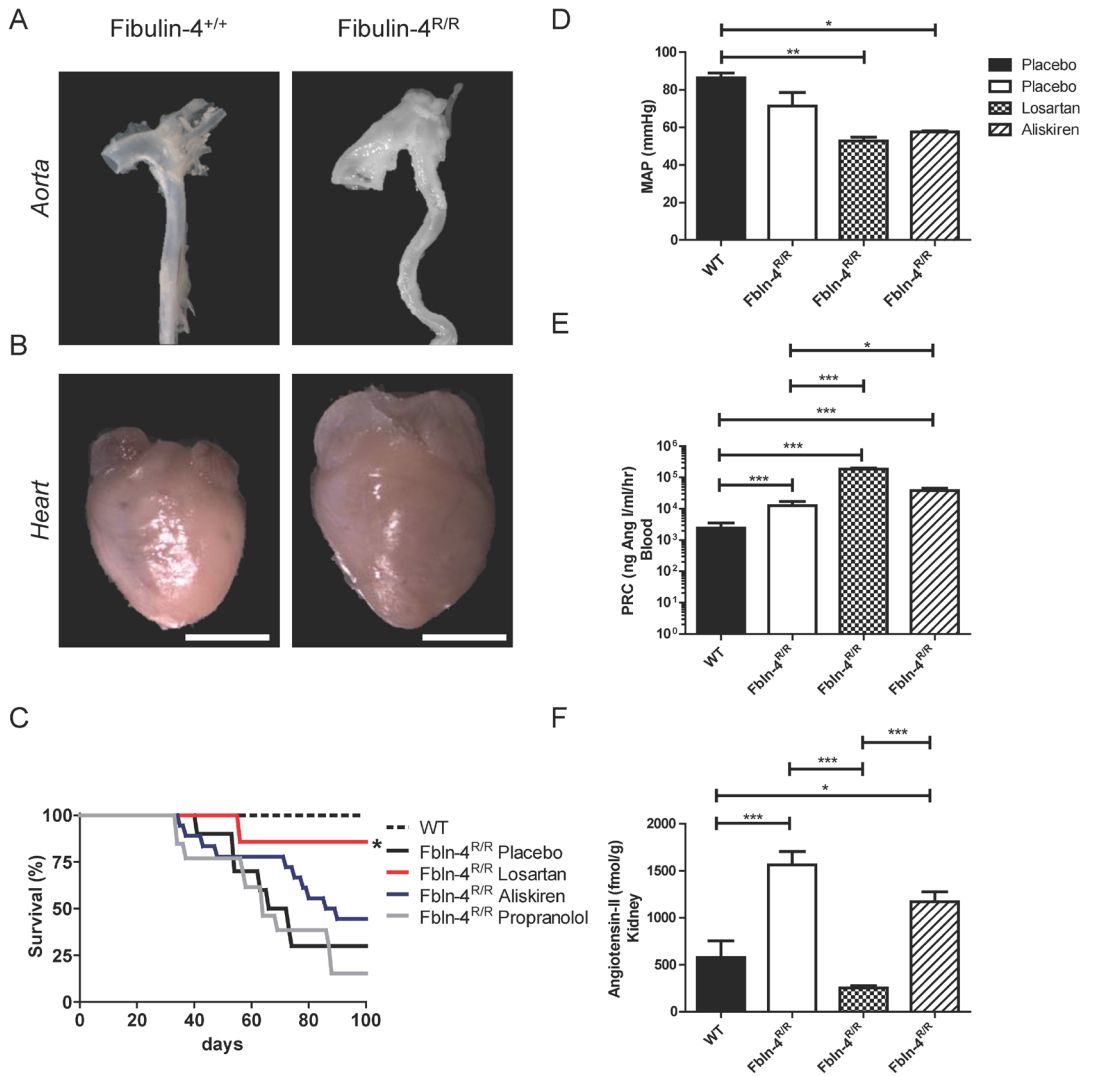


Figure 1

(A-B) Reduced fibulin-4 expression results in thoracic aorta aneurysms and cardiac hypertrophy in 100-day old Fibulin-4^{R/R} mice (white bars represent 4 mm). (C) Kaplan-Meier survival curves of WT and treated Fibulin-4^{R/R} mice (n=7-19). *P<0.05 vs. placebo. (D-F) Mean arterial pressure (MAP; n=3-5), plasma renin concentration (PRC; n=10-18), and renal angiotensin II levels (n=5) in Fibulin-4^{R/R} mice treated for 65 days with placebo, losartan, aliskiren or propranolol vs. untreated age-matched WT mice. Data are mean±SEM. *P<0.05, **P<0.01, ***P<0.001.

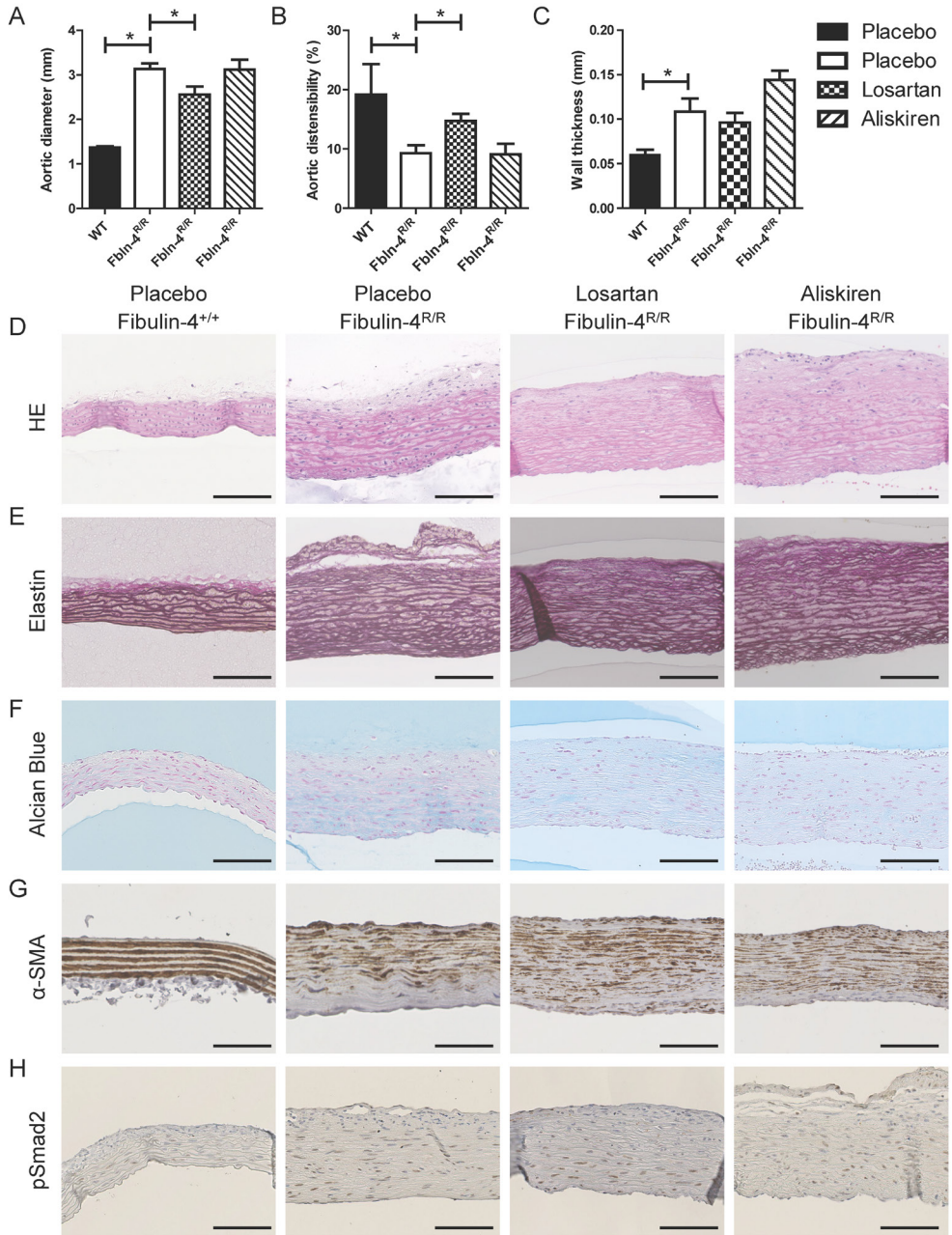


Figure 2

(A-C) Aortic diameter, distensibility and wall diameter in Fibulin-4^{R/R} mice treated for 65 days with placebo, losartan or aliskiren vs. age-matched untreated WT mice (mean±SEM of n=6-10) (black bars represent 100 μm); *P<0.05 vs. placebo. Treatment did not affect aortic wall morphology (D), elastic fiber fragmentation (E), extracellular matrix deposition (Alcian Blue) (F), α-smooth muscle actin (SMA) deposition (G), or pSmad2-signaling (H).

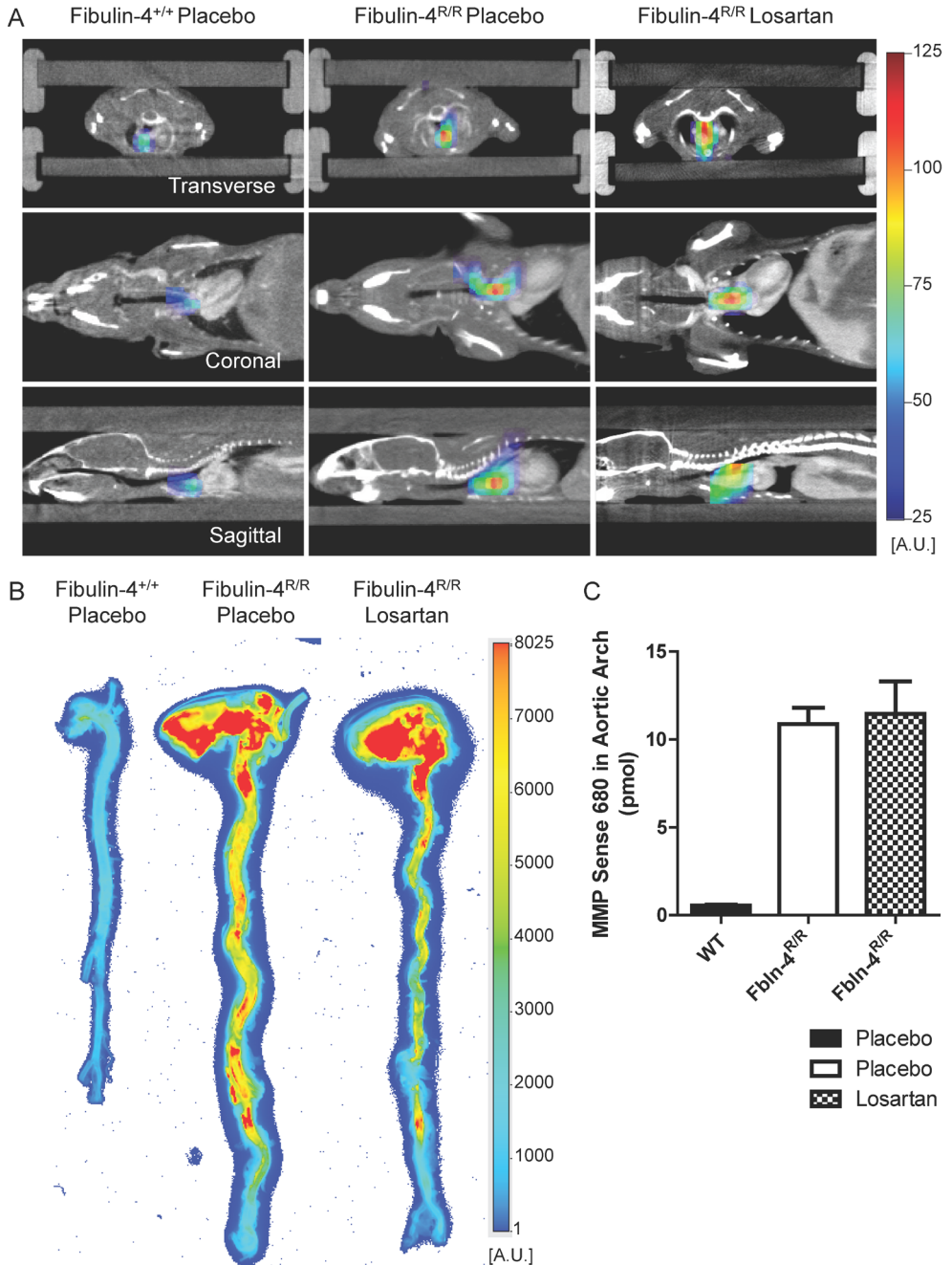


Figure 3

(A) In-vivo three-dimensional FMT-CT co-registration of heart and aorta in Fibulin-4^{R/R} mice treated for 65 days with placebo or losartan vs. age-matched untreated WT mice, after injection of MMPsense 680 to determine matrix metalloproteinase (MMP) activity. (B) MMP activity determined ex-vivo in whole aortas, and (C) its quantification (mean±SEM of n=2).

Data analysis

Normally distributed data are presented as mean±SEM. One-way ANOVA was applied for the analysis between groups, followed by a post-hoc Dunnett's test when appropriate. All statistical tests were two-sided and $P < 0.05$ was considered statistically significant.

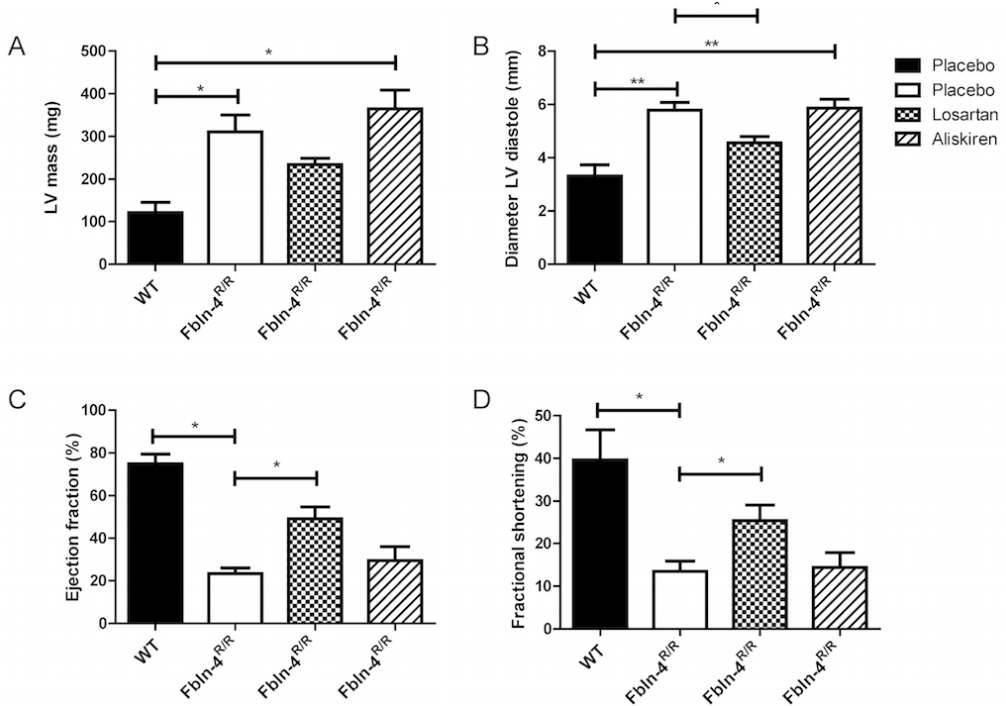


Figure 4

A-D) Left ventricular (LV) mass, LV diameter, ejection fraction and fractional shortening determined by in-vivo transthoracic echocardiography in Fibulin-4^{R/R} mice treated for 65 days with placebo, losartan or aliskiren vs. age-matched untreated WT mice (mean±SEM of $n=6-10$). * $P < 0.05$, ** $P < 0.01$.

RESULTS

Losartan increases survival of adult Fibulin-4^{R/R} animals independently of its effect on blood pressure and the degree of RAS blockade

Reduced fibulin-4 expression resulted in severe TAA, cardiac hypertrophy, and diminished survival (Figures 1A-1B), in full agreement with previous observations^{12,13}. Losartan, but not aliskiren treatment, significantly improved survival (Figures 1C). Propranolol even tended to diminish survival ($P=0.25$), and no animal survived up to 100 days with this treatment. As a consequence, blood pressure data could not be obtained in propranolol-treated mice, and in only 3 surviving aliskiren-treated mice versus 5 losartan-treated mice. MAP tended to be diminished in Fibulin-4^{R/R} mice ($P=0.17$). Both RAS blockers similarly reduced MAP at 100 days (Figure 1D). PRC

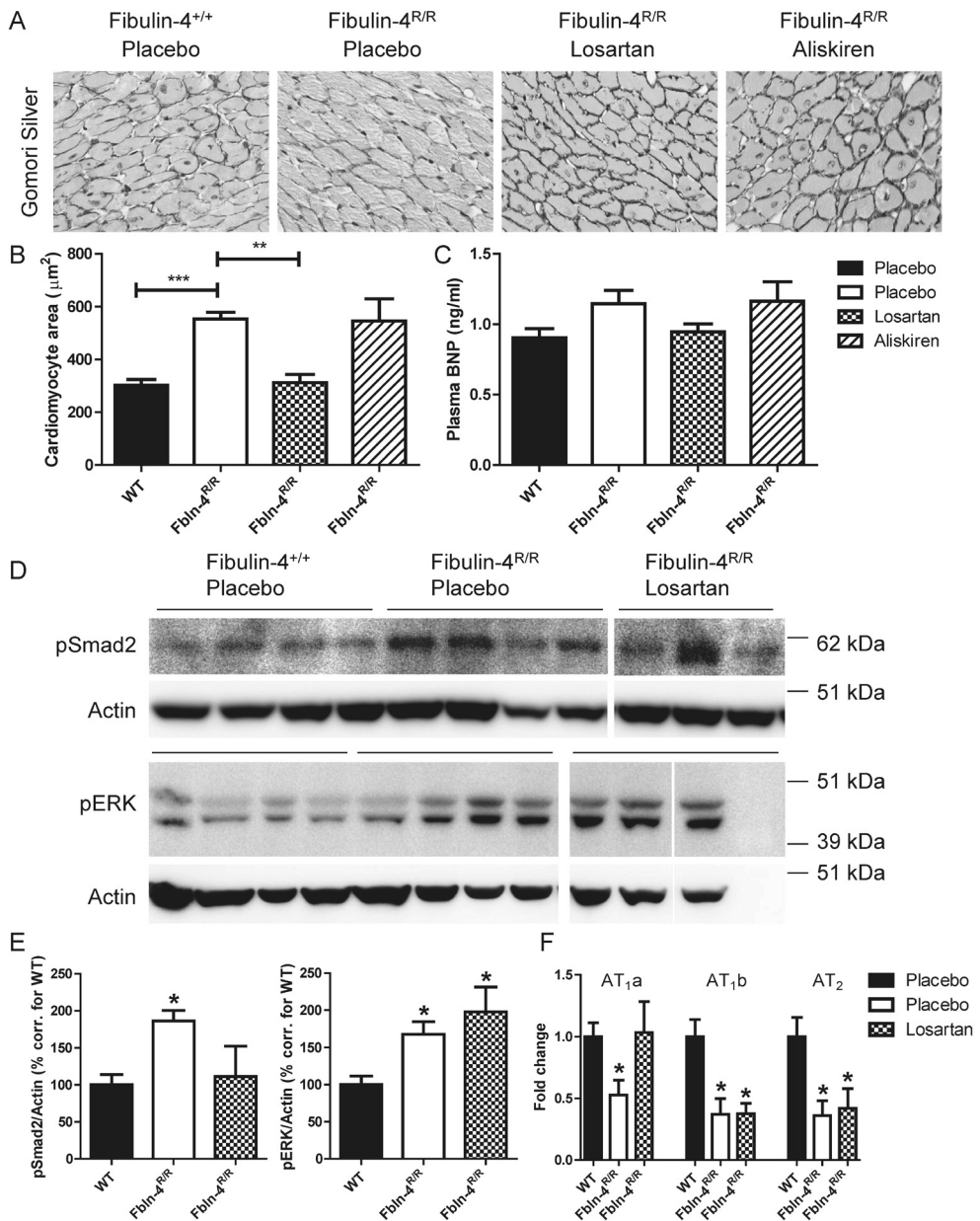


Figure 5

(A-B) Cardiomyocyte area (n=5-12; panel A shows a representative example) and (C) plasma brain natriuretic peptide (BNP; n=10-18) levels in Fibulin-4^{R/R} mice treated for 65 days with placebo, losartan or aliskiren vs. age-matched untreated WT mice. Data are mean±SEM, **P<0.01, ***P<0.001 vs. WT or placebo. (D-E) pSmad2, pERK, and β -actin protein levels in hearts of Fibulin-4^{R/R} mice treated for 65 days with placebo or losartan vs. age-matched untreated WT mice (n=3-4). *P<0.05 vs. WT. (F) Relative gene expression of LV Ang II receptors (n=3-10). *P<0.05 vs. WT.

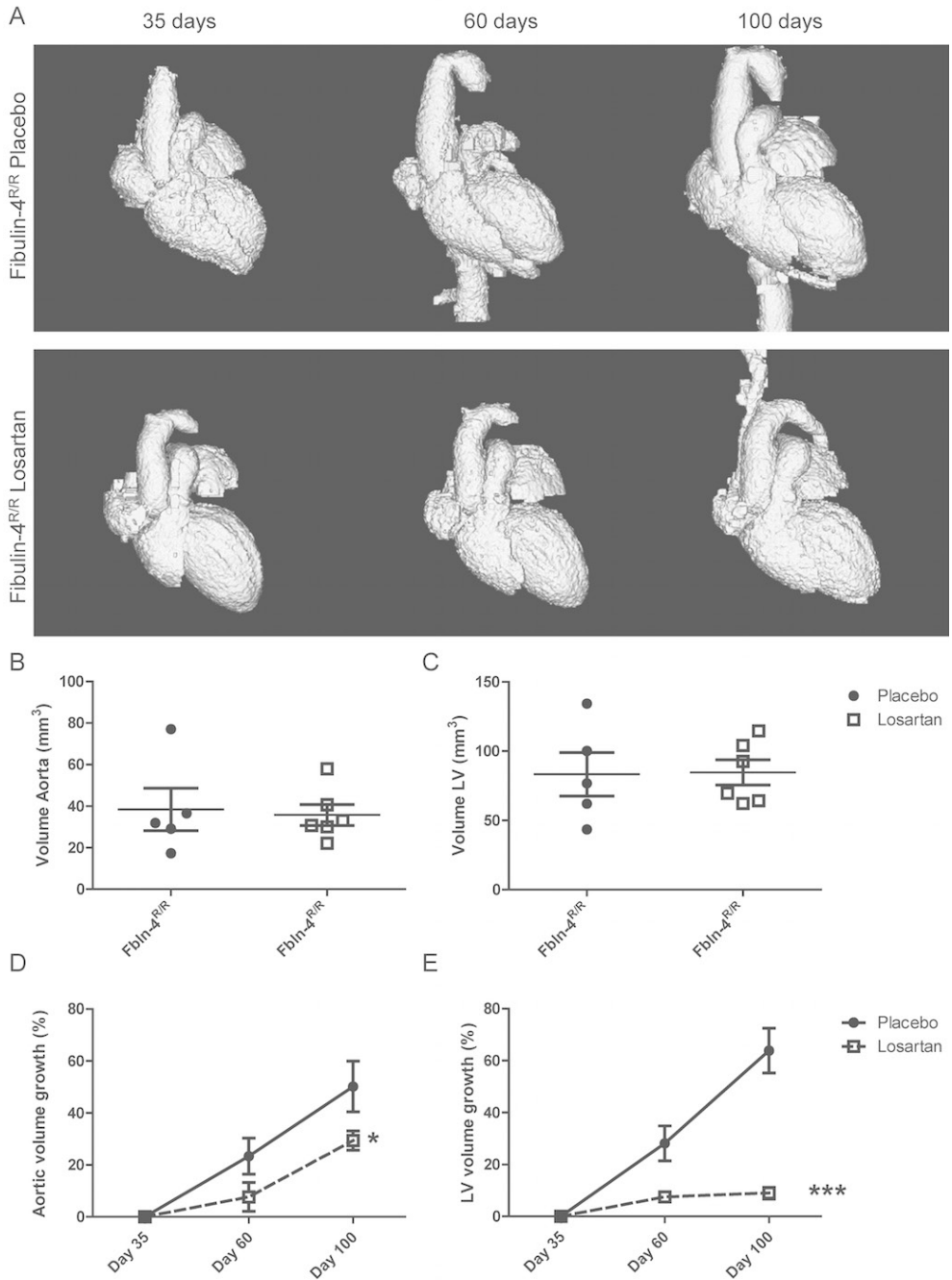


Figure 6
 A) 3D overview of CT-angiography with contrast agent Exia160. (B-C) Aortic and LV volume of placebo and losartan treated Fibulin-4^{R/R} mice at baseline. (D-E) Percentage growth of ascending aortas and left ventricle (LV). Data are mean±SEM of n=4-6. *P<0.05, ***P<0.001 vs. placebo.

and renal Ang II were higher in fibulin-4^{R/R} mice than in wild-type animals (Figures 1E-1F). Losartan and aliskiren comparably increased PRC versus placebo, suggesting a similar degree of RAS blockade. Losartan, but not aliskiren, additionally suppressed renal Ang II.

Losartan improves aneurysm size and aortic distensibility without affecting structural changes and matrix metalloproteinases (MMPs)

At the age of 100 days, the ascending aortic diameter in Fibulin-4^{R/R} mice was almost 3 times enlarged compared to wild-type mice (Figure 2A). This widening was accompanied by an approximately 50% decrease in distensibility (Figure 2B) and an increased wall thickness (Figure 2C). Losartan improved diameter and distensibility without affecting thoracic aortic wall thickness, whereas aliskiren had no significant effect on any of these parameters (Figures 2A-2C). For reasons discussed above, similar data could not be obtained for propranolol. Neither losartan nor aliskiren affected the disturbed aortic wall morphology, the severe alterations in elastic fiber organization, or the increased glycosaminoglycan deposition in Fibulin-4^{R/R} mice (Figures 2D-2F). These drugs also did not significantly improve the reduced VSMC content, or diminish the increased pSmad2-signaling in these animals (Figures 2G-2H). Non-canonical (pERK) TGFβ signaling was similarly unaffected (data not shown).

In-vivo MMP activity, measured by 3D FMT-CT, was undetectable in aortas of wild-type mice, but greatly increased in the aortic arch of placebo- or losartan-treated Fibulin-4^{R/R} mice (Figure 3A). Abdominal aorta MMP measurements were inaccurate due to the high fluorescent signal from the liver. Removal of the aortas after sacrifice allowed ex-vivo imaging at much great sensitivity (Figure 3B), and confirmed the in-vivo observations. Losartan did not affect MMP activity as compared to placebo (Figure 3C). Consequently, MMP activity was not determined in aliskiren-treated mice.

Losartan improves cardiac morphology and function

Transthoracic echocardiography in placebo-treated Fibulin-4^{R/R} mice revealed a tripling of LV mass and a doubling of LV diameter versus wild-type mice (Figures 4A-4B) at the age of 100 days. Ejection fraction and fractional shortening were both greatly reduced (Figures 4C-4D). Losartan improved all parameters, although significance was not reached for LV mass. Aliskiren affected none of these parameters. Data for propranolol in 100-day old mice could not be obtained.

Losartan prevents cardiomyocyte hypertrophy and reduces canonical TGFβ signaling

Cardiomyocyte area doubled in Fibulin-4^{R/R} versus wild-type mice, and losartan (but not aliskiren) fully prevented this hypertrophic response (Figures 5A-5B). As expected, changes in plasma BNP paralleled this pattern, although no significant differences were observed for this parameter (Figure 5C). Both canonical (pSmad2) and non-canonical (pERK) TGFβ signaling were upregulated in hearts of Fibulin-4^{R/R} mice, but losartan reduced only the former to wild-type levels (Figure 5D-5E). Smad2 and ERK levels were identical under all conditions (data not shown). LV AT_{1a}R⁻, AT_{1b}R⁻, and AT₂R expression were downregulated in Fibulin-4^{R/R} mice versus wild-type mice, and losartan treatment exclusively normalized AT_{1a}R expression (Figure 5F). Unfortunately, due to scarcity of available tissue, similar data could not be obtained in aliskiren- or propranolol-treated mice.

Losartan prevents LV and aneurysm growth rate

We used a novel micro-CT method in combination with the vascular contrast agent Exia 160, yielding longitudinal 3D data sets in which each animal serves as its own baseline control (Figure 6A). At the start of treatment, both aortic volume and LV volume were not different in placebo- and losartan-treated Fibulin-4^{R/R} mice (Figures 6B-6C). Both volumes increased by approximately 60% during placebo treatment, and losartan largely (aortic volume), if not completely (LV volume) prevented this (Figures 6D-6E).

DISCUSSION

The present study shows that losartan, but not aliskiren or propranolol, increased survival in Fibulin-4^{R/R} mice, and that this predominantly related to its capacity to improve cardiac function and structure. Although losartan also stabilized aortic growth, these effects were more modest than its effects on LV growth, and they did not result in any change in aortic wall morphology, TGF β -signaling, or MMP-activity. Nevertheless, there was an improvement in aortic distensibility. The larger effects on the heart most likely reflect the fact that the heart profits both from the local (cardiac) effects of losartan and its effects on aortic root remodeling. Since none of these effects were seen with aliskiren, despite the fact that this RAS blocker lowered blood pressure and inhibited the RAS to the same degree as losartan, we conclude that they are blood pressure-independent, and that losartan exerts effects beyond blockade of the classical Ang II-AT₁R axis. This most likely concerns its unique capacity to induce AT₂R stimulation. A second possibility would be activation of the angiotensin-(1-7)-Mas receptor axis. However, a study making use of *Fbn1*^{C1039G/+} mice (an alternative, albeit less severe, TAA model) supports the former only, since it observed no effect of an ACE inhibitor, although such a drug, like an AT₁R blocker, activates the angiotensin-(1-7)-Mas receptor axis^{20,30}. Our study is the first to directly compare renin inhibition and AT₁R blockade in a mouse TAA model.

RAS activation, both in the circulation and at the tissue level, is an established characteristic of Fibulin-4^{R/R} mice^{13,31}. Given the low Ang II levels in the aorta and its relatively small size³², we measured Ang II in renal tissue to confirm the upregulated tissue RAS activity in this model. Increased Ang II levels will facilitate TGF β -signaling, which is known to be enhanced in patients and mice with MFS^{29,33-36}. In fact, increased serum TGF β levels correlated directly with aortic root dilation³³. In agreement with the causative role of Ang II, we showed in an earlier study that prenatal treatment with losartan successfully improved elastic fiber fragmentation and reduced vessel wall thickness in Fibulin-4^{R/R} mice¹³. Moreover, in mice that lack fibulin-4 in VSMCs (*Fbln4*^{SMKO} mice), aneurysm formation could be prevented completely when RAS blockade was started within a narrow therapeutic window during the first month of life³¹. In this latter study, ACE inhibition with captopril and losartan treatment were equally effective. Yet, in contrast with our study, no cardiac phenotype was reported in *Fbln4*^{SMKO} mice.

The present study in Fibulin-4^{R/R} mice now evaluated postnatal losartan versus aliskiren treatment, started on day 35, i.e., when aneurysm formation is already present. This is not only more clinically relevant, as treatment in TAA patients usually starts in the presence of an aneurysm, but also more realistic given the fact that such blockade is contraindicated during pregnancy. Propranolol, a classical MFS drug, was used as a comparator, but exerted no effect, in agreement with its lack of effect at the same dose (50 mg/kg p.o. per day) in *Fbn1*^{C1039G/+} mice¹⁵. All drugs were given orally, since the fragility of our model, resulting in a very low survival, was not compatible with the operation required to implant osmotic minipumps. Although aliskiren displays a low bioavailability³⁷, and is highly species-specific³⁸, it blocks mouse renin at the same concentration range as human renin³⁹. Consequently, by applying oral doses that were over 10 times higher than those used in humans (62.5 mg/kg p.o. per day versus 150-300 mg/day in humans), we were able, as in previous studies^{21,22}, to achieve a degree of RAS blockade that yielded the same blood pressure-lowering effects as losartan at 60 mg/kg p.o. per day. Importantly, as an indication of RAS blockade, losartan and aliskiren increased circulating renin similarly. Probably as a consequence of this rise in renin release, aliskiren did not significantly decrease renal Ang II. Similar observations were made previously in the rat kidney⁴⁰. Yet, losartan decreased renal Ang II, in agreement with the fact that tissue Ang II largely reflects Ang II that is bound to, or has been internalized via, AT₁R^{41,42}. Therefore, during losartan treatment, the reduction in tissue Ang II is an indication of the degree of AT₁R blockade. Unfortunately, we were unable to obtain comparable data for propranolol-treated mice, since none of these mice survived until the age of 100 days, i.e., the day of sacrifice for our RAS component measurements, at which timepoint blood pressure was measured. Nevertheless, it might be speculated that propranolol, given its modest renin-suppressing effects⁴³, did reduce Ang II. Long-term treatment with propranolol was feasible

in *Fbn1*^{C1039G/+} mice, in which aneurysm formation starts only at the age of 2 months^{3,44}. Propranolol affected blood pressure in *Fbn1*^{C1039G/+} mice to the same extent as losartan¹⁵. Even if this had also been the case in our model, e.g., based on Ang II reduction, this effect would have resembled that of aliskiren, i.e., it could not have resulted in enhanced AT₂R stimulation. Thus, once TAA are established, both renin suppression with propranolol and renin inhibition with aliskiren lack the beneficial effects of losartan. In contrast, when treatment is started before the onset of TAA, like in the *Fbln4*^{SMKO} mice model described above³¹, captopril yielded the same effects as losartan. Since captopril does not allow AT₂R stimulation, these data suggest that, at a very early stage of TAA, AT₁R are predominant, while at a later stage AT₂R may additionally come into play. This correlates well with the widely accepted phenomenon that AT₂Rs normally display low-to-undetectable levels, which increase only under pathological conditions, e.g., post-myocardial infarction, during hypertension-induced remodeling, and in heart failure⁴⁵⁻⁴⁷. Clearly, timing of treatment is of utmost importance, and different ages at the start of treatment (e.g. children/adolescents versus adults) may explain the success (or lack thereof) of different RAS blockers in clinical trials^{17,18,48}. Moreover, when classifying *FBN1* mutations into 'haploinsufficiency' (decreased amount of normal fibrillin-1), and 'dominant negative' (normal fibrillin-1 abundance with mutant fibrillin-1 incorporated in the matrix), Franken et al. observed that Marfan patients with haploinsufficient *FBN1* mutations were more responsive to losartan⁴⁹. Since the *Fbn1*^{C1039G/+} and Fibulin-4^{R/R} TAA models closely correspond with the haploinsufficiency situation, it appears that the underlying mutation is an additional determinant of the success of AT₁R blockade in Marfan patients. Taken together, simultaneous AT₂R stimulation may not always offer an additional advantage, and thus selective AT₂R agonists should not by definition be preferred over AT₁R antagonists.

Given the predominant effects of losartan on the heart, we focused on canonical (pSmad2) and non-canonical (pERK) TGFβ signaling in cardiac tissue. Both were upregulated in Fibulin-4^{R/R} mice, comparable to their upregulation in aortic tissue in *Fbln4*^{SMKO} and *Fbn1*^{C1039G/+} mice^{20,31}. Yet, although losartan suppressed both types of signaling in aortic tissue in these latter models, in the hearts of our mice only the canonical signaling was found to be suppressed after losartan, while no pSmad2 suppression was seen in the aortic wall (Figure 5E). These findings concur with the heart-specific effect of this AT₁R antagonist in our model, and suggest that the AT₂R stimulatory effects, if occurring, result in reduced canonical TGFβ signaling in the heart. Studies in transgenic animals support the concept that AT₂Rs are antihypertrophic and prevent remodeling^{50,51}. The lack of effect on pERK signaling in our Fibulin-4^{R/R} mice is in agreement with a recent study by Cook et al.⁵², who demonstrated that ERK1/2 activation peaks at a very early stage of the disease only, while pSmad2 remains elevated throughout the disease. From this perspective, effects of losartan on pERK1/2 are no longer expected after 100 days, simply because pERK1/2 is not activated anymore at that stage.

Gene expression studies in LV tissue revealed a reduction of all Ang II receptor types in Fibulin-4^{R/R} mice compared to wild type mice. It should be noted that mice, unlike humans, display two AT₁R subtypes, AT_{1a}R and AT_{1b}R, and that losartan blocks both AT₁Rs equally well. AT₁R downregulation is also known to occur in heart failure patients⁵³. It was not observed in the aortic arch or kidney of our Fibulin-4^{R/R} mice¹³, implying that its downregulation was cardiac-specific. Importantly, although the raw Ct values for the AT_{1b}R, the AT₂R and the housekeeping genes β-actin and β₂-microglobin were identical in LV tissue and aorta (B.S. van Thiel, data not shown), the raw Ct values for the AT_{1a}R in the LV were approximately 6 cycles lower than in the aorta. This suggests that AT_{1a}R expression in the heart greatly exceeds that in the aorta. Losartan treatment exclusively normalized cardiac AT_{1a}R expression in Fibulin-4^{R/R} mice. Such upregulation is a well-known physiological response to receptor antagonism, once again supporting effective AT_{1a}R blockade by losartan in the heart. Yet, it does not imply that AT_{1a}R activation had now normalized (due to the simultaneous presence of losartan), and thus predominant AT₂R stimulation by the elevated levels of Ang II during losartan treatment is still highly likely.

Our data are the first to show the losartan-induced stabilization of LV growth over time with longitudinal microCT measurements. Using each animal as its own baseline control, this novel approach enabled us to conclude that the effects of losartan on LV growth exceeded those on aortic growth. Combined with the FMT to co-regulate MMP-activity, this approach allows monitoring of cardiac and aortic remodeling in a unique, non-

invasive manner. It would also reduce the required number of animals. Given the major limitation of our animal model, i.e. a complicated breeding scheme and a high death rate resulting in low n-numbers, this is an important advantage.

In conclusion, losartan, but not aliskiren or propranolol, improved survival in Fibulin-4^{R/R} mice, by simultaneously stabilizing aortic growth, reducing aortic distensibility, and improving cardiac function and structure. The absence of these effects during aliskiren treatment, despite a similar reduction in blood pressure and degree of RAS blockade, suggests that it might be due to AT₂R stimulation and/or activation of the angiotensin-(1-7)/Mas receptor axis. Future studies, making use of AT₂R/Mas receptor knockout animals, AT₂R/Mas receptor antagonists (e.g., PD123319 and A779, respectively) or AT₂R/Mas receptor agonists (e.g., C21 and AVE0991, respectively) may help to substantiate this view. However, given the non-specific effects of the latter types of drugs^{54,55}, the possibility that AT₂R heterodimerize with Mas receptors⁵⁶, and the consequences of AT₂R deletion on cardiac development and remodeling⁵⁷, the results of such studies may not be straightforward. In addition, none of these approaches is currently feasible in humans.

ACKNOWLEDGMENTS

This work was supported through the use of imaging equipment provided by the Applied Molecular Imaging Erasmus MC facility. We also thank Lambert Speelman for his assistance with the Vevo2100 ultrasound. Funding: This work was supported by a Lijf en Leven grant (2008): 'Early Detection and Diagnosis of Aneurysms and Heart Valve Abnormalities'.

REFERENCES

- Isselbacher EM. Thoracic and abdominal aortic aneurysms. *Circulation* 2005;**111**:816-828.
- Dietz HC, Cutting GR, Pyeritz RE, Maslen CL, Sakai LY, Corson GM, Puffenberger EG, Hamosh A, Nanthakumar EJ, Curristin SM, Stetten G, Meyers DA, Francomano CA. Marfan-Syndrome Caused by a Recurrent Denovo Missense Mutation in the Fibrillin Gene. *Nature* 1991;**352**:337-339.
- Judge DP, Biery NJ, Keene DR, Geubtner J, Myers L, Huso DL, Sakai LY, Dietz HC. Evidence for a critical contribution of haploinsufficiency in the complex pathogenesis of Marfan syndrome. *J Clin Invest* 2004;**114**:172-181.
- Horiguchi M, Inoue T, Ohbayashi T, Hirai M, Noda K, Marmorstein LY, Yabe D, Takagi K, Akama TO, Kita T, Kimura T, Nakamura T. Fibulin-4 conducts proper elastogenesis via interaction with cross-linking enzyme lysyl oxidase. *Proc Natl Acad Sci U S A* 2009;**106**:19029-19034.
- Papke CL, Yanagisawa H. Fibulin-4 and fibulin-5 in elastogenesis and beyond: Insights from mouse and human studies. *Matrix Biol* 2014.
- Dasouki M, Markova D, Garola R, Sasaki T, Charbonneau NL, Sakai LY, Chu ML. Compound heterozygous mutations in fibulin-4 causing neonatal lethal pulmonary artery occlusion, aortic aneurysm, arachnodactyly, and mild cutis laxa. *Am J Med Genet A* 2007;**143A**:2635-2641.
- Hoyer J, Kraus C, Hammersen G, Geppert JP, Rauch A. Lethal cutis laxa with contractural arachnodactyly, overgrowth and soft tissue bleeding due to a novel homozygous fibulin-4 gene mutation. *Clin Genet* 2009;**76**:276-281.
- Huchtagowder V, Sausgruber N, Kim KH, Angle B, Marmorstein LY, Urban Z. Fibulin-4: a novel gene for an autosomal recessive cutis laxa syndrome. *Am J Hum Genet* 2006;**78**:1075-1080.
- Renard M, Holm T, Veith R, Callewaert BL, Ades LC, Baspinar O, Pickart A, Dasouki M, Hoyer J, Rauch A, Trapane P, Earing MG, Coucke PJ, Sakai LY, Dietz HC, De Paepe AM, Loeys BL. Altered TGFbeta signaling and cardiovascular manifestations in patients with autosomal recessive cutis laxa type I caused by fibulin-4 deficiency. *Eur J Hum Genet* 2010;**18**:895-901.
- Roussin I, Sheppard MN, Rubens M, Kaddoura S, Pepper J, Mohiaddin RH. Cardiovascular complications of cutis laxa syndrome: successful diagnosis and surgical management. *Circulation* 2011;**124**:100-102.
- Sawyer SL, Dicke F, Kirton A, Rajapakse T, Rebeyka IM, McInnes B, Parboosingh JS, Bernier FP. Longer term survival of a child with autosomal recessive cutis laxa due to a mutation in FBLN4. *Am J Med Genet A* 2013;**161A**:1148-1153.
- Hanada K, Vermeij M, Garinis GA, de Waard MC, Kunen MG, Myers L, Maas A, Duncker DJ, Meijers C, Dietz HC, Kanaar R, Essers J. Perturbations of vascular homeostasis and aortic valve abnormalities in fibulin-4 deficient mice. *Circ Res* 2007;**100**:738-746.
- Moltzer E, te Riet L, Swagemakers SMA, van Heijningen PM, Vermeij M, van Veghel R, Bouhuizen AM, van Esch JHM, Lankhorst S, Ramnath NWM, de Waard MC, Duncker DJ, van der Spek PJ, Rouwet EV, Danser AHJ, Essers J. Impaired Vascular Contractility and Aortic Wall Degeneration in Fibulin-4 Deficient Mice: Effect of Angiotensin II Type 1 (AT1) Receptor Blockade. *PLoS One* 2011;**6**:e23411.
- McLaughlin PJ, Chen Q, Horiguchi M, Starcher BC, Stanton JB, Broekelmann TJ, Marmorstein AD, McKay B, Mecham R, Nakamura T, Marmorstein LY. Targeted disruption of fibulin-4 abolishes elastogenesis and causes perinatal lethality in mice. *Mol Cell Biol* 2006;**26**:1700-1709.
- Habashi JP, Judge DP, Holm TM, Cohn RD, Loeys BL, Cooper TK, Myers L, Klein EC, Liu GS, Calvi C, Podowski M, Neptune ER, Halushka MK, Bedja D, Gabrielson K, Rifkin DB, Carta L, Ramirez F, Huso DL, Dietz HC. Losartan, an AT1 antagonist, prevents aortic aneurysm in a mouse model of Marfan syndrome. *Science* 2006;**312**:117-121.
- Isogai Z, Ono RN, Ushiro S, Keene DR, Chen Y, Mazzieri R, Charbonneau NL, Reinhardt DP, Rifkin DB, Sakai LY. Latent transforming growth factor beta-binding protein 1 interacts with fibrillin and is a microfibril-associated protein. *J Biol Chem* 2003;**278**:2750-2757.
- Groenink M, den Hartog AW, Franken R, Radonic T, de Waard V, Timmermans J, Scholte AJ, van den Berg MP, Spijkerboer AM, Marquering HA, Zwinderman AH, Mulder BJ. Losartan reduces aortic dilatation rate in adults with Marfan syndrome: a randomized controlled trial. *Eur Heart J* 2013;**34**:3491-3500.
- Lacro RV, Dietz HC, Sleeper LA, Yetman AT, Bradley TJ, Colan SD, Pearson GD, Selamet Tierney ES, Levine JC, Atz AM, Benson DW, Braverman AC, Chen S, De Backer J, Gelb BD, Grossfeld PD, Klein GL, Lai WW, Liou A, Loeys BL, Markham LW, Olson AK, Paridon SM, Pemberton

- VL, Pierpont ME, Pyeritz RE, Radojewski E, Roman MJ, Sharkey AM, Stylianou MP, Wechsler SB, Young LT, Mahony L, Pediatric Heart Network I. Atenolol versus losartan in children and young adults with Marfan's syndrome. *N Engl J Med* 2014;**371**:2061-2071.
19. Verdonk K, Danser AHJ, van Esch JHM. Angiotensin II type 2 receptor agonists: where should they be applied? *Expert Opin Inv Drug* 2012;**21**:501-513.
 20. Habashi JP, Doyle JJ, Holm TM, Aziz H, Schoenhoff F, Bedja D, Chen YC, Modiri AN, Judge DP, Dietz HC. Angiotensin II Type 2 Receptor Signaling Attenuates Aortic Aneurysm in Mice Through ERK Antagonism. *Science* 2011;**332**:361-365.
 21. Ye Y, Qian J, Castillo AC, Perez-Polo JR, Birnbaum Y. Aliskiren and Valsartan reduce myocardial AT1 receptor expression and limit myocardial infarct size in diabetic mice. *Cardiovasc Drugs Ther* 2011;**25**:505-515.
 22. Weng LQ, Zhang WB, Ye Y, Yin PP, Yuan J, Wang XX, Kang L, Jiang SS, You JY, Wu J, Gong H, Ge JB, Zou YZ. Aliskiren ameliorates pressure overload-induced heart hypertrophy and fibrosis in mice. *Acta Pharmacol Sin* 2014;**35**:1005-1014.
 23. Hawinkels LJ, Verspaget HW, van der Reijden JJ, van der Zon JM, Verheijen JH, Hommes DW, Lamers CB, Sier CF. Active TGF-beta1 correlates with myofibroblasts and malignancy in the colorectal adenoma-carcinoma sequence. *Cancer Sci* 2009;**100**:663-670.
 24. van Kerckhoven R, Saxena PR, Schoemaker RG. Restored capillary density in spared myocardium of infarcted rats improves ischemic tolerance. *J Cardiovasc Pharmacol* 2002;**40**:370-380.
 25. Danser AHJ, van Kats JP, Admiraal PJJ, Derkx FHM, Lamers JMJ, Verdouw PD, Saxena PR, Schalekamp MA. Cardiac renin and angiotensins. Uptake from plasma versus in situ synthesis. *Hypertension* 1994;**24**:37-48.
 26. de Lannoy LM, Danser AHJ, van Kats JP, Schoemaker RG, Saxena PR, Schalekamp MADH. Renin-angiotensin system components in the interstitial fluid of the isolated perfused rat heart. Local production of angiotensin I. *Hypertension* 1997;**29**:1240-1251.
 27. van den Bos EJ, Mees BM, de Waard MC, de Crom R, Duncker DJ. A novel model of cryoinjury-induced myocardial infarction in the mouse: a comparison with coronary artery ligation. *Am J Physiol Heart Circ Physiol* 2005;**289**:H1291-1300.
 28. van Deel ED, de Boer M, Kuster DW, Boontje NM, Holemans P, Sipido KR, van der Velden J, Duncker DJ. Exercise training does not improve cardiac function in compensated or decompensated left ventricular hypertrophy induced by aortic stenosis. *J Mol Cell Cardiol* 2011;**50**:1017-1025.
 29. Kaijzel EL, van Heijningen PM, Wielopolski PA, Vermeij M, Koning GA, van Cappellen WA, Que I, Chan A, Dijkstra J, Ramnath NW, Hawinkels LJ, Bernsen MR, Lowik CW, Essers J. Multimodality imaging reveals a gradual increase in matrix metalloproteinase activity at aneurysmal lesions in live fibulin-4 mice. *Circ Cardiovasc Imaging* 2010;**3**:567-577.
 30. Seva Pessoa B, van der Lubbe N, Verdonk K, Roks AJM, Hoorn EJ, Danser AHJ. Key developments in renin-angiotensin-aldosterone system inhibition. *Nat Rev Nephrol* 2013;**9**:26-36.
 31. Huang JB, Yamashiro Y, Papke CL, Ikeda Y, Lin YL, Patel M, Inagami T, Le VP, Wagenseil JE, Yanagisawa H. Angiotensin-Converting Enzyme-Induced Activation of Local Angiotensin Signaling Is Required for Ascending Aortic Aneurysms in Fibulin-4-Deficient Mice. *Sci Transl Med* 2013;**5**.
 32. Campbell DJ, Kladis A, Duncan AM. Nephrectomy, converting enzyme inhibition, and angiotensin peptides. *Hypertension* 1993;**22**:513-522.
 33. Matt P, Schoenhoff F, Habashi J, Holm T, Van Erp C, Loch D, Carlson OD, Griswold BF, Fu Q, De Backer J, Loeys B, Huso DL, McDonnell NB, Van Eyk JE, Dietz HC, Consortium G. Circulating Transforming Growth Factor-beta in Marfan Syndrome. *Circulation* 2009;**120**:526-532.
 34. Renard M, Holm T, Veith R, Callewaert BL, Ades LC, Baspinar O, Pickart A, Dasouki M, Hoyer J, Rauch A, Trapane P, Earing MG, Coucke PJ, Sakai LY, Dietz HC, De Paepe AM, Loeys BL. Altered TGF beta signaling and cardiovascular manifestations in patients with autosomal recessive cutis laxa type I caused by fibulin-4 deficiency. *Eur J Hum Genet* 2010;**18**:895-901.
 35. Neptune ER, Frischmeyer PA, Arking DE, Myers L, Bunton TE, Gayraud B, Ramirez F, Sakai LY, Dietz HC. Dysregulation of TGF-beta activation contributes to pathogenesis in Marfan syndrome. *Nat Genet* 2003;**33**:407-411.
 36. Chung AWY, Yeung KA, Sandor GGS, Judge DP, Dietz HC, van Breemen C. Loss of elastic fiber integrity and reduction of vascular smooth muscle contraction resulting from the upregulated activities of matrix metalloproteinase-2 and-9 in the thoracic aortic



- aneurysm in Marfan syndrome. *Circ Res* 2007;**101**:512-522.
37. Wood JM, Schnell CR, Cumin F, Menard J, Webb RL. Aliskiren, a novel, orally effective renin inhibitor, lowers blood pressure in marmosets and spontaneously hypertensive rats. *J Hypertens* 2005;**23**:417-426.
 38. Krop M, van Veghel R, Garrelds IM, de Bruin RJA, van Gool JMG, van den Meiracker AH, Thio M, van Daele PLA, Danser AHJ. Cardiac renin levels are not influenced by the amount of resident mast cells. *Hypertension* 2009;**54**:315-321.
 39. Feldman DL, Jin L, Xuan H, Contrepas A, Zhou Y, Webb RL, Müller DN, Feldt S, Cumin F, Maniara W, Persohn E, Schuetz H, Danser AHJ, Nguyen G. Effects of aliskiren on blood pressure, albuminuria, and (pro)renin receptor expression in diabetic TG(mREN-2)-27 rats. *Hypertension* 2008;**52**:130-136.
 40. van Esch JHM, Moltzer E, van Veghel R, Garrelds IM, Leijten F, Bouhuizen AM, Danser AH. Beneficial cardiac effects of the renin inhibitor aliskiren in spontaneously hypertensive rats. *J Hypertens* 2010;**28**:2145-2155.
 41. Mazzolai L, Pedrazzini T, Nicoud F, Gabbiani G, Brunner HR, Nussberger J. Increased cardiac angiotensin II levels induce right and left ventricular hypertrophy in normotensive mice. *Hypertension* 2000;**35**:985-991.
 42. van Esch JHM, Gembardt F, Sterner-Kock A, Heringer-Walther S, Le T, Lassner D, Stijnen T, Coffman T, Schultheiss H-P, Danser AHJ, Walther T. Cardiac phenotype and angiotensin II levels in AT1a, AT1b and AT2 receptor single, double and triple knockouts. *Cardiovasc Res* 2010;**86**:401-409.
 43. Danser AHJ, Derckx FHM, Schalekamp MADH, Hense HW, Riegger GAJ, Schunkert H. Determinants of interindividual variation of renin and prorenin concentrations: evidence for a sexual dimorphism of (pro)renin levels in humans. *J Hypertens* 1998;**16**:853-862.
 44. Moltzer E, Essers J, van Esch JHM, Roos-Hesselink JW, Danser AHJ. The role of the renin-angiotensin system in thoracic aortic aneurysms: Clinical implications. *Pharmacol Therapeut* 2011;**131**:50-60.
 45. Wagenaar LJ, Voors AA, Buikema H, van Gilst WH. Angiotensin receptors in the cardiovascular system. *Can J Cardiol* 2002;**18**:1331-1339.
 46. Utsunomiya H, Nakamura M, Kakudo K, Inagami T, Tamura M. Angiotensin II AT(2) receptor localization in cardiovascular tissues by its antibody developed in AT(2) gene-deleted mice. *Regul Peptides* 2005;**126**:155-161.
 47. Lopez JJ, Lorell BH, Ingelfinger JR, Weinberg EO, Schunkert H, Diamant D, Tang SS. Distribution and Function of Cardiac Angiotensin at(1)-Receptor and at(2)-Receptor Subtypes in Hypertrophied Rat Hearts. *Am J Physiol* 1994;**267**:H844-H852.
 48. Dietz HC. Potential Phenotype-Genotype Correlation in Marfan Syndrome: When Less is More? *Circ Cardiovasc Genet* 2015;**8**:256-260.
 49. Franken R, den Hartog AW, Radonic T, Micha D, Maugeri A, van Dijk FS, Meijers-Heijboer HE, Timmermans J, Scholte AJ, van den Berg MP, Groenink M, Mulder BJM, Zwinderman AH, de Waard V, Pals G. Beneficial Outcome of Losartan Therapy Depends on Type of FBN1 Mutation in Marfan Syndrome. *Circ-Cardiovasc Gene* 2015;**8**:383-388.
 50. Booz GW, Baker KM. Role of type 1 and type 2 angiotensin receptors in angiotensin II-induced cardiomyocyte hypertrophy. *Hypertension* 1996;**28**:635-640.
 51. van Kesteren CAM, van Heugten HAA, Lamers JMJ, Saxena PR, Schalekamp MADH, Danser AHJ. Angiotensin II mediated growth and antigrowth effects in cultured neonatal rat cardiac angiotensin system. *Circ Res* 2013;**112**:1104-1111.
 52. Villela D, Leonhardt J, Patel N, Joseph J, Kirsch S, Hallberg A, Unger T, Bader M, Santos RA, Sumners C, Steckelings UM. Angiotensin type 2 receptor (AT2R) and receptor Mas: a complex liaison. *Clin Sci (Lond)* 2015;**128**:227-234.
 53. Biermann D, Heilmann A, Didie M, Schlossarek S, Wahab A, Grimm M, Romer M, Reichenspurner H, Sultan KR, Steenpass A, Ergun S, Donzelli S, Carrier L, Ehmke H, Zimmermann WH, Hein L, Boger RH, Benndorf RA. Impact of AT2 receptor deficiency on postnatal cardiovascular development. *PLoS One* 2012;**7**:e47916.



CHAPTER 6

Fibulin-4 deficiency increases TGF- β signalling in aortic smooth muscle cells due to elevated TGF- β 2 levels

N.W.M. Ramnath[#], L.J.A.C. Hawinkels[#], P.M. van Heijningen, L. te Riet, M. Paauwe, M. Vermeij, A. H. J. Danser, R. Kanaar, P. ten Dijke, J. Essers

[#]Authors contributed equally

Scientific Reports. 2015; 5:16872



ABSTRACT

Fibulins are extracellular matrix proteins associated with elastic fibres. Homozygous Fibulin-4 mutations lead to life-threatening abnormalities such as aortic aneurysms. Aortic aneurysms in Fibulin-4 mutant mice were associated with upregulation of TGF- β signalling. How Fibulin-4 deficiency leads to deregulation of the TGF- β pathway is largely unknown. Isolated aortic smooth muscle cells (SMCs) from Fibulin-4 deficient mice showed reduced growth, which could be reversed by treatment with TGF- β neutralizing antibodies. In Fibulin-4 deficient SMCs increased TGF- β signalling was detected using a transcriptional reporter assay and by increased SMAD2 phosphorylation. Next, we investigated if the increased activity was due to increased levels of the three TGF- β isoforms. These data revealed slightly increased TGF- β 1 and markedly increased TGF- β 2 levels. Significantly increased TGF- β 2 levels were also detectable in plasma from homozygous *Fibulin-4^{RR}* mice, not in wild type mice. TGF- β 2 levels were reduced after losartan treatment, an angiotensin-II type-1 receptor blocker, known to prevent aortic aneurysm formation. In conclusion, we have shown increased TGF- β signalling in isolated SMCs from Fibulin-4 deficient mouse aortas, not only caused by increased levels of TGF- β 1, but especially TGF- β 2. These data provide new insights in the molecular interaction between Fibulin-4 and TGF- β pathway regulation in the pathogenesis of aortic aneurysms.

INTRODUCTION

In developed countries 1-2% of all deaths are caused by aortic aneurysms and dissections¹. In these countries the incidence of thoracic aortic aneurysm (TAA) is approximately 25 per 100,000 persons per year². In general, a TAA is characterized by degeneration of the extracellular matrix (ECM) and vascular smooth muscle cells (SMCs), including (phenotypic) loss of SMCs and changes in SMC proliferation³⁻⁵. Several genes have been identified in both syndromic and non-syndromic forms of TAA, including ECM genes, genes encoding contractile proteins in SMCs and genes involved in the regulation of the transforming growth factor (TGF)- β pathway⁶⁻⁸.

There are three mammalian TGF- β isoforms; TGF- β 1, - β 2 and - β 3. They are encoded by different genes, but show a high degree of amino acid sequence homology. All TGF- β isoforms bind to the latency-associated protein (LAP) and via the latent TGF- β binding protein (LTBP) to the ECM. Upon activation TGF- β s can bind to the type-II TGF- β receptors (T β RII), which recruit the type-I TGF- β receptor (T β RI), also called activin receptor-like kinase (ALK)-5. ALK-5 is transphosphorylated by T β RII and subsequently downstream SMAD proteins (i.e. SMAD2/3) are phosphorylated. Activated SMAD2 and -3 associate with SMAD4, leading to translocation to the nucleus where they interact with target gene promoters and regulate transcription of genes encoding for plasminogen activator inhibitor (PAI)-1, matrix metalloproteinases (MMPs) and ECM proteins⁹.

A crucial role for the TGF- β pathway in syndromes associated with TAA became evident from both studies in patients and in mouse models¹⁰⁻¹⁴. Although TAAs are usually associated with increased TGF- β signalling, this association has also been observed with loss of function mutations in TGF- β and TGF- β receptors¹⁵. The identification of these mutations has led to new insights in the pathogenesis of aneurysm formation, but the molecular mechanism remains to be elucidated.

Mutations in genes of the TGF- β pathway and the ECM lead to phenotypic and functional SMC loss: *Tgfb2* mutations in Loeys-Dietz syndrome leads to decreased expression of SMC contractile proteins⁵. Furthermore, SMCs from mice with Marfan syndrome, another syndromic form of TAAs caused by mutations in the ECM glycoprotein Fibrillin-1, display an altered expression profile with morphological changes, but retain expression of vascular SMC markers⁴. In addition, increased TGF- β signalling inhibits proliferation of SMCs¹⁶.

Upregulated TGF- β signalling has been observed in another heritable form of TAA caused by a deficiency in the extracellular matrix protein Fibulin-4^{13, 17-20}. Fibulin-4 regulates proper elastogenesis by tethering lysyl oxidase to tropoelastin to facilitate crosslinking^{21, 22}. In Fibulin-4 deficient patients and mice elevated TGF- β signalling has been shown^{12, 13, 20}. However, the exact mechanism by which Fibulin-4 deficiency leads to increased TGF- β signalling remains to be determined. To further investigate this we isolated SMCs from the aortic arch of hypomorphic Fibulin-4 (*Fibulin-4^{R/R}*) mice, displaying a 4-fold reduction of Fibulin-4 expression. This leads to congenital vascular abnormalities in these mice, including TAAs and vascular tortuosity¹². Heterozygous *Fibulin-4^{+R}* mice, which have a 2-fold reduced Fibulin-4 expression, show minor irregularities and ECM changes in the aortic wall. Our data reveal that TGF- β signalling is enhanced in isolated SMCs derived from the aortas of Fibulin-4 deficient mice. We observed a decreased proliferation rate in *Fibulin-4^{R/R}* SMCs, which could be reverted by addition of TGF- β neutralizing antibodies. We found that this increased TGF- β signal transduction activity is not only associated with increased levels of TGF- β 1, but especially with enhanced TGF- β 2 levels. Increased levels of TGF- β 2 could also be detected in blood and aortic tissue lysates of the *Fibulin-4^{R/R}* mice. Treatment of *Fibulin-4^{R/R}* mice with losartan, an angiotensin II type-1 receptor blocker, reduced the increased TGF- β 2 levels in blood plasma. This study shows that increased TGF- β signalling in SMCs of Fibulin-4 deficient mice leads to decreased proliferation of SMCs and could be caused by increased bioavailability of TGF- β 1 and especially TGF- β 2.

RESULTS

Characterization of SMCs derived from Fibulin-4 deficient aortas

To examine TGF- β signalling in Fibulin-4 deficient SMCs, we isolated SMCs from the aortic arches of *Fibulin-4^{+/+}*, *Fibulin-4^{+/-}* and *Fibulin-4^{R/R}* mice. To confirm that the cells we isolated were SMCs, the cells were analysed for the presence of SMC markers, including α -smooth muscle actin (α -SMA), smooth muscle specific protein-22 (SM22), smooth muscle myosin heavy chain II (MHC II) and fibroblast specific protein 1 (FSP1), which stains SMCs with a rhomboid phenotype^{23,24}. Human umbilical vein endothelial cells (HUVECs) were taken along as positive control for CD31 staining and were negative for all other markers, while mouse embryonic fibroblasts (MEFs) were positive controls for FSP1, and SMA and SM22 staining²⁵. Isolated SMCs showed positive staining for α -SMA, SM22, MHC II, FSP1 and were negative for CD31 (Figure 1A) confirming the SMC phenotype. QPCR expression analysis also showed no detectable CD31 and von Willebrand Factor (an additional endothelial marker) mRNA expression (data not shown). α -SMA was highly expressed and seemed somewhat increased in *Fibulin-4^{+/-}* and *Fibulin-4^{R/R}* SMCs (Figure 1B). Next, the levels of Fibulin-4 were analysed by QPCR. These data revealed that expression levels of Fibulin-4 mRNA in *Fibulin-4^{+/-}* and *Fibulin-4^{R/R}* SMCs was downregulated (Figure 1C). These data show that we isolated a population of SMCs with a gradual reduced Fibulin-4 expression level, which we used for further cell biological and molecular analyses.

TGF- β reduces proliferation of *Fibulin-4^{R/R}* SMCs

Previously we showed in 10 days old *Fibulin-4^{R/R}* mice increased BrdU uptake indicating increased proliferation of SMCs, leading to changes in the tunica adventitia of the aorta¹². However, in adult *Fibulin-4^{R/R}* mice (100 days old) increased proliferation was observed specifically in the endothelial layer (Figure 2A). No proliferation of SMCs in the adventitia or media of the aortic wall was observed. Next, we analysed proliferation rates of the SMCs with reduced Fibulin-4 expression *in vitro*. Figure 2B shows similar growth rates of all three genotypes until day 5, after which proliferation was decreased in *Fibulin-4^{R/R}* SMCs. As TGF- β can inhibit cell proliferation, we determined whether the reduced growth of *Fibulin-4^{R/R}* SMCs is a consequence of increased TGF- β activity. Therefore SMCs were treated with TGF- β neutralizing antibodies (nAb), which neutralize all three TGF- β isoforms^{26,27}. Treatment with the TGF- β nAb reversed the growth inhibition observed in *Fibulin-4^{R/R}* SMCs compared to *Fibulin-4^{+/+}* SMCs (Figure 2C-F). On day 7 the number of *Fibulin-4^{R/R}* SMCs was significantly increased after treatment with TGF- β nAb compared to non-treated *Fibulin-4^{R/R}* SMCs. Moreover, proliferation was similar to *Fibulin-4^{+/+}* SMCs. These data indicate that Fibulin-4 deficiency leads to increased TGF- β , which inhibits proliferation of SMCs.

Fibulin-4 expression regulates TGF- β signalling in aortic SMCs

Since we observed that TGF- β neutralizing antibodies revert the decreased proliferation rates of *Fibulin-4^{R/R}* SMCs, we further analysed transcriptional consequences of increased TGF- β signalling in these cells using a SMAD3/SMAD4 dependent promoter transcriptional reporter construct (CAGA-luciferase)²⁸. Although there was a difference in proliferation between different genotypes at later time points, this was not observed during the shorter duration of this assay (Figure 3A). To determine whether transfection efficiency was similar between the different genotypes a green fluorescent protein (GFP) expressing construct was transfected and GFP expression determined. Flow cytometric analysis showed no differences between the percentages of GFP expressing *Fibulin-4^{+/+}*, *Fibulin-4^{+/-}* and *Fibulin-4^{R/R}* SMCs (Figure 3B) and thus no differences in transfection efficiencies among these different genotype. Next, we used the CAGA-luciferase reporter construct to assess TGF- β signalling activity in *Fibulin-4^{+/+}*, *Fibulin-4^{+/-}* and *Fibulin-4^{R/R}* SMCs. Stimulation with TGF- β of *Fibulin-4^{+/+}*, *Fibulin-4^{+/-}* and *Fibulin-4^{R/R}* SMCs showed a strong induction of luciferase activity, which was increased in a Fibulin-4 dose-dependent manner (Figure 3C). Addition of the T β RI kinase inhibitor SB431542, a compound selectively blocking TGF- β binding²⁹, abolished TGF- β -induced transcriptional responses. Analysis of downstream pSMAD2 and pSMAD3 by western blotting revealed a gradual increase in SMAD2 and SMAD3 phosphorylation after stimulation with TGF- β in *Fibulin-4^{+/-}* and *Fibulin-4^{R/R}* SMCs compared to *Fibulin-4^{+/+}* SMCs (Figure 3D), confirming

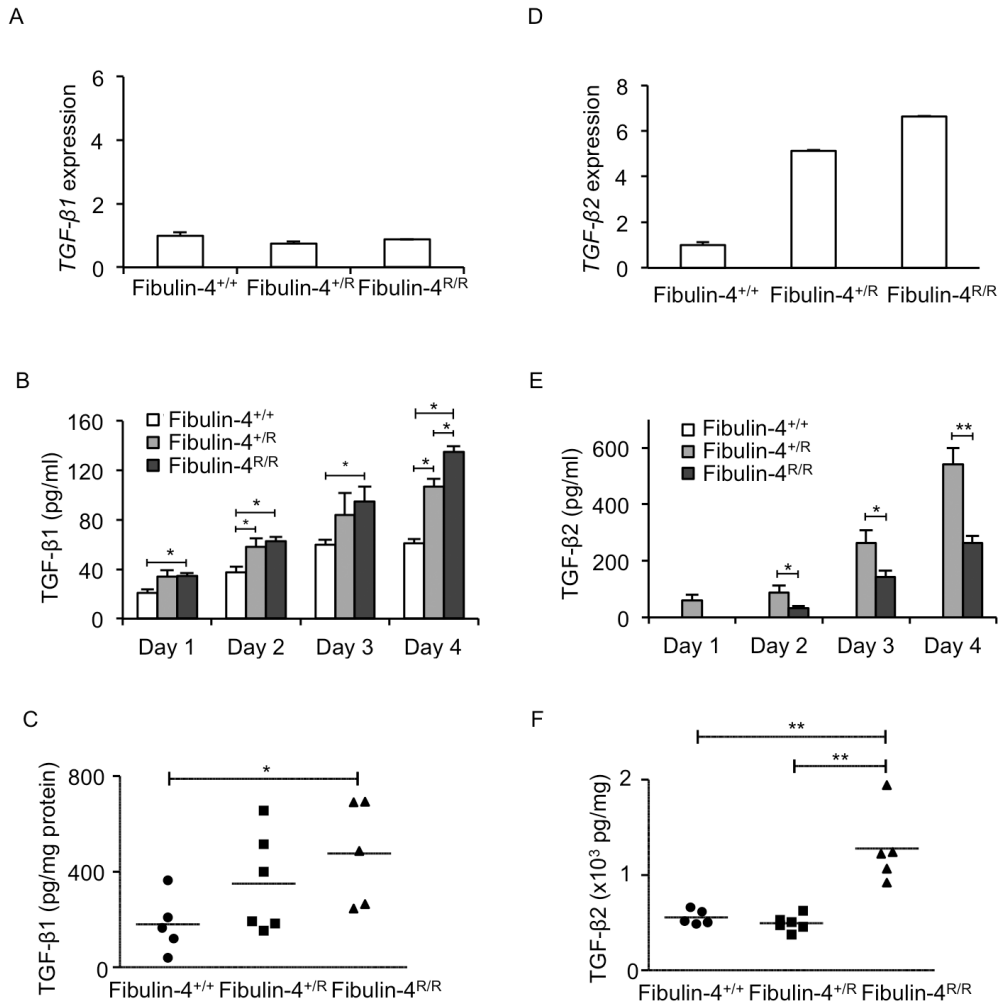


Figure 1

Characterization of isolated SMCs from the aortic arch. (a) Immunofluorescent staining of aortic SMCs isolated from Fibulin-4^{+/+}, Fibulin-4^{+/R} and Fibulin-4^{R/R} mice showed that these cells stained positively for SMA, SM22, MHC II and FSP1. The SMCs were negative for the endothelial marker CD31, while HUVECs were positive. HUVECs were negative for all other stainings. MEFs stained positive for SMA, SM22 and FSP1 and were negative for MHC II and CD31. Magnification 20x, scale bar 100 μ m. (b) Fibulin-4^{+/R} and Fibulin-4^{R/R} SMCs show gradual increased SMA mRNA expression levels compared to Fibulin-4^{+/+} SMCs. (c) Fibulin-4^{R/R} SMCs show gradual decreased Fibulin-4 mRNA expression levels compared to Fibulin-4^{+/+} SMCs.

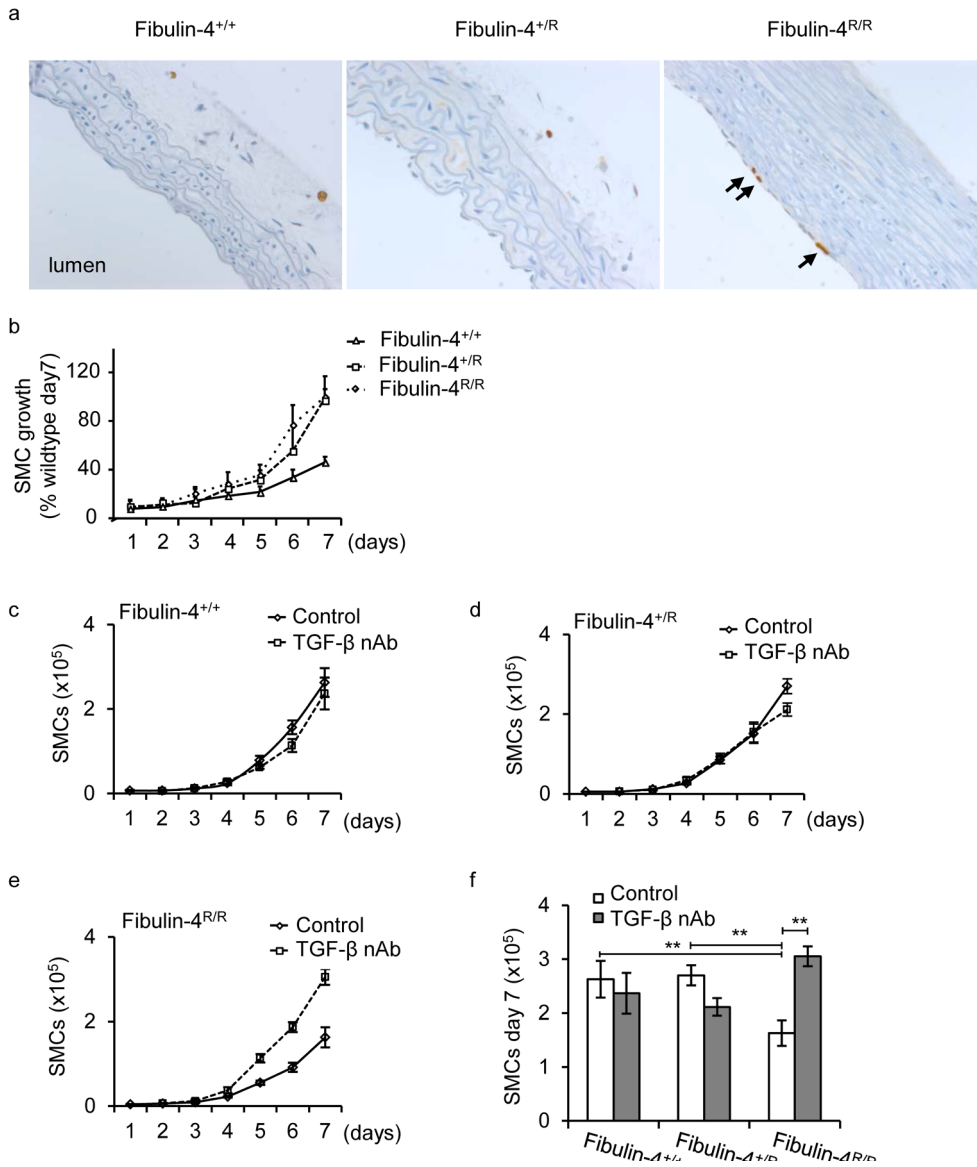


Figure 2

Reduced proliferation of Fibulin-4^{R/R} SMCs is reversed by inhibition of the TGF-β pathway. (a) Increased proliferation of endothelial cells is present in the aortic wall from 100 days old Fibulin-4^{R/R} mice and is indicated by the arrows.

(b) Growth analyses of Fibulin-4^{+/+}, Fibulin-4^{+R} and Fibulin-4^{R/R} SMCs revealed a reduced growth starting from day 5 for Fibulin-4^{R/R} SMCs as compared to Fibulin-4^{+/+} SMCs (3 dishes per experiment were counted and the average of 3 independent experiments is shown). Treatment of (c) Fibulin-4^{+/+}, (d) Fibulin-4^{+R} and (e and f) Fibulin-4^{R/R} SMCs with TGF-β neutralizing antibodies significantly increased proliferation of Fibulin-4^{R/R} SMCs from day 5. (f) At day 7 the number of treated Fibulin-4^{R/R} SMCs was significantly higher and comparable to the amount of Fibulin-4^{+/+} SMCs (* p<0.05, ** p<0.01). Data represent 3 independent experiments performed in triplicate.

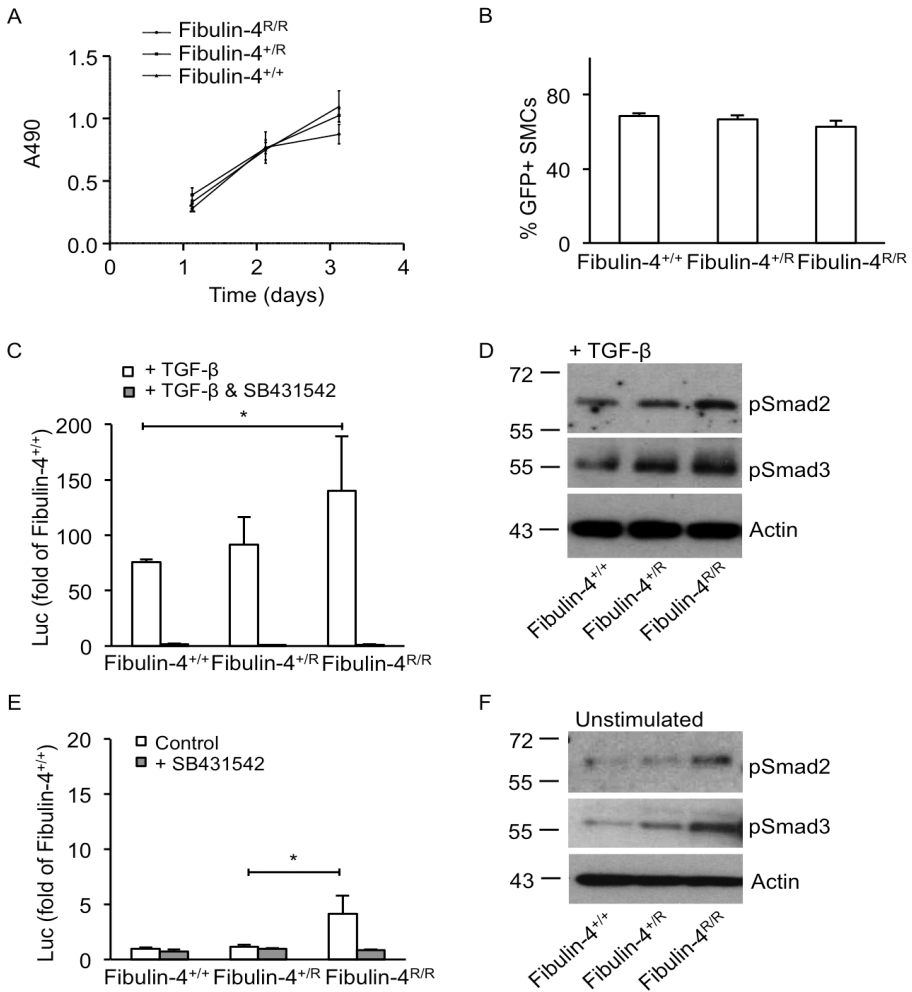


Figure 3

Increased TGF- β signalling in Fibulin-4 deficient SMCs. (a) *Fibulin-4^{+/+}*, *Fibulin-4^{+/R}* and *Fibulin-4^{R/R}* SMCs show similar proliferation rates in the time course of the experiment (MTS proliferation assay) (b) Transfection with green fluorescent protein (GFP) encoding plasmids display no difference in percentage of transfected SMCs between *Fibulin-4^{+/+}*, *Fibulin-4^{+/R}* and *Fibulin-4^{R/R}* SMCs. (c) The TGF- β response assay reveals a gradual increase in TGF- β activity in *Fibulin-4^{+/R}* and *Fibulin-4^{R/R}* SMCs compared to *Fibulin-4^{+/+}* SMCs, after stimulation with exogenous TGF- β . Data represent fold change relative to unstimulated *Fibulin-4^{+/+}* SMCs. Addition of the ALK-5 kinase inhibitor (SB431542) abolishes the TGF- β response in *Fibulin-4^{+/+}*, *Fibulin-4^{+/R}* and *Fibulin-4^{R/R}* SMCs. (d) Western blot analyses for TGF- β signalling downstream mediators pSMAD2 and pSMAD3 on TGF- β stimulated SMCs show a gradual increase in TGF- β signalling in Fibulin-4 deficient SMCs compared to *Fibulin-4^{+/+}* SMCs. (e) Measurement of basal TGF- β activity (no stimulation by exogenous TGF- β) by the CAGA-luciferase reporter show increased TGF- β activity in *Fibulin-4^{R/R}* SMCs compared to *Fibulin-4^{+/+}* SMCs, which can be inhibited by the β RI kinase inhibitor SB431542. (f) These data were confirmed by western blot analyses for pSMAD2 and pSMAD3. All data shown are representative for in total n=3 independent experiments and all performed under serum starved conditions (*p<0.05, **p<0.01).

the CAGA-luciferase reporter data. These data indicate that Fibulin-4 deficient cells show increased signalling upon exogenous TGF- β stimulation.

To explore whether basal TGF- β signalling is also affected in Fibulin-4 deficient cells, SMCs were transfected with the CAGA-luciferase reporter and TGF- β signalling without exogenous addition of TGF- β ligand was analysed. This showed that luciferase activity was already increased in untreated *Fibulin-4^{R/R}* SMCs compared to *Fibulin-4^{+/+}* SMCs (Figure 3E). This could be reversed by SB431542, suggesting a TGF- β mediated effect. Western blot analysis showed gradually increased basal phosphorylation of SMAD2 and SMAD3 in untreated *Fibulin-4^{+/+}* and *Fibulin-4^{R/R}* SMCs (Figure 3F). Taken together, these data indicate that increased phosphorylation of Smad2/3 leads to enhanced transcriptional activation of downstream TGF- β signalling genes and reduced growth in Fibulin-4 mutant cells.

Increased TGF- β 1 and TGF- β 2 levels in Fibulin-4 deficient SMCs

Since we observed increased basal TGF- β signalling in Fibulin-4 deficient SMCs, we analysed whether this was due to increased TGF- β levels. Subconfluent *Fibulin-4^{+/+}*, *Fibulin-4^{+/R}* and *Fibulin-4^{R/R}* SMCs were serum-starved and conditioned medium was collected for 4 consecutive days to determine TGF- β 1, -2 and -3 levels. TGF- β 3 levels were very low and did not differ between the different genotypes (data not shown). Although *Tgf- β 1* mRNA levels in SMCs did not differ between the genotypes (Figure 4A), TGF- β 1 levels in *Fibulin-4^{R/R}* SMCs conditioned medium were higher compared to *Fibulin-4^{+/+}* SMCs (Figure 4B). Conditioned medium from *Fibulin-4^{+/R}* SMCs showed intermediate TGF- β 1 levels. To analyse whether the increased TGF- β 1 levels were also observed *in vivo*, we prepared lysates from aortic arches of *Fibulin-4^{+/+}*, *Fibulin-4^{+/R}* and *Fibulin-4^{R/R}* mice and measured TGF- β 1 levels. These data revealed a similar gradual increase in TGF- β 1 levels in aortic arch lysates of *Fibulin-4^{+/R}* and *Fibulin-4^{R/R}* mice (Figure 4C).

Next, we analysed TGF- β 2 expression in the SMCs. *Fibulin-4^{+/R}* and *Fibulin-4^{R/R}* SMCs showed >5-fold increased *Tgf- β 2* mRNA expression levels (Figure 4D). ELISA analysis on conditioned medium from *Fibulin-4^{+/+}*, *Fibulin-4^{+/R}* and *Fibulin-4^{R/R}* SMCs revealed strongly increased TGF- β 2 levels in medium from *Fibulin-4^{+/R}* and *Fibulin-4^{R/R}* SMCs compared to *Fibulin-4^{+/+}* SMCs, in which TGF- β 2 was undetectable (Figure 4E). TGF- β 2 levels were already significantly higher in conditioned medium from *Fibulin-4^{+/R}* SMCs. Increased TGF- β 2 levels were also detectable in *Fibulin-4^{R/R}* aortic arch lysates, when compared to aortic arch lysates from *Fibulin-4^{+/+}* and *Fibulin-4^{+/R}* mice (Figure 4F). Given the increased TGF- β levels in SMCs and aortic tissue derived from Fibulin-4 deficient mice, we determined TGF- β 1 and TGF- β 2 levels in plasma samples from these mice. TGF- β 1 levels were not significantly different among plasma from *Fibulin-4^{+/+}*, *Fibulin-4^{+/R}* and *Fibulin-4^{R/R}* mice (Figure 5A). In contrast, plasma TGF- β 2 levels were very low in wild type mice and could be detected in 2 out of 15 *Fibulin-4^{+/+}* mice and 2 out of 19 *Fibulin-4^{+/R}* mice (Figure 5B). In contrast TGF- β 2 levels could be detected in plasma from 12 out of 24 *Fibulin-4^{R/R}* mice with significantly higher concentrations compared to *Fibulin-4^{+/+}* and *Fibulin-4^{+/R}* mice. These data show that specifically TGF- β 2 levels in aortic tissue and plasma of Fibulin-4 deficient mice are strongly increased.

Losartan treatment rescues lethality and lowers plasma TGF- β 2 levels in *Fibulin-4^{R/R}* mice

Next, adult mice were treated with Losartan, an angiotensin-II type-I receptor blocker, which prevents aortic root enlargement and reduces circulating TGF- β 1 in a Marfan mouse model³⁰. Compared to the increased secretion of TGF- β 2 in placebo treated *Fibulin-4^{R/R}* mice we observed, TGF- β 2 levels were not detectable in the 10 losartan treated *Fibulin-4^{R/R}* mice. Consistent with previous studies³¹, Losartan treatment of wild type, *Fibulin-4^{+/R}* and *Fibulin-4^{R/R}* mice showed improved survival rates of Losartan treated *Fibulin-4^{R/R}* mice until at least the age of 160 days compared to placebo treated *Fibulin-4^{R/R}* mice, which maximally survive until the age of 100 days (Figure 5C). All losartan and placebo treated wild type and *Fibulin-4^{+/R}* mice survived at least until the duration of the experiment (data not shown). Despite improved survival, 160 days old Losartan treated *Fibulin-4^{R/R}* mice developed significantly enlarged aortic diameters compared to losartan treated wild type mice (Figure 5D), and a thickened and degenerated aortic wall architecture as evidenced by fragmentation of its elastin layers (Figure 5E). Previously we showed a reduced SMA staining in the aortic wall of 100 days old Fibulin-4 deficient mice,

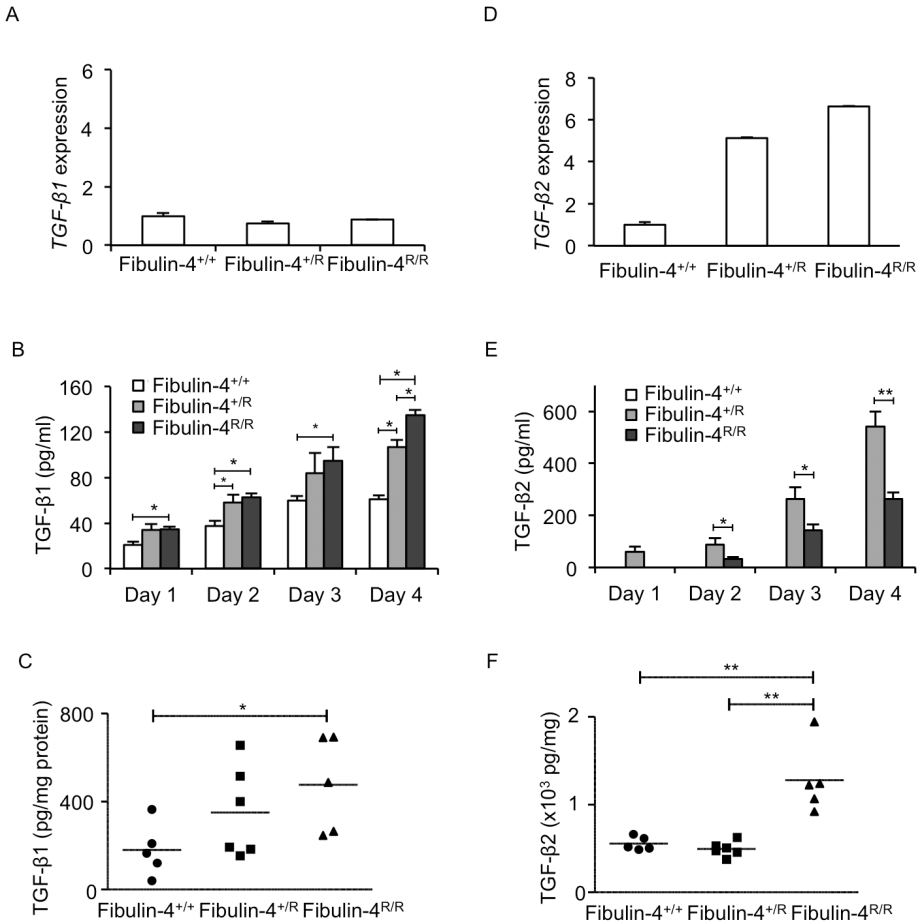


Figure 4

Strong increase of TGF- β 2 levels in Fibulin-4 deficient SMCs. (a) *Fibulin-4^{+/-}* and *Fibulin-4^{-/-}* SMCs show equal *Tgf- β 1* mRNA expression levels compared to *Fibulin-4^{+/+}* SMCs. (b) Increased TGF- β 1 levels measured in conditioned medium (CM) from *Fibulin-4^{-/-}* SMCs compared to *Fibulin-4^{+/+}* CM on day 1-4 after serum starvation. *Fibulin-4^{+/-}* SMCs showed significant increased TGF- β 1 levels on day 2 and 4 after serum starvation compared to *Fibulin-4^{+/+}* SMCs. Furthermore, on day 4 *Fibulin-4^{-/-}* SMCs show significant increased TGF- β 1 levels compared to *Fibulin-4^{+/-}* SMCs (n=4 per day for each genotype). Two-way ANOVA analysis for genotype and between days p<0.05. (c) Gradually increased TGF- β 1 is also observed in aortic arch lysates of *Fibulin-4^{+/-}* (n=6) and *Fibulin-4^{-/-}* mice (n=5) compared to *Fibulin-4^{+/+}* aortas (n=5). This increase is significant in *Fibulin-4^{-/-}* aortic arch lysates compared to *Fibulin-4^{+/+}* aortic arch lysates. (d) *Fibulin-4^{+/-}* and *Fibulin-4^{-/-}* SMCs show gradual increased *Tgf- β 2* mRNA expression levels compared to *Fibulin-4^{+/+}* SMCs. (e) Measurement of TGF- β 2 revealed markedly increased levels in CM of *Fibulin-4^{+/-}* and *Fibulin-4^{-/-}* SMCs, while TGF- β 2 was undetectable in CM of *Fibulin-4^{+/+}* SMCs (experiments were performed in at least 3 independent experiments). Two-way ANOVA analysis for genotype and between days p<0.05. (f) Measurements in aortic arch lysates display significantly increased TGF- β 2 in *Fibulin-4^{-/-}* aortas compared to *Fibulin-4^{+/-}* and *Fibulin-4^{+/+}* aortas (*p<0.05, **p<0.01).

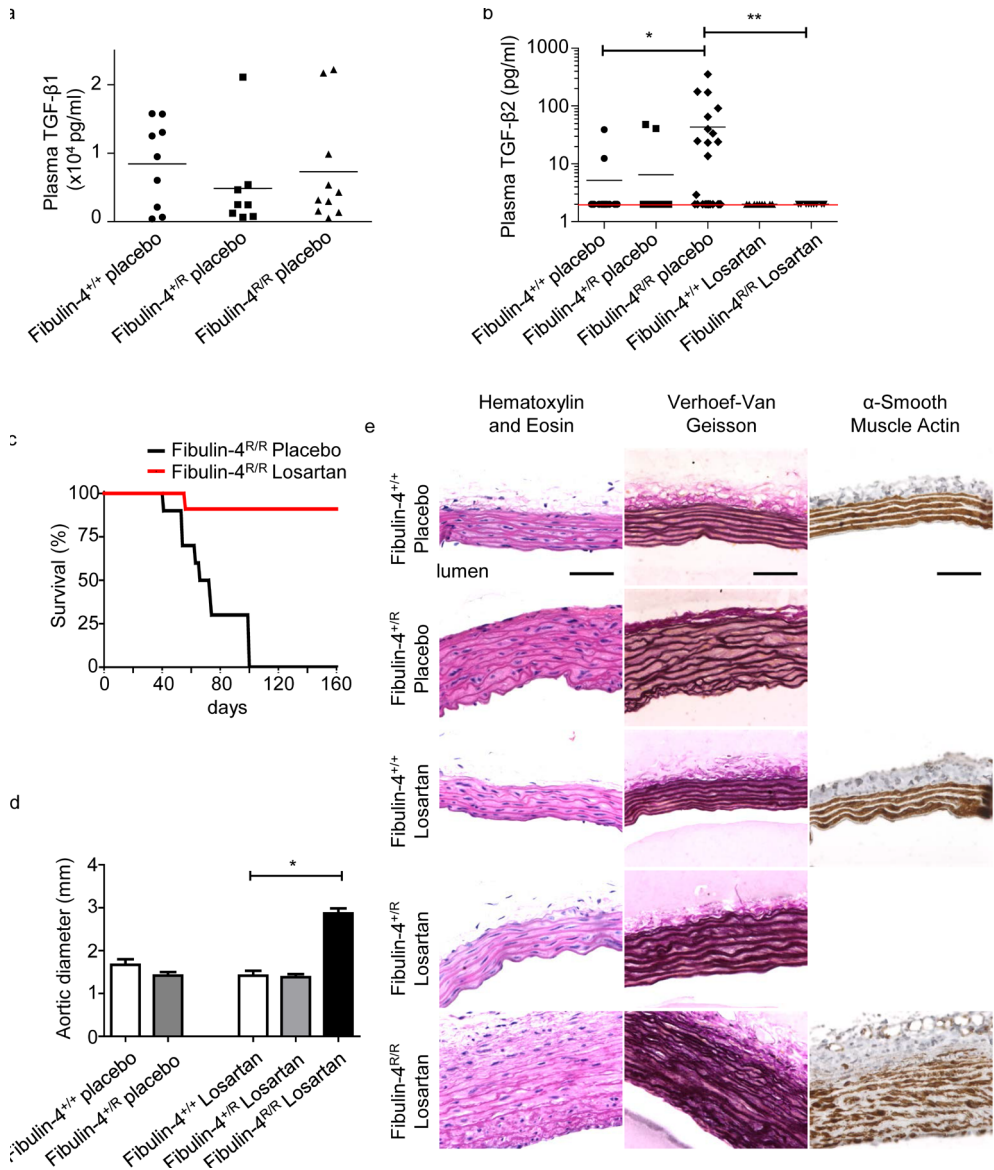


Figure 5

Increased levels of TGF-β2 are detectable in plasma from 100 days old Fibulin-4^{R/R} mice, which reduces on Losartan treatment. (a) TGF-β1 measurements in plasma samples showed no difference between placebo treated Fibulin-4^{+/+} (n=9), Fibulin-4^{+/-} (n=8) and Fibulin-4^{R/R} mice (n=10). (b) TGF-β2 was detectable in plasma of 12 out of 24 placebo treated Fibulin-4^{+/-} mice compared and only 2 out of 15 in placebo treated Fibulin-4^{+/+} mice and 2 out of 19 in Fibulin-4^{R/R} mice. TGF-β2 levels are significantly higher in Fibulin-4^{R/R} mice compared to placebo treated Fibulin-4^{+/+} and Fibulin-4^{+/-} mice. Losartan treatment of Fibulin-4^{R/R} mice seemed to reduce the TGF-β2 levels (0 out of 9) as compared to placebo treated Fibulin-4^{R/R} mice. The red line indicates the detection of the ELISA (Chi-square p<0.001). (c) Kaplan-meier survival curve shows

and increased survival of Losartan treated Fibulin-4^{R/R} mice compared to placebo treated Fibulin-4^{R/R} mice. (d) Aortic diameter of 160 days old placebo and losartan treated Fibulin-4^{+/+}, Fibulin-4^{+R} mice and Losartan treated Fibulin-4^{R/R} mice. Losartan treated Fibulin-4^{R/R} mice have significantly enlarged aortic diameters compared to wild type mice, while there are no differences between placebo and Losartan Fibulin-4^{+R} mice and wild type mice. (e) HE, elastin and α SMA staining of ascending thoracic aortas. Placebo and losartan treated Fibulin-4^{+R} mice (160 days old) show an increase in aortic wall thickness and some elastin breaks compared to Fibulin-4^{+/+} mice. Losartan treated Fibulin-4^{R/R} mice show despite of their survival disrupted aortic wall architecture. In addition, despite losartan treatment there is loss of smooth muscle cell content in the media of Fibulin-4^{R/R} mice. (*p<0.05, **p<0.01).

indicative for SMC loss³¹. This SMC loss is not ameliorated by losartan treatment of *Fibulin-4^{R/R}* mice (Figure 5E). Both placebo and Losartan treated *Fibulin-4^{+R}* mice showed an increase in aortic wall thickness and minor elastin breaks compared to wild type mice, which was also previously observed in non-treated *Fibulin-4^{+R}* mice¹². These results show that lethality and increased plasma TGF- β 2 levels in *Fibulin-4^{R/R}* mice can be reduced by losartan treatment, showing a causal relation between increased TGF- β signalling and lethality in aneurysmal Fibulin-4 mice.

DISCUSSION

In this study we show that TGF- β signalling is gradually enhanced in Fibulin-4 deficient SMCs in a Fibulin-4 dose-dependent manner and influences proliferation of these cells. The increased TGF- β signalling is consistent with increased TGF- β 1 levels, and especially with increased TGF- β 2 levels, detected in plasma from Fibulin-4 deficient mice.

Previous analyses on aortas from Fibulin-4 deficient mice showed increased TGF- β signalling associated with aneurysm formation by gene expression analysis and increased nuclear pSMAD2 staining in the SMCs of these aortas¹². Isolation of aortic SMCs from these mice provided the opportunity to assess TGF- β signalling *in vitro*. *Fibulin-4^{R/R}* SMCs have a reduced proliferation rate compared to *Fibulin-4^{+R}* and wild type SMCs, which is reversed by TGF- β inhibition. Reduced proliferation only takes place after a prolonged incubation time, which is most probably caused by the requirement of certain levels of TGF- β before it affects the proliferation rates of the SMCs. However, in the aortic wall local active TGF- β concentrations can be much higher, due to local activation of the ECM bound TGF- β . In our previous studies we found a hyperproliferation of SMCs as well as a decreased SMC content in the aortic wall of Fibulin-4 deficient mice^{12, 31}. The hyperproliferation of SMCs was specifically found in the adventitial layers of the aortic wall of newborns. Tsai et al showed that TGF- β can transform from an inhibitor to a stimulant of SMC proliferation in the context of elevated Smad3³². We observed a gradual increase in TGF- β signalling in Fibulin-4 deficient SMCs, which could be reverted by inhibition of TGF- β . These data indicate that the proliferation of Fibulin-4 deficient SMCs is reduced due to increased TGF- β signalling, thereby potentially contributing to aortic aneurysm formation.

ELISA analyses point to increased TGF- β 1 levels in Fibulin-4 deficient SMCs and strongly increased TGF- β 2 levels, also detected in plasma of *Fibulin-4^{R/R}* mice. The three TGF- β isoforms are involved in both overlapping and divergent roles. While *Tgf- β 1* null mice develop an autoimmune-like inflammatory disease³³ and *Tgf- β 3* knockout mice show abnormal lung development and cleft palate³⁴ *Tgf- β 2* knockout mice have multiple developmental defects, including cardiovascular, pulmonary, skeletal, ocular, inner ear and urogenital manifestations³⁵. *Tgf- β 2* heterozygous mutations in patients result in a different phenotype compared to *Tgf- β 2* knock-out mice¹⁵. TGF- β 2 haplo-insufficiency predisposes for adult-onset vascular disease, including aortic tortuosity and dilation, cerebrovascular disease and mitral valve disease, which overlaps with the phenotype of Fibulin-4 deficient

patients. The phenotype of the TGF- β 2 deficient patients also shows overlap with other TGF- β signalopathies including Marfan syndrome, Loeys-Dietz syndrome, the aneurysm-osteoarthritis syndrome and similarly present with a paradoxical, probably compensatory, local increase in TGF- β 1 and TGF- β 2. Furthermore, increased *Tgf- β 2* expression has been detected in patients with the Loeys-Dietz syndrome³⁶. The fact that TGF- β 2 haploinsufficiency results in a cardiovascular phenotype and local increased TGF- β 2, stresses the potential importance of TGF- β 2 in the vasculopathy. For various TGF- β superfamily members it is known that their effects are very concentration dependent^{37, 38}. Very high or very low levels of these cytokines can have similar or opposite effects on cells. In addition, crucial in the regulation of TGF- β activity is its activation from the latent ECM-bound complexes. This might explain the, at first sight, contradictory findings. This also suggests that increased TGF- β 2 expression is part of a common pathophysiologic process involved in aortic aneurysm formation in these syndromes. Whether it is a direct or indirect consequence of Fibulin-4 deficiency has to be determined in further studies.

We observed that specifically the TGF- β 2 isoform is elevated and detected at higher levels in the conditioned medium from these cells and *in vivo* in aortic lysates and blood. TGF- β 2 differs in its receptor binding properties from TGF- β 1 and TGF- β 3. While TGF- β 1 and TGF- β 3 have a high affinity for binding to T β RII, TGF- β 2 primarily binds to the transforming growth factor type-III receptor (T β RIII), also called betaglycan, after which it presents the ligand to the T β RI-T β RII signalling complex³⁹. Bee *et al.* showed a specific regulatory role for the TGF- β receptor-IIb (T β RIIb), an alternatively spliced variant of T β RII, in TGF- β 2 signal transduction. T β RIIb mutations result in TGF- β 2 dependent increased SMAD2 phosphorylation, which is involved in aortic aneurysm progression⁴⁰. Human SMCs express T β RI, T β RII and T β RIII, while in SMCs derived from atherosclerotic lesions T β RII expression is decreased⁴¹. This indicates that alterations in TGF- β receptor expression probably contribute to the regulation of the TGF- β pathway. As our data point to markedly increased TGF- β 2 levels in Fibulin-4 deficient SMCs, analyses on TGF- β receptors on these SMCs might further clarify the process of TGF- β regulation and determine its role in the pathogenesis of Fibulin-4 associated aortic aneurysms.

Increased TGF- β levels or TGF- β signalling is associated with multiple diseases. Enhanced TGF- β signalling is known to mediate a pathologic increase in ECM secretion and deposition and is causative for fibrosis in multiple disorders throughout the body⁴². Overexpression of TGF- β 2 is likely to induce trabecular meshwork ECM deposition⁴³ and increased ECM deposition is also observed in aortic aneurysm formation. TGF- β 2 is also frequently overexpressed in malignant cancers, where it induces immunosuppression and stimulates metastasis formation⁴⁴. TGF- β 2 expression can be targeted with antisense oligonucleotides, which are currently under investigation in clinical trials⁴⁵. As inhibition with pan TGF- β neutralizing antibodies is likely to induce side effects, aortic aneurysms associated with increased TGF- β 2 might benefit from a TGF- β 2 specific intervention decreasing systemic side effects by targeting the other isoforms. In Marfan patients, mouse models for Loeys-Dietz syndrome and transverse aortic constriction (TAC), losartan treatment prevents aortic aneurysm formation accompanied by reduced TGF- β 1 levels in patients with Marfan syndrome, and reduced TGF- β 1 and TGF- β 2 levels in Loeys-Dietz syndrome and TAC mice^{30, 36, 46, 47}. Our data indicate that losartan could also serve as an important therapeutic agent. The exact mechanism how losartan treatment leads to reduced TGF- β signalling needs to be determined.

Fibulin-4 binds LTBP-1 with high affinity and therefore an important role for Fibulin-4 in the association of LTBP-1 with microfibrils is predicted. The large latent complex (LLC), which is formed by LTBP and LAP-bound TGF- β , is linked to microfibrils through binding of LTBP-1 to Fibrillin-1. Therefore, Fibulin-4 might be additionally involved in sequestering of the LLC through LTBP-1 binding⁴⁸. We speculate that reduced Fibulin-4 levels lead to defective sequestering to the ECM and thereby increased free TGF- β 1 and TGF- β 2. In conclusion, these data show that SMC derived TGF- β 2 is associated with aortic aneurysm formation and levels decrease upon losartan treatment, which improves survival of Fibulin-4 deficient mice. Specific intervention on TGF- β 2 could provide more information on its role in the pathogenesis of aortic aneurysm formation. *In vitro* analyses on isolated SMCs provide the opportunity to determine the molecular link between Fibulin-4 and TGF- β pathway regulation, and to further unravel its role in aortic aneurysm formation.

MATERIAL AND METHODS

Animals

Mice containing the *Fibulin-4^R* allele were generated as previously described¹². All mice used were bred in a C57Bl/6J background and were kept in individually ventilated cages to keep animals consistently micro-flora and disease free. To avoid stress-related vascular injury, mice were earmarked and genotyped 4 weeks after birth. Animals were housed at the Animal Resource Centre (Erasmus University Medical Centre), which operates in compliance with the "Animal Welfare Act" of the Dutch government, using the "Guide for the Care and Use of Laboratory Animals" as its standard. As required by Dutch law, formal permission to generate and use genetically modified animals was obtained from the responsible local and national authorities. All animal studies were approved by an independent Animal Ethical Committee (Dutch equivalent of the IACUC).

Treatment of mice

Fibulin-4^{+/+} and *Fibulin-4^{R/R}* mice received 0.6 gram/liter losartan (Sigma, Zwijndrecht, the Netherlands) or placebo in their drinking water as previously described^{30, 31}. Adult *Fibulin-4^{R/R}* mice and their wild type littermates were treated during 10 weeks or 18 weeks, starting at the age of 5 weeks. Blood samples from placebo or losartan treated *Fibulin-4^{+/+}* and *Fibulin-4^{R/R}* mice were obtained by cardiac puncture and collected in lithium heparin vials (Sarstedt, Numbrecht, Germany).

Isolation of SMCs and cell culture

Vascular SMCs were isolated from the luminal side of the aortic arch from *Fibulin-4^{+/+}*, *Fibulin-4^{+/R}* and *Fibulin-4^{R/R}* male mice. The tissue was washed with phosphate-buffered saline (PBS), cut into 5-mm pieces with the luminal side on the 0.1% gelatine coated cell culture dishes and incubated. After 7–10 days, smooth muscle-like cell outgrowth was observed. SMCs were maintained in DMEM (Lonza, Leusden, the Netherlands), supplemented with 10% foetal calf serum (HyClone, Thermo Scientific, Breda, the Netherlands), 100 U/ml penicillin and 100 μ g/ml streptomycin (Sigma-Aldrich, Zwijndrecht, the Netherlands). Cells were used at passage 5–11.

Immuno-fluorescent and –histochemical stainings

Subconfluent SMCs, Human Umbilical Vein Endothelial Cells (HUVECs), isolated as described before⁴⁹, and Mouse Embryonic Fibroblasts (MEFs), isolated from 8 day old C57/bl6 mouse embryos, were grown on coverslips and fixed in 1% paraformaldehyde. Cells were permeabilised with 0.1% Triton/PBS and blocked with PBS containing 1.5% bovine serum albumin/0.15% glycine (Sigma). Next, coverslips were incubated overnight at 4°C with the primary antibodies; mouse anti-smooth muscle actin 1:1500 (Progen, Heidelberg, Germany), rabbit polyclonal anti-SM22 alpha antibody 1:400 (Abcam, Cambridge, UK), mouse monoclonal anti-smooth muscle myosin heavy chain II 1G12 1:500 (Abcam, Cambridge, UK), rabbit anti-CD31 1:800 (Santa Cruz Biotechnologies, Santa Cruz, USA) and rabbit anti-FSP1/S100A4 1:1600 (Millipore, MA, USA). The next day cells were incubated with secondary antibodies anti-mouse alexafluor 488 1:1000 (Molecular Probes, Eugene, Oregon) for SMA and MHC II and anti-rabbit alexafluor 594 1:1000 (Molecular Probes, Eugene, Oregon) for SM22, CD31 and Fibroblast Specific Protein1 (FSP-1), and mounted with DAPI. Slides were analysed with the LEICA DMRBE Aristoplan Microscope equipped with the Hamamatsu ORCA-ER Camera. Pictures were taken at 25 x magnification. To analyse *in vivo* SMC content and proliferation 4 μ m sections of paraffin embedded aortas were stained with haematoxylin and eosin, elastin (Verhoeff-van Gieson), and α -smooth muscle actin as described before³¹. BrdU staining was performed according to the manufacturers' protocol (Roche, Basel, Switzerland).

Proliferation assay

Fibulin-4^{+/+}, *Fibulin-4^{+/R}* and *Fibulin-4^{R/R}* SMCs were seeded in triplicate in 6 cm dishes (5000 cells/well) and allowed to attach overnight. Next cells were treated with TGF- β neutralizing antibodies (kindly provided by Dr. E. de Heer, Leiden University Medical Centre, Dept. of Pathology^{26, 27}) and counted every day using a Burker cell counting

chamber. Medium was replaced every other day. The MTS proliferation assay was performed according to the manufacturer's instructions (Promega, Madison, USA). In short SMCs were seeded in 96-well plates (1500 cells/well) and allowed to attach overnight. At day-1, -2 and -3 medium was changed to 100 μ l complete DMEM + 20 μ l MTS substrate and the metabolic activity of the cells was analysed by absorbance change at 490 nm after 2 hours.

TGF- β response assay

TGF- β response in SMCs was determined using (CAGA)₁₂-MLP-Luciferase promoter reporter construct²⁸. This construct contains 12 palindromic repeats of the SMAD3/4 binding element derived from the *PAI-1* promoter and was shown to be highly specific and sensitive to TGF- β . The assay was performed as described previously²⁹. In short SMCs were seeded in 1% gelatine coated 24-well plates and allowed to attach overnight. Subconfluent cells were transfected using Lipofectamin 2000 (Invitrogen, Carlsbad, California, USA) according to the manufacturer's protocol. A β -galactosidase plasmid was co-transfected to correct for transfection efficiency. After 6 hours, medium was changed to DMEM containing 10% FCS and the cells were incubated for 24 hours. Next cells were serum-starved overnight and stimulated with 5 ng/ml TGF- β 3 (kindly provided by Kenneth K. Iwata, OSI, Inc., New York, USA) in the presence or absence of 10 μ M SB431542 (Tocris/R&D systems, Abington, UK) for 6 hours. After stimulation the cells were washed, lysed and luciferase activity was determined according to the manufacturer's protocol (Promega). β -Galactosidase activity in the lysates was determined using β -gal substrate (0.2M H₂PO₄, 2mM MgCl₂, 4mM ortho-nitrophenyl-phosphate, 0.25% β -mercaptoethanol) and measuring absorbance change at 405 nm. The luciferase count was corrected for β -galactosidase activity. The relative increase in luciferase activity was calculated versus controls. All experiments were performed at least three times in triplicate. To determine the transfection efficiency of *Fibulin-4*^{+/+}, *Fibulin-4*^{+/R} and *Fibulin-4*^{R/R} SMCs they were transfected with a GFP plasmid as described above, trypsinised and fixed with 1% PFA. Subsequently, SMCs were analysed with flow cytometry for the percentage of GFP transfected SMCs compared to the total amount of SMCs.

Western blot analysis

Western blot analysis was performed as described before⁵⁰. In short, equal amounts of protein (DC protein assay, Bio-Rad Laboratories, Hercules, CA, USA) were separated on 10% SDS-polyacrylamide gel electrophoresis under reducing conditions. Proteins were transferred to nitrocellulose membranes (Whatman, Dassel, Germany) and blocked with 5% milk powder in Tris-HCl buffered saline containing 0.05% Tween-20 (Merck, Darmstadt, Germany). After washing, blots were overnight incubated with rabbit anti-pSMAD2 (Cell signaling Technologies, USA) and rabbit anti-pSMAD3 (kindly provided by Dr. E. Leof, Mayo Clinic, Rochester, MN, USA) followed by horseradish peroxidase-conjugated secondary antibodies (all GE Healthcare, Waukesha, WI, USA). Detection was performed by chemoluminescence according to the manufacturer's protocol (Pierce, Rockford, IL, USA). Afterwards, blots were stripped and probed with mouse anti- β -actin antibodies as a loading control.

RNA isolation and real-time PCR

Expression of *Fibulin-4* and *Tgf- β 2* were analysed in SMCs. RNA was isolated using RNeasy Mini Kit according to the manufacturer's instructions (Qiagen, Hilden, Germany). RNA concentration and purity was determined spectrometrically. Complementary DNA synthesis was performed using random primers. cDNA samples were subjected to 40 cycles real-time PCR analysis using maxima SYBR Green qPCR Master Mix 2x (Fermentas, Vilnius, Lithuania) and primers shown in table I. Reactions were performed in triplicates for each sample. Product specificity was determined by melting curve analysis and gel electrophoresis. The average Ct values of the triple reactions were calculated for each gene and all values were normalized for cDNA content by *Hprt* expression. The levels of fold-change for each gene were calculated relative to the gene expression levels in baseline wild type SMCs. RNA isolated from HUVECs and fibroblasts were used as controls for the genes analysed.

TGF- β ELISAs

SMC conditioned medium was prepared by seeding the cells and growing them to subconfluence. Medium was changed to serum-free DMEM, containing antibiotics as described above, and incubated for 4 days. Samples were collected every day and frozen at -20 until analysis. Lysates were prepared from aortic arches of 14-15 week old *Fibulin-4^{+/+}*, *Fibulin-4^{+/-}* and *Fibulin-4^{R/R}* mice and protein amounts were determined (Pierce BCA protein assay kit, Thermo Scientific). Total TGF- β 1, TGF- β 2, and TGF- β 3 levels in CM samples, aortic arch lysates and plasma samples were determined by commercially available duo-sets (R&D Systems) using transient acidification as described before⁵¹.

Statistical analysis

Data are presented as mean \pm SEM. The non-parametric Mann-Whitney U-test and unpaired student's t-test were performed to analyse the specific sample groups for significant differences. The two-way ANOVA test was used to test significant differences between independent variables. A p-value of <0.05 was considered to indicate a significant difference between groups. All analyses were performed using IBM SPSS Statistics version 20.0 and 22.0 (SPSS Inc., Chicago, IL, USA).

REFERENCES

- Lindsay ME, Dietz HC. Lessons on the pathogenesis of aneurysm from heritable conditions. *Nature* 2011;**473**:308-316.
- Olsson C, Thelin S, Stahle E, Ekbom A, Granath F. Thoracic aortic aneurysm and dissection: increasing prevalence and improved outcomes reported in a nationwide population-based study of more than 14,000 cases from 1987 to 2002. *Circulation* 2006;**114**:2611-2618.
- Isselbacher EM. Thoracic and abdominal aortic aneurysms. *Circulation* 2005;**111**:816-828.
- Bunton TE, Biery NJ, Myers L, Gayraud B, Ramirez F, Dietz HC. Phenotypic alteration of vascular smooth muscle cells precedes elastolysis in a mouse model of Marfan syndrome. *Circ Res* 2001;**88**:37-43.
- Inamoto S, Kwartler CS, Lafont AL, Liang YY, Fadulu VT, Duraisamy S, Willing M, Estrera A, Safi H, Hannibal MC, Carey J, Wiktorowicz J, Tan FK, Feng XH, Pannu H, Milewicz DM. TGFBR2 mutations alter smooth muscle cell phenotype and predispose to thoracic aortic aneurysms and dissections. *Cardiovasc Res* 2010;**88**:520-529.
- Dietz HC, Cutting GR, Pyeritz RE, Maslen CL, Sakai LY, Corson GM, Puffenberger EG, Hamosh A, Nanthakumar EJ, Curristin SM, et al. Marfan syndrome caused by a recurrent de novo missense mutation in the fibrillin gene. *Nature* 1991;**352**:337-339.
- Wang L, Guo DC, Cao J, Gong L, Kamm KE, Regalado E, Li L, Shete S, He WQ, Zhu MS, Offermanns S, Gilchrist D, Eleftheriades J, Stull JT, Milewicz DM. Mutations in myosin light chain kinase cause familial aortic dissections. *Am J Hum Genet* 2010;**87**:701-707.
- van de Laar IM, Oldenburg RA, Pals G, Roos-Hesselink JW, de Graaf BM, Verhagen JM, Hoedemaekers YM, Willemsen R, Severijnen LA, Venselaar H, Vriend G, Pattynama PM, Collee M, Majoer-Krakauer D, Poldermans D, Frohn-Mulder IM, Micha D, Timmermans J, Hilhorst-Hofstee Y, Bierma-Zeinstra SM, Willems PJ, Kros JM, Oei EH, Oostra BA, Wessels MW, Bertoli-Avella AM. Mutations in SMAD3 cause a syndromic form of aortic aneurysms and dissections with early-onset osteoarthritis. *Nat Genet* 2011;**43**:121-126.
- ten Dijke P, Arthur HM. Extracellular control of TGFbeta signalling in vascular development and disease. *Nat Rev Mol Cell Biol* 2007;**8**:857-869.
- Loeys BL, Chen J, Neptune ER, Judge DP, Podowski M, Holm T, Meyers J, Leitch CC, Katsanis N, Sharifi N, Xu FL, Myers LA, Spevak PJ, Cameron DE, De Backer J, Hellems J, Chen Y, Davis EC, Webb CL, Kress W, Coucke P, Rifkin DB, De Paepe AM, Dietz HC. A syndrome of altered cardiovascular, craniofacial, neurocognitive and skeletal development caused by mutations in TGFBR1 or TGFBR2. *Nat Genet* 2005;**37**:275-281.
- Neptune ER, Frischmeyer PA, Arking DE, Myers L, Bunton TE, Gayraud B, Ramirez F, Sakai LY, Dietz HC. Dysregulation of TGF-beta activation contributes to pathogenesis in Marfan syndrome. *Nat Genet* 2003;**33**:407-411.
- Hanada K, Vermeij M, Garinis GA, de Waard MC, Kunen MG, Myers L, Maas A, Duncker DJ, Meijers C, Dietz HC, Kanaar R, Essers J. Perturbations of vascular homeostasis and aortic valve abnormalities in fibulin-4 deficient mice. *Circ Res* 2007;**100**:738-746.
- Renard M, Holm T, Veith R, Callewaert BL, Ades LC, Baspinar O, Pickart A, Dasouki M, Hoyer J, Rauch A, Trapane P, Earing MG, Coucke PJ, Sakai LY, Dietz HC, De Paepe AM, Loeys BL. Altered TGFbeta signaling and cardiovascular manifestations in patients with autosomal recessive cutis laxa type I caused by fibulin-4 deficiency. *Eur J Hum Genet* 2010;**18**:895-901.
- Renard M, Callewaert B, Baetens M, Campens L, MacDermot K, Fryns JP, Bonduelle M, Dietz HC, Gaspar IM, Cavaco D, Stattin EL, Schrandt-Stumpel C, Coucke P, Loeys B, De Paepe A, De Backer J. Novel MYH11 and ACTA2 mutations reveal a role for enhanced TGFbeta signaling in FTAAD. *Int J Cardiol* 2013;**165**:314-321.
- Renard M, Callewaert B, Malfait F, Campens L, Sharif S, del Campo M, Valenzuela I, McWilliam C, Coucke P, De Paepe A, De Backer J. Thoracic aortic-aneurysm and dissection in association with significant mitral valve disease caused by mutations in TGFBR2. *Int J Cardiol* 2013;**165**:584-587.
- Merwin JR, Newman W, Beall LD, Tucker A, Madri J. Vascular cells respond differentially to transforming growth factors beta 1 and beta 2 in vitro. *Am J Pathol* 1991;**138**:37-51.
- Erickson LK, Opitz JM, Zhou H. Lethal osteogenesis imperfecta-like condition with cutis laxa and arterial tortuosity in MZ twins due to a homozygous fibulin-4 mutation. *Pediatr Dev Pathol* 2012;**15**:137-141.
- Sawyer SL, Dicke F, Kirton A, Rajapakse T, Rebeyka IM, McInnes B, Parboosingh JS, Bernier FP. Longer term survival of a child with autosomal recessive cutis

- laxa due to a mutation in FBLN4. *Am J Med Genet A* 2013;**161A**:1148-1153.
19. Kappanayil M, Nampoothiri S, Kannan R, Renard M, Coucke P, Malfait F, Menon S, Ravindran HK, Kurup R, Faiyaz-Ul-Haque M, Kumar K, De Paepe A. Characterization of a distinct lethal arteriopathy syndrome in twenty-two infants associated with an identical, novel mutation in FBLN4 gene, confirms fibulin-4 as a critical determinant of human vascular elastogenesis. *Orphanet J Rare Dis* 2012;**7**:61.
 20. Huang J, Davis EC, Chapman SL, Budatha M, Marmorstein LY, Word RA, Yanagisawa H. Fibulin-4 deficiency results in ascending aortic aneurysms: a potential link between abnormal smooth muscle cell phenotype and aneurysm progression. *Circ Res* 2010;**106**:583-592.
 21. Chen Q, Zhang T, Roshetsky JF, Ouyang Z, Essers J, Fan C, Wang Q, Hinek A, Plow EF, Dicorleto PE. Fibulin-4 regulates expression of the tropoelastin gene and consequent elastic-fibre formation by human fibroblasts. *Biochem J* 2009;**423**:79-89.
 22. Horiguchi M, Inoue T, Ohbayashi T, Hirai M, Noda K, Marmorstein LY, Yabe D, Takagi K, Akama TO, Kita T, Kimura T, Nakamura T. Fibulin-4 conducts proper elastogenesis via interaction with cross-linking enzyme lysyl oxidase. *Proc Natl Acad Sci U S A* 2009;**106**:19029-19034.
 23. Brisset AC, Hao H, Camenzind E, Bacchetta M, Geinoz A, Sanchez JC, Chaponnier C, Gabbiani G, Bochaton-Piallat ML. Intimal smooth muscle cells of porcine and human coronary artery express S100A4, a marker of the rhomboid phenotype in vitro. *Circ Res* 2007;**100**:1055-1062.
 24. Hao H, Ropraz P, Verin V, Camenzind E, Geinoz A, Pepper MS, Gabbiani G, Bochaton-Piallat ML. Heterogeneity of smooth muscle cell populations cultured from pig coronary artery. *Arterioscler Thromb Vasc Biol* 2002;**22**:1093-1099.
 25. Wang J, Chen H, Seth A, McCulloch CA. Mechanical force regulation of myofibroblast differentiation in cardiac fibroblasts. *Am J Physiol Heart Circ Physiol* 2003;**285**:H1871-1881.
 26. Lucas C, Bald LN, Fendly BM, Mora-Worms M, Figari IS, Patzer EJ, Palladino MA. The autocrine production of transforming growth factor-beta 1 during lymphocyte activation. A study with a monoclonal antibody-based ELISA. *J Immunol* 1990;**145**:1415-1422.
 27. Arteaga CL, Hurd SD, Winnier AR, Johnson MD, Fendly BM, Forbes JT. Anti-transforming growth factor (TGF)-beta antibodies inhibit breast cancer cell tumorigenicity and increase mouse spleen natural killer cell activity. Implications for a possible role of tumor cell/host TGF-beta interactions in human breast cancer progression. *J Clin Invest* 1993;**92**:2569-2576.
 28. Dennler S, Itoh S, Vivien D, ten Dijke P, Huet S, Gauthier JM. Direct binding of Smad3 and Smad4 to critical TGF beta-inducible elements in the promoter of human plasminogen activator inhibitor-type 1 gene. *EMBO J* 1998;**17**:3091-3100.
 29. Hawinkels LJ, Paauwe M, Verspaget HW, Wiercinska E, van der Zon JM, van der Ploeg K, Koelink PJ, Lindeman JH, Mesker W, ten Dijke P, Sier CF. Interaction with colon cancer cells hyperactivates TGF-beta signaling in cancer-associated fibroblasts. *Oncogene* 2014;**33**:97-107.
 30. Habashi JP, Judge DP, Holm TM, Cohn RD, Loeys BL, Cooper TK, Myers L, Klein EC, Liu G, Calvi C, Podowski M, Neptune ER, Halushka MK, Bedja D, Gabrielson K, Rifkin DB, Carta L, Ramirez F, Huso DL, Dietz HC. Losartan, an AT1 antagonist, prevents aortic aneurysm in a mouse model of Marfan syndrome. *Science* 2006;**312**:117-121.
 31. Moltzer E, te Riet L, Swagemakers SM, van Heijningen PM, Vermeij M, van Veghel R, Bouhuizen AM, van Esch JH, Lankhorst S, Ramnath NW, de Waard MC, Duncker DJ, van der Spek PJ, Rouwet EV, Danser AH, Essers J. Impaired vascular contractility and aortic wall degeneration in fibulin-4 deficient mice: effect of angiotensin II type 1 (AT1) receptor blockade. *PLoS One* 2011;**6**:e23411.
 32. Tsai S, Hollenbeck ST, Ryer EJ, Edlin R, Yamanouchi D, Kundi R, Wang C, Liu B, Kent KC. TGF-beta through Smad3 signaling stimulates vascular smooth muscle cell proliferation and neointimal formation. *Am J Physiol Heart Circ Physiol* 2009;**297**:H540-549.
 33. Shull MM, Ormsby I, Kier AB, Pawlowski S, Diebold RJ, Yin M, Allen R, Sidman C, Proetzel G, Calvin D, et al. Targeted disruption of the mouse transforming growth factor-beta 1 gene results in multifocal inflammatory disease. *Nature* 1992;**359**:693-699.
 34. Kaartinen V, Voncken JW, Shuler C, Warburton D, Bu D, Heisterkamp N, Groffen J. Abnormal lung development and cleft palate in mice lacking TGF-beta 3 indicates

- defects of epithelial-mesenchymal interaction. *Nat Genet* 1995;**11**:415-421.
35. Bartram U, Molin DG, Wisse LJ, Mohamad A, Sanford LP, Doetschman T, Speer CP, Poelmann RE, Gittenberger-de Groot AC. Double-outlet right ventricle and overriding tricuspid valve reflect disturbances of looping, myocardialization, endocardial cushion differentiation, and apoptosis in TGF-beta(2)-knockout mice. *Circulation* 2001;**103**:2745-2752.
 36. Gallo EM, Loch DC, Habashi JP, Calderon JF, Chen Y, Bedja D, van Erp C, Gerber EE, Parker SJ, Sauls K, Judge DP, Cooke SK, Lindsay ME, Rouf R, Myers L, ap Rhys CM, Kent KC, Norris RA, Huso DL, Dietz HC. Angiotensin II-dependent TGF-beta signaling contributes to Loews-Dietz syndrome vascular pathogenesis. *J Clin Invest* 2014;**124**:448-460.
 37. Battegay EJ, Raines EW, Seifert RA, Bowen-Pope DF, Ross R. TGF-beta induces bimodal proliferation of connective tissue cells via complex control of an autocrine PDGF loop. *Cell* 1990;**63**:515-524.
 38. Jacobsen SE, Keller JR, Ruscetti FW, Kondaiah P, Roberts AB, Falk LA. Bidirectional effects of transforming growth factor beta (TGF-beta) on colony-stimulating factor-induced human myelopoiesis in vitro: differential effects of distinct TGF-beta isoforms. *Blood* 1991;**78**:2239-2247.
 39. Lopez-Casillas F, Wrana JL, Massague J. Betaglycan presents ligand to the TGF beta signaling receptor. *Cell* 1993;**73**:1435-1444.
 40. Bee KJ, Wilkes DC, Devereux RB, Basson CT, Hatcher CJ. TGFbetaRIIb mutations trigger aortic aneurysm pathogenesis by altering transforming growth factor beta2 signal transduction. *Circ Cardiovasc Genet* 2012;**5**:621-629.
 41. McCaffrey TA, Consigli S, Du B, Falcone DJ, Sanborn TA, Spokojny AM, Bush HL, Jr. Decreased type II/type I TGF-beta receptor ratio in cells derived from human atherosclerotic lesions. Conversion from an antiproliferative to profibrotic response to TGF-beta1. *J Clin Invest* 1995;**96**:2667-2675.
 42. Samarakoon R, Overstreet JM, Higgins PJ. TGF-beta signaling in tissue fibrosis: redox controls, target genes and therapeutic opportunities. *Cell Signal* 2013;**25**:264-268.
 43. Fuchshofer R, Tamm ER. The role of TGF-beta in the pathogenesis of primary open-angle glaucoma. *Cell Tissue Res* 2012;**347**:279-290.
 44. Jaschinski F, Rothhammer T, Jachimczak P, Seitz C, Schneider A, Schlingensiepen KH. The antisense oligonucleotide trabedersen (AP 12009) for the targeted inhibition of TGF-beta2. *Curr Pharm Biotechnol* 2011;**12**:2203-2213.
 45. Hawinkels LJ, Ten Dijke P. Exploring anti-TGF-beta therapies in cancer and fibrosis. *Growth Factors* 2011;**29**:140-152.
 46. Brooke BS, Habashi JP, Judge DP, Patel N, Loeyes B, Dietz HC, 3rd. Angiotensin II blockade and aortic-root dilation in Marfan's syndrome. *N Engl J Med* 2008;**358**:2787-2795.
 47. Kuang SQ, Geng L, Prakash SK, Cao JM, Guo S, Villamizar C, Kwartler CS, Peters AM, Brasier AR, Milewicz DM. Aortic remodeling after transverse aortic constriction in mice is attenuated with AT1 receptor blockade. *Arterioscler Thromb Vasc Biol* 2013;**33**:2172-2179.
 48. Massam-Wu T, Chiu M, Choudhury R, Chaudhry SS, Baldwin AK, McGovern A, Baldock C, Shuttleworth CA, Kiely CM. Assembly of fibrillin microfibrils governs extracellular deposition of latent TGF beta. *J Cell Sci* 2010;**123**:3006-3018.
 49. Hawinkels LJ, Zuidwijk K, Verspaget HW, de Jonge-Muller ES, van Duijn W, Ferreira V, Fontijn RD, David G, Hommes DW, Lamers CB, Sier CF. VEGF release by MMP-9 mediated heparan sulphate cleavage induces colorectal cancer angiogenesis. *Eur J Cancer* 2008;**44**:1904-1913.
 50. Kaijzel EL, van Heijningen PM, Wielopolski PA, Vermeij M, Koning GA, van Cappellen WA, Que I, Chan A, Dijkstra J, Ramnath NW, Hawinkels LJ, Bernsen MR, Lowik CW, Essers J. Multimodality imaging reveals a gradual increase in matrix metalloproteinase activity at aneurysmal lesions in live fibulin-4 mice. *Circ Cardiovasc Imaging* 2010;**3**:567-577.
 51. Hawinkels LJ, Verspaget HW, van der Reijden JJ, van der Zon JM, Verheijen JH, Hommes DW, Lamers CB, Sier CF. Active TGF-beta1 correlates with myofibroblasts and malignancy in the colorectal adenoma-carcinoma sequence. *Cancer Sci* 2009;**100**:663-670.

ACKNOWLEDGEMENTS

We thank Dr. E. de Heer for providing the TGF- β neutralizing antibody and Dr. E. Leof for providing the phospho-SMAD-3 antibody.

SOURCES OF FUNDING

This work was supported by the 'Lijf en Leven' grant (2008): 'early detection and diagnosis of aneurysms and heart valve abnormalities' (to JE and PvH). LH and MP are supported by the Alp d'HuZes/Bas Mulder award 2011 (UL 2011-5051).

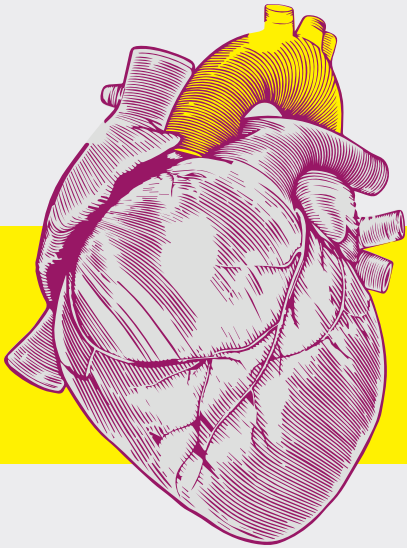
AUTHOR CONTRIBUTIONS

NR and LH designed and performed experiments, analysed data and wrote the main manuscript. PH isolated vSMCs and contributed to the TGF-beta reporter assays. LR contributed to the preparation of Figure 5 with the Losartan treatment data. MP contributed to real time PCR and ELISA data. MV contributed to immunohistochemical stainings. RK, PD and JE supervised the project. All authors reviewed the manuscript.

Table 1

Primers used for quantitative real time PCR. Forward and reverse primers are displayed for each gene from 5' to 3'.

Genes	Forward primers	Reverse primers
Fibulin-4	5'-GGGTTATTTGTGTCTGCCTCG-3'	5'-TGGTAGGAGCCAGGAAGGTT-3'
SMA	5'-GTCCCAGACATCAGGGAGTAA-3'	5'-TCGGATACTTCAGCGTCAGGA-3
TGF- β 1	5'-CAACAATTCCTGGCGTTACC-3'	5'-TGCTGTCACAAGAGCAGTGA-3'
TGF- β 2	5'-CCGCCCACTTTCTACAGACCC-3'	5'-GCGCTGGGTGGGAGATGTAA-3'



Part III

The Identification of Genetic Factors Involved
in Aneurysms

CHAPTER 7

RNA Expression Profiling of Abdominal Aortic Aneurysmal Disease Identifies Signaling Cross-talk Between TGF β and BMP

L. te Riet[#], A. Ijpma[#], K. M. van de Luitgaarden, P. M. van Heijningen, D. Majoor-Krakauer, E. V. Rouwet, H. J. M. Verhagen, J. Essers, I. van der Pluijm

*#*Authors contributed equally

(in progress)



ABSTRACT

An abdominal aortic aneurysm (AAA) is a widening of the aorta below the renal arteries, usually asymptomatic until rupture causes fatal bleeding, which is a major vascular health problem. Abdominal aortic aneurysms are associated with high age, male gender and cardiovascular risk factors such as hypertension and smoking, however the underlying genetic changes remain to be elucidated. In order to develop proper treatment strategies, it is crucial to understand the mechanisms and targets that play a role in AAA. Strikingly, AAA has many if not all risk factors in common with aortic occlusive disease (AOD), yet the outcome is quite opposite; dilation versus occlusion of the aorta. We therefore compared RNA expression profiles of abdominal aortic samples of AAA patients using 'best match control' material of patients with AOD to identify molecular mechanisms that underlie AAA disease. In addition, to identify novel biological mechanisms, pathways and key regulators, we designed an analysis pipeline to select genes based on their level of expression, their potential as blood marker and their possible relevance for aneurysmal disease, resulting in a list of potential targets and markers for further study in blood of AAA patients. The list of significantly changed genes included COL11A1 (32-fold increase, $p=0.00012$), ADIPOQ, LPL (21-fold increase, $p=0.0003$) that have previously been associated with AAA, validating our approach. The list also included genes such as CXCL13, SLC7A5, FDC-5P, for which the connection with aneurysmal disease is novel. IPA analysis revealed an overrepresentation of significantly altered immune related pathways next to pathways previously associated with aneurysmal disease. Our gene expression profiling approach not only identifies genes and pathways previously associated with AAA genes, but also reveals that simultaneous inhibition of BMP and activation of TGF- β signaling controls aneurysm growth in the abdominal aorta.

INTRODUCTION

Aneurysms are life-threatening arterial diseases identified by the dilatation of a blood vessel with a more than 50% increase of the diameter compared to normal. Aortic aneurysms can arise at different locations, and most common are thoracic and abdominal aortic aneurysms (TAA and AAA). Both these types are associated with high age, male gender and atherosclerosis, as well as with environmental and familial components. Around 5% of TAAs are present in a syndromic form, with early onset, and several responsible genes have been identified so far.¹⁻³

Genes that have directly been linked to syndromic forms of TAA encode for transforming growth factor β (TGF β) components, cytoskeleton proteins, or extracellular matrix (ECM) proteins. Well-known examples are Marfan syndrome (MFS) with a mutation in the extracellular matrix protein Fibrillin-1, and Loeys-Dietz syndrome with mutations in genes including the TGF β -receptors 1 and 2, and SMAD3.⁴⁻⁶ Histological staining of aortic aneurysm sections of these patients usually show abnormalities in the extracellular matrix (ECM), loss of smooth muscle cells and disorganization of elastin and collagen structure.⁷ Furthermore, TGF β -signaling is increased in TAAs of patients and mice, and high serum TGF β levels correlated directly with aortic root dilation.⁸⁻¹² It is unclear if genetic factors affected in TAA also play a role in AAA, though a recent study identified overlapping genetic defects between AAA and familial TAA.¹³ The prevalence of AAA is ~8% among men older than 65 years of age and is much higher than for TAA.¹⁴ Yet, in contrast to TAA, for AAA causative genes are hard to identify.

Interestingly, aneurysm formation and arterial occlusive disease (AOD) share a number of important risk factors, such as smoking, hypertension, and older age. In men over 65 years of age, 48% have atherosclerosis in the aorta, of which 9-16% will also develop an aortic aneurysm.¹⁵⁻¹⁷ Based on this common clinical risk profile, aneurysm formation was formerly ascribed to atherosclerosis. Of the many types of cardiovascular diseases, atherosclerosis is most common and contributes to major morbidity and mortality in developed countries. Contributing factors such as dyslipidemia, diabetes and hypertension will result in the manifestation of plaque development, vascular smooth muscle cell (VSMC) proliferation, and extracellular matrix modulation, eventually resulting into obstruction of the blood vessel as seen in AOD. Abdominal aneurysms, with similar risk factors and alike pathologic processes as AOD, shows another form of extracellular matrix modulation and a different role of VSMCs. The process of matrix modulation results in enzymatic degradation of the elastin laminae causing disruption of arterial wall integrity, therefore weakening and dilatation of the aortic wall, resulting in an aneurysm.² Pathologically, aneurysm formation is characterized by destruction of elastin and collagen in the media and adventitia of the arterial wall, loss of medial smooth muscle cells, and transmural infiltration of lymphocytes and macrophages. However, despite many similarities in risk factors for AAA and AOD, the two diseases have opposite outcomes, i.e. dilatation versus stenosis/occlusion.

Targeted ultrasound screening of high risk cases may allow reduction of AAA related mortality and early diagnosis therein is crucial. Thus, a clinical risk prediction model will aid in earlier, and more efficient, identification of persons at risk. Identifying the underlying processes and genes that differentiate these two diseases will be a first step towards such a risk prediction model. In this study we therefore investigated the transcriptional profiles and molecular processes that differentiate AAA from AOD.



MATERIALS AND METHODS

Tissue analysis

Patient cohort Micro-array

Aortic tissue was derived from patients undergoing elective open surgical reconstruction of the infrarenal abdominal aorta for either abdominal aortic aneurysm (AAA) or aortoiliac occlusive disease (AOD) in the Erasmus University Medical Center between 2008 and 2012. The study complies with the Helsinki declaration on research ethics. Aortic biopsies were obtained by protocol approved by the institutional Medical Ethics Committee (MEC-2012-387, MEC 2013-265, MEC-2014-057).

Aortic biopsies

Full thickness aortic tissue samples for RNA expression profiling in AAA patients were collected from the infrarenal anterior aneurysm wall in AAA patients. Full thickness aortic tissue samples in AOD patients were obtained from the infrarenal anterior aortic wall at the site of the proximal anastomosis of the prosthetic graft. Tissue samples were snap frozen in liquid nitrogen directly after harvesting and stored at -80°C until RNA isolation.

RNA isolation and Microarray hybridization

Total RNA including miRNAs were isolated using the miRNeasy Mini Kit (Qiagen, Hilden, Germany). Tissues were disrupted with a 5mm steel bead by a disruption program of 2 times 20Hz in the TissueLyser II (Qiagen, Hilden, Germany). RNA quality was checked with the Bioanalyzer 2100 (Agilent Technologies, Santa Clara, CA, USA). Samples with a high quality RNA Integrity number (RIN) and with a 28S/18S ratio of >0.9 were used for hybridization. Microarray hybridization and scanning were performed at SkylineDiagnostics (Skyline Diagnostics, Rotterdam, The Netherlands). In short, 625 ng RNA was processed to generate cRNA. Fragmented and biotinylated cRNA was subsequently hybridized on Affymetrix U133 plus 2.0 microarrays (Affymetrix Inc, Santa Clara, CA, USA) and these microarrays were scanned with an Affymetrix Genechip System 3000Dx v.2 microarray scanner (Affymetrix Inc, Santa Clara, CA, USA).

RNA expression analysis

The CEL files generated by the Affymetrix Genechip System 3000Dx v.2 microarray scanner were subsequently imported into Partek Genomics Suite version 6.4 (Partek Inc, St Louis, MO, USA). Quantile normalization and background correction was applied to the raw intensity values of all samples via GC Robust Multichip Analysis. As the data was processed in 3 hybridization batches, hybridization batch effect correction was applied. To visualize the correlation between the samples, principal component analysis and unsupervised hierarchical clustering were used. For the comparison of AAA with AOD samples, 2-sample T-test statistics were applied to calculate the fold changes with associated p-values.

Microarray data processing

During data processing within Partek Genomics Suite 6.4, all microarray CEL files were assessed for passing of quality control (QC) thresholds. We started the analysis with 14 AAA samples and 7 AOD samples. One AAA samples failed QC due to bad hybridization and this sample was removed from the analysis. During unsupervised clustering, all AAA samples grouped together and all AOD samples also grouped together. One AAA sample grouped together with the AOD samples. Since the two groups clustered into 2 clear groups we suspected a potential sample misidentification and therefore this AAA sample was removed from the analysis.

IPA analysis

A set of differential expressed genes was uploaded into Ingenuity/Qiagen IPA (Qiagen, Redwood City, CA, USA) and a core analysis was performed on 1047 significant expressed genes ($-2 \leq \text{FC} \leq 2$ and $p\text{-value} \leq 0.05$), as part of the core analysis we looked at functions, pathways and upstream regulator. First the $\log_2\text{Ratio}$ (fold change)

and p-value data generated from the 2-sample test analysis in Partek Genomics Suite 6.4, was uploaded into IPA. For the Ingenuity Pathway Analysis (IPA), significance thresholds of $\log_2\text{Ratio}=1$ (this equals $-2 \leq \text{FC} \leq 2$) and $p\text{-value} < 0.05$ were applied for the comparison of the AAA vs AOD groups. During upload of the data into IPA, the probe level data was mapped to the gene level and averaged based on the median Fold Change values. For the upstream analysis the z-score significance thresholds were set to $-1.8 \leq z\text{-score} \leq 1.8$ and $p\text{-value} < 0.01$.

Selection of genes

A list of 50 genes that could serve as potential markers for AAA was generated by applying the following potential prioritization protocol, which was designed to identify best possible markers. The two parts of the IPA core analysis that contributed to this prioritization schedule were the list of significantly upregulated genes scored by highest fold change and p-value together with the list of significant Upstream Regulators (Figure 2). These are genes that are not necessarily themselves differentially regulated, but are identified based on the prediction to regulate a significant (or substantial) set of genes present within the gene expression dataset being analyzed. The final selection list consists of 30 genes; 15 based on selection of the most significantly upregulated genes (left selection procedure in Figure 2) and 15 genes based on the most significant Upstream regulators (right selection procedure in Figure 2).

Steps to prioritize the 15 most significantly upregulated genes were as follows (1) The normalized raw expression values were divided into 3 categories: Low (< 80), Medium (80-800) and High (> 800). Only genes with High or Medium expression levels were considered as we reasoned it will be technically difficult to detect a gene with low expression values. (2) Only genes that showed an increase in expression levels in the AAA samples relative to the AOD samples were selected since detection of increased expression (presence) is more robust than detection of decreased expression (absence). (3) Genes that at the protein level are expressed on the cell membrane or that are secreted extracellularly were selected as we reasoned that this would improve the ability to detect a potential marker in blood. (4) All genes were marked that were part of our in-house developed Vascular Gene Set. The Vascular Gene Set (4209 genes; Supplemental Table II) is a list of genes with relevance to vascular tissue development, maintenance and disease, including aortic aneurysms, that are selected based on HGMD and OMIM information, GO terms, KEGG pathways, Ingenuity IPA pathways, GWAS studies and literature (Supplemental Table I). (5) As a last step we also marked the genes that were identified as significant upstream regulators. Here we reasoned that prioritization via two independent analyses gives increased overall confidence in the proper selection.

Steps to prioritize the 15 most significantly upstream regulators: (1) Upstream regulators were prioritized based on the highest Upstream Regulator z-score with a minimal p-value of 0.01. (2) All genes that were part the Vascular Gene Set were marked. (3) Upstream regulators that were identified as being significantly upregulated at the mRNA level in our dataset, above the threshold of $\log_2\text{Ratio}=1$ (fold change=2) were also marked. Here we reasoned that prioritization via two independent analysis gives increased overall confidence in the proper selection.

QPCR analysis

Expression data of COL11A, Adiponectin, CXCL13, SLC7A5 and FDC-SP were analyzed in diseased aortic tissue. Total RNA was reverse transcribed using iScript cDNA Synthesis Kit (Bio-Rad, Veenendaal, The Netherlands). cDNA samples were subjected to 40 cycles real-time PCR analysis using SYBR Green qPCR Master Mix 2x (Bio-Rad, Veenendaal, Netherlands) and primers; Actin- β 5'-CTCCCTGGAGAAGAGCTACG-3'; 5'-GAAGGAAGGCTGGAAGAGTG-3'; Hypoxanthine-guanine phosphoribosyltransferase (HPRT) 5'-TGACACTGGCAAACAATGCA-3'; 5'-GGTCTTTTCACCAGCAAGCT-3'; COL11a1 5'-ACAATAGCACAGACGGAGGC-3'; 5'-GGATTTGGCTCATTTGTCCCAG-3'; Adiponectin 5'-GTGATGGCAGAGATGGCACC-3'; 5'-ACTCCGGTTTCACCGATGTC-3'; CXCL13 5'-CGAATTC AATCTTGCCCCGT-3';

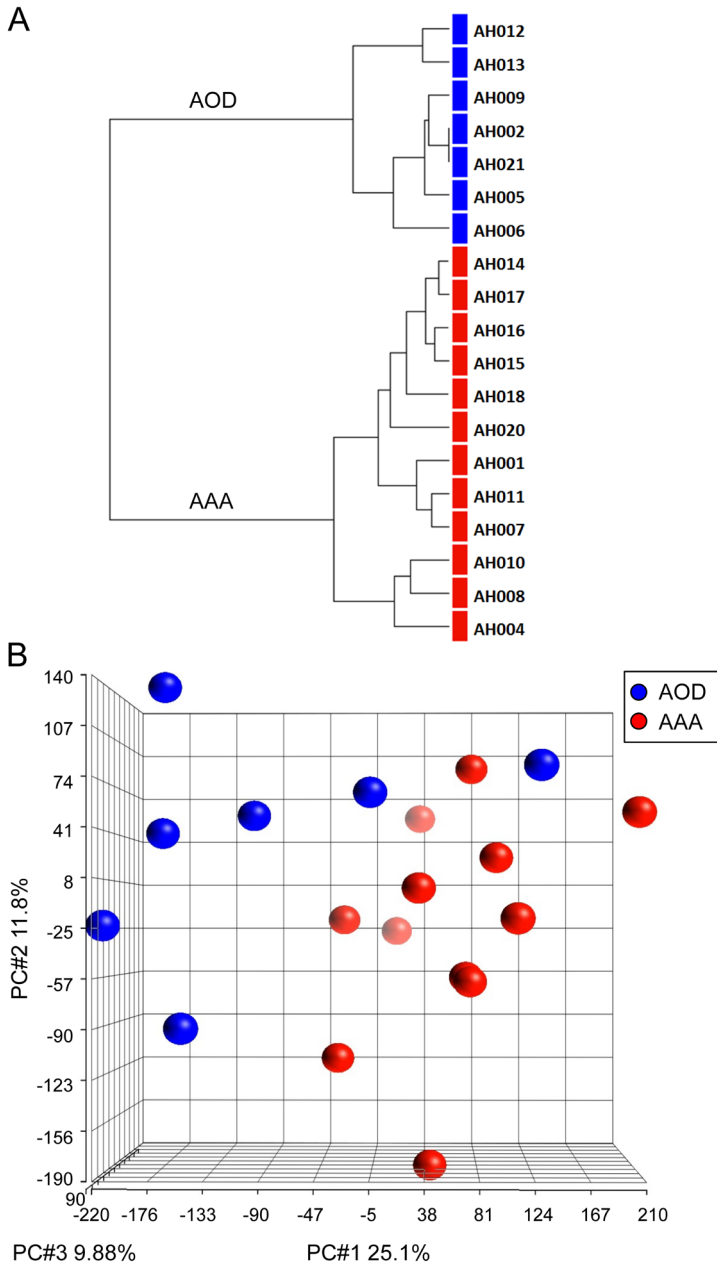


Figure 1

(A) Non-supervised hierarchical clustering dendrogram of AAA and AOD samples. (B) Principal Component Analysis plot of AAA and AOD samples. In red the AAA patient samples, in blue the AOD patient samples. On the x, y, and z axis: PC#1 25.1%, PC#2 11.8%, PC#3 9.88%, respectively.

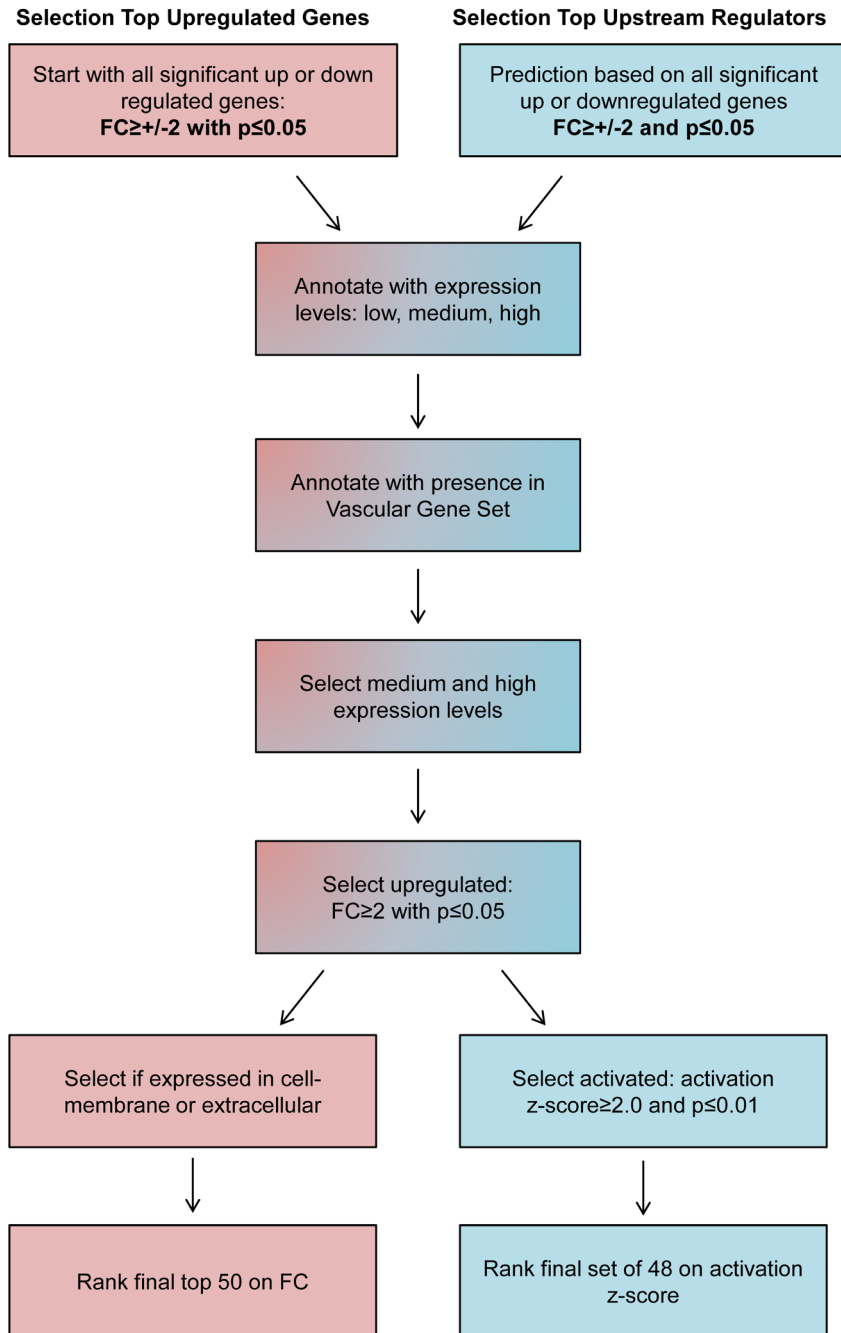


Figure 2
Selection procedure flowchart of the top upregulated genes (left) and top upstream regulators (right).

5'-ACTTGTTCTTCTCCAGACTATGA-3'; SLC7a5 5'-TCATCATCCGGCCTTCATCG-3'; 5'-AGCAGCAGCACGCAGAG-3'; and FDC-SP 5'-GGCTGTTGTTTCCAGTCTC-3'; 5'-TGTTGGAAGTGGGCGAAATG-3'. Gene expression was calculated using actin- β and HPRT as housekeeping genes and the comparative Ct method ($\Delta\Delta C_t$) was used for relative quantification of gene expression.

Vascular surgery aortic tissue sample collection

The study population consisted of a cohort of vascular surgery patients consecutively operated at the Erasmus Medical Center in Rotterdam. Patients undergoing elective open or endovascular surgery for aortic aneurysm repair, peripheral arterial disease or carotid artery disease, were included in the study. Patients were classified as aneurysmal disease (AA) or arterial occlusive disease (peripheral arterial disease or carotid artery disease). The study complies with the Helsinki declaration on research ethics and was approved by the institutional Review Board of the Erasmus Medical Center (MEC 2011-510).

Clinical characteristics vascular surgery patient cohort

The clinical characteristics of the index AAA patients were obtained from medical files and included gender, age at diagnosis, age at surgery, body mass index (BMI), as well as the cardiovascular comorbidities and risk factors. Cardiovascular comorbidities included congestive heart failure, ischemic heart disease (history of myocardial infarction, angina pectoris, coronary revascularisation or pathologic Q-waves on the electrocardiogram), and cerebrovascular disease (history of ischemic/hemorrhagic stroke or transient ischemic attack). Cardiovascular risk factors included kidney disease (serum creatinine ≥ 2.0 mg/dL), diabetes mellitus (fasting plasma glucose ≥ 7.0 mmol/L, non-fasting glucose ≥ 11.1 mmol/L or use of anti-diabetic medication), and hypertension (blood pressure $\geq 140/90$ mmHg in non-diabetics, $\geq 130/80$ mmHg in diabetics or use of antihypertensive medication). Smoking status was obtained and included current smoking and ever smoking (ie, patients who are currently smoking OR patients with a history of smoking). Prescription medications were recorded and included the use of statins, beta-blockers, renin-angiotensin system inhibitors, diuretics, and antiplatelets.

Lipoprotein and inflammatory parameters

Serum levels of triglycerides, high-density lipoprotein, low-density lipoprotein and high-sensitive C-reactive protein (hs-CRP) were determined as described.¹⁸ Patients with an hs-CRP higher than 10 mmol/L were excluded from analysis due to the chance of active inflammation status.¹⁹

Statistical analysis

Dichotomous data are presented as numbers and percentages. Continuous variables are presented as mean \pm standard deviation or median and interquartile range (IQR) when not normally distributed. Categorical data were analysed with Fisher's exact test or chi-square test and continuous variables with t-test, ANOVA or Kruskal-Wallis test. Linear univariable and multivariable regression analyses were performed to evaluate the difference in lipoprotein and inflammatory markers (triglycerides, high-density lipoprotein, low-density lipoprotein and hs-CRP) between patients with aortic aneurysm and those with arterial occlusive disease. Multivariable analyses were adjusted for age, gender, body mass index, congestive heart failure, ischemic heart disease, cerebrovascular disease, kidney disease, diabetes mellitus, hypertension, current smoking, and the use of statins, beta-blockers, renin-angiotensin system inhibitors, diuretics and antiplatelets. Covariates were chosen on the basis of biological plausibility. For all tests, a p-value < 0.05 (two-sided) was considered significant. Analyses were performed using Graphpad Software (Graphpad Software inc, La Jolla, CA, USA) or SPSS statistics (version 21.0; IBM Inc, Chicago, IL, USA).

RESULTS

AAA and AOD patient and sample characteristics

Based on high quality RNA RIN values, 14 AAA and 7 AOD samples were selected for microarray hybridization. During the quality control of the microarray data, 2 AAA samples were removed from the analysis: one due to bad microarray hybridization and the other as it was an outlier in the principal component analysis (PCA) and the non-supervised hierarchical clustering. The final selection of patient samples therefore included 12 AAA samples and 7 AOD samples. Patient characteristics are depicted in Table 1 accordingly. The baseline characteristics showed a difference in age and gender, though as expected, no significant differences were found in cardiovascular risk factors such as diabetes mellitus, ischemic heart disease, renal insufficiency, hypertension, dyslipidemia and smoking status.

Gender difference exclusion

Both age and gender are important risk factors for AAA. In our dataset, 11 out of 12 AAA patients were male and 5 out of 7 AOD patients were female. Due to the overlap of gender with disease phenotype, our analysis could also potentially identify differences between males and females. To identify genes that are differentially expressed between male and female aortic samples we obtained microarray expression data from another study investigating AAA.²⁰ We downloaded the expression data from GEO (GSE 7084) and performed a 2 sample t-test on the male and female sample groups within the control group only. This dataset consisted of an Affymetrix array based analysis and an Illumina array based analysis (for both array based analysis: 2 females vs. 4 males). We identified genes as significantly differentially expressed in the Affymetrix analysis with p-value<0.05 and FC cut off of >3.5 whereas in the Illumina analysis we applied p value<0.05 and FC > 2.5. With these stringent settings we identified 137 gender specific genes. As in the present study, we were specifically interested in the genes that differentiate aneurysmal disease from occlusive disease irrespective of gender, these 137 gender specific genes were removed from our AAA vs AOD analysis. For example, we show in Table 2 a top selection of 50 upregulated genes with 10 gender specific genes marked (see M symbol in column). For our AAA specific gene selection, all marked 'gender-specific' genes were excluded. In addition we performed an IPA core analysis on the dataset with and without the gender specific genes (1077 and 1047 ready molecules, respectively). Both analyses showed very similar results regarding functions, pathways and upstream regulators, suggesting that the differences between AAA and AOD state are the predominant state difference in this dataset (data not shown).

Non supervised hierarchical clustering and Principal Component Analysis

Non-supervised hierarchical clustering was performed on the genome wide microarray gene expression data of the 19 samples (Figure 1A). This analysis showed a clear separation of the AAA and AOD groups, and thus can be considered a validation of clear microarray gene expression differences between the two groups. In addition, Principal Component Analysis (PCA) was performed on the samples and again a clear separation of the AAA and AOD samples was observed (Figure 1B).

Selection procedure of top upregulated genes reveals 'known' and novel 'marker genes' for AAA

Top upregulated genes were selected based on fold change and p-value (Figure 2), and categorized by location and type. In addition, we checked the presence of filtered genes in our Vascular Gene Set, which is an enriched gene set consisting of genes expressed in vascular tissues and/or having a role in vascular related pathways and functions. The top 10 upregulated genes with highest fold changes are depicted in Table 3. In the columns of this table, fold change, p-value, location, and presence in the Vascular Gene Set are depicted. A literature search of these top 10 upregulated genes was performed where we screened for relevance in AAA or atherosclerotic disease, which is summarized in Table 3. Collagen-alpha1(XI) (COL11A1) appears highly relevant for AAA based

on its location in the ECM and its previous association with aneurysmal disease.²¹ Also Adiponectin (ADIPOQ) seems relevant, as ADIPOQ is elevated in Kawasaki patients (aneurysms in coronary artery).²² (aneurysms in coronary artery). Both associations show that our filtering is able to identify potential or known AAA-relevant genes. Furthermore, many highly upregulated genes are associated with the immune system, for instance CXC motif chemokine 13 (CXCL13), follicular dendritic cell secreted protein (FDC-SP), POU domain class 2-associating factor 1 (POU2AF1), membrane-spanning 4A (MS4A1 or CD20), and marginal zone B and B1 cell-specific protein (MZB1). Upregulation of these genes indicates that our gene expression profiling approach identifies the prominence of inflammation genes in AAA. In our literature research many of these genes showed no direct link with aneurysmal disease, therefore these genes could be 'novel' for aneurysmal disease.

A subset of 5 potential 'marker genes' were selected from Table 3 to be verified by QPCR, as additional check for the micro-array results. Selection criteria were; increased fold change, extracellular location and an association with aneurysmal disease, resulting in selection of CXCL13, COL11A1 and ADIPOQ. Additionally, FDC-SP and Solute carrier family 7 member 5 (SLC7A5) were selected as they had not previously been associated with aneurysmal disease. QPCR data shows that COL11A1, ADIPOQ, CXCL13, SLC7A5 and FDC-SP are upregulated in AAA compared to AOD (Figure 3), which corresponds to the micro-array data, although only COL11A1 and FDC-SP were significantly upregulated. The other genes were upregulated, but not significantly, probably due to small availability of samples.

Selection of top upstream regulators indicating potential key regulators in AAA

The parallel selection procedure to identify novel genes in AAA was performed by prioritizing our data with upstream regulator information available within IPA (Figure 2). The upstream regulator analysis is based on the idea that the activation state of a known upstream regulator can be determined by assessing the expression fold changes of all of its downstream targets and then using a z-score based algorithm to test if there is a good correlation between the hypothetical regulatory state of the upstream regulator and the regulatory state of all of its known downstream targets. The data was prioritized by highest upstream regulator z-score, with a minimal p-value of 0.01, and a threshold of $\log_2\text{Ratio}=1$, resulting in a gene list selected on the basis of upstream regulators. In Table 4 we show 46 genes which are upregulated with a cut-off z-score of >2 , together with their respective fold changes in the gene expression dataset. This list of genes could indicate novel markers and key regulators involved in AAA disease.

Pathway selection by Ingenuity Pathway Analysis shows a clear inflammatory component

Functional analysis, pathway analysis and upstream regulator analysis was performed with the data set of 1047 ready genes. In Figure 4 we show a top 10 IPA list of pathways which are significantly altered in AAA disease. Interestingly these top 10 pathways are all of an inflammatory nature, indicating the immune system as an important component in the differences between AAA and AOD phenotype. Therefore, the immune system and its associated markers would be interesting to further investigate in these patient groups. However our analysis was not sufficient to pinpoint one inflammation pathway which exclusively differentiates AAA disease from AOD. More likely, we need to look for a combination of different significantly altered immune pathways, together providing an 'immune signature' that is different for AAA compared to AOD. This could subsequently further be explored in blood of AAA and AOD patients.

Inflammation changes in a large vascular surgery patient cohort with aneurysmal or arterial occlusive disease

We analyzed 1393 cardiovascular patients for indications of inflammation changes. The patient and baseline characteristics are depicted in Table 5. The baseline population consisted of 1393 patients with either aortic aneurysm (n=614), peripheral arterial disease (n=491) or carotid artery disease (n=288). Endovascular procedures were performed in 598 patients (43%). The mean age of the population was 68 ± 10 years and the majority of patients were men (75%). The clinical characteristics of the patients were as follows; 614 patients (44%) were

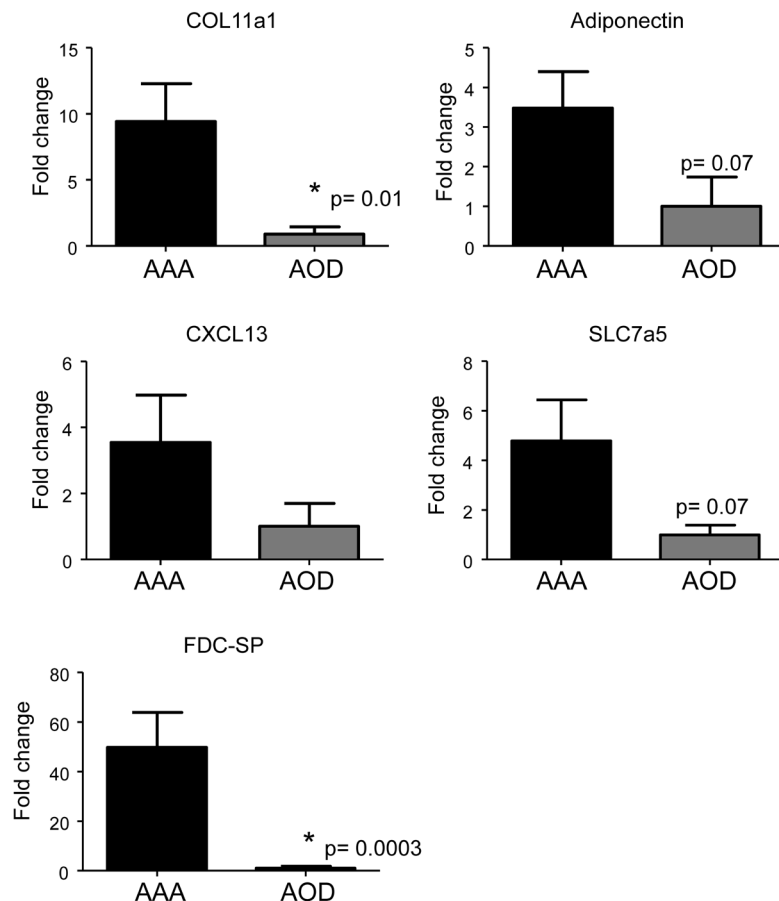


Figure 3
Significantly regulated genes from the top 10 selection (Table 4), verified by QPCR. Plotted are the fold changes of COL11A1, ADIPOQ, CXCL13, SLC7a5 and FDCSP gene (AAA vs AOD n=5). *p<0.05 vs AAA.

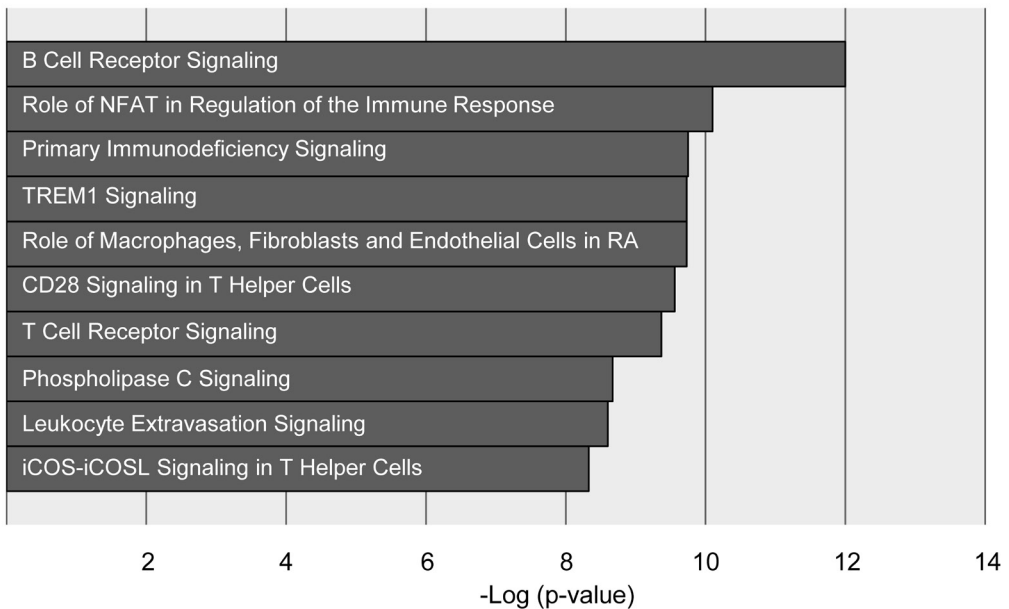
classified as aortic aneurysms and 779 patients (56%) as arterial occlusive disease. The patient and baseline characteristics are depicted in Table 5. A significant difference was observed between aneurysmal and occlusive disease patients in age (71 versus 66 years, respectively) and male gender (86% versus 67%, respectively), as was likewise present in our small patient group used for gene expression profiling, showing the representative nature of this database for the general population, and the samples used in this study. In Table 6 it is shown that the inflammatory marker high-sensitivity C-reactive protein (hs-CRP) was slightly, though significantly higher in patients with AAA compared to occlusive disease (4.07 mg/L versus 3.06 mg/L). Although this is a rather small difference and clinically this difference cannot be used to distinguish both groups, an adult population with a hs-CRP of >3.0 mg/L have a 2 fold increased relative risk for cardiovascular disease as compared with patients with a hs-CRP<1.0 mg/L.¹⁹. Multivariable regression analysis showed unadjusted differences for hs-CRP (β -0.51, 95% CI: -0.78 : -0.25, P<.001), as shown in Table 7. Importantly hs-CRP, remained significant in multivariable

analysis after adjustment for potential confounding factors (β -0.55, 95% CI: -0.99 : -0.11, $P=0.015$).

Taken together, these differences in gene expression as well as in the broader patient population study hint towards differences in the immune system of AAA and AOD patients, which might explain at least part of the different arterial outcomes. Therefore, it would be interesting to perform immunoprofiling studies on the blood of these two patient groups.

The TGF β pathway is significantly regulated at both gene and upstream regulator level

Although IPA analysis showed many significantly altered inflammation pathways, also other interesting pathways were significantly altered, amongst which the TGF β signaling pathway. As the TGF β pathway is also an important factor in the development of TAA, we next examined this pathway more closely. In figure 5 we show the TGF β signaling and the BMP-pathway, as derived from IPA, with all genes and upstream regulators that are significantly



RA= rheumatoid arthritis

Figure 4

Top 10 IPA list of upregulated pathways in AAA disease. The $-\log(p)$ value depicted on the x-axis represents significance of the depicted pathways.

altered. As shown, many genes and upstream regulators from our dataset are upregulated in the TGF β pathway, e.g. the known factors TGF β , ERK1/2, SMAD2/SMAD3 and Pai-1. Notably, IRF7 is not only upregulated at the mRNA level but also predicted to be upregulated at the upstream regulator level. Interestingly, many genes in the BMP signaling pathway were significantly downregulated, which implies that the pathway itself is inhibited in AAA disease compared to AOD. Moreover, genes involved in the pERK pathway are predicted to be upregulated. This pathway has been previously associated with (thoracic) aneurysmal disease, and it is interesting to note that it can regulate both the TGF β as well as the BMP signaling pathway, which warrants further investigation.

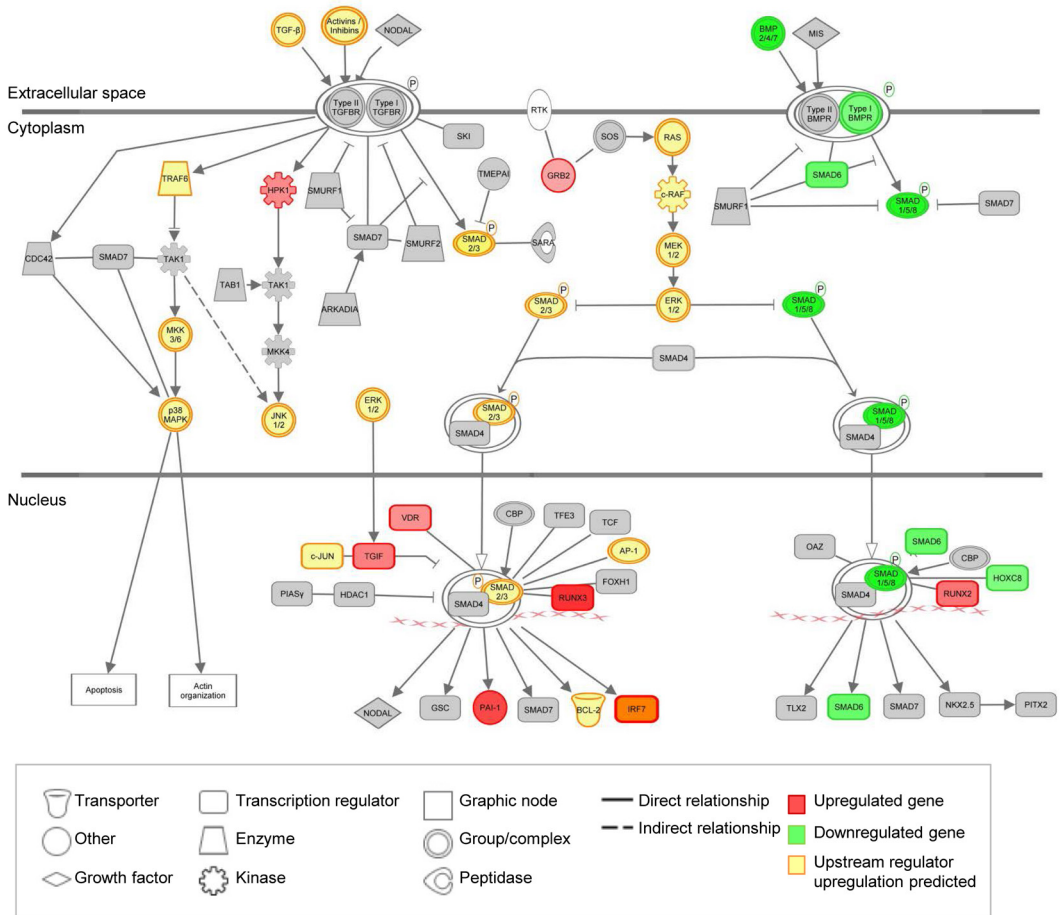


Figure 5 TGFβ signaling pathway with mediators in the TGFβ pathway and BMP pathway are depicted, adapted from IPA. Upregulated genes in red, downregulated genes in green, and upstream regulators which are predicted to be upregulated in yellow.

DISCUSSION

In this study we investigated the genetic factors and molecular processes that differentiate abdominal aortic aneurysm from arterial occlusive disease, despite overlapping characteristics between both diseases. By comparing the gene expression profiles of both diseases we show important pathway differences, in particular differences in upregulation of distinct inflammation pathways, but also differences in two previously identified TAA-related pathways; TGF β and BMP signaling.

Non-hierarchical clustering and Principal Component Analysis of the data showed two distinct datasets of genes which are up- or downregulated in AAA compared to AOD (Figure 1). Clinical characteristics of the 19 patients included in our microarray dataset were analyzed and we observed no differences in the cardiovascular risk factors, indicating that indeed these factors do not explain the observed phenotypic differences between AAA and AOD. Additionally, the subsequent database study of 1393 patients likewise showed no differences in cardiovascular risk factors, strengthening our findings. Smoking, gender, obesity, age, hypertension, and dyslipidemia are associated with an increased risk for AAA, whereas diabetes, is associated with a reduced risk.²³ Interestingly, we observe that diabetes is significantly lower in the AAA compared to the AOD group. In line with this observation, it has been described that diabetes seems to be protective when it comes to AAA formation and growth.^{24, 25}

In both the micro-array and database study (Tables 1 and 5) we show a gender and age difference between AAA and occlusive disease patients with a male dominance in AAA compared to occlusive disease patients (85.5% vs. 66.9%, $p < 0.001$, Table 5). This observation has been described earlier as it is known that the incidence of AAA disease rises rapidly after the age of 55 years in men.¹⁴ Therefore, these datasets reflect the actual AAA and occlusive disease patient population. We used a dataset of gender specific genes to correct our data for sex differences, as gender could be an influencing factor for several upregulated genes. However, comparison of the gender-dependent and gender-independent datasets revealed only minor differences. We performed an IPA core analysis on the dataset with and without the gender specific genes and both analyses showed very similar results regarding functions, pathways and upstream regulators, suggesting that the differences between AAA and AOD are the predominant determinant in this dataset. To select AAA-specific genes irrespective of gender, we used the list of gender-independent significantly regulated genes, for further IPA analysis of AAA disease (Table 2).

From the list with significantly upregulated genes we selected a top 10 of potential markers, based on their expression level, significance and presence in vascular tissue, and performed literature research to identify possible connections of these genes to AAA or AOD. Of these 10 genes, 4 showed an association with aneurysmal disease, showing that our selection procedure indeed can reveal aneurysm relevant markers. At the same time, the other 6 genes showed no previously known association, making them potential novel markers for AAA disease. We performed an additional validation step of 5 upregulated genes by QPCR. As determined by microarray analysis, all these genes showed upregulation, however, probably due to small sample size only COL11A1 and FDC-SP were significantly upregulated. At this point upregulation of potential AAA markers at the transcriptional level should be further verified in blood of AAA and control patients, for which an independent AAA patient cohort is needed.

The IPA analysis showed an overrepresentation of significantly regulated immune-specific pathways for AAA disease (Table 3). Moreover, analysis of hs-CRP levels in an additional patient cohort of 1393 patients showed slightly increased hs-CRP levels in AAA compared to occlusive disease patients, both in the unadjusted and adjusted data analysis. Although in this larger cohort we show increased inflammation based on hs-CRP, data of other known inflammation markers were not available. However, the significance of increased hs-CRP in already established aneurysms is unknown, as inflammation is a multifactorial process. Similar to what we find, other studies reported the role of the immune-related genes and pathways in AOD and AAA disease.^{26, 27} Though, we used additional IPA analysis and upstream regulator information to go in depth of distinct pathways to distinguish both pathogenic mechanisms. Together the changes in distinct inflammation pathways derived

from our gene expression analysis, as well as the finding that hs-CRP levels differ significantly between AAA and occlusive disease patients, imply that a more thorough analysis of immune factors in the blood for these two patient groups would be a very relevant next step.

Dysregulation of the TGF β and BMP signaling pathway, previously described for TAA patients¹¹, was also shown for AAA patients in our IPA analysis. While we find most components of the TGF β signaling pathway were significantly upregulated, most components of the BMP-pathway were downregulated in AAA compared to AOD. Moreover, many upstream regulators involved in the TGF β pathway were predicted to be upregulated in our analysis. Interestingly, TGF β signaling was mostly reported to be upregulated in TAA, and intervention therapy aimed at reducing TGF β is able to reduce aneurysmal growth. In addition, blockade of TGF β -signaling by TGF β -neutralizing antibody (Nab) showed beneficial effects in MFS rodent models. In contrast, TGF β -Nab administration exacerbated the pathology of aneurysms in angiotensin-II induced AAA mice models.^{28, 29} Consequently, in AAA (dys)regulation of the TGF β signaling pathway is not clear yet. For example, a small study in 12 AAA and 6 control biopsies showed downregulation of T β RII subtype mRNA³⁰. Yet, about 20-30% of AAA patients later in life also develop a TAA.^{31, 32} Vice versa, many TAA patients have aneurysms at multiple sites, including the abdominal part.³³ Therefore similar mechanisms might be at work in both AAA and TAA patient groups. In this respect it is very interesting that our data show that the TGF β signaling pathway might be dysregulated in AAA aorta samples, with predictions that the pathway is upregulated. At the same time, the closely associated BMP pathway is predicted to be downregulated. These data could indicate that an imbalance between TGF β and BMP signaling causes part of the AAA phenotype. This might also explain the different findings described above on TGF β signaling pathway involvement in AAA versus TAA. It would therefore be interesting to further investigate factors involved in both the TGF β and BMP signaling pathways in tissue or serum samples from AAA patients. In particular, measuring the TGF β ligands 1-3 in the serum could be of great importance, in parallel to measurements of TGF β R subtype mRNA levels.

In conclusion, our data show that gene expression profiling is an important tool to distinguish AAA from AOD, clinical entities that share the same risk factors, but show completely different disease progression. As we reveals that simultaneous inhibition of BMP and activation of TGF β signaling plays a role in abdominal aortic aneurysms. Besides, these profiles are important in the identification of novel genes, markers and processes that can shed light on the molecular mechanisms underlying abdominal aneurysm formation.

Limitation of the study

One limitation of this micro-array study is the small number of samples in the AAA and AOD groups, however previously other studies showed novel differences of upregulated genes and pathways in comparison analysis of similar small patient groups.^{26, 27} In addition, we did identify novel markers and pathways with significant p-values, that separate AAA disease from aortic occlusive disease. One reason for these small sample groups is that it is becoming increasingly difficult to obtain the abdominal aortic tissue as nowadays AAA disease and occlusive patients are generally operated by endovascular procedures.. Another limitation of the study is that one disease (AAA) is compared with another disease (AOD) without a 'healthy' control group as part of this comparison. Because of this limitation, genes that are considered upregulated in AAA in this study, could be higher expressed in AAA as compared to a healthy individuals or they could be genes that are downregulated in AOD as compared to a healthy individual. Nonetheless, this study clearly demonstrates that interesting biological interpretations can be made from this comparison as TGF-beta signaling is identified both as a significant differentially regulated pathway and several of its components are identified as significant upstream regulators of the AAA versus AOD differentially expressed dataset.



ACKNOWLEDGEMENTS

This work was supported by the 'Lijf en Leven' grant (2011): 'dilating versus stenosing arterial disease (DIVERS)' (PvH, ER, HV, JE, IvdP). Eurotrans-Bio grant 2011 'Development of novel non-invasive diagnostics for aneurysms (Aneudia)' (PvH, JE).

REFERENCES

1. Hoel AW. Aneurysmal Disease: Thoracic Aorta. *Surg Clin N Am* 2013;**93**:893-+.
2. Isselbacher EM. Thoracic and abdominal aortic aneurysms. *Circulation* 2005;**111**:816-828.
3. Albornoz G, Coady MA, Roberts M, Davies RR, Tranquilli M, Rizzo JA, Elefteriades JA. Familial thoracic aortic aneurysms and dissections--incidence, modes of inheritance, and phenotypic patterns. *Ann Thorac Surg* 2006;**82**:1400-1405.
4. Dietz HC, Cutting GR, Pyeritz RE, Maslen CL, Sakai LY, Corson GM, Puffenberger EG, Hamosh A, Nanthakumar EJ, Curristin SM, Stetten G, Meyers DA, Francomano CA. Marfan-Syndrome Caused by a Recurrent Denovo Missense Mutation in the Fibrillin Gene. *Nature* 1991;**352**:337-339.
5. Loeys BL, Chen J, Neptune ER, Judge DP, Podowski M, Holm T, Meyers J, Leitch CC, Katsanis N, Sharifi N, Xu FL, Myers LA, Spevak PJ, Cameron DE, De Backer J, Hellemans J, Chen Y, Davis EC, Webb CL, Kress W, Coucke P, Rifkin DB, De Paepe AM, Dietz HC. A syndrome of altered cardiovascular, craniofacial, neurocognitive and skeletal development caused by mutations in TGFBR1 or TGFBR2. *Nat Genet* 2005;**37**:275-281.
6. van de Laar IM, Oldenburg RA, Pals G, Roos-Hesselink JW, de Graaf BM, Verhagen JM, Hoedemaekers YM, Willemsen R, Severijnen LA, Venselaar H, Vriend G, Pattynama PM, Collee M, Majoor-Krakauer D, Poldermans D, Frohn-Mulder IM, Micha D, Timmermans J, Hilhorst-Hofstee Y, Bierma-Zeinstra SM, Willems PJ, Kros JM, Oei EH, Oostra BA, Wessels MW, Bertoli-Avella AM. Mutations in SMAD3 cause a syndromic form of aortic aneurysms and dissections with early-onset osteoarthritis. *Nat Genet* 2011;**43**:121-126.
7. Borges LF, Touat Z, Leclercq A, Zen AA, Jondeau G, Franc B, Philippe M, Meilhac O, Gutierrez PS, Michel JB. Tissue diffusion and retention of metalloproteinases in ascending aortic aneurysms and dissections. *Hum Pathol* 2009;**40**:306-313.
8. Kaijzel EL, van Heijningen PM, Wielopolski PA, Vermeij M, Koning GA, van Cappellen WA, Que I, Chan A, Dijkstra J, Ramnath NW, Hawinkels LJ, Bernsen MR, Lowik CW, Essers J. Multimodality imaging reveals a gradual increase in matrix metalloproteinase activity at aneurysmal lesions in live fibulin-4 mice. *Circ Cardiovasc Imaging* 2010;**3**:567-577.
9. Matt P, Schoenhoff F, Habashi J, Holm T, Van Erp C, Loch D, Carlson OD, Griswold BF, Fu Q, De Backer J, Loeys B, Huso DL, McDonnell NB, Van Eyk JE, Dietz HC, Consortium G. Circulating Transforming Growth Factor-beta in Marfan Syndrome. *Circulation* 2009;**120**:526-532.
10. Renard M, Holm T, Veith R, Callewaert BL, Ades LC, Baspinar O, Pickart A, Dasouki M, Hoyer J, Rauch A, Trapane P, Earing MG, Coucke PJ, Sakai LY, Dietz HC, De Paepe AM, Loeys BL. Altered TGF beta signaling and cardiovascular manifestations in patients with autosomal recessive cutis laxa type I caused by fibulin-4 deficiency. *Eur J Hum Genet* 2010;**18**:895-901.
11. Neptune ER, Frischmeyer PA, Arking DE, Myers L, Bunton TE, Gayraud B, Ramirez F, Sakai LY, Dietz HC. Dysregulation of TGF-beta activation contributes to pathogenesis in Marfan syndrome. *Nat Genet* 2003;**33**:407-411.
12. Chung AWY, Yeung KA, Sandor GGS, Judge DP, Dietz HC, van Breemen C. Loss of elastic fiber integrity and reduction of vascular smooth muscle contraction resulting from the upregulated activities of matrix metalloproteinase-2 and-9 in the thoracic aortic aneurysm in Marfan syndrome. *Circ Res* 2007;**101**:512-522.
13. van de Luitgaarden KM, Heijnsman D, Maugeri A, Weiss MM, Verhagen HJ, A IJ, Bruggenwirth HT, Majoor-Krakauer D. First genetic analysis of aneurysm genes in familial and sporadic abdominal aortic aneurysm. *Hum Genet* 2015;**134**:881-893.
14. Ashton HA, Buxton MJ, Campbell HE, Day NE, Kim LG, Marteau TM, Scott RAP, Thompson SG, Barker P, Collin J, Morris G, Sutton G, Wilson NK, Bridgewater S, Druce PS, Hardy EJ, Lodge S, Pettifer M, Woronowski H, Dewbury K, Jarvis LJ, Langham-Brown J, Lindsell D, Page A, Buxton MJ, Campbell HE, Colehan J, Holland J, Hankins M, Marteau TM, Couto E, Day NE, Duffy SW, Kim LG, Styles M, Thompson SG, Vardulaki KA, Walker NM, Collin J, Hardy EJ, Lodge S, Cuzick J, Parmar MKB, Ruckley CV, Warlow C, Emmett G, Kay DN, Peake J, Stu MAS. Multicentre aneurysm screening study (MASS): cost effectiveness analysis of screening for abdominal aortic aneurysms based on four year results from randomised controlled trial. *Brit Med J* 2002;**325**:1135-1138B.
15. Lederle FA, Johnson GR, Wilson SE, Chute EP, Littooy FN, Bandyk D, Krupski WC, Barone GW, Acher CW, Ballard

- DJ. Prevalence and associations of abdominal aortic aneurysm detected through screening. Aneurysm Detection and Management (ADAM) Veterans Affairs Cooperative Study Group. *Ann Intern Med* 1997;**126**:441-449.
16. Lederle FA, Johnson GR, Wilson SE, Aneurysm D, Management Veterans Affairs Cooperative S. Abdominal aortic aneurysm in women. *J Vasc Surg* 2001;**34**:122-126.
 17. Gallino A, Aboyans V, Diehm C, Cosentino F, Stricker H, Falk E, Schouten O, Lekakis J, Amann-Vesti B, Siclari F, Poredos P, Novo S, Brodmann M, Schulte KL, Vlachopoulos C, De Caterina R, Libby P, Baumgartner I, European Society of Cardiology Working Group on Peripheral C. Non-coronary atherosclerosis. *Eur Heart J* 2014;**35**:1112-1119.
 18. Ramnath NW, van de Luijngaarden KM, van der Pluijm I, van Nimwegen M, van Heijningen PM, Swagemakers SM, van Thiel BS, Ridwan RY, van Vliet N, Vermeij M, Hawinkels LJ, de Munck A, Dzyubachyk O, Meijering E, van der Spek P, Rottier R, Yanagisawa H, Hendriks RW, Kanaar R, Rouwet EV, Kleinjan A, Essers J. Extracellular matrix defects in aneurysmal Fibulin-4 mice predispose to lung emphysema. *Plos One* 2014;**9**:e106054.
 19. Pearson TA, Mensah GA, Alexander RW, Anderson JL, Cannon RO, 3rd, Criqui M, Fadl YY, Fortmann SP, Hong Y, Myers GL, Rifai N, Smith SC, Jr., Taubert K, Tracy RP, Vinicor F, Centers for Disease C, Prevention, American Heart A. Markers of inflammation and cardiovascular disease: application to clinical and public health practice: A statement for healthcare professionals from the Centers for Disease Control and Prevention and the American Heart Association. *Circulation* 2003;**107**:499-511.
 20. Hinterseher I, Erdman R, Donoso LA, Vrabec TR, Schworer CM, Lillvis JH, Boddy AM, Derr K, Golden A, Bowen WD, Gatalica Z, Tapinos N, Elmore JR, Franklin DP, Gray JL, Garvin RP, Gerhard GS, Carey DJ, Tromp G, Kuivaniemi H. Role of complement cascade in abdominal aortic aneurysms. *Arterioscler Thromb Vasc Biol* 2011;**31**:1653-1660.
 21. Black KM, Masuzawa A, Hagberg RC, Khabbaz KR, Trovato ME, Rettagliati VM, Bhasin MK, Dillon ST, Libermann TA, Toumpoulis IK, Levitsky S, McCully JD. Preliminary Biomarkers for Identification of Human Ascending Thoracic Aortic Aneurysm. *J Am Heart Assoc* 2013;**2**.
 22. Takeshita S, Takabayashi H, Yoshida N. Circulating adiponectin levels in Kawasaki disease. *Acta Paediatr* 2006;**95**:1312-1314.
 23. Kent KC, Zwolak RM, Egorova NN, Riles TS, Manganaro A, Moskowitz AJ, Gelijs AC, Greco G. Analysis of risk factors for abdominal aortic aneurysm in a cohort of more than 3 million individuals. *J Vasc Surg* 2010;**52**:539-548.
 24. Shantikumar S, Ajjan R, Porter KE, Scott DJ. Diabetes and the abdominal aortic aneurysm. *Eur J Vasc Endovasc Surg* 2010;**39**:200-207.
 25. Lederle FA, Johnson GR, Wilson SE, Chute EP, Hye RJ, Makaroun MS, Barone GW, Bandyk D, Moneta GL, Makhoul RG. The aneurysm detection and management study screening program: validation cohort and final results. Aneurysm Detection and Management Veterans Affairs Cooperative Study Investigators. *Arch Intern Med* 2000;**160**:1425-1430.
 26. Biros E, Gabel G, Moran CS, Schreurs C, Lindeman JH, Walker PJ, Nataatmadja M, West M, Holdt LM, Hinterseher I, Pilarsky C, Gollledge J. Differential gene expression in human abdominal aortic aneurysm and aortic occlusive disease. *Oncotarget* 2015;**6**:12984-12996.
 27. Armstrong PJ, Johanning JM, Calton WC, Jr., Delatore JR, Franklin DP, Han DC, Carey DJ, Elmore JR. Differential gene expression in human abdominal aorta: aneurysmal versus occlusive disease. *J Vasc Surg* 2002;**35**:346-355.
 28. Dai JP, Losy F, Guinault AM, Pages C, Anegon I, Desgranges P, Becquemin JP, Allaire E. Overexpression of transforming growth factor-beta 1 stabilizes already-formed aortic aneurysms - A first approach to induction of functional healing by endovascular gene therapy. *Circulation* 2005;**112**:1008-1015.
 29. Wang Y, Ait-Oufella H, Herbin O, Bonnin P, Ramkhalawon B, Taleb S, Huang J, Offenstadt G, Combadiere C, Renia L, Johnson JL, Tharaux PL, Tedgui A, Mallat Z. TGF-beta activity protects against inflammatory aortic aneurysm progression and complications in angiotensin II-infused mice. *J Clin Invest* 2010;**120**:422-432.
 30. Biros E, Walker PJ, Nataatmadja M, West M, Gollledge J. Downregulation of transforming growth factor, beta receptor 2 and Notch signaling pathway in human abdominal aortic aneurysm. *Atherosclerosis* 2012;**221**:383-386.
 31. Gillis E, Van Laer L, Loeyls BL. Genetics of thoracic aortic aneurysm: at the crossroad of transforming growth factor-beta signaling and vascular smooth muscle cell

- contractility. *Circ Res* 2013;**113**:327-340.
32. Akhurst RJ, Hata A. Targeting the TGFβ signalling pathway in disease. *Nat Rev Drug Discov* 2012;**11**:790-811.
 33. Szmídt J, Rowinski O, Galazka Z, Jakimowicz T, Nazarewski S, Grochowicki T, Pachó R. Simultaneous endovascular exclusion of thoracic aortic aneurysm with open abdominal aortic aneurysm repair. *Eur J Vasc Endovasc Surg* 2004;**28**:442-448.
 34. Ansel KM, Ngo VN, Hyman PL, Luther SA, Forster R, Sedgwick JD, Browning JL, Lipp M, Cyster JG. A chemokine-driven positive feedback loop organizes lymphoid follicles. *Nature* 2000;**406**:309-314.
 35. Houtkamp MA, de Boer OJ, van der Loos CM, van der Wal AC, Becker AE. Adventitial infiltrates associated with advanced atherosclerotic plaques: structural organization suggests generation of local humoral immune responses. *J Pathol* 2001;**193**:263-269.
 36. Mohanta SK, Yin CJ, Peng L, Srikakulapu P, Bontha V, Hu DS, Weih F, Weber C, Gerdes N, Habenicht AJR. Artery Tertiary Lymphoid Organs Contribute to Innate and Adaptive Immune Responses in Advanced Mouse Atherosclerosis. *Circ Res* 2014;**114**:1772-1787.
 37. Tilson MD, Ro CY. The candidate gene approach to susceptibility for abdominal aortic aneurysm - TIMP1, HLA-DR-15, ferritin light chain, and collagen XI-Alpha-1. *Ann Ny Acad Sci* 2006;**1085**:282-290.
 38. Toumpoulis IK, Oxford JT, Cowan DB, Anagnostopoulos CE, Rokkas CK, Chamogeorgakis TP, Angouras DC, Shemin RJ, Navab M, Ericsson M, Federman M, Levitsky S, McCully JD. Differential Expression of Collagen Type V and XI alpha-1 in Human Ascending Thoracic Aortic Aneurysms. *Ann Thorac Surg* 2009;**88**:506-514.
 39. Urieli-Shoval S, Linke RP, Matzner Y. Expression and function of serum amyloid A, a major acute-phase protein, in normal and disease states. *Curr Opin Hematol* 2000;**7**:64-69.
 40. Steel DM, Sellar GC, Uhlár CM, Simon S, Debeer FC, Whitehead AS. A Constitutively Expressed Serum Amyloid-a Protein Gene (Saa4) Is Closely Linked to, and Shares Structural Similarities with, an Acute-Phase Serum Amyloid-a Protein Gene (Saa2). *Genomics* 1993;**16**:447-454.
 41. De Beer MC, Wroblewski JM, Noffsinger VP, Rateri DL, Howatt DA, Balakrishnan A, Ji AL, Shridas P, Thompson JC, van der Westhuyzen DR, Tannock LR, Daugherty A, Webb NR, De Beer FC. Deficiency of Endogenous Acute Phase Serum Amyloid A Does Not Affect Atherosclerotic Lesions in Apolipoprotein E-Deficient Mice. *Arterioscl Throm Vas* 2014;**34**:255-261.
 42. Ridker PM, Hennekens CH, Buring JE, Rifai N. C-reactive protein and other markers of inflammation in the prediction of cardiovascular disease in women. *New Engl J Med* 2000;**342**:836-843.
 43. Yamauchi T, Kamon J, Waki H, Terauchi Y, Kubota N, Hara K, Mori Y, Ide T, Murakami K, Tsuboyama-Kasaoka N, Ezaki O, Akanuma Y, Gavrilova O, Vinson C, Reitman ML, Kagechika H, Shudo K, Yoda M, Nakano Y, Tobe K, Nagai R, Kimura S, Tomita M, Froguel P, Kadowaki T. The fat-derived hormone adiponectin reverses insulin resistance associated with both lipodystrophy and obesity. *Nat Med* 2001;**7**:941-946.
 44. Yoshida S, Fuster JJ, Walsh K. Adiponectin attenuates abdominal aortic aneurysm formation in hyperlipidemic mice. *Atherosclerosis* 2014;**235**:339-346.
 45. Okamoto Y, Kihara S, Ouchi N, Nishida M, Arita Y, Kumada M, Ohashi K, Sakai N, Shimomura I, Kobayashi H, Terasaka N, Inaba T, Funahashi T, Matsuzawa Y. Adiponectin reduces atherosclerosis in apolipoprotein E-deficient mice. *Circulation* 2002;**106**:2767-2770.
 46. Marshall AJ, Du Q, Draves KE, Shikishima Y, HayGlass KT, Clark EA. FDC-SP, a novel secreted protein expressed by follicular dendritic cells. *Journal of Immunology* 2002;**169**:2381-2389.
 47. Al-Alwan M, Du Q, Hou S, Nashed B, Fan Y, Yang X, Marshall AJ. Follicular dendritic cell secreted protein (FDC-SP) regulates germinal center and antibody responses. *Journal of Immunology* 2007;**178**:7859-7867.
 48. Teitel MA. OCA-B regulation of B-cell development and function. *Trends Immunol* 2003;**24**:546-553.
 49. Hagg S, Salehpour M, Noori P, Lundstrom J, Possnert G, Takolander R, Konrad P, Rosfors S, Ruusalepp A, Skogsberg J, Tegner J, Björkegren J. Carotid plaque age is a feature of plaque stability inversely related to levels of plasma insulin. *PLoS One* 2011;**6**:e18248.
 50. Treska V, Kocova J, Boudova L, Neprasova P, Topolcan O, Pecan L, Tonar Z. Inflammation in the wall of abdominal aortic aneurysm and its role in the symptomatology of aneurysm. *Cytokines Cell Mol Ther* 2002;**7**:91-97.
 51. Ait-Oufella H, Herbin O, Bouaziz JD, Binder CJ, Uyttenhove C, Laurant L, Taleb S, Van Vre E, Esposito B, Vilar J, Sirvent J, Van Snick J, Tedgui A, Tedder TF, Mallat Z. B cell depletion reduces the development of atherosclerosis in mice. *J Exp Med* 2010;**207**:1579-1587.
 52. Kyaw T, Tay C, Hosseini H, Kanellakis P, Gadowski T, MacKay F, Tipping P, Bobik A, Toh BH. Depletion of B2

- but not B1a B cells in BAFF receptor-deficient ApoE mice attenuates atherosclerosis by potently ameliorating arterial inflammation. *Plos One* 2012;**7**:e29371.
53. Kyaw T, Tay C, Krishnamurthi S, Kanellakis P, Agrotis A, Tipping P, Bobik A, Toh BH. B1a B lymphocytes are atheroprotective by secreting natural IgM that increases IgM deposits and reduces necrotic cores in atherosclerotic lesions. *Circ Res* 2011;**109**:830-840.
 54. Flach H, Rosenbaum M, Duchniewicz M, Kim S, Zhang SL, Cahalan MD, Mittler G, Grosschedl R. Mzb1 protein regulates calcium homeostasis, antibody secretion, and integrin activation in innate-like B cells. *Immunity* 2010;**33**:723-735.
 55. Verrey F, Closs EI, Wagner CA, Palacin M, Endou H, Kanai Y. CATs and HATs: the SLC7 family of amino acid transporters. *Pflugers Arch* 2004;**447**:532-542.
 56. Allison MB, Myers MG, Jr. 20 YEARS OF LEPTIN: Connecting leptin signaling to biological function. *J Endocrinol* 2014;**223**:T25-T35.
 57. Tao M, Yu P, Nguyen BT, Mizrahi B, Savion N, Kolodgie FD, Virmani R, Hao S, Ozaki CK, Schneiderman J. Locally applied leptin induces regional aortic wall degeneration preceding aneurysm formation in apolipoprotein E-deficient mice. *Arterioscler Thromb Vasc Biol* 2013;**33**:311-320.
 58. Schneiderman J, Schaefer K, Kolodgie FD, Savion N, Kotev-Emeth S, Dardik R, Simon AJ, Halak M, Pariente C, Engelberg I, Konstantinides S, Virmani R. Leptin locally synthesized in carotid atherosclerotic plaques could be associated with lesion instability and cerebral emboli. *J Am Heart Assoc* 2012;**1**:e001727.
 59. Chiba T, Shinozaki S, Nakazawa T, Kawakami A, Ai M, Kaneko E, Kitagawa M, Kondo K, Chait A, Shimokado K. Leptin deficiency suppresses progression of atherosclerosis in apoE-deficient mice. *Atherosclerosis* 2008;**196**:68-75.
 60. Bodary PF, Gu S, Shen Y, Hasty AH, Buckler JM, Eitzman DT. Recombinant leptin promotes atherosclerosis and thrombosis in apolipoprotein E-deficient mice. *Arterioscler Thromb Vasc Biol* 2005;**25**:e119-122.

TABLES

Characteristic	AAA (n=12)	AOD (n=7)	P-value
Male gender – n (%)	11 (92)	2 (29)	.0095
Age – (y, mean ± SD)	68 ± 6.7	56 ± 5.7	.001
Diabetes mellitus – n (%)	0 (0)	1 (14)	.3684
Ischemic heart disease – n (%)	2 (17)	1 (14)	1
Renal insufficiency – n (%)	4 (33)	1 (14)	.6027
Hypertension – n (%)	9 (75)	5 (71)	1
Dyslipidemia – n (%)	9 (75)	6 (86)	1
Current smoking – n (%)	6 (50)	4 (57)	1
Ever smoking – n (%)	4 (33)	3 (43)	1

Table 1

A t-test (continuous data) or Fisher’s exact test (categorical data) was applied for the analysis between groups. All statistical analyses were performed using Graphpad Software (Graphpad Software inc, La Jolla, CA, USA). All statistical tests were two-sided and P<0.05 was considered statistically significant.



Gene Symbol	Entrez Gene Name	Fold Change	p-value	Gender Specific
RPS4Y1	ribosomal protein S4, Y-linked 1	48,386	0,00238	M
CXCL13	chemokine (C-X-C motif) ligand 13	32,269	0,000112	
DDX3Y	DEAD (Asp-Glu-Ala-Asp) box helicase 3, Y-linked	30,326	0,00208	M
COL11A1	collagen, type XI, alpha 1	27,046	5,29E-05	
SAA2	serum amyloid A2	24,96	3,95E-07	
PLIN1	perilipin 1	23,989	9,49E-05	M
ADIPOQ	adiponectin, C1Q and collagen domain containing	21,454	0,000301	
FDCSP	follicular dendritic cell secreted protein	21,38	0,000101	
PTX3	pentraxin 3, long	19,063	1,10E-05	M
POU2AF1	POU class 2 associating factor 1	18,842	0,000479	
MS4A1	membrane-spanning 4-domains, subfamily A, member 1	18,414	0,000261	
KDM5D	lysine (K)-specific demethylase 5D	17,854	0,00275	M
MZB1	marginal zone B and B1 cell-specific protein	17,072	0,00126	
SLC7A5	solute carrier family 7 (amino acid transporter light chain, L system), member 5	15,716	5,37E-07	
LEP	leptin	14,288	1,94E-06	
MARCO	macrophage receptor with collagenous structure	13,563	0,000412	
LPL	lipoprotein lipase	12,984	3,51E-05	
IL1RN	interleukin 1 receptor antagonist	12,873	0,00116	
IGLL5	immunoglobulin lambda-like polypeptide 1	12,848	0,000973	
CR2	complement component (3d/Epstein Barr vir-us) receptor 2	12,123	0,00113	
KIAA1199	KIAA1199	12,122	0,0016	

Gene Symbol	Entrez Gene Name	Fold Change	p-value	Gender Specific
TREM1	triggering receptor expressed on myeloid cells 1	11,851	0,000433	
P2RX5	purinergic receptor P2X, ligand-gated ion channel, 5	11,706	8,53E-05	
EIF1AY	eukaryotic translation initiation factor 1A, Y-linked	11,554	0,00304	M
SPAG4	sperm associated antigen 4	11,463	0,00106	M
HMOX1	heme oxygenase (decycling) 1	10,932	5,47E-05	
IGLJ3	immunoglobulin lambda joining 3	10,776	0,00729	
IGH	immunoglobulin heavy locus	10,257	0,000424	
ISG20	interferon stimulated exonuclease gene 20kDa	10,238	1,31E-05	
CCL18	chemokine (C-C motif) ligand 18 (pulmonary and activation-regulated)	10,164	0,000151	
CD79A	CD79a molecule, immunoglobulin-associated alpha	10,064	0,000197	
FNDC1	fibronectin type III domain containing 1	10,028	0,00028	
IL8	interleukin 8	9,89	0,00235	M
TIMD4	T-cell immunoglobulin and mucin domain containing 4	9,859	0,00259	
PIM2	pim-2 oncogene	9,838	0,000235	
CXCL5	chemokine (C-X-C motif) ligand 5	9,659	0,000276	
FCRL5	Fc receptor-like 5	9,596	0,00249	
CXCL3	chemokine (C-X-C motif) ligand 3	9,526	3,06E-06	
MIAT	myocardial infarction associated transcript (non-protein coding)	9,359	0,00011	
GZMB	granzyme B (granzyme 2, cytotoxic T-lymphocyte-associated serine esterase 1)	9,211	0,000277	
IGHM	immunoglobulin heavy constant mu	8,93	0,0051	
AQP9	aquaporin 9	8,908	0,00445	



Gene Symbol	Entrez Gene Name	Fold Change	p-value	Gender Specific
COMP	cartilage oligomeric matrix protein	8,739	0,00511	
CXCL1	chemokine (C-X-C motif) ligand 1 (melanoma growth stimulating activity, alpha)	8,677	1,07E-05	M
PAX5	paired box 5	8,41	0,000776	
IGK	immunoglobulin kappa locus	8,403	0,00257	
USP9Y	ubiquitin specific peptidase 9, Y-linked	8,296	0,00493	M
SYTL1	synaptotagmin-like 1	8,235	4,38E-06	
C15orf48	chromosome 15 open reading frame 48	8,225	0,0064	
DPH1	diphthamide biosynthesis 1	8,218	0,00019	

Table 2

Top upregulated genes in AAA vs AOD with the gender specific genes marked (M) that were excluded for further analysis.

Table 3 (next two pages)

Top 10 genes up-regulated genes in AAA vs AOD.

Gene	Function and relation to AAA or atherosclerosis	FC	p-value	Location	Vascular Gene Set
CXCL13 C-X-C motif chemokine 13	Selective chemotactic for B cells (B-1 and B-2 subsets), by interacting with chemokine receptor CXCR5. Control of B cell organization within follicles of lymphoid tissues. High levels of CXCL13 are found in aneurysm and in atherosclerotic lesions ³⁴⁻³⁶ .	32.26	.000112	Extracellular space	YES
COL11A1 Collagen alpha-1(XI) chain	Adds structure and strength to connective tissues supporting muscles, joints, organs, and skin. Col11a1 protein levels are upregulated in TAA and AAA tissue ^{21, 37, 38}	27.05	5.3E-05	Extracellular space	YES
SAA2 Serum amyloid A protein	Production primarily in liver, circulates in low levels in the blood. Although its function is not fully understood, serum amyloid A appears to play a role in the immune system. Different biomarker studies have shown association of SAA with atherosclerotic disease. Patients with atherosclerotic disease show increased levels of Amyloid A protein. ³⁹⁻⁴²	24.96	4.0E-07	Extracellular space	NO
ADIPOQ Adiponectin	Involved in the control of fat metabolism and insulin sensitivity, with direct anti-diabetic, anti-atherogenic and anti-inflammatory activities. Stimulates AMPK phosphorylation and activation in liver and skeletal muscle, enhancing glucose utilization and fatty-acid combustion. Negatively regulates TNF-alpha expression in various tissues such as liver and macrophages. Inhibits endothelial NF κ B signaling through a cAMP-dependent pathway. Adiponectin is dysregulated in aneurysm and atherosclerotic disease. ⁴³⁻⁴⁵	21.45	.000301	Extracellular space	YES
FDCSP follicular dendritic cell-secreted protein	FDCSP bind to the surface of B-lymphoma cells. Functions as a secreted mediator acting upon B-cells. No direct associations of FDCSP with atherosclerotic disease or AAA are described in literature. ^{46, 47}	21.38	.000101	Extracellular space	NO

Gene	Function and relation to AAA or atherosclerosis	FC	p-value	Location	Vascular Gene Set
POU2AF1 POU domain class 2-associating factor 1	Transcriptional coactivator that specifically associates with either OCT1 or OCT2. It boosts the OCT1 mediated promoter activity and to a lesser extent that of OCT2. Essential for the response of B-cells to antigens and required for the formation of germinal centers. Little is known about this factor in AAA, though in carotid plaque formation analysis it is shown that POU2AF1 is upregulated, which is related to the immune and inflammatory processes linked to atherosclerosis. ^{48, 49}	18.84	.000479	Nucleus	NO
MS4A1 membrane-spanning 4A / CD20	B-lymphocyte surface molecule which plays a role in the development and differentiation of B-cells into plasma cells. B-lymphocytes with MS4A1 expressed are found in aneurysm and atherosclerotic. ⁵⁰⁻⁵³	18.41	.000261	Plasma membrane	YES
MZB1 Marginal zone B and B1 cell-specific protein	Associates with immunoglobulin M (IgM) heavy and light chains and promotes IgM assembly and secretion. Acts as a hormone-regulated adipokine/proinflammatory cytokine implicated in causing chronic inflammation, affecting cellular expansion and blunting insulin response in adipocytes. No direct association of MZB1 with atherosclerotic disease or AAA are described in literature. ⁵⁴	17.07	.00126	Extracellular space	NO
SLC7A5 Solute carrier family 7 member 5	Encodes for a protein called y+L amino acid transporter 1 (y+LAT-1). Involved in transport of amino acids, namely lysine, arginine, and ornithine. The y+LAT-1 protein forms one part (the light subunit) of a complex called the heterodimeric cationic amino acid transporter, responsible for binding to the amino acids that are transported. There is no direct association of SLC7A5 with atherosclerotic disease or AAA described in the literature. ⁵⁵	15.72	5.4E-07	Plasma membrane	YES
LEP Leptin	Hormone involved in the regulation of body weight. As fat accumulates in cells, more leptin is produced, indicating that fat stores are increasing. Increased leptin levels are associated with atherosclerotic disease. Furthermore, in an AAA animal model mRNA and protein levels of leptin were found to be upregulated in aneurysmatic tissue. ⁵⁶⁻⁶⁰	14.29	1.9E-06	Extracellular space	YES

Upstream Regulator	Activation z-score	p-value of overlap	FC	Molecule Type	Predicted Activation State	Target molecules in dataset
IL1B	<u>7.3</u>	9E-27	6.7	cytokine	Activated	ABCG2,ACTA2,ADAM8,ADM,AIF1,AMPD3,ANGPT1,ANGPTL4,APOB,APOE,ARC,ARG1,BCL2L1,BCL3,BGN,BIRC3,BMP4,CCL3,CCL5,CCR1,CCR5,CCR6,CCR7,CCR2L2,CD14,CD4,CD44,CD83,CD86,CEBPB,CEBPD,CFLAR,CHI3L1,COL10A1,CREM,CSF2RB,CSF3,CTSB,CTSS,CTS2,CX3CL1,CXCL1,CXCL2,CXCL3,CXCL5,CXCR4,CYBA,CYBB,CYSLTR1,CYTIP,DAB2,DDIT4,DUSP5,EDN1,ENPP1,ERBB2,ESR1,F2RL1,FABP5,FAM129A,FCG R2B,FGF2,FOSL1,FST,G0S2,GAD1,GADD45B,GBP1,GCH1,GLA,GM2A,HAS1,HEY2,HGF,HIF1A,HK2,HMGA1,HMOX1,HSD11B1,IBSP,ICAM1,IER3,IGFBP5,IGFBP6,IL10,IL10RA,IL16,IL18,IL18R1,IL18RAP,IL18,IL18R2,IL1RN,IL33,IL6,IL6R,IL8,IRAK1,IRF1,IRF7,ISG20,ITGAM,LCP1,LEP,LIF,MCL1,MMP1,MMP12,MMP3,MMP9,M,YEF2,MYH11,NAMPT,NFIL3,NR4A3,OCLN,OLR1,OSM,PCDH7,PDE4B,PIM1,PLA2,PLAU,PRKCD,PTGS1,PTGS2,PTP4A1,PTX3,RAC2,REL,RUNX2,S100A8,S100A9,SAA2,SCUBE2,SDC1,SERPINE9,SERPINE1,SLAMF1,SLC12A1,SLC14A1,SLC1A3,SLC20A1,SOD2,SPP1,SRGN,STAT4,STMN2,TAC1,TACR1,THBS1,THrsp,THY1,TLR2,TLR3,TLR8,TMEM176B,TNFAIP3,TNFRSF11A,TNFRSF1B,TREM1,TREM2,TYMP,UAP1,UGCG,VDR,VEGFA,XYLT1,ZC3H12A
CEBPA	<u>4.9</u>	1E-20	3.1	transcription regulator	Activated	ACSL1,ADCY7,ADH1B,ADIPOQ,AGT,ALOX5AP,ANPEP,APOB,ARG1,ARL4C,BCL2L1A,BTG1,C3AR1,CCR1,C D14,CD19,CD3G,CEBPA,CEBPB,CEBPD,CHI3L1,COL10A1,CSF1R,CSF3,CSF3R,CXCR4,DDX21,DGAT2,EFN B2,EMCN,FABP4,FASN,FCAR,FHL1,G0S2,GABPB1,GAS1,GATA6,GBP1,GCH1,GLRX,HCAR3,HGF,HMOX1, HSD11B1,ICAM1,IER3,IL10,IL1RN,IL6,IL6R,IL8,ITGAL,ITGAM,ITGAX,LCK,LEP,LPL,LST1,LTf,MALTI,MNDA, NFATC2,NFIL3,OLR1,PAX5,PCK1,PFN2,PGD,PLIN2,PPP1R3C,PTAFR,PTGS1,PTGS2,PTPN3,PTPRC,PTPRE,PTX3,RGS2,RUNX2,RUNX3,S100A8,S100A9,SCD,SEMA3E,SERPINE1,SMPDL3A,SOD2,SPP1,TAC1,TBXAS1, THRB,TRIB1,VDR,VLDLR
IL6	<u>4.6</u>	3E-19	4.0	cytokine	Activated	ABCA1,ABCG2,ACP5,AGT,ANPEP,APOB,APOE,ARG1,ARL4C,BATF,BCL2L11,BCL3,BGN,C5AR1,CCL5,CCR1, CCR5,CCR6,CCR7,CD14,CD163,CD209,CD36,CD48,CD53,CD68,CD79A,CD86,CDKN2B,CEBPA,CEB PB,CEBPD,CFLAR,CLU,CSF2RB,CSF3R,CXCL1,CXCL13,CXCL2,CXCL3,CXCL5,CXCR4,CYBB,CYTIP,EZH2,GA DD45B,GLRX,GSTA4,GZMB,HGF,HIF1A,HLA-DQA1,HMOX1,ICAM1,ICAM3,ICOS,IGFBP5,IGFBP6,IGHM1,IGJ,IL10,IL1RN,IL6,IL6R,IL7R,IL8,IRF1,IRF4,ITGA M,JAK1,JAK2,KIAA0101,KLRB1,KRT14,LEFTY2,LEP,LIF,LPL,LRG1,LRP6,LTf,LY86,MCL1,MERTK,MMP1,MM P12,MMP3,MMP9,MRV1,MSR1,NAMPT,NCF2,PIM1,PLAT,PLAU,PRF1,PROK2,PTGS2,PTPRC,PTTG1,RAB2 7A,RNASE6,RRM2,S100A9,SAA2,SEMA4A,SERPINE1,SERPIN1,SGL1,SLC14A1,SLC7A7,SNX10,SOD2,SPP 1,SRA1,STAT4,TAC1,TBXAS1,THBS1,THrsp,TLR1,TLR10,TLR2,TLR3,TLR8,TNFRSF11A,TNFRSF17,TNFRSF 1B, TOP2A,VEGFA,VLDLR,XBP1

IL18	<u>4.4</u>	4E-11	2,6	cytokine	Activated	ADIPOQ,CC13,CC15,CCR7,CD44,CD69,CD83,CD86,CFLAR,CXCL16,CXCL3,GADD45B,GZMB,HAVC R2,ICAM1,IL10,IL12RB1,IL18,IL18R1,IL1B,IL6,IL8,INPP5D,IRF1,ITGAM,KLR4-KLR1/KLRK1,MMP1,MMP3,MMP9,PRF1,PTGS2,SELL,SPP1,TACR1,TKX,VEGFA
IRF7	<u>4.3</u>	2E-03	2,6	transcription regulator	Activated	CC15,CCR2,CD69,CTLA4,FAM26F,GBP1,GBP5,IRF1,IRF7,IRF8,ISG20,ITGAM,ITGAX,IAK2,MCL1,MX2,NA MPT,PEL1,PLAC8,PMAIP1,S100A8,TLR8,TMBIM6,TNFAIP8,ZBP1,ZC3HAV1
TLR2	<u>4.1</u>	9E-09	4,3	transmembrane receptor	Activated	ARG1,CCL5,CCR1,CCR5,CD69,CD86,CEBPB,CEBPD,CSF3,CXCL2,CXCL3,CYLD,GRIN2A,GZMB,HLA-DQA1,HMOX1,ICAM1,IL10,IL18,IL18R1,IL1B,IL1RN,IL6,IL8,IRAK1,IRF1,ITGA4,LEP,MMP1,MMP9,PTGS2,TREM1,V DR,XBP1
CEBPB	<u>4.0</u>	3E-12	2,4	transcription regulator	Activated	ACTA2,ADIPOQ,AGT,ALDH1A1,ALOX5AP,APOB,ARG1,BCL2A1,BLNK,CCL3,CCL5,CCR5,CD14,CDKN2B,C EBPA,CEBPB,CEBPD,CIRBP,COL10A1,CSF1R,CSF3,CSF3R,CXCL2,CXCL3,CXCL5,DAB2,DGAT2,EFNB2,EMC N,FABP4,FBLN1,FCAR,FHL1,GAS1,HGF,HSD11B1,ICAM1,IER3,IGKC,IL10,IL11RA,IL1B,IL1RN,IL6,IL8,ITGAL ,LCP2,LEP,LYN,MBP,MGP,MMP1,MMP3,MSR1,NFATC2,NFKBID,PCK1,PLAUR,PRKCD,PTGS1,PTGS2,RAC2, RUNX2,SAA2,SAT1,SCD,SEMA3E,SERPINA1,SERPINE1,SGK1,SPP1,TAC1,TLR8,TMEM176B,TRIB3,UPP1,V DR,VLDLR,XIST
CCL5	<u>3.9</u>	2E-08	2,4	cytokine	Activated	C5AR1,CCL3,CCL5,CCR1,CCR5,CCR2,CD163,CD44,CXCL2,CXCL3,EMP1,F2RL1,IL1B,IL6,IL8,MM P19,MMP9,NAMPT,OLR1,PLAUR,PNP,PP1F,SGK1
OSM	<u>3.8</u>	3E-13	6,1	cytokine	Activated	ABCA1,ABCG1,ADAM17,ADH5,AMPD3,AQP9,ARG1,ARHGEF12,ARL4C,BHLHE40,BTC,CALB2,CCL5,CEBP A,CEBPD,CH25H,CHD1,CPM,CSF3,CTSL,CXADR,CXCL1,CXCL13,CXCL2,CXCL3,CXCL5,CYP4F3,DNAJ3,D SC2,ECM2,FGF2,FOXO1,GAB1,GBP1,GLUL,GRIN2A,HGF,HIF1A,HK2,HMOX1,HOXA9,HSD11B1,ICAM1,IG FBP6,IL10,IL18,IL1B,IL1RN,IL3,IL6,IL6R,IL8,IRAK1,IRF1,IRF7,ISG20,ITGAL,JAAG1,ILF,LRFRIP1,MAP2,MARC KS,MICA,MLLT11,MMP1,MMP3,MMP9,MYE2,MYH10,NAMPT,NEDD4,NELL2,NOTCH3,NUAK1,OSM,P2R Y10,PDPN,PFKFB3,PLAU,PRDM1,PTP4A1,PTPN21,S100A12,S100A8,S100A9,S100P,SELL,SERPINA1,SER PINE1,SLC16A3,SLC16A6,SOST,STK4,STX11,TLR2,TLR3,TMBIM6,TNC,TNFRSF11A,TOP2A,TPM1,TYMP,U AP1,VDR,VEGFA,ZBTB43,ZC3HAV1
XBP1	<u>3.8</u>	5E-04	3,3	transcription regulator	Activated	COL10A1,CXCL2,DERL1,DNAJB9,DNAJC3,EDEM1,ERO1LB,ESR1,ET51,FASN,FKBP11,FKBP7,HMOX1,HSP A13,ICAM1,IL6,IL8,IRF4,NCF1,PDIA4,POU2AF1,PRDM1,RUNX2,SDF2L1,SEC11C,SEC24D,SEC61A1,SERPI NA1,SPCS3,SRPB,SSR4,STAR5,TXNDC11,TXNDC5
SELP1G	<u>3.7</u>	5E-07	3,5	other	Activated	BCL2A1,CCL3,CXCL2,CXCR4,HCAR3,HCK,IL10,IL1B,IL1RN,IL2,IL8,ITGAM,PLAUR,PRKCD,SERPINB9
STAT4	<u>3.6</u>	3E-06	3,1	transcription regulator	Activated	ACADL,ACAP1,ARMCX1,BCL2L11,BCL3,CCR5,CXCL2,CXCL3,ERO1L,FCER1G,FYB,GRTP1,IER3,IL10,IL10R A,IL12RB1,IL18R1,IL18RAP,IL6,IRF1,IRF4,ISG20,ITGA7,KDM6B,LRFRIP1,MAP3K1,MGARP,PCGF5,PKD1,PL AC8,PRDM16,RASL12,RGCC,SAT1,SELENBP1,SELP1G,SERPINE1,SLC2A3,SMPDL3A,STC2,TPD52,VEGFA,

VLDLR

CD2	<u>3.6</u>	8E-05	2,9	transmembrane receptor	Activated	CCR7,CD4,CD44,CD48,CD86,CD8A,HLA-DPA1,ICAM1,IL10,ITGAL,PTPRC,SELL,STAT4
CD44	<u>3.6</u>	2E-09	2,5	enzyme	Activated	ADAM8,ARHGEF12,BCAM,BGN,BIRC3,CCL5,CCR5,CCR7,CD36,CD44,CD69,CD8A,CIDECL,CEC7A,CX3CL1,CXADR,ERBB2,FASN,IL10,IL1B,IL1R2,IL1RN,IL6,ITGA4,ITGAX,LI,MS2,LTBP1,MCL1,MMP12,MMP3,MMP9,NPNT,PLAU,SELL,SMAD1,SPP1,THBS1,THY1,TLR8,TNFRSF11A,TPM2,WNT2
TYROBP	<u>3.4</u>	1E-06	2,6	transmembrane receptor	Activated	CCL3,CCR7,CD69,CD83,CD86,FCGR2B,ICAM1,IL6,IL8,ITGAX,NOD2,TYROBP
POU2AF1	<u>3.3</u>	9E-11	18,8	transcription regulator	Activated	CCND3,CCR5,CD79A,CD79B,JDHZ,IGH,IGHA1,IGHG1,IGHM,IGK,KCNN4,LCK,MS4A6A,PAX5,PRDM1,RBP1,SD5,SPIB,SPP1
TREM1	<u>3.3</u>	2E-15	11,9	transmembrane receptor	Activated	ABL2,AREG/AREGB,ATP1B1,CCL18,CCL3,CCL5,CCR2,CD14,CD86,CDKN2B,CEBPB,CKS2,CRTAM,CXCL1,CXCL2,CXCL3,CXCL5,DUSP14,DUSP4,EDN1,FOSL1,GADD45B,GCLM,GLA,HAS1,HS3ST3B1,IL10,IL1B,IL6,IL6R,IL8,IRF1,ITGAX,KANK1,LAMP3,LI,LP,LL,Y9,MAFF,MCOLN2,MFL1P,MMP1,MMP19,NOD2,NRP3,PIM2,PLAC8,PLCXD1,PTGS2,RGS1,SCG5,SFMBT2,SLAMF7,SLC1A3,SPP1,TARP,THBS1,TLR2,TNFSF15
PLAU	<u>3.3</u>	7E-06	4,2	peptidase	Activated	ABCG1,ARG1,CSAR1,CCL5,CCR5,CXCL3,HGF,ICAM1,IL1B,IL6,MMP1,MMP12,MMP9,PLAU,PLAUR,S100A8,S100A9,SERPINE1
ETS1	<u>3.3</u>	2E-15	2,9	transcription regulator	Activated	ANPEP,ARL4C,ATP2A3,BCL11A,BMP4,CD14,CD27,CD79A,CD79B,CRTAM,CSF1R,ERBB2,ETS1,FCGR2A,FOXD1,GZMB,GZMK,HCST1,HGF,HMOX1,HPSE,HSPA6,HSPB8,ICAM1,IL10,IL2RB,INSIG1,ITGB2,ITK,IAK1,KLRC4,KLRK1/KLRK1,LAIR1,LCK,LTB,MCL1,MMP1,MMP3,MMP9,MSR1,NCF1,NFIL3,NPR1,PLAU,PRF1,RUNX2,RUNX3,SELL,SERPINE1,SLAMF6,SPP1,SRGN,TBXAS1,TGFA,THY1,TRPC1,VEGFA,WAS,ZAP70,ZEB1
NFATC2	<u>3.3</u>	2E-06	2,5	transcription regulator	Activated	ABCA1,ACF5,BATF,CD3G,CFLAR,CTLA4,CXCL3,DAB2,E2F5,EDN1,ICOS,IKZF1,IL10,IL18,IRF1,IRF4,IRF7,ISG20,MERTK,NFATC1,PELI1,PLAT,PLK2,PPP3R1,PTGS2,PTPN1,REL,RGS1,RGS2,RILPL1,TLR3,TNFSF8
VEGFA	<u>3.3</u>	5E-06	2,1	growth factor	Activated	ACSL1,ADH5,ANEP,BCL2A1,BTK,CCR2,CD34,CTSB,CTSS,CXCR4,DUSP4,DUSP5,EFNB2,ETS1,FABP4,FGF2,GBP1,GRIA2,HMOX1,ICAM1,IGFBP5,IL6,IL8,INPP5D,MCL1,MEOX2,MMP1,MMP12,MMP9,NME1,OCLN,PIM1,PLAT,PLAU,PTGS1,PTGS2,RUNX2,SCO2,SERPINE1,SCNG,SOD2,THBS1,VEGFA
MAP3K1	<u>3.2</u>	6E-04	2,0	kinase	Activated	BIRC3,CSA,HMOX1,IL8,MMP3,PGR,PLAU,PLAUR,PTGS2,SERPINE1,THBS1,TNCT,TP2A,TPH1
CSAR1	<u>3.1</u>	8E-07	4,8	G-protein coupled receptor	Activated	CSAR1,CD28,CD86,CSF3,CXCL2,FCERT1,FCERT2,FCERT3,FCGR2B,IL1B,IL6,IL8,SERPINE1
IL6R	<u>3.1</u>	1E-08	2,9	transmembrane receptor	Activated	CCL3,CCL5,CD36,CXCL2,CXCL3,CXCL5,ICAM1,ICAM3,IGFBP5,IL10,IL6,IL8,IRF1,MCL1,MMP3,MMP9,NAMPT,PTGS2,TAC1,TNFRSF11A,VEGFA

IL17RA	<u>3.1</u>	1E-06	2,2	transmembrane receptor	Activated	CCR1,CSF3,CSF3R,CXCL2,CXCL3,CXCR2,IL1B,IL6,IL8,MMMP3,S100A8,S100A9
PLAUR	<u>3.0</u>	1E-03	7,1	transmembrane receptor	Activated	C5AR1,CCL5,CTSB,CXCL3,CYBB,ITGAM,MMMP3,MMMP9,PLAU,PLAUR
CD14	<u>3.0</u>	1E-04	3,0	transmembrane receptor	Activated	BCL2A1,CCL3,CCL5,CXCL2,CXCR2,IL10,IL10RA,IL1B,IL6,IL8,PTGS2,TLR2,TNFAIP3
ICAM1	<u>2.9</u>	9E-06	2,4	transmembrane receptor	Activated	ACTA2,CCL5,CD69,CD86,CXCL2,CXCL3,ICAM1,IL1B,IL6,ITGA4,ITGAL,MMMP9,VEGFA
SAMSN1	<u>2.8</u>	4E-05	4,7	other	Activated	BATF,CXCL2,DAB2,EDN1,IL18,IL6,IRF1,IRF7,ISG20,MARCO,MERTK,PEL1,PLAT,PTGS2,RGCC,RILPL1,SDC1,TLR3,TNFSF8,XBP1,ZC3H12A
NAMPT	<u>2.8</u>	2E-06	3,5	cytokine	Activated	CXCL1,CXCL2,IL6,IL8,MMP1,MMMP3,MMMP9,NAMPT,NELL2,NPY1R,TMSB15A
SPP1	<u>2.7</u>	5E-09	7,1	cytokine	Activated	ABCG2,ACP5,ADIPOQ,ANGPT1,BCL2L11,CCL18,CCL3,CCL5,CD44,CXCL1,CXCL2,CXCL3,CXCL5,HMOX1,ICAM1,IL10,IL1B,IL6,IL8,INSIG1,JAG1,MMP1,MMMP9,PLAU,RUNX2,SPP1
PRKCB	<u>2.7</u>	5E-03	5,5	kinase	Activated	CD83,CD86,FASN,ICAM1,IL10,IL6,MMMP9,PRKCB,PTGS2,SERPINE1,SOD2
BTK	<u>2.7</u>	1E-04	3,3	kinase	Activated	BCL2A1,BTK,CCND3,CD2,CD86,CXCL3,FABP5,HMOX1,IGLL1/IGLL5,IL10,IL18,IL6,IL8,ITGAX,NFATC1
PTGS2	<u>2.7</u>	2E-08	2,6	enzyme	Activated	ANGPT1,AQP1,AREG/AREGB,BIRC3,CCL5,CCR7,CD44,CD68,CLU,CTSD,CXCL3,CXCL5,CXCR2,CXCR4,EDNRA,ERBB2,EZR,ICAM1,IL10,IL1B,IL6,IL8,ITGAL,LEP,MCL1,MMMP9,MSR1,NOP2,PTGER2,PTGS1,PTGS2,RUNX2,SELL,SOST,VEGFA
CEBPD	<u>2.7</u>	3E-07	2,0	transcription regulator	Activated	ALOX5AP,BCL2A1,CD14,CEBPB,COL10A1,CSF1R,CSF3R,CXCL1,CXCL3,FABP4,HGF,IGFBP5,IL10,IL1B,IL6,IL8,ITGAM,ITGAX,MBP,MMMP3,PTAFR,PTGS2,TLR8,VLDR
LEP	<u>2.6</u>	1E-07	14,3	growth factor	Activated	ACADL,ADAM8,ADIPOQ,ANGPTL4,AQP3,AQP9,AR,BCL2A1,CCL5,CD14,CD36,CD68,CEBPB,CPT1B,CSF3,CTSL,CYBA,CYBB,EDN1,ERBB2,ESR1,FABP4,FASN,GPAM,HEY2,IBSP,ICAM1,IL10,IL1B,IL1R2,IL1RN,IL6,ITGAM,JAK2,KISS1R,LEP,LIPA,LP,MBP,MCL1,MMP1,MMMP12,MMMP19,MMMP3,NAMPT,NCF1,NCF2,NP1,NPR1,NPR2,NPY1R,NTS,PCK1,PGR,PLAT,PLIN1,PLIN2,PLN,PRF1,PTGS2,SCD,SERPINE1,SOD2,SPP1,THBS1,THSRP,UCP2,VEGFA
REL	<u>2.5</u>	8E-05	3,6	transcription regulator	Activated	BCL2A1,BCL3,CD86,CCR2,CREM,ESR1,GADD45B,ICAM1,IER3,IGHG1,IGHM,IGK,IL18,IL6,IL8,IRF4,IRF5,MMMP9,NFKBID,PMAIP1,RELSL,C25A27,SOD2,TNFAIP3,TNFRSF10C
TGIF1	<u>2.4</u>	7E-04	2,9	transcription regulator	Activated	CXCL1,CXCL2,CXCL3,IL1B,IL6,IL8
CYBB	<u>2.4</u>	3E-03	2,6	enzyme	Activated	CCL5,CXCL3,CYBA,CYBB,ICAM1,IL1B,IL6,TNFRSF11A

IRF8	<u>2.3</u>	4E-10	3,5	transcription regulator	Activated	CCL5,CCR6,CCR7,CD4,CD83,CD86,CEBPA,CSF1R,CSF3R,CTSS,CXCL16,CYBB,DAB2,GBP1,ICAM1,IL17RA,IL18,IL1B,IL6,IRF8,ITGAM,JAK1,ILF,MMP9,MSR1,PCDH7,PRDM1,TLR3,TYROBP
IRF1	<u>2.3</u>	5E-03	2,9	transcription regulator	Activated	ADAM8,CCL5,CTSS,CXCL16,CYBB,DST,IL10,IL12RB1,IL17RA,IL18,IL1B,IL6,IL8,IRF1,IRF4,IRF5,IRF7,JAK2,ILTB,MMP9,PCDH7,PTGS2,SELL,TLR3
CSF3	<u>2.2</u>	1E-21	5,8	cytokine	Activated	ARG1,ARHGDI3,BATF,BIRC3,C3AR1,CAPG,CCL3,CCL5,CCND3,CCR7,CD14,CD300LF,CD44,CEBPA,CEBPB,CSF3R,CTLA4,CTSD,CXCL5,CXCR4,CYBB,EDN1,ETS1,FPRI,GADD45B,GPR183,GZMB,HGF,HLA-DPA1,HLA-DQA1,HMOX1,HOXA7,HOXB7,ICAM1,IL10,IL1RN,IL6,IL8,ITGAM,ITGB2,JAK3,LTB,LTG,LTG,LTG,MMP9,NFATC1,NFIL3,PIM1,PRKCB,PROK2,PYHIN1,RAB27A,RS1,RS100P,SELL,TFRC,TLR2,TLR8,TNFAIP3,TNFRSF1B,VEGFA,PEL3
PTPRE	<u>2.2</u>	8E-03	2,6	phosphatase	Activated	CXCL2,CXCL3,IL18,MARCO,SLA
INHBB	<u>2.2</u>	7E-04	2,3	growth factor	Activated	FST,HGF,MMP3,SERPINE1,THBS1,TNC
CD86	<u>2.1</u>	4E-06	3,0	transmembrane receptor	Activated	CCL3,CD28,CD69,CD86,CTLA4,ICAM1,ICOS,IL10,IL6,POUZ2,TNFAIP3,TNFRSF1A,XBP1
DOCK8	<u>2.0</u>	3E-04	2,9	other	Activated	DAB2,EDN1,IL18,IL6,IRF1,IRF7,ISG20,MERTK,PELI1,PIAT,PTGS2,REL,RS1,RILPL1,TLR3,TNFSF8

Table 4
List of up-regulated genes prioritized by upstream regulator selection (z-score; p<0.01) in AAA vs AOD.

	Total	Aneurysmal disease	Occlusive disease	P-value
	n=1393	n=614	n=779	
Baseline characteristics				
Male gender (%)	1046 (75.1)	525 (85.5)	521 (66.9)	<.001
Age (years±SD)	68.1 ±10.1	71.3 ±7.8	65.6 ±11.0	<.001
Body mass index (kg/m ²), mean(±SD)	26.1 ±4.1	26.1 ±3.9	26.2 ±4.3	.540
Cardiovascular comorbidities (%)				
Congestive heart failure	155 (11.1)	66 (10.7)	89 (11.4)	.692
Ischemic heart disease	578 (41.5)	272 (44.3)	306 (39.3)	.059
Cerebrovascular disease	455 (32.7)	89 (14.5)	366 (47.0)	<.001
Cardiovascular risk factors (%)				
Kidney disease (≥2.0mg/dl)	200 (14.4)	94 (15.3)	106 (13.6)	.368
Diabetes mellitus	328 (23.5)	103 (16.8)	225 (28.9)	<.001
Hypertension	932 (66.9)	408 (66.4)	524 (67.2)	.761
Hypercholesterolemia	1240 (89.0)	534 (87.0)	706 (90.6)	.030
Smoking – ever	1086 (78.0)	473 (77.0)	613 (78.7)	.459
Smoking – current	576 (41.7)	236 (39.0)	338 (43.9)	.068
Medication (%)				
Statins (%)	1079 (77.4)	446 (72.6)	633 (81.2)	<.001
Beta-blockers (%)	1123 (80.6)	531 (86.4)	592 (75.9)	<.001
RAAS inhibitors (%)	640 (45.9)	271 (44.1)	369 (47.3)	.247
Diuretics (%)	349 (25.0)	138 (22.4)	211 (27.0)	.052
Antiplatelets (%)	934 (67.0)	353 (57.4)	581 (74.5)	<.001

Table 5

Clinical characteristics of patients with aneurysmal or arterial occlusive disease. Abbreviations: RAAS inhibitors; renin-angiotensin system inhibitors.

Inflammatory marker	Number	Total	Aneurysm	Occlusive	P-value
triglyceride (mmol/L)	1307	1.61 [1.16-2.27]	1.58 [1.13-2.19]	1.63 [1.18-2.34]	.053
high-density lipoprotein (mmol/L)	1314	1.20 [0.97-1.46]	1.18 [0.97-1.42]	0.97 [1.20-1.48]	.275
low-density lipoprotein (mmol/L)	1297	2.72 [2.04-3.47]	2.83 [2.13-3.53]	2.59 [1.95-3.41]	.003
hs-CRP (mg/l) [IQR]	872	3.53 [1.58-5.73]	4.07 [2.21-6.39]	3.06 [1.52-5.22]	<.0001

Table 6
Inflammatory markers of patients with aneurysmal or arterial occlusive disease. Abbreviations: hs CRP, high sensitive C-reactive protein. Data presented in median with inter quartile range.

Inflammatory marker	β	95% CI for β	P-value
triglyceride	unadjusted	.06 : .13	.005
	adjusted*	.01 : .25	.079
high-density lipoprotein	unadjusted	-.03 : .08	.334
	adjusted*	-.06 : .06	.913
low-density lipoprotein	unadjusted	-.26 : -.21	.021
	adjusted*	-.22 : .51	.226
hs-CRP	unadjusted	-1.07 : -.35	<.0001
	adjusted*	-.99 : -.11	.015

Table 7
Multivariable logistic regression models for inflammatory markers in patients with aneurysmal or arterial occlusive disease. Abbreviations: CI, confidence interval; hs-CRP, high sensitive C-reactive protein. * adjusted for: age, gender, body mass index, congestive heart failure, ischemic heart disease, cerebrovascular disease, kidney disease, diabetes mellitus, hypertension, current smoking, and the use of statins, beta-blockers, renin-angiotensin system inhibitors, diuretics and antiplatelets.

KEGG pathways

Vascular Smooth Muscle Contraction hsa04270

Tight Junction hsa04530

ECM receptor interaction hsa04512

TGF β signaling hsa04350

notch signaling hsa04330

Focal Adhesion hsa04510

Adherens junctions hsa04520

Fat Dig and Absorption hsa04975

Renin-Angiotensin-System hsa04614

GO-Terms

Vasculogenesis GO 0001570

Vasculature Development 0001944

Relaxation of smooth muscle GO 0060087

Cardiovascular system development GO:0072358

Vascular smooth muscle contraction GO:0014829

Reg. of vascular permeability GO 0002528

Regulation of vascular smooth muscle contraction GO:0003056

Cardiac vascular smooth muscle cell differentiation GO:0060947

macrophage derived foam cell differentiation GO:0010742

Negative regulation of macrophage derived foam cell differentiation GO 0010745

positive regulation of macrophage derived foam cell differentiation GO 0010744

regulation of macrophage derived foam cell diff GO 0010743

IPA functions and pathways

Adherens Junction IPA

Cardiovascular IPA

Extracellular matrix IPA

Fat Digestion and Absorption IPA

Foam Cell IPA

Focal Adhesion IPA

Supplemental Table I

The Vascular Gene Set, constructed from HGMD, OMIM, relevant GO terms, relevant KEGG pathways, relevant Ingenuity IPA pathways, GWAS studies and the literature.

Notch Signaling IPA

Renin Angiotensin IPA

TGF β Signaling IPA

Tight Junction IPA

vascular smooth muscle IPA

Vasculature Development IPA

Vasculogenesis IPA

Vascular Permeability IPA

AAA GWAS gene

aneurysm HGMD genes

aneurysm OMIM

aneurysm custom

Supplemental Table II

This Vascular Gene Set consists of 4209 genes, which are implicated to have a role in the vascular tissue system.
(See digital excel list)

CHAPTER 8

Long range polymerase chain reaction amplification of
Aortic Aneurysm Genes

L. te Riet, P. Elfferich, Z. Çakmak, I. van der Pluijm, J. Essers

(in progress)

**ABSTRACT**

Aortic aneurysms are complex multifactorial diseases with genetic and environmental risk factors. Genetic factors have been shown to play a role in the etiology of thoracic aortic aneurysms mostly present in a syndromic form, with early onset. Responsible aneurysm-associated gene mutations have been identified, such as mutations in cytoplasmic, contractile, extracellular matrix (ECM) and transforming growth factor β associated proteins. Aneurysms are identified in patients with ultrasound, CT or MRI imaging methods. In addition the genome is sequenced for potential mutations, as genetic profiling will identify patients at high risk of aneurysm development, allowing early follow-up. Our goal is to set up a method for reliable massive parallel genomic DNA sequencing of aneurysm-associated genes. In this report we show the essential enrichment of complete TAA genes, by optimization of long range-PCR of TAA linked genes, covering 14 aneurysm-associated genes, including intron, exon and regulatory sequences. The next step will be massive parallel sequencing to screen for potential pathological mutations, which can be performed from this point.

INTRODUCTION

The regular definition of an aneurysm is an increase of 50% or more in vessel diameter size. Aortic aneurysms are divided into thoracic aortic aneurysms (TAA) and abdominal aortic aneurysms (AAA) based upon their location. Due to dilation of the aortic wall, the wall weakens, thereby increasing the risk of rupture.¹ Aortic aneurysmal disease, either of the abdominal or thoracic aorta, contributes significantly to the disease burden of the elderly population. Age and gender are important risk factors for AAA, and currently AAA has a prevalence rate ranging from 1.7% to 7.2% for men above the age of 65.² Although various environmental factors, such as smoking and hypertension, are implicated in the development of the pathology, there is also a clear hereditary component. Yet, although 15% of the AAA patients show a positive family history, the direct causative genes have not been identified.²⁻⁵

TAA and thoraco-abdominal aortic aneurysms (TAAA) are less common, with an incidence of 10.4 new aneurysms per 100,000 person-years for TAA and 2.2 new aneurysms per 100,000 person-years for TAAA.^{6,7} There is a strong genetic factor in TAA and TAAA disease, they mostly present in a syndromic form, with early onset, and responsible genes have been identified. Mutations are found in genes encoding for cytoplasmic, contractile and extracellular matrix (ECM) proteins as well as for transforming growth factor β (TGF β) components. A well-known example is Marfan syndrome (MFS) with a mutation in the extracellular matrix protein Fibrillin-1, which was the first gene described causing TAA disease.⁸ Another example is Loeys-Dietz syndrome with mutations in TGF β signaling pathway components, such as TGF β R1⁹, TGF β R2⁹⁻¹¹, and SMAD3 (also known as aneurysm osteoarthritis syndrome).¹² Furthermore, mutations in contractile proteins of smooth muscle cells have been described, such as ACTA2¹³ and MYH11.¹⁴ Despite the fact that a spectrum of different genetic mutations causing aneurysm disease have been identified, hallmark histological anomalies like fragmentation of the elastic lamina and loss of extracellular matrix integrity are similar. Clinically, aneurysms are identified with ultrasound CT or MRI. If necessary aneurysms are treated by open or endovascular surgery. Normally, surgery is indicated for TAA at a diameter of ≥ 5.5 cm, for males with AAA at a diameter of ≥ 5.5 cm, and for women with AAA at a diameter of ≥ 4.5 cm.¹ However, the loss of vessel wall integrity that precedes aortic dilatation can neither be detected, nor treated in time.¹ Nevertheless, for existing AAAs and TAAs β -blocker therapy is considered important in reducing the risk of aortic aneurysm expansion and rupture.¹⁵ Consequently, genetic sequencing of familial TAA associated genes is necessary to detect patients with high probability in developing aneurysm disease, as about 20% of all TAAs are familial.⁵ Nowadays, at least 14 genes are directly linked to TAA disease (see table 1). Accordingly, patients and family members are screened when there is a suspicion of mutations in one of the TAA linked genes by genetic sequencing.

At present, different TAA genes are routinely analyzed for mutations in the coding part of genes through targeted Sanger sequencing of individual genes or next generation exome sequencing, with the exome being the part of the genome formed by exons. Our goal is to set up reliable massive parallel DNA sequencing for mutation analysis of complete genomic sequences, including intron, exon and regulatory sequences, of these 14 aneurysm-related genes. To this end we set up selective amplification of targeted genomic regions spanning the entire aneurysm-associated gene length. Genetic profiling will identify people at high risk of aneurysm development, allowing early follow-up of these patients using ultrasound and other molecular imaging methods. In this study we show long range polymerase chain reaction (LR-PCR) optimization and the enrichment of DNA fragments of 14 TAA associated genes. This represents the first step in the set up for mutation analysis with massive parallel DNA sequencing.

MATERIALS AND METHODS

TAA genes

TAA linked genes were selected from literature and can be categorized in: extracellular matrix proteins: collagen α -1 III (COL3A1), collagen α -1 IV (COL4A1), fibulin-4 (EFEMP2); elastin (ELN) and fibrillin-1 (FBN1); cytoskeleton proteins: α -smooth muscle actin (ACTA2), smooth muscle myosin (MYH11), myosin light chain kinase (MYLK) and myosin light chain 9 (MYL9); Transforming Growth Factor beta (TGF- β) associated components; TGF- β receptor type 1 (TGFBR1), receptor type 2 (TGFBR2) and SMAD family member 3 (SMAD3); other proteins: Notch1 and glucose transporter type 10 (SLC2A10).

LR-PCR Primer Design

Human gene sequences of the 14 selected TAA genes, were imported from the NCBI database to the Vector NTI software program (Vector NTIO express, Life Technologies). The gene sequences were extended with an additional 5000 base pair (bp) upstream and an additional 1000 bp downstream. All exons were marked, and the gene sequences were divided into fragments of roughly 1500 up to 10.000 bp. The exons were generally combined into bundles of several exons to generate these 1500 - 10.000 bp fragments. Primers were designed in a 300 bp region, at least 500 bp upstream and downstream of the exons, except upstream of exon 1; there the primer was at least 1000 bp upstream. The sequences were exported to the Primer 3 website (Primer 3 version 0.4.0, //bioinfo.ut.ee/primer3-0.4.0/) and primers were designed using this program. The following parameters were used and adjusted from standard settings; primers must be in the 300 bp regions upstream and downstream of the bundled sequences; product size should be 1000-10.000 bp, primer size of 25-35 bp with an optimal size of 30 bp; melting temperature (T_m) between 59-64°C with an optimal of 62°C, a T_m difference of only 0.5°C at maximum; and preferably a GC-clamp. Designed primers were checked for single-nucleotide polymorphism (SNP) in their prime region, for which the SNP Check3 program was used (//nrgl.manchester.ac.uk/SNPCheckV3). Only primers without a SNP or without a significant SNP were used in this study, since a SNP variation could prevent a primer from annealing properly in patient cohorts. Primers using the desalt purification method were ordered from Life Technologies, dissolved in TE-buffer (10 mM Tris, pH8 and 1 mM EDTA) at 100 μ M, and stored in the freezer (-20 °C).

Optimization of Primers

Although annealing temperatures were preferably calculated to be the same for all *in silico* designed primers, they were first optimized and tested by using a gradient PCR thermocycler. The optimal annealing temperature was determined for each primer set by using an annealing gradient of 56°C up to 63°C. If necessary, new primers were designed. The annealing temperatures generally turned out to be 2 degrees lower in these LR-PCR reactions than the calculated T_m .

Genomic DNA

Genomic DNA (gDNA) was extracted from a cultured human lymphoblast cell-line clone, and obtained from ThermoFisher (control DNA from CEPH individual 1347-02)²⁶. Accordingly control DNA from CEPH individual 1347-02 was used as normal healthy gDNA.

Long Range Polymerase Chain Reaction

Kapa HiFi HotStart Readymix (2x) (Kapa Biosystems) was used in the Long Range-PCR (LR-PCR), as it is able to amplify long DNA targets up to 15.000 bp. The concentration for each PCR reaction was as follows; 1x Kapa HiFi HotStart Readymix, 0.3 μ M Forward and 0.3 μ M Reverse primer (10 μ M stocks), 10 ng gDNA (5 ng/ μ l) and PCR-grade water was added to obtain an end-volume of 25 μ l. Standard conditions were changed if necessary to improve reactions and these changes are noted in the supplemental table I. The PCR program settings for an amplicon size of 1000-2000 bp were as follows; (1) denaturation at 95°C for 5 minutes. (2) denaturation at 98°C

Gene	Description	Category
COL3A1 ¹⁶ (collagen α 1(III))	COL3A1 gene encodes for type III collagen, and is found in extendable tissues.	Extracellular matrix protein
COL4A1 ¹⁷ (collagen α 1(IV))	COL4A1 gene encodes for the type IV alpha collagen chain of basement membranes.	Extracellular matrix protein
EFEMP2 ¹⁸ (fibulin-4)	EFEMP2 gene encodes for a protein involved in the formation of elastic fibers.	Extracellular matrix protein
ELN ¹⁹ (elastin)	ELN gene encodes for a protein forming elastin fibers. Mutations in this gene cause cutis laxa.	Extracellular matrix protein
FBN1 ¹⁰ (fibrillin-1)	FBN1 gene encodes for the fibrillin-1 protein. It provides force bearing structures. Mutations in this gene are associated with Marfan syndrome.	Extracellular matrix protein
ACTA2 ¹³ (α -smooth muscle actin)	ACTA2 gene encodes for a member of the actin family proteins. α -Actin is found in the skeletal muscle and is a component of the contractile apparatus.	Cytoskeleton proteins
MYH11 ²⁰ (smooth muscle myosin)	Smooth muscle myosin belongs to the myosin heavy chain family. MYH11 hydrolyses ATP to obtain mechanical energy for its contractile function.	Cytoskeleton proteins
MYLK ²¹ (myosin light chain kinase)	MYLK gene encodes for myosin light chain kinase, and this enzyme phosphorylates myosin light chains with actin filaments to produce contractile activity.	Cytoskeleton proteins
MYL9 ²² (myosin light chain 9)	MYL9 gene encodes for a myosin light chain protein, it binds calcium to regulate muscle contraction and is activated by myosin light chain kinase.	Cytoskeleton proteins
TGFBR1 ¹¹ (TGF- β receptor type 1)	TGFBR1 gene encodes for a protein forming the TGF- β receptor, which binds TGF- β . Mutations in this receptor can cause Loeys-Dietz syndrome.	TGF- β associated components
TGFBR2 ⁹ (TGF- β receptor type 2)	TGFBR2 gene encodes for a protein forming TGF- β receptor protein, which binds TGF- β . It phosphorylates other proteins that enter the nucleus and regulate transcription processes.	TGF- β associated components
SMAD3 ²³ (SMAD family member 3)	SMAD3 protein belongs to the SMAD family and is a signal transducer and transcriptional modulator. SMAD3 is activated by TGF- β signaling.	TGF- β associated components
Notch1 ²⁴	Notch1 is part of the intracellular signaling pathway and controls cell fate decisions. The exact interaction of NOTCH1 in aneurysm disease is not yet determined.	Other
SLC2A10 ²⁵ (glucose transporter type 10)	SLC2A10 gene encodes for a glucose transporter protein and is involved in glucose homeostasis.	Other

Table 1

General information about the TAA associated genes.



for 20 seconds. (3) annealing at 56-66°C for 15 seconds. (4) extension at 72°C for 1 minute, with PCR reaction 2-4 being repeated going 34 times, followed by (5) extension at 72°C for 2 minutes. With increasing amplicon sizes the extension times were increased with 30 seconds per 1000 bp. Consequently, for amplicons of 8.000-9.000 bp the annealing time in step 4 is increased up to 4.5 minutes and in step 5 up to 5.5 minutes. Finished PCR reactions were cooled to a temperature of 10°C or stored at 4°C upon further processing.

PCR Product Verification

LR-PCR products were initially verified on an agarose gel (1% agarose in TBE buffer with 0.005% ethidium bromide) with a λ BstEII or λ PstI (Invitrogen) marker. One third of LR-PCR reaction volumes were mixed with loading dye (6X Orange G DNA Loading Dye, homemade), loaded and ran for at least 2 hours at 100 Volt. Gels were visualized by a Typhoon imager (Typhoon FLA 9500, GE Healthcare Life Sciences). If the observed bands were of the correct size and showed a sharp and single banded pattern, the corresponding settings were approved and depicted in the tables. In addition, LR-PCR products were verified by using a restriction enzyme procedure. The total sequence of PCR products was obtained from the UCSC genome browser (<https://genome.ucsc.edu>) by inserting only forward and reverse primer sequences. Selection of the single cutting restriction enzymes was attained by uploading total sequences in the NEBcutter website (<http://nc2.neb.com/NEBcutter2/>). About 5 μ l of each LR-PCR product was digested in an end-volume of 25 μ l, using a single cutting restriction enzyme (Biolabs ~20 Units (20000 units/ml)), the associated 10x buffer (Biolabs), and PCR-grade water. Samples were digested at 37°C for an hour, loaded and verified on agarose gel as described previously.

RESULTS

ACTA2

Pathogenic ACTA2 mutations lead to altered cell mobility, resulting in a different structure and integrity of the aortic wall.¹³ Of all inherited TAAs 14% is caused by mutations in the ACTA2 gene. The following settings were used to enrich DNA covering the promotor region, all exons and large parts of the introns (table 2 and/or supplemental table I). In figure 1 an overview of ACTA2 PCR products is shown.

Lane	Primers	Sequence	Annealing temperature (°C)	Amplicon Size (bp)	Extension Time (min)
1	ACTA2ex1LRFNew	tatgtctgatcttgtatttgactcatctg	60	2338	1,5
	ACTA2ex1LRR	aggttgaaactacagcagaagcctttag	60		1,5
2	ACTA2ex2LRF	gtaaagtaaaagtcctcatgattcaaaaag	59	2952	1,5
	ACTA2ex3LRR	ttgtagagacaggatcttactactgttacc	59		1,5
3	ACTA2ex4LRF	attaggtttcaagtaagcgtcattattc	60	5528	3
	ACTA2ex7LRR	tgctcttatctatctcctaattctcac	60		3
4	ACTA2ex8LRFNew	ttacagagatagataaagagcacttagcc	63	4698	2,5
	ACTA2ex9LRRNew	cataaaagtcagaccacctgtttctatag	63		2,5

Table 2

ACTA2 gene details of primer sequence, annealing temperature, amplicon size and extension times

In addition, all LR-PCR products were verified by restriction enzyme analysis to confirm the size of each product and specificity of the primers. The total sequences were obtained from the UCSC genome browser, and enzymes with a unique restriction site in this sequence were selected from the NEBcutter website (<http://nc2.neb.com/NEBcutter2/>). This procedure was performed for all primer sets. (for an example see lane 5 figure1). Supplemental Table I contains all the restriction enzymes used for each primer set, and their expected DNA fragment sizes.

MYH11

The MYH11 gene encodes for smooth muscle myosin heavy chain 11, and this cytoplasmic protein hydrolyses ATP to obtain mechanical energy for its contractile function. Mutations, in MYH11 result in TAA disease.²⁰ The PCR conditions are listed in supplemental table I, Figure 2 shows the result of amplification of the complete genomic MYH11 DNA sequence covering the promotor region, all exons and large parts of the introns.

SMAD3

SMAD3 belongs to the SMAD family and is a signal transducer and transcriptional modulator. SMAD3 is activated by TGF- β signaling, and mutations in SMAD3 result in SMAD3-related aneurysms-osteoarthritis syndrome, also called Loeys-Dietz syndrome, and results in aortic aneurysms.²³ The PCR conditions are listed in supplemental table I, Figure 3 shows the result of amplification of the complete genomic SMAD3 DNA sequences, covering the promoter region, all exons, and large parts of the introns.

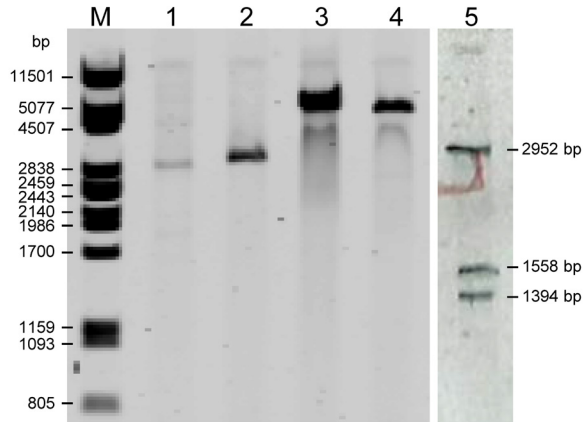


Figure 1

Overview of the ACTA2 genomic PCR products obtained with the primer sets listed in suppl. table I. Marker λ PstI, lane 1 primer set covering exon 1, lane 2 covering exon 2 up to exon 3, lane 3 covering exon 4 up to exon 7, and lane 4 covering exon 8 up to exon 9. Lane 5 the verification of Amplicon 2 of ACTA2 by restriction enzyme analysis. ACTA2 amplicon 2 was cut by EcoRI and the expected DNA fragment lengths of 1558 bp and 1394 bp were obtained. The 2952 bp band is still visible, as the novel LR-PCR product was not digested completely. The lanes corresponds with suppl. table I.

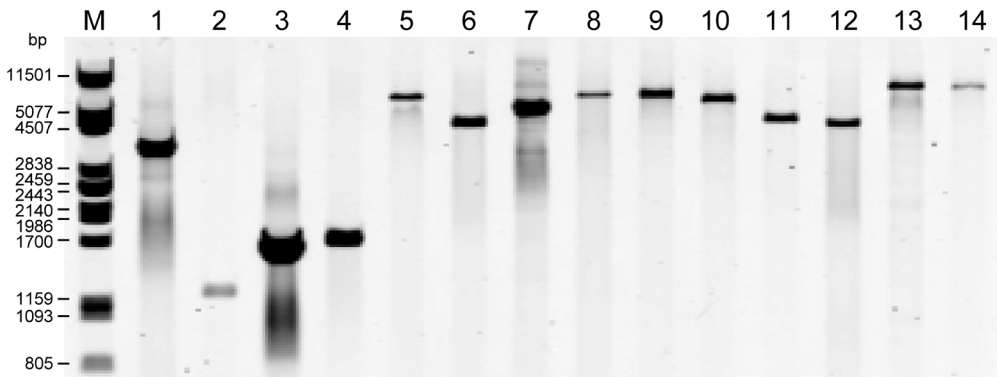


Figure 2

Overview of the MYH11 genomic PCR products obtained with the primer sets listed in suppl. table I. The lanes corresponds with suppl. table I, marker λ PstI.

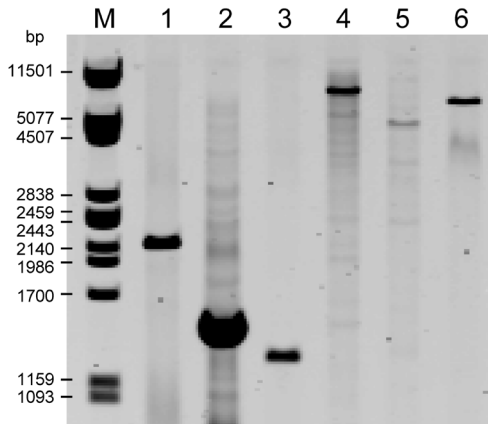
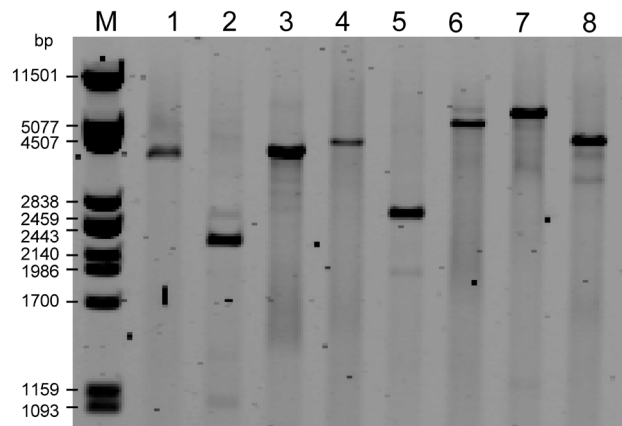


Figure 3

Overview of the SMAD3 genomic PCR products obtained with the primer sets listed in suppl. table I. The lanes corresponds with suppl. table I, marker λ PstI.

Figure 4

Overview of the NOTCH genomic PCR products obtained with the primer sets listed in suppl. table I. The lanes corresponds with suppl. table I, marker λ PstI.



NOTCH1

Notch1 encodes a member of the Notch family. Members of this Type 1 transmembrane protein family share structural characteristics including an extracellular domain consisting of multiple epidermal growth factor-like (EGF) repeats, and an intracellular domain consisting of multiple different domain types. Notch family members play a role in a variety of developmental processes by controlling cell fate decisions. The Notch signaling network is an evolutionarily conserved intercellular signaling pathway which regulates interactions between physically adjacent cells. The molecular role of NOTCH1 in aneurysms is not known.²⁴ PCR conditions for NOTCH1 are listed in supplemental table I. Figure 4 shows the result of amplification of the complete genomic NOTCH1 DNA sequences covering promoter region, all exons and large parts of the introns.

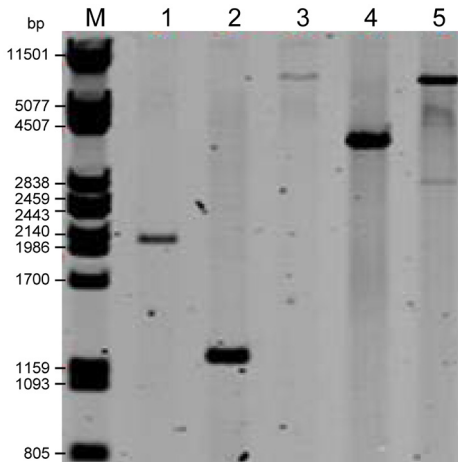


Figure 5
Overview of the SLC2A10 genomic PCR products obtained with the primer sets listed in suppl. table I. The lanes corresponds with suppl. table I, marker λ PstI.

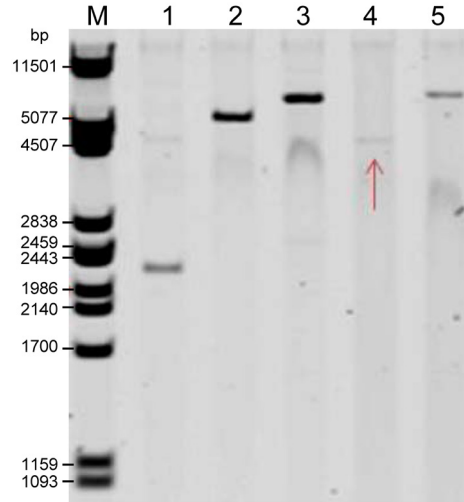


Figure 6
Overview of the TGFBR1 genomic PCR products obtained with the primer sets listed in suppl. table I. The lanes corresponds with suppl. table I, marker λ PstI.

SLC2A10

The SLC2A10 gene encodes for a glucose transporter protein and is involved in glucose homeostasis.²⁵ Mutations in this gene alter angiogenesis and cause arterial tortuosity syndrome. Furthermore this syndrome is characterized by elongation, stenosis and aneurysm formation in the major arteries owing to disruption of elastic fibers in the medial layer of the arterial wall. SLC2A10 PCR conditions are listed in supplemental table I. Figure 5 shows the result of amplification of the complete genomic SLC2A10 DNA sequences covering promoter region, all exons and large parts of the introns.

TGFBR1

The TGFBR1 gene encodes for the transforming growth factor-beta (TGF- β) receptor type 1, which binds TGF- β . Mutations in this receptor can cause Loey-Dietz syndrome, with presentation of aortic aneurysm dissection.¹¹ Many patients are characterized by the triad of 1) widely spaced eyes (hypertelorism); 2) a bifid uvula, cleft palate, or both; and 3) generalized arterial tortuosity with widespread vascular aneurysms and dissections.⁸ The TGFBR1 receptor together with TGFBR2 forms a heterodimeric complex, which phosphorylates other proteins that enter the nucleus, thereby regulating transcriptional processes, for instance cell proliferation. The TGFBR1 PCR conditions are listed in supplemental table I. Figure 6 shows the result of amplification of the complete genomic TGFBR1 DNA sequences covering promoter region, all exons and large parts of the introns.

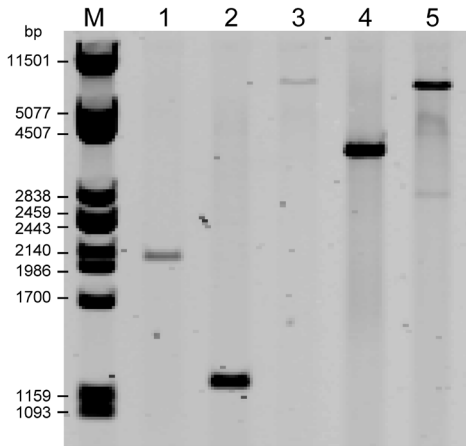


Figure 7

Overview of the TGFB2 genomic PCR products obtained with the primer sets listed in suppl. table I. The lanes corresponds with suppl. table I, marker λ PstI.

TGFB2

The TGFB2 gene encodes for the transforming growth factor-beta (TGF- β) receptor type 2, which binds TGF- β . Likewise, mutations in this receptor can cause Loey-Dietz syndrome, with presentation of aortic aneurysm dissection. As the TGFB2 receptor forms a heterodimeric complex with TGFB1, mutations in this receptor show a similar phenotype as mutations in TGFB1.⁹ PCR conditions for TGFB2 are listed in supplemental table I. Figure 7 shows the result of amplification of the complete genomic TGFB2 DNA sequences covering promoter region, all exons and large parts of the introns.

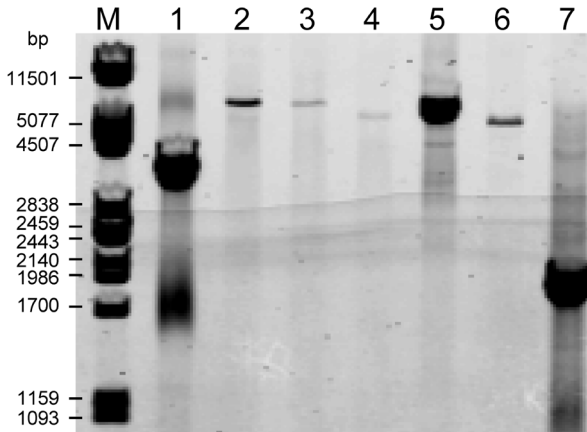


Figure 8

Overview of the COL3A1 genomic PCR products obtained with the primer sets listed in suppl. table I. The lanes corresponds with suppl. table I, marker λ PstI.

COL3A1

The COL3A1 gene encodes for type III collagen, and is found in extensible connective tissues such as skin, lung and the vascular system.¹⁶ Haploinsufficiency for the COL3A1 allele of type III procollagen results in a phenotype similar to the vascular form of Ehlers-Danlos Syndrome; type IV. COL3A1 PCR conditions are listed in supplemental table I. Figure 8 shows the results of amplification of the complete genomic COL3A1 DNA sequences covering promoter region, all exons and large parts of the introns.

COL4A1

The COL4A1 gene encodes for the type IV alpha collagen chain of basement membranes.¹⁷ COL4A1 is a candidate gene for unexplained familial syndromes with autosomal dominant hematuria, cystic kidney disease, muscle cramps, and mutations can result in intracranial aneurysms.¹⁷ This aneurysm-related gene could be involved in aortic aneurysm formation, however a direct link is not yet been described.²⁷ The PCR conditions for COL4A1 are listed in supplemental table I. Figure 9 shows the result of amplification of the complete genomic COL4A1 DNA sequences covering promoter region, all exons and large parts of the introns.

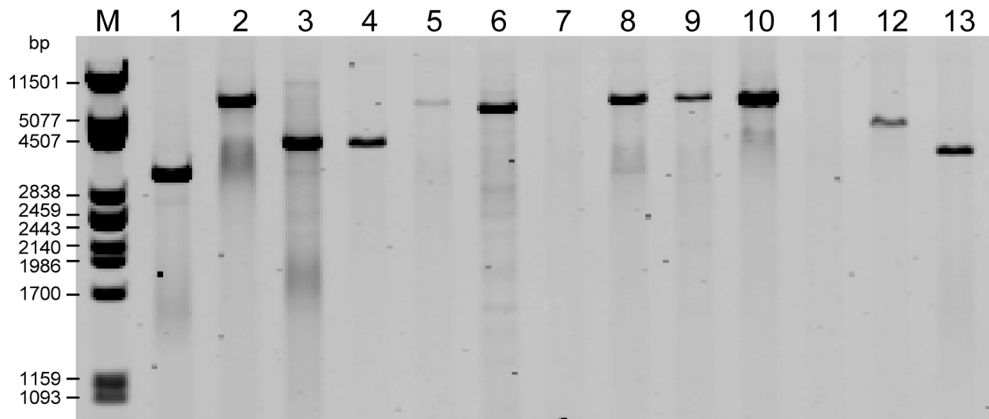


Figure 9

Overview of the COL4A1 genomic PCR products obtained with the primer sets listed in suppl. table I. The lanes corresponds with suppl. table I, marker λ PstI.

EFEMP2

The EFEMP2 gene encodes for the Fibulin-4 protein, which is involved in the formation of elastic fibers and in connective tissue development.^{18,28} Patients are diagnosed with cutis laxa, vascular tortuosity, ascending aortic aneurysm, developmental emphysema, inguinal and diaphragmatic hernia, joint laxity, and pectus excavatum. The EFEMP2 PCR conditions are listed in supplemental table I. Figure 10 shows the result of amplification of the complete genomic EFEMP2 DNA sequences covering promoter region, all exons and large parts of the introns.

ELN

The ELN gene encodes for a protein that forms the elastin fibers. Heterozygous mutations in the ELN gene have been shown to cause autosomal dominant cutis laxa, and mutations can cause severe aortic disease in patients.¹⁹ ELN PCR conditions are listed in supplemental table I. Figure 11 shows the result of amplification of the complete genomic ELN DNA sequences covering promoter region, all exons and large parts of the introns.

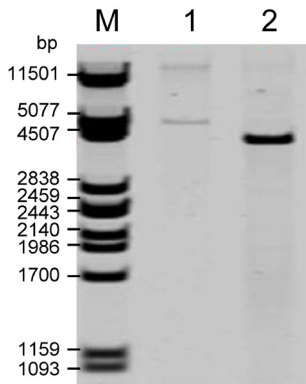


Figure 10
Overview of the EFEMP2 genomic PCR products obtained with the primer sets listed in suppl. table I. The lanes corresponds with suppl. table I, marker λ PstI.

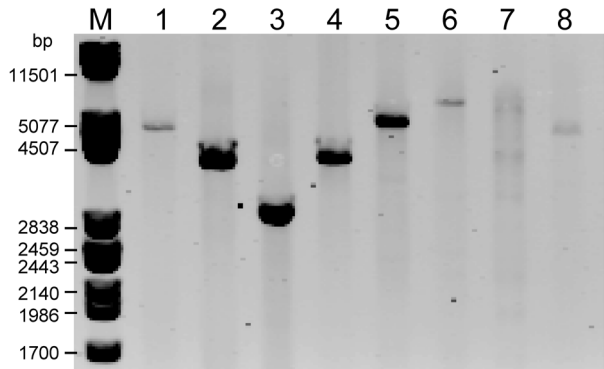


Figure 11
Overview of the ELN genomic PCR products obtained with the primer sets listed in suppl. table I. The lanes corresponds with suppl. table I, marker λ PstI.

FBLN1

The FBLN1 gene encodes for the fibrillin-1 protein, which provides force bearing structures to the extracellular matrix. Mutations in this gene are associated with Marfan syndrome,¹⁰ which is an inherited disorder of connective tissue with an incidence of 1 in 5000 patients. Marfan syndrome manifests in the ocular, skeletal and cardiovascular systems, and is mainly characterized by mitral valve prolapse and medial degeneration of the aorta resulting in aneurysm formation. The FBLN1 PCR conditions are listed in supplemental table I. Figure 12 shows the results of amplification of the complete genomic FBLN1 DNA sequences covering promotor region, all exons and large parts of the introns.

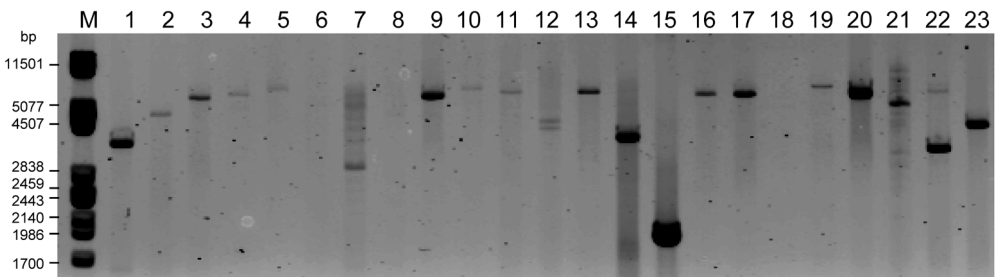


Figure 12
Overview of the FBLN1 genomic PCR products obtained with the primer sets listed in suppl. table I. The lanes corresponds with suppl. table I, marker λ PstI.

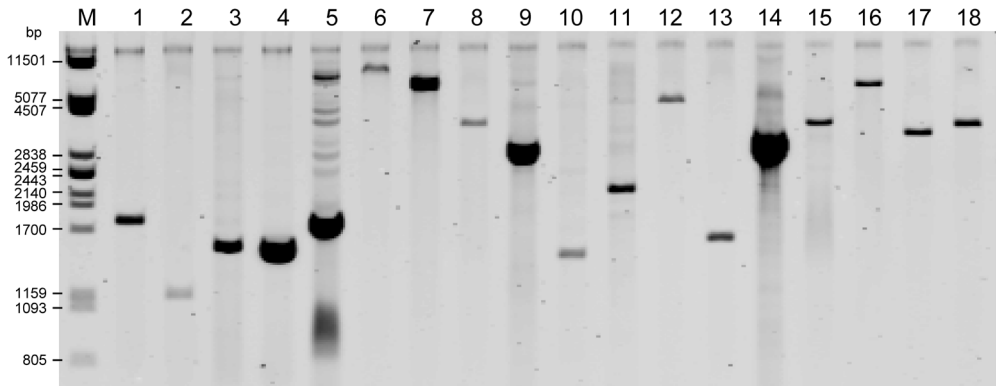
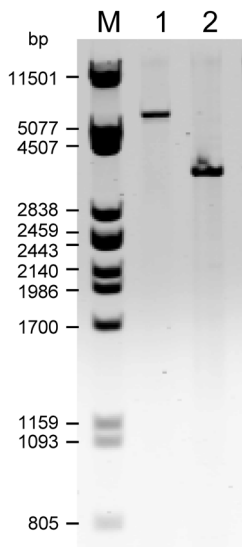


Figure 13

Overview of the FBLN1 genomic MYLK products obtained with the primer sets listed in suppl. table I. The lanes corresponds with suppl. table I, marker λ PstI.

MYLK

The MYLK gene encodes for myosin light chain kinase, and this enzyme phosphorylates myosin light chains with actin filaments to produce contractile activity.²¹ Genetic and functional studies showed that heterozygous loss-of-function mutations in MYLK are associated with aortic dissections. The MYLK PCR conditions are listed in supplemental table I. Figure 13 shows the result of amplification of the complete genomic MYLK DNA sequences covering promoter region, all exons and large parts of the introns.



MYL9

The MYL9 gene encodes for a myosin light chain protein, that is activated by myosin light chain kinase and binds calcium to regulate muscle contraction.²² The exact connection of MYL9 to aneurysmal disease is not yet determined. MYL9 PCR conditions are listed in supplemental table I. Figure 14 shows the result of amplification of the complete genomic MYL9 DNA sequences covering promoter region, all exons and large parts of the introns.

Figure 14

Overview of the MYL9 genomic MYLK products obtained with the primer sets listed in suppl. table I. The lanes corresponds with suppl. table I, marker λ PstI.

DISCUSSION

In this study we show LR-PCR optimization of 14 TAA linked genes, which allows massive parallel sequencing for these aneurysm genes, including promotor regions, exons and a large part of the introns. Genomic DNA enrichment of aneurysm-associated genes by LR-PCR amplification is an important step in massive parallel sequencing, since it improves sensitivity, specificity, uniformity and reproducibility.²⁹ After complete genomic TAA gene enrichment these PCR products can subsequently be used in massive parallel sequencing. For this purpose, products are sonicated into small fragments, and these genomic DNA fragments are ligated to adapters to both ends of the fragments. With a range of unique adapters for each PCR product it is then possible to sequence multiple different PCR products of TAA associated genes from different patients pooled into one sample run with next generation sequencing. With this new phase of pooling and next generation sequencing it is possible to screen patients or complete families for mutations on a very large scale. Moreover, it is less time consuming and can be performed at lower costs than the conventional methods.

The first target of this study was to design primers to amplify complete genes including exons and the surrounding intron sequences for at least 500 bp. Average product sizes were up to 8000 bp, covering exons and most introns completely. Furthermore, at least 1000 bp of the promotor region upstream of exon 1 was amplified, in order to screen mutations in the promotor-sequence and in the adjacent responsive elements. By amplification of all exons, a large part of the intron sequences, the promotor-sequence and the 3'-untranslated region (UTR)-sequence, it becomes possible to screen for mutations outside the exome, as these sequences contain binding sites for gene regulation, thus mutations in these regions could influence protein expression levels.³⁰ Accordingly, transcriptional regulatory DNA sequences recruit transcription factors (TFs) in a DNA sequence-specific manner, allowing cells to precisely control the rates of chromatin decompaction, transcription initiation, and the release of RNA polymerase II (RNAPII) into productive elongation.^{31, 32} Though, the TAA linked gene mutations that were selected for this study are thus far reported in the coding region or intron-exon splice junctions, which results in a dysfunctional protein causing aneurysm disease (table 1). However, since 15% of aneurysm patients show a positive family history with late onset of the disease,^{2, 5} the direct causative genes have not been identified. In these cases, gene expression dysregulation of known aneurysm-linked genes could potentially be causative.

Important regulatory sequences are promoters and enhancers. A promoter is a regulatory region located upstream of a gene that binds transcription factor II D (TFIID) and allows the subsequent coordination of components of the transcription (pre-)initiation complex (PIC), facilitating recruitment of RNA polymerase II and initiation of transcription.^{33, 34} The core promoter generally spans approximately 80 bp around the transcription start site (TSS), and can be separated into two distinct classes: conserved TATA-box enriched promoters that initiate at a single TSS, and variable CpG-rich promoters containing multiple TSS.³⁵ Multiple TSS promoter elements are involved in regulation of transcription initiation. Both upstream and downstream promoter elements (UPE and DPE) contain transcription factor binding sites (TFBS), and may act independently or synergistically with the core promoter that facilitates transcription initiation.^{33, 34} Other enhancer elements within the promoter region are the insulators, activators and repressors. All these factors selectively contribute to transcription initiation activity. It is therefore of importance to screen this promoter region for mutations or presence of sequences binding these core elements, especially within the promoter region spanning approximately 80 bp. Deletion analyses implicated sequences lying -300 to -50 bp upstream of the TSS generally having a positive effect on promoter activity, while elements negatively affecting promoter activity were located -1,000 to -500 bp upstream of the TSS for 55 % of the genes examined.^{30, 36} Hence, also wider screening for mutations in the promoter sequence region could give extra insight into aneurysmal disease.

The 5'-UTR is a regulatory region in the DNA situated at the 5' end of all protein-coding genes that is transcribed into mRNA but not translated into protein. The 5'-UTRs contain various regulatory elements and plays a role in translation initiation. Besides, 5'-UTRs are highly conserved across species, indicative of functional conservation.³⁷ The 5' cap is a modification added to the 5' end of precursor mRNA³⁸, and this structure is essential

for efficient translation of mRNA, serving as a binding site for the pre-initiation complex (PIC).³⁹ Additionally, upstream open reading frames (uORF) occur in 5'-UTRs when there is an in-frame stop codon following an upstream AUG (uAUG) codon, prior to the main start codon.^{30, 40} uORFs are present in ~50% of human 5'-UTRs, and their presence correlates with reduced protein expression and with mutation studies indicating that uORFs reduce mRNA levels by 30% and reduce protein expression by 30-80% on average.⁴¹ Ribosomes binding to an uAUG codon may translate an uORF, which can impact on downstream expression by altering the efficiency of translation or initiation at the main ORF. Mutations involving uORFs are likely to be detrimental, as they can disrupt the control of gene expression, resulting in aberrant gene expression levels.⁴²

Introns are regions of DNA that are transcribed into pre-messenger RNA but are removed during splicing to generate a mature mRNA. Specific mutations in the introns of TAA associated genes could disrupt the assembly of a spliceosome,³⁰ resulting in disrupted splicing that could lead to problems in normal mRNA maturation. Though intron-exon boundary splice mutations are usually also identified by conventional Sanger Sequencing of amplified exons, as these amplicons usually contain a few base pairs of the intron as well. Furthermore, introns could have deleterious effects on gene expression, such as a delay in mature transcript production due to aberrant splicing or increased pre-mRNA length. Furthermore, introns are sources of non-coding RNAs, carriers of transcriptional regulatory elements (enhancers) and contributors to alternative splicing. However, these kind of mutations have not been found or reported yet in aneurysmal disease.

The 3'-UTR is a regulatory region in the DNA situated downstream of the protein-coding sequence, and is transcribed into a mature mRNA sequence. The 3'-UTR has been found to be involved in numerous regulatory processes including transcript cleavage, stability and polyadenylation, translation and mRNA localization, and is therefore critical in determining the fate of an mRNA. In addition, 3'-UTRs are highly conserved across species, indicating functional conservation.³⁷ Furthermore, the 3'-UTR serves as a binding site for numerous regulatory proteins as well as microRNAs (miRNAs). The binding sites in the 3'-UTR can bind miRNAs, which are single-stranded non-coding RNA molecules of approximately 22 nucleotides in length that interact post-transcriptionally with mRNA targets to regulate expression. Generally miRNAs exert their effect by partial basepairing to a miRNA response element (MRE) on a target mRNA via a seed sequence at the 5' end of the miRNA, which then recruits proteins of the Argonaute family and inhibits translation of the mRNA⁴³⁻⁴⁵. Recently, miRNAs such as miR-24, miR-155, miR-205, miR-712, miR-21, miR-26a, miR-143/145, miR-29, and miR-195, have been demonstrated to be differentially expressed in diseased aortic tissues and were shown to be strongly associated with the development of aortic aneurysms.^{46, 47}

To recapitulate, regulatory sequences such as the promoter sequence, upstream and downstream promoter elements (UPE and DPE) sequences, enhancer element sequences, uORF sequences, recognition sequences in the introns for the spliceosome, and MRE sequences are all of interest as they could contain pathogenic mutations causing aneurysm disease. Pinpointing pathogen mutations in these transcription factor binding sites (TFBS) is quite challenging,⁴⁸ but gradually the ability to read individual genomes is in progress and along with sequencing the introns, promoters, 5'-UTR and 3'-UTR-sequences we will get a better understanding of initiation and progression of aneurysmal disease.

There is great potency to gain extra information by sequencing more than the exome alone, thus the next generation sequencing technique presented in this study could be more beneficial than the conventional methods. The next step is to screen patient cohorts along with their relatives on the short-term, for which 14 TAA genes were completely covered and enriched. The next step of massive parallel sequencing to screen for mutations resulting in damaged or dysregulated proteins can now be performed.

ACKNOWLEDGEMENTS

This work was supported by the 'Lijf en Leven' grant (2011): 'dilating versus stenosing arterial disease (DIVERS)' (JE, IvdP). We thank Tamara Pesic, Randall de Joode, Precious Griffith and Frank Bouwman from the Hogeschool Rotterdam for their assistance with optimization of the LR-PCR. Set-up of the PCR protocol was proposed and initially discussed with Yvete Barrois, Wanwisa Jamnongluk and Arthur van den Wijngaarden of Maastricht University.

REFERENCES

- Isselbacher EM. Thoracic and abdominal aortic aneurysms. *Circulation* 2005;**111**:816-828.
- Svensjo S, Bjorck M, Gurtelschmid M, Gidlund KD, Hellberg A, Wanhainen A. Low Prevalence of Abdominal Aortic Aneurysm Among 65-Year-Old Swedish Men Indicates a Change in the Epidemiology of the Disease. *Circulation* 2011;**124**:1118-1123.
- Saratzis A, Bown MJ. The genetic basis for aortic aneurysmal disease. *Heart* 2014;**100**:916-922.
- Cosford PA, Leng GC. Screening for abdominal aortic aneurysm (Review). *Cochrane Db Syst Rev* 2007.
- Albornoz G, Coady MA, Roberts M, Davies RR, Tranquilli M, Rizzo JA, Elefteriades JA. Familial thoracic aortic aneurysms and dissections - Incidence, modes of inheritance, and phenotypic patterns. *Ann Thorac Surg* 2006;**82**:1400-1406.
- Clouse WD, Hallett JW, Schaff HV. Improved prognosis of thoracic aortic aneurysms - A population-based study. *Jama-J Am Med Assoc* 1998;**280**:1926-1929.
- Webb TH, Williams GM. Thoracoabdominal aneurysm repair. *Cardiovasc Surg* 1999;**7**:573-585.
- Loeys BL, Schwarze U, Holm T, Callewaert BL, Thomas GH, Pannu H, De Backer JF, Oswald GL, Symoens S, Manouvrier S, Roberts AE, Faravelli F, Greco MA, Pyeritz RE, Milewicz DM, Coucke PJ, Cameron DE, Braverman AC, Byers PH, De Paepe AM, Dietz HC. Aneurysm syndromes caused by mutations in the TGF-beta receptor. *New Engl J Med* 2006;**355**:788-798.
- Mizuguchi T, Collod-Beroud G, Akiyama T, Abifadel M, Harada N, Morisaki T, Allard D, Varret M, Claustres M, Morisaki H, Ihara M, Kinoshita A, Yoshiura K, Junien C, Kajii T, Jondeau G, Ohta T, Kishino T, Furukawa Y, Nakamura Y, Niikawa N, Boileau C, Matsumoto N. Heterozygous TGFBR2 mutations in Marfan syndrome. *Nat Genet* 2004;**36**:855-860.
- Dietz HC, Cutting GR, Pyeritz RE, Maslen CL, Sakai LY, Corson GM, Puffenberger EG, Hamosh A, Nanthakumar EJ, Curristin SM, Stetten G, Meyers DA, Francomano CA. Marfan-Syndrome Caused by a Recurrent Denovo Missense Mutation in the Fibrillin Gene. *Nature* 1991;**352**:337-339.
- Loeys BL, Chen J, Neptune ER, Judge DP, Podowski M, Holm T, Meyers J, Leitch CC, Katsanis N, Sharifi N, Xu FL, Myers LA, Spevak PJ, Cameron DE, De Backer J, Hellemsans J, Chen Y, Davis EC, Webb CL, Kress W, Coucke P, Rifkin DB, De Paepe AM, Dietz HC. A syndrome of altered cardiovascular, craniofacial, neurocognitive and skeletal development caused by mutations in TGFBR1 or TGFBR2. *Nat Genet* 2005;**37**:275-281.
- van der Linde D, van de Laar I, Wessels MW, Oldenburg RA, Bekkers JA, Mattace-Raso FU, van den Meiracker AH, Moelker A, Tanghe HL, van Kooten F, Bertoli-Avella AM, Roos-Hesselink JW. Cardiovascular Phenotype of the Recently Discovered Aggressive Aneurysms-Osteoarthritis Syndrome (aos) Caused by Smad(3) Mutations. *Circulation* 2011;**124**.
- Guo DC, Pannu H, Tran-Fadulu V, Papke CL, Yu RK, Avidan N, Bourgeois S, Estrera AL, Safi HJ, Sparks E, Amor D, Ades L, McConnell V, Willoughby CE, Abuelo D, Willing M, Lewis RA, Kim DH, Scherer S, Tung PP, Ahn C, Buja LM, Raman CS, Shete SS, Milewicz DM. Mutations in smooth muscle alpha-actin (ACTA2) lead to thoracic aortic aneurysms and dissections. *Nat Genet* 2007;**39**:1488-1493.
- Zhu LM, Vranckx R, Van Kien PK, Lalande A, Boisset N, Mathieu F, Wegman M, Glancy L, Gasc JM, Brunotte FO, Bruneval P, Wolf JE, Michel JB, Jeunemaitre X. Mutations in myosin heavy chain 11 cause a syndrome associating thoracic aortic aneurysm/aortic dissection and patent ductus arteriosus. *Nat Genet* 2006;**38**:343-349.
- Gadowski GR, Pilcher DB, Ricci MA. Abdominal aortic aneurysm expansion rate: effect of size and beta-adrenergic blockade. *J Vasc Surg* 1994;**19**:727-731.
- Schwarze U, Schievink WI, Petty E, Jaff MR, Babovic-Vuksanovic D, Cherry KJ, Pepin M, Byers PH. Haploinsufficiency for one COL3A1 allele of type III procollagen results in a phenotype similar to the vascular form of Ehlers-Danlos syndrome, Ehlers-Danlos syndrome type IV. *American Journal of Human Genetics* 2001;**69**:989-1001.
- Plaisier E, Gribouval O, Alamowitch S, Mougnot B, Prost C, Verpont MC, Marro B, Desmettre T, Cohen SY, Rouillet E, Dracon M, Fardeau M, Van Agtmael T, Kerjaschki D, Antignac C, Ronco P. COL4A1 mutations and hereditary angiopathy, nephropathy, aneurysms, and muscle cramps. *New Engl J Med* 2007;**357**:2687-2695.
- Huchtagowder V, Sausgruber N, Kim KH, Angle B, Marmorstein LY, Urban Z. Fibulin-4: a novel gene for an autosomal recessive cutis laxa syndrome. *Am J Hum Genet* 2006;**78**:1075-1080.
- Szabo Z, Crepeau MW, Mitchell AL, Stephan MJ, Puntel RA, Yin Loke K, Kirk RC, Urban Z. Aortic aneurysmal disease and cutis laxa caused by defects in the elastin

- gene. *J Med Genet* 2006;**43**:255-258.
20. Pannu H, Tran-Fadulu V, Papke CL, Scherer S, Liu Y, Presley C, Guo D, Estrera AL, Safi HJ, Brasier AR, Vick GW, Marian AJ, Raman CS, Buja LM, Milewicz DM. MYH11 mutations result in a distinct vascular pathology driven by insulin-like growth factor 1 and angiotensin II. *Hum Mol Genet* 2007;**16**:2453-2462.
 21. Wang L, Guo DC, Cao JM, Gong LM, Kamm KE, Regalado E, Li L, Shete S, He WQ, Zhu MS, Offermanns S, Gilchrist D, Eleftheriades J, Stull JT, Milewicz DM. Mutations in Myosin Light Chain Kinase Cause Familial Aortic Dissections. *American Journal of Human Genetics* 2010;**87**:701-707.
 22. Chen L, Fan Y, Wan J. Screening of key genes of unruptured intracranial aneurysms by using DNA microarray data analysis techniques. *Genet Mol Res* 2014;**13**:758-767.
 23. van de Laar IM, Oldenburg RA, Pals G, Roos-Hesselink JW, de Graaf BM, Verhagen JM, Hoedemaekers YM, Willemsen R, Severijnen LA, Venselaar H, Vriend G, Pattynama PM, Collee M, Majoor-Krakauer D, Poldermans D, Frohn-Mulder IM, Micha D, Timmermans J, Hilhorst-Hofstee Y, Bierma-Zeinstra SM, Willems PJ, Kros JM, Oei EH, Oostra BA, Wessels MW, Bertoli-Avella AM. Mutations in SMAD3 cause a syndromic form of aortic aneurysms and dissections with early-onset osteoarthritis. *Nat Genet* 2011;**43**:121-126.
 24. McKellar SH, Tester DJ, Yagubyan M, Majumdar R, Ackerman MJ, Sundt TM, 3rd. Novel NOTCH1 mutations in patients with bicuspid aortic valve disease and thoracic aortic aneurysms. *J Thorac Cardiovasc Surg* 2007;**134**:290-296.
 25. Coucke PJ, Willaert A, Wessels MW, Callewaert B, Zoppi N, De Backer J, Fox JE, Mancini GM, Kambouris M, Gardella R, Facchetti F, Willems PJ, Forsyth R, Dietz HC, Barlati S, Colombi M, Loeys B, De Paep A. Mutations in the facilitative glucose transporter GLUT10 alter angiogenesis and cause arterial tortuosity syndrome. *Nat Genet* 2006;**38**:452-457.
 26. Hawkins JR, Hawkins M, Boyle J, Gray E, Matejtschuk P, Metcalfe P. Genetic reference materials and their application to haematology. *Biologicals* 2010;**38**:467-473.
 27. Jones JA, Zavadzkas JA, Chang EI, Sheats N, Koval C, Stroud RE, Spinale FG, Ikonomidis JS. Cellular phenotype transformation occurs during thoracic aortic aneurysm development. *J Thorac Cardiovasc Surg* 2010;**140**:653-659.
 28. Moltzer E, te Riet L, Swagemakers SMA, van Heijningen PM, Vermeij M, van Veghel R, Bouhuizen AM, van Esch JHM, Lankhorst S, Ramnath NWM, de Waard MC, Duncker DJ, van der Spek PJ, Rouwet EV, Danser AHJ, Essers J. Impaired Vascular Contractility and Aortic Wall Degeneration in Fibulin-4 Deficient Mice: Effect of Angiotensin II Type 1 (AT(1)) Receptor Blockade. *Plos One* 2011;**6**:e23411.
 29. Mamanova L, Coffey AJ, Scott CE, Kozarewa I, Turner EH, Kumar A, Howard E, Shendure J, Turner DJ. Target-enrichment strategies for next-generation sequencing. *Nat Methods* 2010;**7**:111-118.
 30. Barrett LW, Fletcher S, Wilton SD. Regulation of eukaryotic gene expression by the untranslated gene regions and other non-coding elements. *Cell Mol Life Sci* 2012;**69**:3613-3634.
 31. Fuda NJ, Ardehali MB, Lis JT. Defining mechanisms that regulate RNA polymerase II transcription in vivo. *Nature* 2009;**461**:186-192.
 32. Plank JL, Dean A. Enhancer function: mechanistic and genome-wide insights come together. *Mol Cell* 2014;**55**:5-14.
 33. Juven-Gershon T, Hsu JY, Theisen JW, Kadonaga JT. The RNA polymerase II core promoter - the gateway to transcription. *Curr Opin Cell Biol* 2008;**20**:253-259.
 34. Smale ST, Kadonaga JT. The RNA polymerase II core promoter. *Annu Rev Biochem* 2003;**72**:449-479.
 35. Carninci P, Sandelin A, Lenhard B, Katayama S, Shimokawa K, Ponjavic J, Semple CA, Taylor MS, Engstrom PG, Frith MC, Forrest AR, Alkema WB, Tan SL, Plessy C, Kodzius R, Ravasi T, Kasukawa T, Fukuda S, Kanamori-Katayama M, Kitazume Y, Kawaji H, Kai C, Nakamura M, Konno H, Nakano K, Mottagui-Tabar S, Arner P, Chesi A, Gustincich S, Persichetti F, Suzuki H, Grimmond SM, Wells CA, Orlando V, Wahlestedt C, Liu ET, Harbers M, Kawai J, Bajic VB, Hume DA, Hayashizaki Y. Genome-wide analysis of mammalian promoter architecture and evolution. *Nat Genet* 2006;**38**:626-635.
 36. Cooper SJ, Trinklein ND, Anton ED, Nguyen L, Myers RM. Comprehensive analysis of transcriptional promoter structure and function in 1% of the human genome. *Genome Res* 2006;**16**:1-10.
 37. Siepel A, Bejerano G, Pedersen JS, Hinrichs AS, Hou M, Rosenbloom K, Clawson H, Spieth J, Hillier LW, Richards S, Weinstock GM, Wilson RK, Gibbs RA, Kent WJ, Miller W, Haussler D. Evolutionarily conserved elements in

- vertebrate, insect, worm, and yeast genomes. *Genome Res* 2005;**15**:1034-1050.
38. Banerjee AK. 5'-terminal cap structure in eucaryotic messenger ribonucleic acids. *Microbiol Rev* 1980;**44**:175-205.
 39. Jackson RJ, Hellen CU, Pestova TV. The mechanism of eukaryotic translation initiation and principles of its regulation. *Nat Rev Mol Cell Biol* 2010;**11**:113-127.
 40. Morris DR, Geballe AP. Upstream open reading frames as regulators of mRNA translation. *Mol Cell Biol* 2000;**20**:8635-8642.
 41. Calvo SE, Pagliarini DJ, Mootha VK. Upstream open reading frames cause widespread reduction of protein expression and are polymorphic among humans. *Proc Natl Acad Sci U S A* 2009;**106**:7507-7512.
 42. Chatterjee S, Pal JK. Role of 5'- and 3'-untranslated regions of mRNAs in human diseases. *Biol Cell* 2009;**101**:251-262.
 43. Gerin I, Clerbaux LA, Haumont O, Lanthier N, Das AK, Burant CF, Leclercq IA, MacDougald OA, Bommer GT. Expression of miR-33 from an SREBP2 intron inhibits cholesterol export and fatty acid oxidation. *J Biol Chem* 2010;**285**:33652-33661.
 44. Paik JH, Jang JY, Jeon YK, Kim WY, Kim TM, Heo DS, Kim CW. MicroRNA-146a downregulates NFkappaB activity via targeting TRAF6 and functions as a tumor suppressor having strong prognostic implications in NK/T cell lymphoma. *Clin Cancer Res* 2011;**17**:4761-4771.
 45. Song B, Wang Y, Kudo K, Gavin EJ, Xi Y, Ju J. miR-192 Regulates dihydrofolate reductase and cellular proliferation through the p53-microRNA circuit. *Clin Cancer Res* 2008;**14**:8080-8086.
 46. Fu XM, Zhou YZ, Cheng Z, Liao XB, Zhou XM. MicroRNAs: Novel Players in Aortic Aneurysm. *Biomed Res Int* 2015;**2015**:831641.
 47. Boon RA, Seeger T, Heydt S, Fischer A, Hergenreider E, Horrevoets AJ, Vinciguerra M, Rosenthal N, Sciacca S, Pilato M, van Heijningen P, Essers J, Brandes RP, Zeiher AM, Dimmeler S. MicroRNA-29 in aortic dilation: implications for aneurysm formation. *Circ Res* 2011;**109**:1115-1119.
 48. Levo M, Segal E. In pursuit of design principles of regulatory sequences. *Nat Rev Genet* 2014;**15**:453-468.

Supplemental data table 1

Set	Primer Name:	Sequence	T (°C)	Size (bp)	Extension Time (min)	Restriction enzyme	Cutsite	Formed Fragments (bp)	Cycli	Primers (µl/well)	gDNA (ng)
1	ACTA2ex1LRF New	tatgctgatcttggtaattttgactctctg	60	2338	1,5	EcoRI	G/AATTC	1096/1242	35	0,75	10
	ACTA2ex1LRR	agggtgaactcaagcagaagcctttag	60		1,5	BamHI	G/GATCC	835/1503			
2	ACTA2ex2LRF	gtaaagaaaagtcctcatgattcaaaaag	59	2952	1,5	EccorI	G/AAATTC	1390/1562	35	0,75	10
	ACTA2ex3LRR	ttgagagcaggattctactatgtacc	59		1,5	NcoI	C/CATGG	1456/1496			
3	ACTA2ex4LRF	atagagtttcaagaagcgctattatc	60	5528	3	NdeI	C/ATATG	3846/1682	35	0,75	10
	ACTA2ex7LRR	tgctcttatctctcctgtaattctcac	60		3	MfeI	C/AAATG	3112/2416			
4	ACTA2ex8LRF New	ttacagagatagataaagagcacttagcc	63	4698	2,5	ApaI	GGGCC/C	2041/2657	35	0,75	10
	ACTA2ex8LRR New	caaaaagt-cagaccacctgtttctatag	63		2,5	NdeI	CA/TATG	1935/2763			
Set	Primer Name:	Sequence	T (°C)	Size (bp)	Extension Time (min)	Restriction enzyme	Cutsite	Formed Fragments (bp)	Cycli	Primers (µl/well)	gDNA (ng)
1	FBLN4ex1LRF	cccttaagagcgtattattaacctctctg	58	4691	2,5	EagI	C/GGCCG	1705/3358	35	0,75	10
	FBLN4ex7LRR	gattattttatgaatcctcccaacaac	58		2,5	MluI	A/CGCGT	3211/1480			
2	FBLNex8LRF	ctaggaagtagattttctctctctac	58,6	3995	2	ApaI	G/GGCC	1366/2629	35	0,75	10
	FBLNex11LRR	atggaatcacccttaaccatgcttc	58,6		2	AvrII	C/CTAGG	3418/577			
Set	Primer Name:	Sequence	T (°C)	Size (bp)	Extension Time (min)	Restriction enzyme	Cutsite	Formed Fragments (bp)	Cycli	Primers (µl/well)	gDNA (ng)
1	SLC2A10ex1LRF	atataatgatgctctctcttctccaac	57	1852	1	-	-	-	35	0,75	10
	SLC2A10ex1LRR	gtttatgctattttgtcattgctgaag	57		1	-	-	-			
2	SLC2A10ex2LRF	gaataaaggtatagataaattggacatgag	59-	5640	3	-	-	-	35	0,75	10
	SLC2A10ex4LRR	gttttaagattactctctagcctctctg	61		3	-	-	-			
3	SLC2A10ex5LRF	cattctcacatgctatgaagaataactg	59	3807	2	SpeI	A/CTAGT	2834/973	35	0,75	10
	SLC2A10ex5LRR	caagctattttaagttggaatcaactg	59		2	HindIII	A/AGCTT	2258/1549			

Set	Primer Name:	Sequence	T (°C)	Size (bp)	Extension Time (min)	Restriction enzyme	Cutsite	Formed Fragments (bp)	Cycli	Primers (µl/well)	gDNA (ng)
1	TGFBR1ex1LRF New	agaaagactgactgctgacaggagaataac	60.4	2113	1.5	PvuI	CGATCG	840/1273	35	0.75	10
	TGFBR1ex1LRR New	aggaaataaaaagcgttaatacactaac	60.4		1.5	MscI	TGGCCA	893/1220			
2	TGFBR1ex2LRF	gtagtattgttacagggtgtagctctgtg	58	5136	3	EcoRI	G/AATTC	2837/2309	35	0.75	10
	TGFBR1ex3LRR	atagactgagaaagaacacgcatatagg	58		3	XmaI	C/CCGGG	3668/1468			
3	TGFBR1ex4LRF	gaaaatgctctggtgattttactgac	60	6137	3.5	PvuII	CAG/CTG	5826/311	35	0.75	10
	TGFBR1ex5LRR	agcacttcacattcatttggactactac	60		3.5	BamHI	G/GATCC	5383/754			
4	TGFBR1ex6LRF	gaagaactgcatactatcttctaagatg	61	4262	2.5	Asel	A/ITTAAT	2116/2146	35	0.75	10
	TGFBR1ex8LRR	gctctgctcccaalattgtaabtagaac	61		2.5	MscI	TGG/CCA	1473/2789			
5	TGFBR1ex9LRF	gctataaaaagctgttcagttcagatgtg	60	6367	3.5	BamHI	G/GATCC	2068/4299	35	0.75	10
	TGFBR1ex9LRR	tfgcaggtaaacgtagggtactaaaatagg	60		3.5	PvuII	CAG/CTG	3552/2815			
Set	Primer Name:	Sequence	T (°C)	Size (bp)	Extension Time (min)	Restriction enzyme	Cutsite	Formed Fragments (bp)	Cycli	Primers (µl/well)	gDNA (ng)
1	SMAD3ex1LRF	aacaacaccctgtatgtaaatttttc	60	2164	1.5	SapI	GCTCTCN/NNIN	1203/1021	35	0.75	10
	SMAD3ex1LRR	tctaaaaataactcgataaaaaagctaatcc	60		1.5	SacI	GAGCT/C	1348/876			
2	SMAD3ex2.1LRF	aagcagttgttgaaaggctacag	59	1500	1	SacII	CCGC/GG	477/756	35	0.75	10
	SMAD3ex2.1LRR	cagaatagaaatcaaacaccctcagtg	59		1	ApaLI	G/TGCAC	1050/450			
3	SMAD3ex2.2LRF	aaataitttcatgagatcactacttcc	59	1325	1	HindIII	A/AGCTT	481/844	35	0.75	10
	SMAD3ex2.2LRR	atatacaatagccatggaaacagctcac	59		1	AvrII	C/CTAGG	673/652			
4	SMAD3ex2.3LRF new	aaatcaccaagaagacatggttcc	57/58	7497	4	SphI	G/CATGC	4140/3339	35	0.75	10
	SMAD3ex5LRR new	cggtttacaataatacaagaagaaag	57/58		4	XbaI	T/CTAGA	5479/2000			
5	SMAD3ex6LRF	ataagtggaatatgttctgtgatagg	61.36	7551	4		-	-	35	0.75	10
	SMAD3ex8LRR	agcgagaaaatttttcccttaactac	61.71		4		-	-			
5	SMAD3ex6LRF New	agactgacagacactgggacaataac	62.11	7587	4		-	-	35	0.75	10
	SMAD3ex8LRR New	cttccggactctcagtttaataatcc	64.31		4		-	-			
5	SMAD3ex6LRF	ataagtggaatatgttctgtgatagg	61.4	7505	4		-	-	35	0.75	10
	SMAD3ex8LRR New	cttcccaactctcaatttaataatcc	64.3		4		-	-			

Set	Primer Name:	Sequence	T (°C)	Size (bp)	Extension Time (min)	Restriction enzyme	Cutsite	Formed Fragments (bp)	Cycli	Primers (µl/well)	gDNA (ng)
5	SMAD3ex6LRF_ZC	gagaagctgcatttactcttcttgag	59-	8164	4.5				35	0.75	10
	SMAD3ex8LRR_ZC	gaaagaaggagctggattctctaacc	64		4.5				35	0.75	10
	SMAD3ex6LRF New	agactgtacagacaatcgagacaatac	62,1	7633	4	-	-	-			
	SMAD3ex8LRR	agcagaaaattttgtctcttaactac	61,7		4	-	-				
6	SMAD3ex9LRF	aaataagcgcgtagatgagaataatacag	59	6011	3.5	BamHI	G/GATCC	4479/1532	35	0.75	10
	SMAD3ex9LRR	tttacatttaactcagcgtttctttatc	59		3.5	XbaI	T/CTAGA	3357/2654			
1	MYLkex1LRF	tgactacatgaaagctcaggttagtggttac		1817	1				35	0.75	10
2	MYLkex1LRR	gagaagtttaccaaaacttccaactg	56 - 61,6		1				35	0.75	10
	MYLkex2LRF	aattgatacttctgtctctgactg		1210	1						
3	MYLkex2LRR	caaaatttactaaagaatacactagacaacc	56 - 62,8		1						
	MYLkex3LRFPG	ataagttattgtccctcctgggaaatg		1544	1				35	0.75	10
4	MYLkex3LRRPG	gatcaccacaatttggaaataatttag	56 - 60,4		1				35	0.75	10
	MYLkex4LRFPG	taaggttcttctgcaagtataccat		1532	1						
5	MYLkex4LRRPG	aactattctcagtgttctctctcttg	56 - 62,8		1				35	0.75	10
	MYLkex5LRFPG	agtagcacattaanaagtagaacaactg		1770	1						
6	MYLkex5LRRPG	aagtagtgaatgagataaacaactg	56 - 58		1						
	MYLkex6LRFPG	ctctcttccagcttctgctactg		8196	4.5				35	0.75	10
6	MYLkex6LRRPG	atacacatgagcaaataggatagaagaac	57-64		4.5						
	MYLkex6LRF_ZC	gccttaagtgaagaatggagtggt	59-	7200	4.5				35	0.75	10
7	MYLkex10LRR_ZC	aagcgaaccctctggagagctca	64		4.5						
	MYLkex11LRRPG	gatatacttbaagcacaatacagttc		5785	3				35	0.75	10
8	MYLkex12LRRPG	aaagtcttctcccctttcttc	59,2 - 61,6		3						
	MYLkex13LRRPG	atgtgatcttcttattttagcaatc		3551	2				35	0.75	10
9	MYLkex15LRRPG	gtggtcttaaaagaactgcaagctc	56 - 59,2		2						
	MYLkex16LRRPG2	tgttaacaactactactagtcacctg		2879	1.5				35	0.75	10
10	MYLkex17LRRPG2	tgctacaagctgaagtattgtgacc	56 - 62,8		1.5						

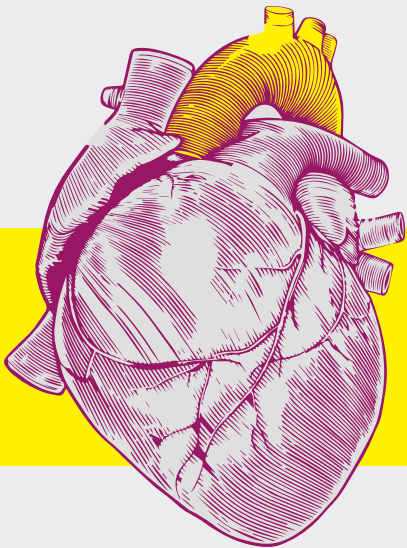
1	MYH11ex1LRF MYH11ex1LRR	gtgggagagaagaagaattgagtg tatgccatggttttaactgattaaatg	57-60,4 57-58	3432 2	2 2	EcoRI	G/AATTC	1364/2068	35 0,75	10
2	MYH11ex2LRF New MYH11ex2LRR	tcttgagcactggtagtattcac atgaaactgtgagaggtatcatcagtc	56-61,6 57-58	1259 1	1 1	MscI MseI	T/GGCCA T/TAA	437/822 462/797	35 0,75	10
3	MYH11ex3LRF New MYH11ex3LRRRC New	atacttaagcaacactgttcaattctgtg ccagaggttgagaccaaccagatag	56-61,6	1659 1	1 1	SphI PvuII	G/CATGC CAG/CTG	763/896 1172/487	35 0,75	10
4	MYH11ex4LRFPG MYH11ex4LRPPG	taatcacatagttcttgatgacctgtg caagtgcttcttgatgattagtgtc	56-59,2	1748 1	1 1	HindIII PvuII	A/AGCTT CAG/CTG	787/861 749/999	35 0,75	10
5	MYH11ex5LRF New MYH11ex7LRR New	agcttctaaactttagctctggtactc caataaaccatgttgctactctatcac	57-61,6	6242 3,5	3,5 3,5	NdeI	CA/TATG	2455/3787	35 0,75	10
6	MYH11ex8LRF New MYH11ex9LRR New	aatatggaaaaaccttcttctgcttag aaaaacttttccctcacacagaggtc	56,3-58	4318 2,5	2,5 2,5	XbaI BamHI	T/CTAGA G/GATCC	1433/2885 1979/2339	35 0,75	10
7	MYH11ex10LRF MYH11ex13LRR	tatggacttagacagatggtctgtttccc taagagatccaataaccagtttctactac	56-59,2	5534 3	3 3	AvrII XmaI	C/CTAGG C/CCGGG	2320/3209 2966/2568	35 0,75	10
8	MYH11ex14LRF New MYH11ex16LRR New	aaaactctggaattaagctcactgactc agacctgacagatagatcttaggtag	58-61,6	6635 3,5	3,5 3,5	EagI AseI	C/GGCCG AT/TAAT	2069/4566 1709/4926	35 0,75	10
9	MYH11ex17LRF New MYH11ex21LRRRCnew2	attccacttaacatctgactctgtc tctctgctatctctgttattgttactcc	56-60,4	7211 4	4 4	BamHI	G/GATCC	2742/4469	35 0,75	10
10	MYH11ex22LRFPG2 MYH11ex26LRFPG2	agaatgctatgaaaggtgaaagaatg gtctgcaaggattgctgaaag	56-59,2	5999 3,5	3,5 3,5	AvrII XmaI	C/CTAGG C/CCGGG	2226/3773 4926/1073	35 0,75	10
11	MYH11ex27LRF MYH11ex28LRR	ataaacacaacaaaaccttaactcac agcctattttatgtttgatbaaggcttc	56-62,8	4498 2,5	2,5 2,5	HindIII PvuII	A/AGCTT C/AGCTG	1627/2871 3401/1097	35 0,75	10
12	MYH11ex29LRF New MYH11ex32LRR New	agaagctgggaatccagattttatg gtactgacatctgtaattgctctgaaatg	56-62,8	4386 2,5	2,5 2,5	XbaI	T/CTAGA	1750/2636	35 0,75	10
13	MYH11ex33LRFPG MYH11ex41LRR	agctcatctcaatgctctgttacc aacatctagacatcttttgggtcac	56,3-59,2	8283 4,5	4,5 4,5	BspHI EcoRI	T/CATGA G/AATTC	1509/6774 1154/7129	35 0,75	10
14	MYH11ex42LRF New MYH11ex43LRR new	SGttcttaaaagtagctctaaaggacagac gtttatcttttaagtgtttcccacagagtg	56,3-60,4	7715 4	4 4	BglII	A/GATCT	3508/4207	35 0,75	10

Set	Primer Name:	Sequence	T (°C)	Size (bp)	Extension Time (min)	Restriction enzyme	Cutsite	Formed Fragments (bp)	Cycli	Primers (µl/well)	gDNA (ng)
1	FBN1ex1LRF FBN1ex2LRR	catacttaaggagctatgctttagatcag aaactggtctgtagtactcttttc	59.2 59.2	3635 2	2 2	XbaI SacI	T/CTAGA GAGCT/C	807/2828 1774/1861	35	0.75	10
2	FBN1ex3LRF FBN1ex4LRR	acagtggttttaagggtttatgcttttg gagacaanaagagagagactaataaag	61.8 61.8	4877 2.5	2.5 2.5	Asel ApaLI	A/TTAAT G/TGCAC	1427/3450 1312/3565	35	0.75	10
3	FBN1ex5LRF FBN1ex6LRR	cattctaaatfactgaacagagatagcc acactctctgctctttgttttccctattac	61.6 61.6	6075 3.5	3.5 3.5	BamHI AvrII	G/GATCC C/CTAGG	2772/3303 905/5170	35	0.75	10
4	FBN1ex7LRF FBN1ex8LRR	atgaaagcaccacagtagttctattag cctatacagagtcacatttatgtcttttg	59.2 59.2	6153 3.5	3.5 3.5	SacI	GAGCT/C	2248/3887	35	0.75	10
5	FBN1ex9LRF FBN1ex10LRR	ccatattgtcttaagggaattttactg tttggctaaatactatgaaagtaaaaaagc	62.24 62.3	7906 4	4 4	-	-	-	35	0.75	10
5	FBN1ex9LRF_ZC FBN1ex10LRR_ZC	agttcattcaaccaaccagaagac acttagcaggaagaaagagctccaa	3.5 3.5	6552 3.5	3.5 3.5				35	0.75	10
6	FBN1ex11LRF FBN1ex13LRR	aaataaaataaatacatcttggaaaactg ctttgtcaaaagagagcaaaataagattaac	58 58	5419 3	3 3	AvrII MscI	C/CTAGG TGG/CCA	2285/3134 2669/2750	35	0.75	10
7	FBN1ex14LRF_ZC2 FBN1ex15LRR_ZC2	ccctcagaatcaatatttttggttg ctagagaaataatgaggaagagatcatg	57- 61	2629 1.5	1.5 1.5				35	0.75	10
8	FBN1ex16LRF_ZC2 FBN1ex16LRR_ZC2	tatacattccaaaaacccttctctttt tctataaatgttcatcatgagataagca	59- 64	798 1	1 1				35	0.75	10
9	FBN1ex17LRF FBN1ex18LRR	tctttttggaaagatacctaattcagac tccaagtcctcaacaacttactatc	58 58	6211 3.5	3.5 3.5	HindIII BamHI	A/AGCTT G/GATCC	2947/3264 2482/3729	35	0.75	10
10	FBN1ex19LRF FBN1ex24LRR	tatatgtcatagaagagtggaagctgg actaagactcaagaatgcatcaactgacatc	59.2 59.2	6771 3.5	3.5 3.5	AgeI ApaI	A/CCGGT GGGCC/C	3147/3624 1678/5104	35	0.75	10
11	FBN1ex25LRF FBN1ex30LRR	tgatcactcagaatttagaataaacaacc ctatgtattaccactttgttctcacc	58 58	6516 3.5	3.5 3.5	XbaI PstI	T/CTAGA CTGCAG	3001/3515 2797/3719	35	0.75	10
12	FBN1ex31LRF FBN1ex32LRR	aagaagagaatttggatttaggaacc gaagctaaaaataaagctgaaccatagac	58 58	4417 2.5	2.5 2.5	ApaLI SacI	G/TGCAC GAGCT/C	879/3538 1688/2729	35	0.75	10
13	FBN1ex33LRF	aaatcatttaattggcttccataaagtaac	62.01	6476	3.5	-	-	-	35	0.75	10

4	COL3a1ex22RF COL3a1ex32RR	aaaattcctaataatgcatcc agaaactcaaatgcaaacacc	53.6 58.1	528 3	3	Apal	G/TGCAC	3477/1851	35	0,75	10
5	COL3a1ex33RF COL3a1ex43RR	gtaatactcttgacagactctatgaac ctgttaacttgctctgtcattacc	64.1 64	5968 3.5	3.5	-	-	-	35	0,75	10
5	COL3A1ex33LRF_ZC2 COL3A1ex43LRR_ZC2	gcttcgctttgacagactagatagaag tttccatcatctgcataaaggaagatt	57- 61.6	6352 3.5	3.5	XhoI	C/TCGAG	1608/3380	35	0,75	10
6	COL3a1ex44RF COL3a1ex50RR	gaacattgagtagaagagaatgicag tgcttacttcaaatgtaactctcttag	61.6 61.6	4988 2.5	2.5	-	-	-	35	0,75	10
7	COL3a1ex51RF COL3a1ex51RR	taatagatgataaataaagatagcattgg taacccctaactcaagacaggttagaag	59.2 59.2	2916 2	2	BspHI	T/CATGA	618/2298	35	0,75	10
7	COL3A1ex51LRF_ZC2 COL3A1ex51LRR_ZC2	tattgtatttggacaagaaggaaaaact tttggatccatagactaaactctccaac	59- 64	2016 1.5	1.5	-	-	-	35	0,75	10
Set	Primer Name:	Sequence	T (°C)	Size (bp)	Extension Time (min)	Restriction enzyme	Cutsite	Formed Fragments (bp)	Cycli	Primers (µl/well)	gDNA (ng)
1	COL4a1ex1RF COL4a1ex1RR	ccctactttaacaaaacgataaaatgg tggccaatttctcagacaaaataaagtg	60.9 62	3278 2	2	SphI	G/CATGC	1086/2192	35	0,75	10
2	COL4a1ex2RF COL4a1ex2RR	cttagacatctttgtcgaagaagctaac accagtagattgtattccatttccaac	61.5 62.7	6473 3.5	3.5	-	-	-	35	0,75	10
3	COL4a1ex3RF COL4a1ex8RR	aaattalaaccagttcagtgaaaaaaccc ctatttagaggatctatttctcagtgctc	61.9 61	4020 2.5	2.5	-	-	-	35	0,75	10
4	COL4a1ex9RF COL4a1ex12RR	gaacacgttaggaataagatccataatag aaaattacaactgcatacttccagagtc	61 62.1	3136 2	2	-	-	-	35	0,75	10
5	COL4a1ex13RF COL4a1ex18RR	acaagcagagaacaacagagactaacct aaaattaaagcaactctctgtaggac	62.7 62.5	5950 3.5	3.5	-	-	-	35	0,75	10
6	COL4a1ex19RF COL4a1ex21RR	acgttgaagtaaacattctgtttatgg cagtgattattctgaggagttcaagtg	61.9 62.1	5559 3	3	AflII	C/TTAAG	4968/591	35	0,75	10
7	COL4a1ex22RF COL4a1ex24RR	tcaattcttggacatacttctcagagtc attccacattttaatctactctctgtg	61.6 62.2	5912 3.5	3.5	-	-	-	35	0,75	10
8	COL4a1ex25RF	gatctacagctcaactcttcttggatcag	62.3	6194	3.5	-	-	-	35	0,75	10

Set	Primer Name:	Sequence	T (°C)	Size (bp)	Extension Time (min)	Restriction enzyme	Cutsite	Formed Fragments (bp)	Cycli	Primers (µl/well)	gDNA (ng)
9	COL4a1ex28RR	gfgtggtagcagaagacaaacttccttac	63.4	6254	3.5	-	-	-	35	0.75	10
	COL4a1ex29RF	gcatcaaaagggctgaacaggg	62.3	6254	3.5	-	-	-	35	0.75	10
	COL4a1ex36RR	ctatgtctttatatacagccagctctc	61.3	6402	3.5	-	-	-	35	0.75	10
10	COL4a1ex37RF	tgatacagfcaactttgatgatctcc	61	6402	3.5	-	-	-	35	0.75	10
	COL4a1ex42RR	attggggttaaatatgcaagglc	64.1	6168	3.5	-	-	-	35	0.75	10
11	COL4a1ex43RF	tcacaagaagaaatagcfaaagaataag	63	6168	3.5	-	-	-	35	0.75	10
	COL4a1ex46RR	ttcaacttaaaagtttctctcc	60.1	4481	2.5	-	-	-	35	0.75	10
12	COL4a1ex47RF	aaacatgctctctctattgtaggaac	61.7	4481	2.5	-	-	-	35	0.75	10
	COL4a1ex49RR	ggatggnagcaagtgtaaacagg	63.1	3576	2	-	-	-	35	0.75	10
13	COL4a1ex50RF	ttttaigtctcctgttagtgacatc	62.9	3576	2	-	-	-	35	0.75	10
	COL4a1ex50RR	agcctgcaatcagataaataaagtctc	61.3		2	-	-	-	35	0.75	10
Set	Primer Name:	Sequence	T (°C)	Size (bp)	Extension Time (min)	Restriction enzyme	Cutsite	Formed Fragments (bp)	Cycli	Primers (µl/well)	gDNA (ng)
1	ELNex1LRF	gttctgaccagatactgcaacttc	56-58	4941	3	SphI	GCATG/C	1434/3507	35	0.75	10
	ELNex3LRR	ccacacctctactggaactcc	56-58	3986	3	XbaI	T/CTAGA	3467/1474	35	0.75	10
2	ELNex4LRF	agagatgctacataattgaaacaaacc	59.2-62.8	3986	2	SacI	GAGCT/C	738/2248	35	0.75	10
	ELNex8LRR	gfgactcacagctttgggaaatag	59.2-62.8	3074	2	XbaI	T/CTAGA	985/3001	35	0.75	10
3	ELNex9LRF	aaagctcagctaacagacataagg	59.2-62.8	3074	2	BamHI	G/GATCC	1002/2028	35	0.75	10
	ELNex11LRRPG	ctggagctgaggtattctctacacc	59.2-62.8	4094	2	SphI	GCATG/C	1701/1329	35	0.75	10
4	ELNex11LRRFPG2	gaactgctctttattccaag	56-61.6	4094	2.5	HindIII	A/AGCTT	907/3187	35	0.75	10
	ELNex14LRRPG2	cccaacaagtgctatattctcaag	56-61.6	5335	2.5	XbaI	T/CTAGA	1061/3033	35	0.75	10
5	ELNex15LRRFPG2	accggtgtagaagaataattttagtg	56-62.8	5335	3	EcoRI	G/AATTC	1366/3969	35	0.75	10
	ELNex18LRRPG2	caagtgaaaaagaagctcagtagagag	56-62.8	6413	3	SacI	GAGCT/C	2060/3275	35	0.75	10
6	ELNex19LRF	caatggcctgctgtttgttc	58-59.2	6413	3.5	-	-	-	35	0.75	10
	ELNex25LRR	taaacgtcataaagctcctagaactg	58-59.2	3749	3.5	-	-	-	35	0.75	10
7	ELNex26LRF	gtcgtgatactataccgtttgttttg	57-61.6	3749	2	-	-	-	35	0.75	10
	ELNex29LRR	ctacagcaagtgcttctcaac	57-61.6	3623	2	-	-	-	35	0.75	10
7	ELNex26LRF_ZC2	tactataccgtttgtttgttttg		3623	2	-	-	-	35	0.75	10
	ELNex26LRR_ZC2	cccaactctctctcaactcaactc			2	-	-	-	35	0.75	10

8	ELNex30LRF ELNex21LRR	gcactttaggattcagatgactg ctctgttctattcttccgtaaaaatg	59- 61,6	4860	2,5 2,5	-	-	-	35	0,75	10
Set	Primer Name:	Sequence	T (°C)	Size (bp)	Extension Time (min)	Restriction enzyme	Cutsite	Formed Fragments (bp)	Cycli	Primers (µl/well)	gDNA (ng)
1	MYL9ex1LRFPG MYL9ex2LRPPG	tgcaagttcttctaaccttatcctaagtc ttgattttgacccttgtagtcttaagg	56-60,4	5824	3 3	BglII XbaI	A/GATCT T/CTAGA	3434/2390 2229/3595	35	0,75	10
2	MYL9ex3LRF MYL9ex4LRR	atcttaaatctcaaaagcaatcctattgaaac ctggaggtgataccagggaacttttg	56 - 58	3506	2 2	NdeI XbaI	CA/TATG T/CTAGA	2689/917 1382/2124	35	0,75	10



Part IV

(Pro)Renin Receptor Inhibition in Diabetic Rats

CHAPTER 9

Deterioration of Kidney Function by the (Pro)renin Receptor Blocker Handle Region Peptide in Aliskiren-treated Diabetic Transgenic (mRen2)²⁷ Rats

L. te Riet, M. van den Heuvel, C. J. Peutz-Kootstra, J. H. M. van Esch, R. van Veghel, I. M. Garrelds, U. Musterd-Bhaggoe, A. M. Bouhuizen, F. P. J. Leijten, A.H. J. Danser, W. W. Batenburg

Am J Physiol Renal Physiol 2014; 306: F1179–F1189

**ABSTRACT**

Dual renin-angiotensin system (RAS) blockade in diabetic nephropathy is no longer feasible because of the profit/side effect imbalance. (Pro)renin receptor ((P)RR) blockade with HRP has been reported to exert beneficial effects in various diabetic models in a RAS-independent manner. To what degree (P)RR blockade adds benefit on top of RAS blockade is still unknown. Here we treated diabetic TGR(mREN2)27 rats, a well-established nephropathy model with high prorenin levels (allowing continuous (P)RR stimulation *in vivo*), with HRP on top of renin inhibition with aliskiren. Aliskiren alone lowered blood pressure and exerted renoprotective effects, as evidenced by reduced glomerulosclerosis, diuresis, proteinuria, albuminuria, and urinary aldosterone levels, and diminished renal (P)RR and AT₁ receptor expression. It also suppressed plasma and tissue RAS activity, and suppressed cardiac ANP and BNP expression. HRP, when given on top of aliskiren, did not alter the effects of renin inhibition on blood pressure, RAS activity or aldosterone. Yet, it counteracted the beneficial effects of aliskiren in the kidney, induced hyperkalemia and increased plasma plasminogen activator-inhibitor 1, renal cyclo-oxygenase-2 and the cardiac collagen content. All these effects have been linked to (P)RR stimulation, suggesting that HRP might in fact act as a partial agonist. Therefore, the use of HRP on top of RAS blockade in diabetic nephropathy is not advisable.

INTRODUCTION

Hypertensive patients with diabetes exhibit an increased risk for cardiovascular complications such as nephropathy, stroke and heart failure. The renin-angiotensin system (RAS) is believed to modulate the underlying structural and functional changes in the kidney and heart^{1,2}, thereby explaining the beneficial effects of RAS blockers in this condition. Elevated levels of prorenin, the precursor of renin, are an early indicator of nephropathy in diabetes^{3,4}. Prorenin has been speculated to contribute to angiotensin generation in the kidney via binding to the so-called (pro)renin receptor ((P)RR). Indeed, (P)RR-bound prorenin displays angiotensin I-generating activity^{5,6}. Yet, it also stimulates (P)RR-mediated signal transduction in an angiotensin-independent manner, resulting in the activation of extracellular signal-regulated kinase (ERK) 1/2, cyclo-oxygenase-2 (COX-2) and fibrotic pathways^{5,7}. The latter includes enhanced transforming growth factor- β 1 (TGF β 1) synthesis, plasminogen activator-inhibitor 1 (PAI-1) release, and the upregulation of fibronectin and collagens^{5,7-9}. In agreement with this concept, ubiquitous expression of the human (P)RR in rats led to proteinuria, glomerulosclerosis and nephropathy, which could be reversed by the putative (P)RR blocker, handle region peptide (HRP)¹⁰. Beneficial renal effects of HRP were also observed in angiotensin II type 1a (AT_{1a})-receptor-deficient mice, suggesting that they are not solely due to interference with the RAS. Yet, the capacity of HRP to block the (P)RR is controversial¹¹, and recent studies in knockout animals suggest that (P)RR deletion in cardiomyocytes or podocytes is actually lethal¹²⁻¹⁴. Thus, a relevant question is to what degree HRP should still be used, e.g., on top of RAS blockade in diabetic patients with nephropathy and heart failure. This is of particular importance now that the combination of 2 or more RAS blockers is no longer advocated in diabetic patients, since the side effect profile (hypotension, hyperkalemia) of this approach outweighs the beneficial effects^{15,16}.

In the present study we therefore set out to study the effects of HRP on top of renin inhibition (with aliskiren) in a well-established high prorenin model, the TGR(mRen2)27 (Ren2) rat, which overexpresses the mouse Ren2 gene¹⁷ and also displays elevated (P)RR levels¹⁸. Aliskiren is renoprotective in this model, and its effects are comparable to those observed during AT₁ receptor blockade or ACE inhibition, despite non-equivalent blood pressure-lowering effects of these 3 types of RAS blockers^{19,20}. Cardioprotective effects of aliskiren have also been observed in diabetic rodents^{21,22}.

Rats were made diabetic with streptozotocin (STZ), and treated for 3 weeks with aliskiren and/or HRP. We used a dose of HRP that has been applied before in several rodent studies^{10,23-25}. We reasoned that, if anywhere, the beneficial effects of this putative (P)RR blocker on kidney and heart should be observed in this high-prorenin, high-(P)RR model.

METHODS

Animal studies

Homozygous Ren2 rats (400-500 g; a kind gift of dr. M. Bader, Berlin, Germany) were crossed with Sprague Dawley (SD) rats (Harlan, Boxmeer, The Netherlands) to generate heterozygous Ren2 rats. Heterozygous rats were subsequently used in all studies, since these rats, in contrast to homozygous Ren2 rats, did not require lisinopril treatment (10 µg/ml in drinking water) to decrease mortality. All studies were performed under the regulation and permission of the Animal Care Committee of the Erasmus MC. Rats were housed in individual cages and maintained on a 12-hour light/dark cycle, having access to standard laboratory rat chow and water ad libitum. Radiotelemetry transmitters were implanted as described before²⁶ for continuous measurement of heart rate, blood pressure, and activity. Two weeks later, to induce diabetes mellitus (DM), rats were fasted overnight and administered STZ (1 injection of 55 mg/kg STZ i.p., Sigma-Aldrich, Zwijndrecht, The Netherlands). Rats were checked for non-fasting blood glucose and β-ketone levels by tail incision daily during the first 3 days after STZ injection, and once-weekly thereafter (Precision Xceed, Abbott, Zwolle, The Netherlands). Only rats with a glucose level >15 mM were considered diabetic, and they subsequently received 2-4 U insulin per day (Levemir®, Novo Nordisk, Denmark). Diabetic Ren2 rats had an average blood glucose level of 25.8±0.9 mmol/L. After two weeks of DM status osmotic minipumps (2ML4 ALZET, Cupertino, USA) were implanted subcutaneously under isoflurane anesthesia to infuse vehicle (saline; n=8), aliskiren (a gift of Novartis, 10 mg/kg per day; n=8) or aliskiren + rat HRP (NH₂-RILLKKMPSV-COOH, 1 mg/kg per day, Biosynthan, Berlin, Germany; n=7). In the animals receiving aliskiren + HRP, 2 separate minipumps were implanted at both sides of the body. During the study, rats were placed in metabolic cages on day -14 (non-DM), day 0 (DM) and day 21 (DM+treatment) to collect 24-hour urine. Each rat served as its own control for the non-DM state. The urine was frozen and stored until analysis of total protein, albumin, creatinine, Na⁺, endothelin-1 and aldosterone. Three weeks later, animals were anaesthetized by pentobarbital injection i.p., and the hepatic portal vein was cannulated to collect blood for the measurement of angiotensin I and II, aldosterone, endothelin-1, TGFβ1, PAI-1, K⁺, cystatin C (a marker of glomerular filtration that is less dependent on muscle mass compared to creatinine), and creatinine (day 21). Kidney and heart were excised, weighed, divided into transverse segments, and fixated in 4% paraformaldehyde for histological analysis or frozen in liquid nitrogen for gene expression analysis. Blood and organs were also obtained from 6 DM Ren2 rats treated with saline for 3 weeks and 8 untreated non-DM Ren2 rats, which did not undergo hemodynamic measurements.

Biochemical measurements

ET-1 was assessed using a chemiluminescent ELISA (QuantiGlo, R&D Systems), albumin by enzyme immunoassay (Spi-Bio, Montigny-Le-Bretonneux, France), and aldosterone by radioimmunoassay (Coat-a-Count, Siemens Medical Solutions Diagnostics, Los Angeles, USA). TGFβ1, cystatin C (Quantikine, R&D systems) and PAI-1 (Zymutest, Tebu-Bio, Le Perray-en-Yvelines, France) were measured by ELISA. Creatinine, K⁺, Na⁺ and total protein were measured at the clinical chemical laboratory of the Erasmus MC. Angiotensin I and II were measured by radioimmunoassay, after SepPak extraction and reversed phase high performance liquid chromatography (HPLC) separation as described before^{27, 28}.

Histology

After fixation, kidney and heart sections were dehydrated and paraffin embedded. Gomori silver staining was applied to sections (5 µm) of the left ventricle of the heart to visualize individual cardiomyocytes. Sirius red staining was applied to visualize collagen as a measure of cardiac fibrosis. Cardiomyocyte size and the amount of collagen was measured using Qwin (Leica).

Transversely sliced kidney sections (deparaffinized, 2 µm) were stained with periodic acid Schiff (PAS) to localize kidney damage and α-smooth muscle actin (SMA) to identify interlobar arteries. In the sections, glomerular volume, arterial wall thickness and lumen diameter of interlobar arteries were blindly assessed. To measure

glomerular volume, 50 individual glomeruli from each kidney section were traced along Bowman's capsule to measure glomerular circumference using the system of NanoZoomer Digital Pathology. Glomerular volume was calculated from the glomerular circumference and radius according to the method of van Damme et al.²⁹ using the formula $4/3\pi r^2$. To measure arterial wall thickness to lumen diameter ratio, the arterial and lumen circumference of 6 interlobar arteries per kidney section was measured using the system of NanoZoomer Digital Pathology. Arterial wall thickness was calculated by deduction of lumen radius from the arterial outerradius. Data were also expressed as arterial wall thickness divided by lumen diameter ratio to correct for the size of the arteries measured.

The presence of focal segmental glomerulosclerosis was assessed in all glomeruli of one kidney section per animal with a mean of 181 ± 4 glomeruli per section. All sections were semiquantitatively scored by a renal pathologist in a blinded manner. Renal scarring of all glomeruli was scored on an arbitrary scale from 0 to 4. Grade 0 (n_0) indicated no glomerulosclerosis; grade 1 (n_1), less than 25% of sclerosis; grade 2 (n_2), 25-50% of sclerosis; grade 3 (n_3), 50-75% of sclerosis; and grade 4 (n_4), more than 75% of sclerosis per glomerulus. Hereafter, the individual glomerulosclerosis index (GSI) was calculated for each rat with the following formula: $[(1 \times n_1) + (2 \times n_2) + (3 \times n_3) + (4 \times n_4)] / [n_0 + n_1 + n_2 + n_3 + n_4]$. Furthermore, 10 images of each kidney section (100x magnification) were analyzed for arterial hyalinosis, intima fibrosis and media hypertrophy as well as tubular atrophy, interstitial fibrosis and renal inflammation according to the BANFF classification³⁰. Each parameter was graded in 10 fields with a score of 0-3 in which 0 meant no changes in pathology; grade 1, less than 25% of change; grade 2, 25-50% of change; grade 3, more than 50% of affected tissue. From these data, the tubulointerstitial score (TIS) was calculated by dividing the combined score of tubular atrophy, interstitial fibrosis and renal inflammation with the number of parameters.

Quantitative Real-Time RT-PCR

Total RNA was isolated from snap-frozen rat kidney and heart using Trizol (Life Technologies, Grand Island, USA) and reverse transcribed into cDNA using the QuantiTect Reverse Transcription Kit (Qiagen, Venlo, The Netherlands). The resulting cDNA was amplified in 40 cycles (denaturation at 95°C for 10 min; thermal cycling at 95°C for 15 sec, annealing/extension at 60°C for 1 min) with a Step-One cycler (NYSE, Life Technologies) using the SYBR® Green PCR Master Mix (Life Technologies). The intron-spanning oligonucleotide primers for qPCR were designed with NCBI (Primer-BLAST; Table 1). The comparative cycle time method ($\Delta\Delta CT$) was used for relative quantification of gene expression, using the geometric mean of the housekeeping genes hypoxanthine phosphoribosyl transferase-1 (HPRT1), β_2 -microglobulin and β -actin for normalization. In cardiac left ventricular tissue gene expression of atrial natriuretic peptide (ANP), brain natriuretic peptide (BNP), β -myosin heavy chain (β -MHC), the (P)RR and the AT_1 receptor was determined. Gene expression of rat renin, the (P)RR, the AT_1 receptor, collagen-1, $TGF\beta_1$, TNF α , NF- κB , COX-2 and neutrophil gelatinase-associated lipocalin (Ngal, a marker of tubular damage) was measured in kidney medulla and cortex.

Statistical analysis

Statistical analysis was performed using unpaired t-test after one-way ANOVA with Bonferroni post-test confirmed differences between groups. Data are given as mean \pm SEM. $P < 0.05$ was considered significant.

RESULTS

Animal characteristics

Hemodynamic data have been reported before³¹. In brief, diabetic Ren2 rats were severely hypertensive, and a three-week treatment with aliskiren (but not vehicle) lowered blood pressure (Table 2). The effect on blood pressure was unaltered by HRP. Diabetic Ren2 rats displayed a reduced body weight (BW) and heart weight (HW), and an increased kidney weight (KW), and as a result, the HW/BW ratio was unaltered in diabetic animals while their KW/BW ratio was increased (Table 2). Treatment with aliskiren ± HRP did not affect these parameters.

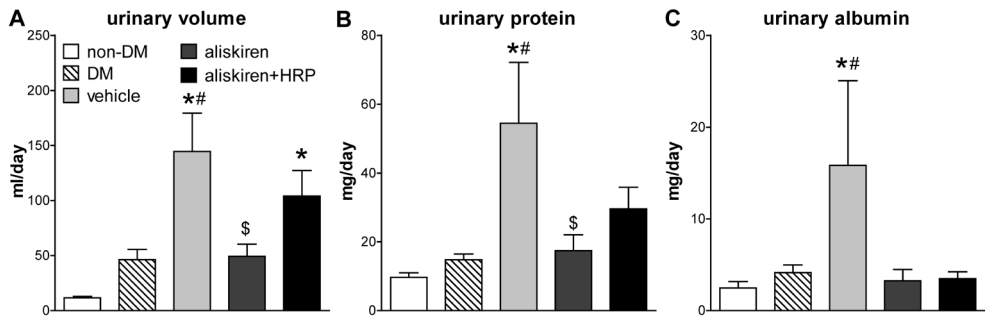


Figure 1

Urinary volume (A), urinary protein (B), and urinary albumin (C) in non-diabetic (non-DM) and DM Ren2 rats, treated with vehicle, aliskiren or aliskiren+HRP. Urine was collected on day -14 (non-DM), day 0 (DM; 2 weeks DM) and day 21 (after 3 weeks treatment; 5 weeks DM, vehicle, aliskiren and aliskiren+HRP). Please note that the Day 0 data (DM) reflect the measurements immediately before the start of treatment. Data are mean ± SEM of n=7-8. *P<0.05 vs non-DM, #P<0.05 vs 2 weeks DM, \$P<0.05 vs vehicle.

Biochemical measurements

STZ-induced DM increased blood glucose in Ren2 rats ≈4-fold, and this was unaffected by treatment (Table 2). DM increased urinary volume time-dependently. It was up ≈4-fold after 2 weeks, and after an additional 3 weeks (during treatment with vehicle) ≈13-fold (Figure 1). Aliskiren prevented this rise in diuresis, most likely due to its effects on blood pressure, while HRP negated the protective effects of aliskiren. Changes in urinary protein and albumin ran in parallel with the changes in urinary volume, although HRP did not prevent the effect of aliskiren on albumin (Figure 1).

DM decreased plasma creatinine, and this was unaffected by aliskiren treatment. HRP, when given on top of aliskiren, normalized plasma creatinine. No significant changes in urinary creatinine or creatinine clearance were observed following DM induction, with or without treatment (Table 2). Likewise, there was no change in plasma cystatin C, indicating no change in glomerular filtration rate due to 5 weeks of DM with or without treatment.

DM marginally decreased PRA (P=NS) and this was accompanied by a significant decrease in angiotensin levels in heart and kidney (Figure 2). Aliskiren further reduced these levels in the kidney, both with and without HRP. Plasma aldosterone levels were also decreased in diabetic Ren2 rats, and this resulted in increased natriuresis and an (nonsignificant) increase in plasma K⁺ levels (Figure 3). Remarkably, despite the reduction in

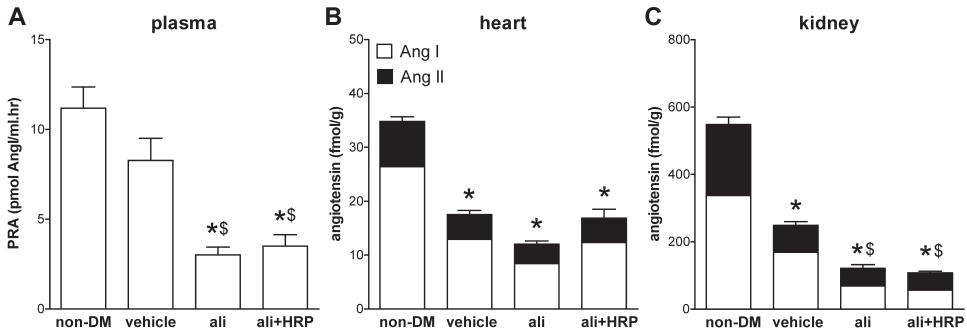


Figure 2

Plasma renin activity (A, PRA) and angiotensin (Ang) levels in heart (B) and kidneys (C) from non-diabetic (non-DM) and DM Ren2 rats, the latter treated for 3 weeks with vehicle, aliskiren or aliskiren+HRP. Data are mean±SEM of n=7-12. *P<0.05 vs non-DM, \$P<0.05 vs vehicle.

plasma aldosterone, urinary aldosterone excretion rose 8-fold. Aliskiren ± HRP greatly reduced the latter and yet non-significantly increased plasma aldosterone. As a result, natriuresis tended to diminish (P=NS). Of interest, HRP on top of aliskiren further increased plasma K⁺.

The plasma levels of TGFβ₁ and PAI-1 were not affected by diabetes or treatment with aliskiren. Yet, HRP on top of aliskiren increased plasma PAI-1 by 50% compared to vehicle or aliskiren treated rats, without affecting TGFβ₁ (Table 2). Plasma and urinary endothelin-1 levels were unaffected by DM or treatment (Table 2).

Kidney – gene expression

DM did not alter rat renin, AT₁ receptor, COX-2 or Ngal expression in medulla or cortex (Figure 4). It increased (P) RR and collagen-1 expression in the medulla, and to a lesser degree (P=NS) in the cortex. DM decreased TGFβ₁ expression in the cortex, whereas it induced a non-significant increase in TGFβ₁ expression in the medulla. Similar changes were observed for TNFα and NF-κB, but these were not significant (data not shown). Aliskiren did not alter the DM-induced changes in TGFβ₁ and collagen-1, and increased cortical rat renin expression. A similar increase in renin expression, albeit non-significant, was observed in the medulla. Aliskiren diminished cortical (P)RR and AT₁ receptor expression, without affecting these parameters in the medulla. Aliskiren tended to increase cortical COX-2 expression (P=NS). Changes by aliskiren were unaltered in the presence of HRP, except for the increase in COX-2, which became significant after addition of HRP.

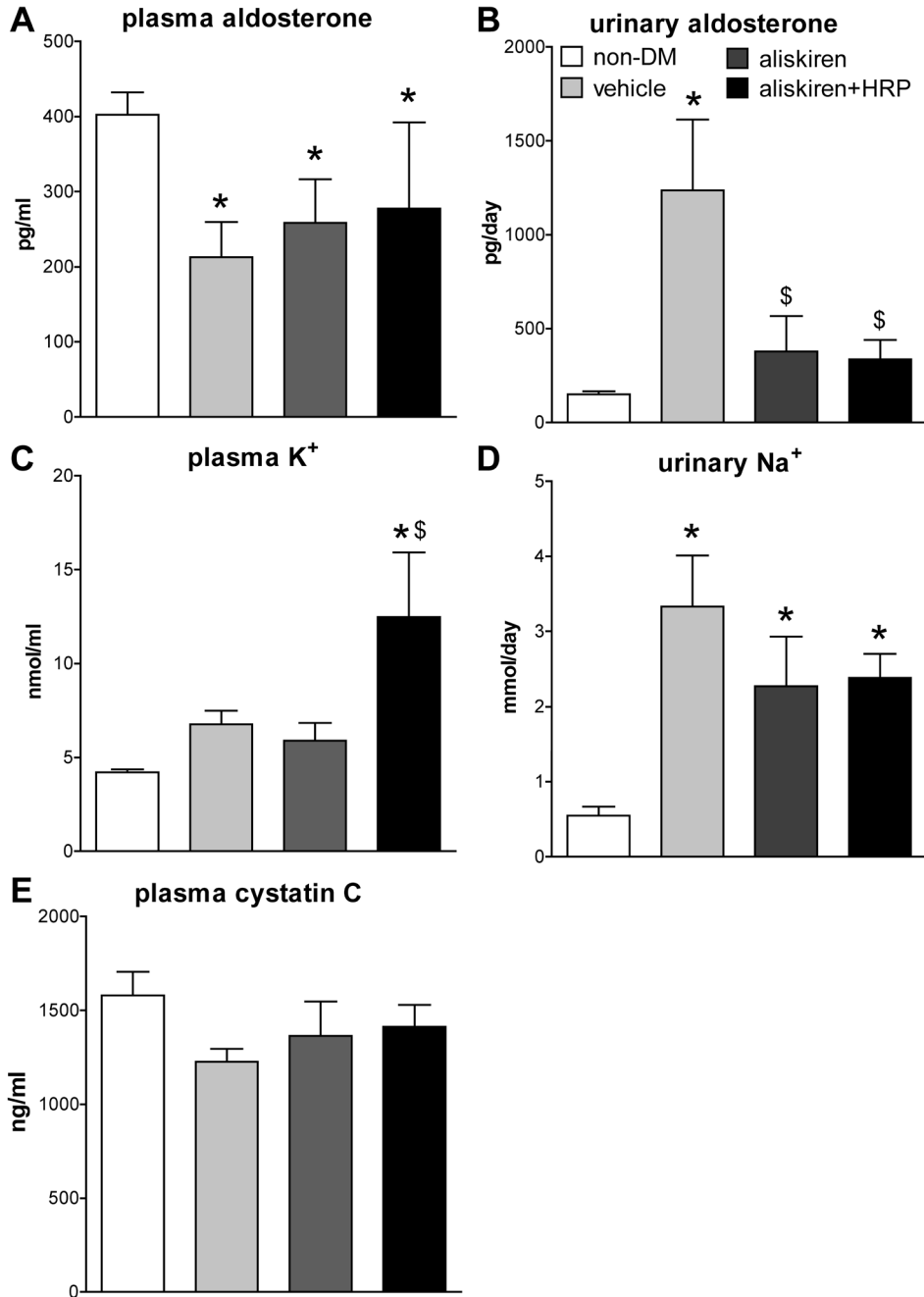


Figure 3

Levels of plasma (A) and urinary aldosterone (B), urinary K⁺ (C), urinary Na⁺ (D) and plasma cystatin C (E) in non-diabetic (non-DM) and DM Ren2 rats, the latter treated for 3 weeks with vehicle, aliskiren or aliskiren+HRP. Data are mean±SEM of n=7-13. *P<0.05 vs non-DM, \$P<0.05 vs vehicle.

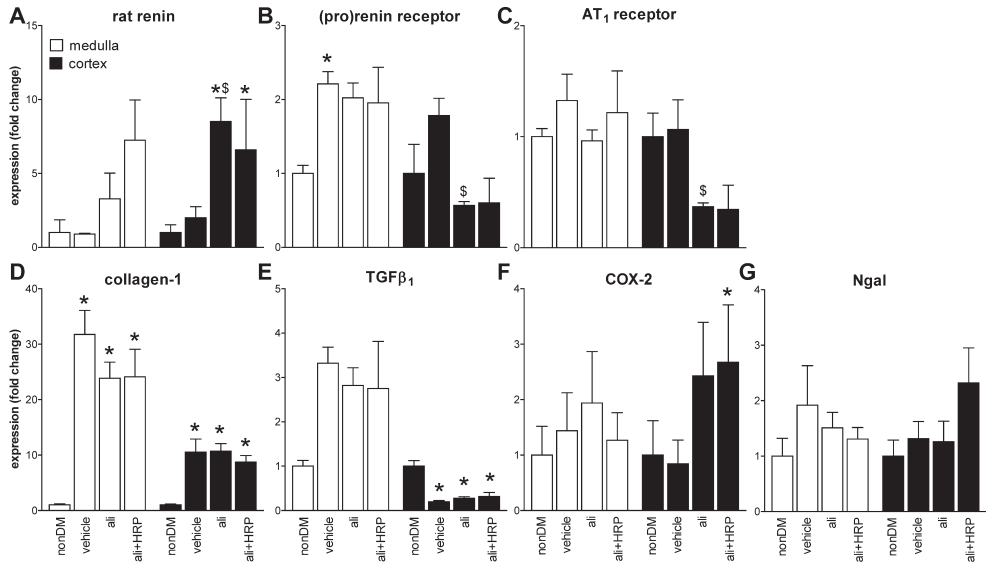


Figure 4 Gene expression analysis of rat renin (A), (pro)renin receptor (B), AT₁ receptor (C), collagen-1 (D), TGFβ₁ (E), COX-2 (F) and Ngal (G) in kidney medulla and cortex from non-diabetic (non-DM) and DM Ren2 rats, the latter treated for 3 weeks with vehicle, aliskiren or aliskiren+HRP. Data are mean±SEM of n=5-9 and have been expressed as fold-change vs. non-DM. *P<0.05 vs non-DM, \$P<0.05 vs vehicle.

Kidney - histology

DM did not alter TIS, glomerular volume, interlobar arterial lumen diameter and wall thickness (nor the ratio of the latter two), and non-significantly decreased GSI (Figure 5). Arterial hyalinose, intima fibrosis and media hypertrophy were not observed. Aliskiren reduced GSI, without affecting any of the other parameters. HRP, when given on top of aliskiren, did not alter its effects on GSI, but tended to increase glomerular volume and lumen diameter, the latter resulting in a decrease in lumen diameter/wall thickness ratio. However, none of these changes were significant.

Heart - gene expression

DM did not affect cardiac ANP, BNP and (P)RR expression, and increased β-MHC and AT₁ receptor expression (Figure 6). Aliskiren + HRP, but not aliskiren alone, normalized the latter. Drug treatment did not affect (P)RR or β-MHC expression. Aliskiren, with or without HRP, reduced cardiac BNP expression, and similar trends were observed for cardiac ANP expression, although now the changes were significant only during combination treatment.

Heart - histology

DM increased the cardiac collagen content, without altering myocyte size. Aliskiren did not affect these changes, while aliskiren + HRP further increased the collagen content and marginally diminished myocyte size (Figure 7).

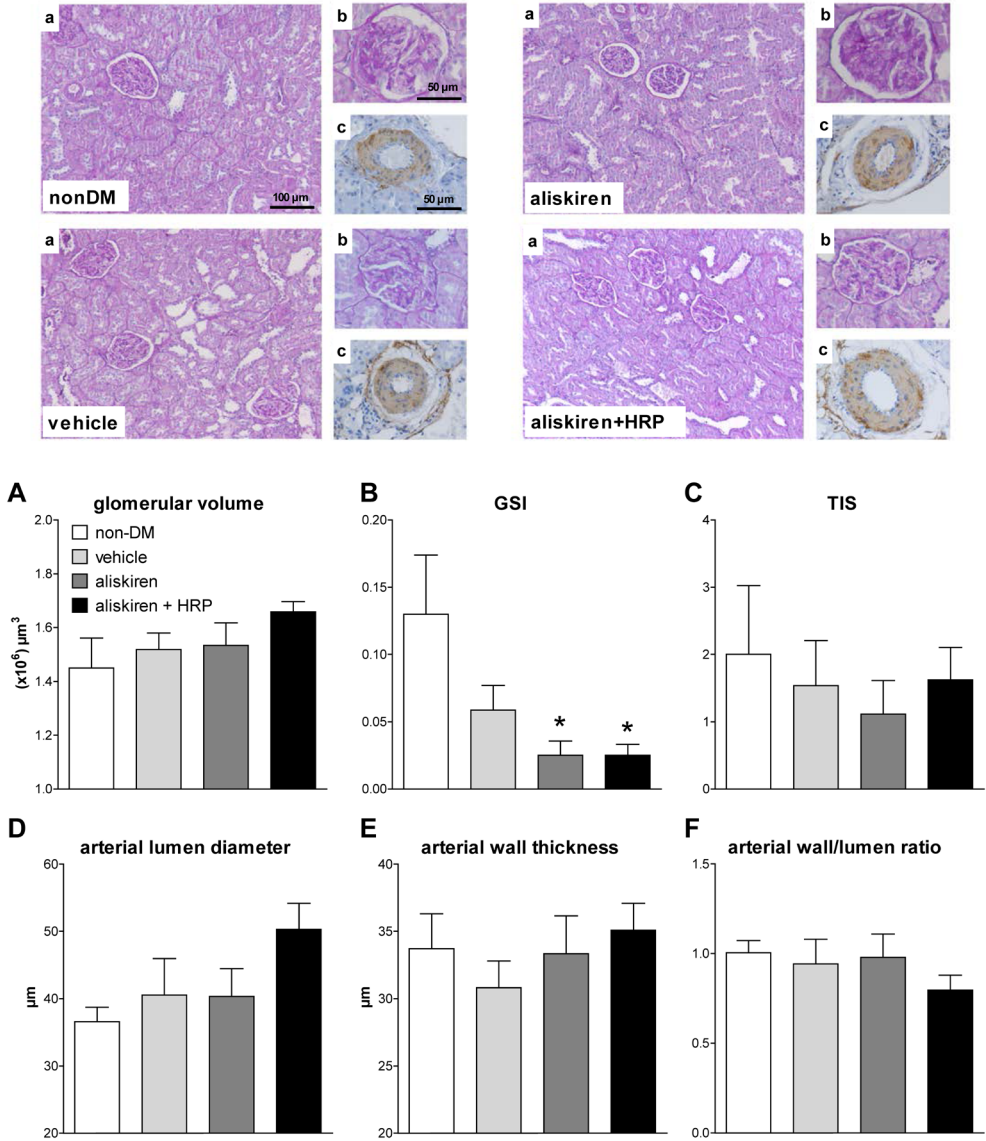


Figure 5

Glomerular volume (A), glomerulosclerosis index (B, GSI), tubulointerstitial score (C, TIS), interlobar arterial lumen diameter (D), wall thickness (E) and wall/lumen ratio (F) in kidney sections from non-diabetic (non-DM) and DM Ren2 rats, the latter treated for 3 weeks with vehicle, aliskiren or aliskiren+HRP. Data are mean+SEM of n=7-8. *P<0.05 vs non-DM. a and b, representative pictures of PAS-stained kidney sections; c, representative pictures of smooth muscle actin-stained interlobar arteries.

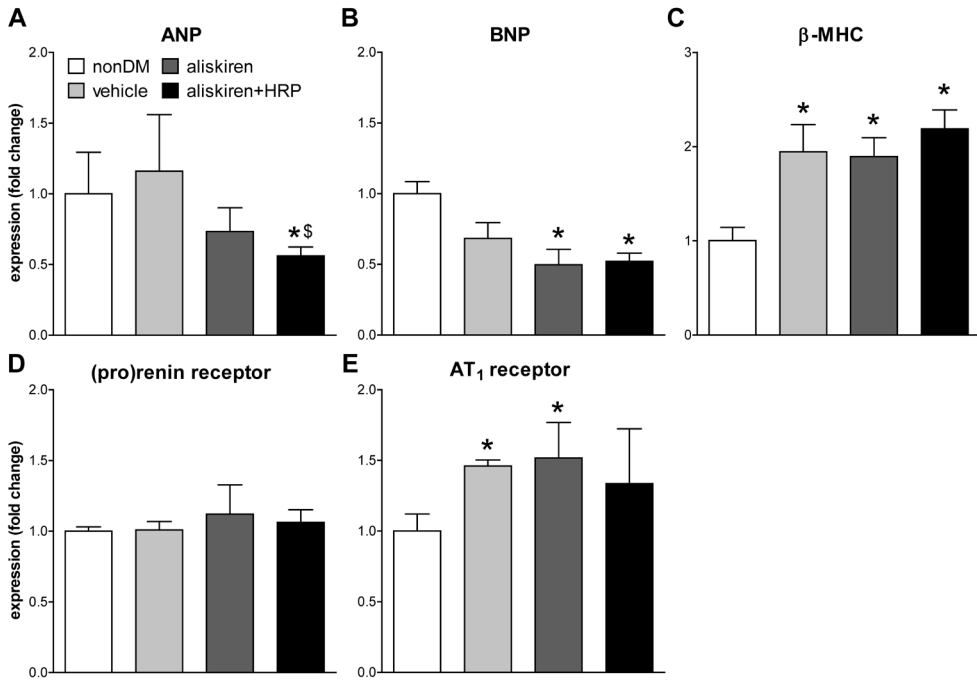


Figure 6

Gene expression analysis of ANP (A), BNP (B), β -MHC (C), (pro)renin receptor (D), and AT_1 receptor (E), in hearts from non-diabetic (non-DM) and DM Ren2 rats, the latter treated for 3 weeks with vehicle, aliskiren or aliskiren+HRP. Data are mean+SEM of n=7-10 and have been expressed as fold-change vs. non-DM. *P<0.05 vs non-DM, \$P<0.05 vs vehicle.

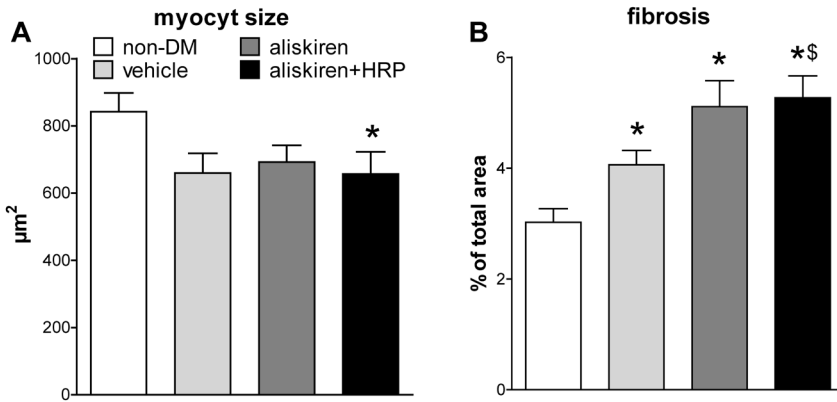
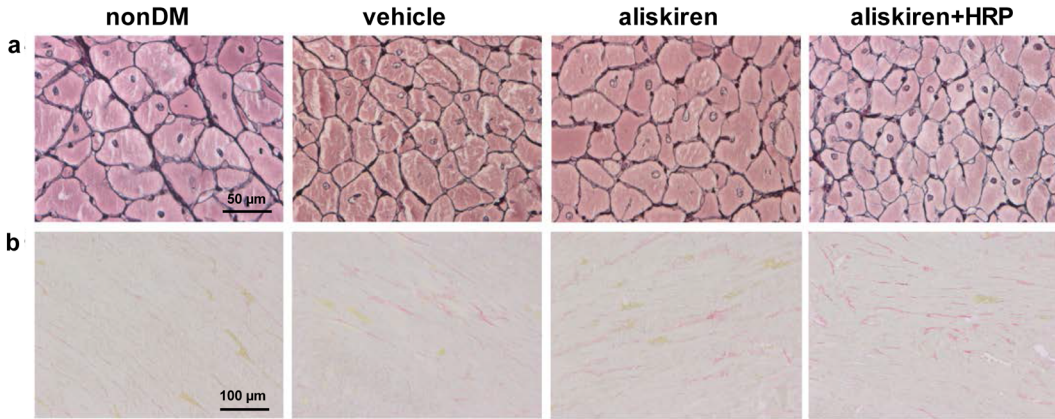


Figure 7

Cardiomyocyte size (A) and fibrotic area (B) in left ventricular tissue of hearts from non-diabetic (non-DM) and DM Ren2 rats, the latter treated for 3 weeks with vehicle, aliskiren or aliskiren+HRP. Data are mean+SEM of n=7-8. a, representative pictures of Gomori-stained cardiomyocytes; b, representative pictures of Sirius red-stained LV tissue. *P<0.05 vs non-DM, \$P<0.05 vs vehicle.

DISCUSSION

This study shows that HRP counteracts the favorable effects of aliskiren on early renal damage in diabetic Ren2 rats. In agreement with previous studies, the hypertensive Ren2 rat, when made diabetic with STZ, displayed mild glomerulosclerosis, accompanied by albuminuria, proteinuria and diuresis^{31, 32}. A three-week treatment with aliskiren improved these parameters, while the addition of HRP on top of aliskiren negated the protective effects of aliskiren on the latter two. HRP also induced hyperkalemia and increased plasma PAI-1, renal COX-2 and the cardiac collagen content. This argues against the application of HRP in combination with aliskiren in diabetic patients.

Plasma creatinine decreased after the induction DM, most likely reflecting the weight (and muscle) loss occurring in these animals. There were no changes in cystatin C or renal Ngal expression, suggesting that indeed the renal damage in our DM animals was at an early stage, not yet resulting in alterations in glomerular filtration or tubular damage. Of interest, aliskiren alone did not alter these parameters, whereas HRP on top of aliskiren increased plasma creatinine and tended to increase (P=NS) cortical Ngal expression, again suggesting that HRP, if anything, worsened renal function when combined with aliskiren.

DM reduced plasma, cardiac and renal RAS activity in the Ren2 rat, although only the reduction in tissue was significant. The reduction in PRA was modest, in full agreement with the consequence of diabetes in humans³³. Along with this RAS suppression, plasma aldosterone decreased by almost 50%. Not surprisingly, this resulted in natriuresis and a (non-significant) rise in plasma K⁺. Yet, urinary aldosterone excretion increased 8-fold. This is suggestive for a net rise in adrenal aldosterone production, most likely to compensate the loss of aldosterone via urine (□1.5 ng/day). Of interest, aliskiren greatly diminished the urinary aldosterone loss, reflecting a reduction in aldosterone production, although plasma aldosterone, if anything tended to go up, thereby counteracting the above effects on natriuresis and hyperkalemia. The effects of aliskiren on aldosterone and natriuresis were unaltered by HRP. Yet, it greatly elevated plasma K⁺. Since this occurred independently of changes in aldosterone, it might be the consequence of direct effects of HRP, e.g., via the (P)RR³⁴.

The aliskiren-induced reduction in renal angiotensin content, together with the reduction of cortical AT₁ receptor expression, probably underlies the beneficial effect of renin inhibition in the kidney. Aliskiren-induced AT₁ receptor suppression has been reported before, both in the kidney and other organs³⁵⁻³⁷. At 5 weeks after STZ injection, we observed modest regional changes in renal TGFβ1, TNFα, NF-κB and collagen-1 expression, although no fibrosis or inflammation could be detected. It is therefore not surprising that aliskiren did not significantly affect these parameters in the kidney. Such effects have been observed before, but this required a longer duration of DM (10 weeks), and aliskiren treatment starting at the moment of STZ injection³⁶. HRP did not alter the effect of aliskiren on TGFβ1, but unexpectedly increased the levels of PAI-1. These observations contrast with the idea that HRP prevents (pro)renin-(P)RR interaction, thereby blocking the rise in PAI-1 that result from such (P)RR stimulation, at least in vitro^{9, 38}. Possibly, the increase in renal (rat) renin expression after aliskiren was too modest to increase PAI-1. In addition, aliskiren suppressed (P)RR expression. Recently, HRP has been reported to act as a partial agonist of the (P)RR^{34, 39}. Thus, its stimulatory effects on PAI-1 on top of aliskiren might also be the consequence of direct (P)RR stimulation.

Hyperglycemia elevates (P)RR expression in rat mesangial cells via protein kinase C, ERK1/2 and JNK⁴⁰, and this has been suggested to facilitate angiotensin II generation and AT₁ receptor-dependent COX-2 induction⁴¹. Ubiquitous overexpression of the human (P)RR in the rat also resulted in COX-2 upregulation¹⁰. Simultaneously, COX-2 inhibition reduced the glucose-induced (P)RR upregulation, suggesting that COX-2 itself upregulates (P)RR⁴². Our study confirms renal (P)RR upregulation in diabetic Ren2 rats. Yet, significant COX-2 upregulation was only seen following concomitant HRP administration, even in the face of aliskiren-induced (P)RR suppression. This suggests that (P)RR upregulation per se is insufficient to increase COX-2, and requires additional (P)RR stimulation, either by renin, HRP or their combination. COX-2 elevation has been reported before in the macula densa after renin upregulation due to salt restriction⁴³. Such COX-2 upregulation has detrimental effects; for instance, COX-2 generated endothelium-derived contractile factors (EDCF) in diabetic Ren2 rats, thereby inducing vascular

dysfunction³¹, and the COX-2 upregulation in human (P)RR-overexpressing rats was accompanied by proteinuria and glomerulosclerosis¹⁰.

Natriuretic peptides are released by the hypertrophied heart, and their levels are elevated in patients with heart failure⁴⁴ and homozygous Ren2 rats⁴⁵. Aliskiren reduced cardiac ANP and BNP expression in the diabetic, heterozygous Ren2 rats of the present study, most likely due to its blood pressure-lowering effect. Yet, aliskiren did not affect cardiac hypertrophy, β -MHC expression, or myocyte size. These effects were unaltered by HRP. Moreover, no changes occurred in cardiac (P)RR expression, suggesting that (P)RR upregulation by hyperglycemia is not a uniform phenomenon. Although aliskiren with or without HRP did not significantly reduce the cardiac angiotensin content, HRP combined with aliskiren did suppress cardiac AT₁ receptor expression, suggesting that this combination may have reduced the consequences of angiotensin II-AT₁ receptor interaction. Yet, this did not result in a reduction of cardiac fibrosis, possibly because the degree of fibrosis in our model was still modest. Remarkably however, cardiac fibrosis increased significantly following co-treatment of aliskiren + HRP. This contrasts with studies showing antifibrotic effects of HRP in stroke-prone spontaneously hypertensive rats⁴⁶, and once again illustrates the partial agonistic capacities of HRP.

In conclusion, renin inhibition improves renal function in diabetic Ren2 rats with early kidney damage, and (P)RR blockade with HRP not only counteracted this effect in a RAS-independent manner, but also increased K⁺, PAI-1, renal COX-2 and cardiac fibrosis. This contrasts with the beneficial cardiac and renal effects of HRP observed in various models^{23,47,48}, but agrees with the deleterious effects of (P)RR knockout in heart and kidney^{12,13}. A uniform explanation might be that HRP acts as a partial agonist^{35,39}. Nevertheless, given these controversial findings, it seems that at this stage, HRP should not be considered as add-on drug in diabetics treated with a RAS inhibitor. Furthermore, given the uncertainty whether HRP is a (P)RR blocker or not, future studies should carefully examine the exact function of the (P)RR in diabetes, e.g., making use of (inducible) renal cell-specific knockout models, in order to define its role as a treatment target.

REFERENCES

1. Kobori H, Kamiyama M, Harrison-Bernard LM, Navar LG. Cardinal role of the intrarenal renin-angiotensin system in the pathogenesis of diabetic nephropathy. *J Investig Med* 2013;**61**:256-264.
2. Mandavia CH, Aroor AR, Demarco VG, Sowers JR. Molecular and metabolic mechanisms of cardiac dysfunction in diabetes. *Life Sci* 2013;**92**:601-608.
3. Deinum J, Ronn B, Mathiesen E, Derckx FHM, Hop WC, Schalekamp MADH. Increase in serum prorenin precedes onset of microalbuminuria in patients with insulin-dependent diabetes mellitus. *Diabetologia* 1999;**42**:1006-1010.
4. Luetscher JA, Kraemer FB, Wilson DM, Schwartz HC, Bryer-Ash M. Increased plasma inactive renin in diabetes mellitus. A marker of microvascular complications. *N Engl J Med* 1985;**312**:1412-1417.
5. Nguyen G, Delarue F, Burcklé C, Bouzahir L, Giller T, Sraer JD. Pivotal role of the renin/prorenin receptor in angiotensin II production and cellular responses to renin. *J Clin Invest* 2002;**109**:1417-1427.
6. Batenburg WW, Krop M, Garrelts IM, de Vries R, de Bruin RJA, Burcklé CA, Müller DN, Bader M, Nguyen G, Danser AHJ. Prorenin is the endogenous agonist of the (pro) renin receptor. Binding kinetics of renin and prorenin in rat vascular smooth muscle cells overexpressing the human (pro)renin receptor. *J Hypertens* 2007;**25**:2441-2453.
7. Batenburg WW, Lu X, Leijten F, Maschke U, Müller DN, Danser AHJ. Renin- and prorenin-induced effects in rat vascular smooth muscle cells overexpressing the human (pro)renin receptor: does (pro)renin-(pro)renin receptor interaction actually occur? *Hypertension* 2011;**58**:1111-1119.
8. Huang Y, Noble NA, Zhang J, Xu C, Border WA. Renin-stimulated TGF- β 1 expression is regulated by a mitogen-activated protein kinase in mesangial cells. *Kidney Int* 2007;**72**:45-52.
9. Huang Y, Wongamorntham S, Kasting J, McQuillan D, Owens RT, Yu L, Noble NA, Border W. Renin increases mesangial cell transforming growth factor- β 1 and matrix proteins through receptor-mediated, angiotensin II-independent mechanisms. *Kidney Int* 2006;**69**:105-113.
10. Kaneshiro Y, Ichihara A, Sakoda M, Takemitsu T, Nabi AH, Uddin MN, Nakagawa T, Nishiyama A, Suzuki F, Inagami T, Itoh H. Slowly Progressive, Angiotensin II-Independent Glomerulosclerosis in Human (Pro) renin Receptor-Transgenic Rats. *J Am Soc Nephrol* 2007;**18**:1789-1795.
11. Maschke U, Muller DN. The (pro)renin receptor and the mystic HRP—is there a role in cardiovascular disease? *Front Biosci (Elite Ed)* 2010;**2**:1250-1253.
12. Kinouchi K, Ichihara A, Sano M, Sun-Wada GH, Wada Y, Kurauchi-Mito A, Bokuda K, Narita T, Oshima Y, Sakoda M, Tamai Y, Sato H, Fukuda K, Itoh H. The (pro) renin receptor/ATP6AP2 is essential for vacuolar H⁺-ATPase assembly in murine cardiomyocytes. *Circ Res* 2010;**107**:30-34.
13. Riediger F, Quack I, Qadri F, Hartleben B, Park JK, Potthoff SA, Sohn D, Sihn G, Rousselle A, Fokuhl V, Maschke U, Purfurst B, Schneider W, Rump LC, Luft FC, Dechend R, Bader M, Huber TB, Nguyen G, Muller DN. Prorenin receptor is essential for podocyte autophagy and survival. *J Am Soc Nephrol* 2011;**22**:2193-2202.
14. Oshima Y, Kinouchi K, Ichihara A, Sakoda M, Kurauchi-Mito A, Bokuda K, Narita T, Kurosawa H, Sun-Wada GH, Wada Y, Yamada T, Takemoto M, Saleem MA, Quaggin SE, Itoh H. Prorenin receptor is essential for normal podocyte structure and function. *J Am Soc Nephrol* 2011;**22**:2203-2212.
15. de Boer RA, Azizi M, Danser AJ, Nguyen G, Nussberger J, Ruilope LM, Schmieder RE, Volpe M. Dual RAAS suppression: recent developments and implications in light of the ALTITUDE study. *J Renin Angiotensin Aldosterone Syst* 2012;**13**:409-412.
16. Parving HH, Brenner BM, McMurray JJ, de Zeeuw D, Haffner SM, Solomon SD, Chaturvedi N, Persson F, Desai AS, Nicolaidis M, Richard A, Xiang Z, Brunel P, Pfeffer MA, Investigators A. Cardiorenal end points in a trial of aliskiren for type 2 diabetes. *N Engl J Med* 2012;**367**:2204-2213.
17. Mullins JJ, Peters J, Ganten D. Fulminant hypertension in transgenic rats harbouring the mouse Ren-2 gene. *Nature* 1990;**344**:541-544.
18. Connelly KA, Advani A, Kim S, Advani SL, Zhang M, White KE, Kim YM, Parker C, Thai K, Krum H, Kelly DJ, Gilbert RE. The cardiac (pro)renin receptor is primarily expressed in myocyte transverse tubules and is increased in experimental diabetic cardiomyopathy. *J Hypertens* 2011;**29**:1175-1184.
19. Kelly DJ, Zhang Y, Moe G, Naik G, Gilbert RE. Aliskiren, a novel renin inhibitor, is renoprotective in a model of

- advanced diabetic nephropathy in rats. *Diabetologia* 2007;**50**:2398-2404.
20. Whaley-Connell A, Nistala R, Habibi J, Hayden MR, Schneider RI, Johnson MS, Tilmon R, Rehmer N, Ferrario CM, Sowers JR. Comparative effect of direct renin inhibition and AT1R blockade on glomerular filtration barrier injury in the transgenic Ren2 rat. *Am J Physiol Renal Physiol* 2010;**298**:F655-661.
 21. Ye Y, Qian J, Castillo AC, Perez-Polo JR, Birnbaum Y. Aliskiren and Valsartan reduce myocardial AT1 receptor expression and limit myocardial infarct size in diabetic mice. *Cardiovasc Drugs Ther* 2011;**25**:505-515.
 22. Dong YF, Liu L, Kataoka K, Nakamura T, Fukuda M, Tokutomi Y, Nako H, Ogawa H, Kim-Mitsuyama S. Aliskiren prevents cardiovascular complications and pancreatic injury in a mouse model of obesity and type 2 diabetes. *Diabetologia* 2010;**53**:180-191.
 23. Ichihara A, Kaneshiro Y, Takemitsu T, Sakoda M, Nakagawa T, Nishiyama A, Kawachi H, Shimizu F, Inagami T. Contribution of nonproteolytically activated prorenin in glomeruli to hypertensive renal damage. *J Am Soc Nephrol* 2006;**17**:2495-2503.
 24. Ichihara A, Kaneshiro Y, Takemitsu T, Sakoda M, Suzuki F, Nakagawa T, Nishiyama A, Inagami T, Hayashi M. Nonproteolytic activation of prorenin contributes to development of cardiac fibrosis in genetic hypertension. *Hypertension* 2006;**47**:894-900.
 25. Feldt S, Maschke U, Dechend R, Luft FC, Müller DN. Role of the (pro)renin receptor in transgenic rats with human renin hypertension. *J Am Soc Nephrol* 2008:in press.
 26. van Esch JHM, Moltzer E, van Veghel R, Garrelds IM, Leijten F, Bouhuizen AM, Danser AHJ. Beneficial cardiac effects of the renin inhibitor aliskiren in spontaneously hypertensive rats. *J Hypertens* 2010;**28**:2145-2155.
 27. de Lannoy LM, Danser AHJ, van Kats JP, Schoemaker RG, Saxena PR, Schalekamp MADH. Renin-angiotensin system components in the interstitial fluid of the isolated perfused rat heart. Local production of angiotensin I. *Hypertension* 1997;**29**:1240-1251.
 28. Danser AHJ, van Kats JP, Admiraal PJJ, Derckx FHM, Lamers MJM, Verdouw PD, Saxena PR, Schalekamp MADH. Cardiac renin and angiotensins. Uptake from plasma versus in situ synthesis. *Hypertension* 1994;**24**:37-48.
 29. van Damme B, Koudstaal J. Measuring glomerular diameters in tissue sections. *Virchows Arch A Pathol Anat Histol* 1976;**369**:283-291.
 30. Mengel M, Reeve J, Bunnag S, Einecke G, Jhangri GS, Sis B, Famulski K, Guembes-Hidalgo L, Halloran PF. Scoring total inflammation is superior to the current Banff inflammation score in predicting outcome and the degree of molecular disturbance in renal allografts. *Am J Transplant* 2009;**9**:1859-1867.
 31. Batenburg WW, van den Heuvel M, van Esch JH, van Veghel R, Garrelds IM, Leijten F, Danser AH. The (pro)renin receptor blocker handle region peptide upregulates endothelium-derived contractile factors in aliskiren-treated diabetic transgenic (mRen2)27 rats. *J Hypertens* 2013;**31**:292-302.
 32. Kelly DJ, Wilkinson-Berka JL, Allen TJ, Cooper ME, Skinner SL. A new model of diabetic nephropathy with progressive renal impairment in the transgenic (mRen-2)27 rat (TGR). *Kidney Int* 1998;**54**:343-352.
 33. Hollenberg NK, Fisher NDL, Nussberger J, Moukarbel GV, Barkoudah E, Danser AHJ. Renal responses to three types of renin-angiotensin system blockers in patients with diabetes mellitus on a high-salt diet: a need for higher doses in diabetic patients? *J Hypertens* 2011;**29**:2454-2461.
 34. Lu X, Garrelds IM, Wagner CA, Danser AH, Meima ME. (Pro)renin receptor is required for prorenin-dependent and -independent regulation of vacuolar H(+)-ATPase activity in MDCK.C11 collecting duct cells. *Am J Physiol Renal Physiol* 2013;**305**:F417-425.
 35. van Esch JHM, van Veghel R, Garrelds IM, Leijten F, Bouhuizen AM, Danser AHJ. Handle region peptide counteracts the beneficial effects of the Renin inhibitor aliskiren in spontaneously hypertensive rats. *Hypertension* 2011;**57**:852-858.
 36. Feldman DL, Jin L, Xuan H, Contrepas A, Zhou Y, Webb RL, Mueller DN, Feldt S, Cumin F, Maniara W, Persohn E, Schuetz H, Jan Danser AH, Nguyen G. Effects of aliskiren on blood pressure, albuminuria, and (pro) renin receptor expression in diabetic TG(mRen-2)27 rats. *Hypertension* 2008;**52**:130-136.
 37. Lastra G, Habibi J, Whaley-Connell AT, Manrique C, Hayden MR, Rehmer J, Patel K, Ferrario C, Sowers JR. Direct renin inhibition improves systemic insulin resistance and skeletal muscle glucose transport in a transgenic rodent model of tissue renin overexpression. *Endocrinology* 2009;**150**:2561-2568.
 38. Zhang J, Noble NA, Border WA, Owens RT, Huang Y. Receptor-dependent prorenin activation and induction of PAI-1 expression in vascular smooth muscle cells. *Am J Physiol Endocrinol Metab* 2008;**295**:E810-819.

39. Wilkinson-Berka JL, Heine R, Tan G, Cooper ME, Hatzopoulos KM, Fletcher EL, Binger KJ, Campbell DJ, Miller AG. RILLKMPVS influences the vasculature, neurons and glia, and (pro)renin receptor expression in the retina. *Hypertension* 2010;**55**:1454-1460.
40. Huang J, Siragy HM. Regulation of (pro)renin receptor expression by glucose-induced mitogen-activated protein kinase, nuclear factor-kappaB, and activator protein-1 signaling pathways. *Endocrinology* 2010;**151**:3317-3325.
41. Gonzalez AA, Luffman C, Bourgeois CR, Vio CP, Prieto MC. Angiotensin II-independent upregulation of cyclooxygenase-2 by activation of the (Pro)renin receptor in rat renal inner medullary cells. *Hypertension* 2013;**61**:443-449.
42. Huang J, Siragy HM. Glucose promotes the production of interleukine-1beta and cyclooxygenase-2 in mesangial cells via enhanced (Pro)renin receptor expression. *Endocrinology* 2009;**150**:5557-5565.
43. Harris RC, McKanna JA, Akai Y, Jacobson HR, Dubois RN, Breyer MD. Cyclooxygenase-2 is associated with the macula densa of rat kidney and increases with salt restriction. *J Clin Invest* 1994;**94**:2504-2510.
44. Burnett JC, Jr., Kao PC, Hu DC, Hesser DW, Heublein D, Granger JP, Opgenorth TJ, Reeder GS. Atrial natriuretic peptide elevation in congestive heart failure in the human. *Science* 1986;**231**:1145-1147.
45. Wegner M, Ganten D, Stasch JP. Neutral endopeptidase inhibition potentiates the effects of natriuretic peptides in renin transgenic rats. *Hypertens Res* 1996;**19**:229-238.
46. Ichihara A, Kaneshiro Y. Response to Cardiovascular Effects of Nonproteolytic Activation of Prorenin. *Hypertension* 2006.
47. Ichihara A, Hayashi M, Kaneshiro Y, Suzuki F, Nakagawa T, Tada Y, Koura Y, Nishiyama A, Okada H, Uddin MN, Nabi AH, Ishida Y, Inagami T, Saruta T. Inhibition of diabetic nephropathy by a decoy peptide corresponding to the "handle" region for nonproteolytic activation of prorenin. *J Clin Invest* 2004;**114**:1128-1135.
48. Ichihara A, Suzuki F, Nakagawa T, Kaneshiro Y, Takemitsu T, Sakoda M, Nabi AH, Nishiyama A, Sugaya T, Hayashi M, Inagami T. Prorenin receptor blockade inhibits development of glomerulosclerosis in diabetic angiotensin II type 1a receptor-deficient mice. *J Am Soc Nephrol* 2006;**17**:1950-1961.

Table 1
Real-time RT-PCR primers

gene	forward primer 5'-3'	reverse primer 5'-3'
HPRT-1	TGGACAGGACTGAAAGACTTGCTCG	CTTCAGCACACAGAGGGCCACA
β -actin	AGCCATGTACGTAGCCATCCA	TCTCCGGAGTCCATCACAATG
β 2-microglobulin	ATGGCTCGCTCGGTGACCG	TGGGGAGTTTTCTGAATGGCAAGCA
rat renin	CGGGAGGAGGATGCCTCTCTGG	CAAGATTCGTCCAAAGCTGGCTGT
Collagen-1	TCTGGCGCAAGAGGCGAGAGA	GTTGCCGGGGGCACCATTGT
TGF β 1	AGTGGCTGAACCAAGGAGACGGA	TGCCCAGGTCACCTCGACGT
(P)RR	TGAAGGAAGACCTGTCTTGCCAGG	ATAATGGTAGCCCGGGGCCGG
AT1R	ACTGCCTGAACCCTCTGTTC	TCGTAGACAGGCTTGAGTGG
COX-2	ATTGCTGGCCGGGTTGCTGG	TCAATGGAGGCCTTTGCCACTGC
TNF- α	GACCCTCACACTCAGATCATCTTCT	TGCTACGACGTGGGCTACG
NF- κ B	TCTGATTGGCCAGAGGCTCCC	GGGCGTGGCCATAGTTCAAGGG
ANP	ATGGGCTCCTTCTCCATCAC	TCTACCGGCATCTTCTCCTC
BNP	ACAATCCACGATGCAGAAGCT	GGGCCTTGGTCCTTTGAGA
β -MHC	ATGGACCTGGAGCGAGCAAA	GTCCTTCTTTTTGAGTCGCTCATCC
Ngal	GGGCTGTCCGATGAACTGAA	CATTGGTCGGTGGGAACAGA

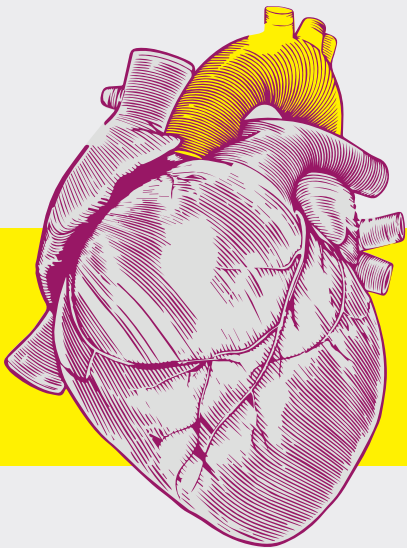
HPRT-1, hypoxanthine phosphoribosyltransferase; TGF β 1, transforming growth factor β 1; (P)RR, (pro)renin receptor; AT1R, angiotensin II type 1 receptor; COX-2, cyclooxygenase 2; TNF- α , tumor necrosis factor- α ; NF- κ B, nuclear factor- κ B; ANP, atrial natriuretic peptide; BNP, B-type natriuretic peptide; β -MHC, β -myosin heavy chain; Ngal, neutrophil gelatinase-associated lipocalin.

Table 2

Main characteristics, urine and plasma analysis in non-diabetic (DM) Ren2 rats and DM rats treated with vehicle, aliskiren or aliskiren + HRP. Data are mean±SEM of n=7-8.

	non-DM	vehicle	aliskiren	aliskiren+HRP
MAP on day 21(mm Hg)#	n.d.	123±7	104±9 [§]	103±4 [§]
Body weight (BW; kg)	0.562±0.02	0.409±0.01*	0.419±0.01*	0.422±0.01*
Heart weight (HW; g)	2.15±0.06	1.55±0.07*	1.51±0.04*	1.60±0.05*
HW/BW (g/kg)	3.9±0.10	3.7±0.11	3.6±0.12	3.7±0.09
Kidney weight (KW; g)	1.48±0.06	1.58±0.07	1.69±0.04*	1.63±0.05
KW/BW (g/kg)	2.7±0.12	4.1±0.15*	4.0±0.10*	3.9±0.12*
Blood glucose (mM)#	6.0±0.5	24.5±0.8*	26.1±1.0*	24.8±1.0*
urine				
creatinine (µmol/day)	128±4	114±9	116±13	109±5
endothelin-1 (pg/day)	3.6±0.7	7±3	0.5±0.5	3.8±2
creatinine clearance (ml/min)	n.d.	3.4±0.3	3.3±0.3	2.8±0.2
plasma				
creatinine (nmol/ml)	32.6±1.6	23.9±0.9*	23.9±0.7*	27.8±1.8
endothelin-1 (pg/mL)	9.1±4	12.4±9	19.6±8	18.4±14
PAI-1 (ng/mL)	3.2±0.5	7.7±1.2	7.6±1.9	11.8±3.9*
TGFβ1 (pg/mL)	423±99	266±78	408±124	268±80

HRP, handle region peptide; PAI-1, plasminogen-activator inhibitor type 1; TGFβ1, transforming growth factor β1; n.d., not determined. *P<0.05 vs non-DM, § P<0.05 vs vehicle. Creatinine clearance in non-DM could not be calculated since plasma and urine creatinine levels in this group were determined on day 21 and day -14, respectively, i.e., not on the same day. #Data are from Batenburg et al.³¹.



Part V

Summary and Discussion

CHAPTER 10

Summary and Discussion

Summary
Discussion
Nederlandse samenvatting
Curriculum Vitae
Publications
PhD Portfolio
Dankwoord

SUMMARY

The aorta is the largest artery that supplies oxygen to the body. Hence, aortic occlusive disease could obstruct the bloodflow, resulting in a pathophysiological outcome, as seen in atherosclerotic patients with aorta or iliac stenosis. Correspondingly, aortic aneurysm disease, which is a widening of the aorta, is an progressive process that is generally asymptomatic; consequently aortic aneurysms are usually only detected at a late and severe stage. Both aortic diseases are important causes of cardiovascular death in elderly patients. Moreover, these diseases share important risk factors, such as increased age and hypertension. As (high) blood pressure has an important effect on the aorta, the renin-angiotensin system (RAS) affects aortic pathology locally, as well as via its effect on blood pressure. Indeed, increasing evidence supports a role for the RAS in aneurysm development, as seen in thoracic aorta aneurysm (TAA) patients. In preclinical research, infusion of angiotensin (Ang) II, the main effector peptide of the RAS, in atherosclerotic apolipoprotein E and LDL receptor knockout mice induces aortic aneurysm.^{1,2} This mouse model provides an experimental model for abdominal aorta aneurysms (AAA) and the findings from this model implicate that the RAS has a pivotal role in aneurysm disease. When focusing on the local effects of the RAS and mainly of Ang II in the vessel wall, it is well-established that activation of Ang II type 1 (AT₁) receptors induces vasoconstriction, endothelial dysfunction, inflammation, growth, and remodeling, whereas Ang II type 2 (AT₂) receptors are believed to counteract these effects (**chapter 1**). Additionally, recent evidence supports a role for the Ang II-transforming growth factor β (TGF β) -axis in aneurysm development.³⁻⁵

When focusing on aneurysm disease, TAAs show degeneration of the medial layer of the aortic wall, characterized by elastic fiber fragmentation, loss of smooth muscle cells (SMC), and the accumulation of amorphous extracellular matrix.⁶ Such aortic wall degeneration is often the consequence of inherited connective tissue disorders. TAAs mostly present in a syndromic form, with early onset, and responsible genes have been identified. Mutations are found in genes encoding for cytoplasmic, contractile, extracellular matrix (ECM) proteins or components of the TGF β signaling pathway. A well-known example is Marfan syndrome (MFS) with a mutation in the extracellular matrix protein fibrillin-1, which was the first gene to be linked to TAA disease.⁸ Furthermore, another example is Loeys-Dietz syndrome with a mutation in TGF β -receptor subtypes (both TGF β R1⁷ and TGF β R2⁸). Finally, mutations in the gene encoding for SMAD3,⁹⁻¹¹ an intracellular mediator of the TGF β pathway, also result in TAA disease. Increased TGF β -signaling in MFS patients and also the dysregulation of the TGF β pathway showed the importance of TGF β in aneurysm disease.

Although mutations in different genes cause aneurysm disease, hallmark histological anomalies of this disease, like fragmentation of the elastic lamina and loss of extracellular matrix integrity, are similar. Likewise, mutations in the ECM protein fibulin-4 have been identified in patients with TAAs.¹² Fibulin-4 is a member of the seven-member family of ECM proteins that play a role in elastic fiber assembly and function.¹³ Fibulin-4 is an ubiquitously expressed protein essential for elastic fiber formation and is expressed in blood vessels, heart valves, basement membranes, and around cardiomyocytes.¹⁴ In humans, mutations in fibulin-4 lead to cutis laxa syndrome that besides loose skin is characterized by cardiovascular pathology, for instance vascular tortuosity and ascending aortic aneurysm.¹² We demonstrated that mice with a systemic 4-fold reduced expression of fibulin-4 (Fibulin-4^{R/R}) (where R stands for reduced) share a number of key features with the human phenotype of connective tissue disease, including aortic wall degeneration, aortic aneurysm formation, aortic valve disease, increased TGF β -signaling and impaired cardiac function (**chapter 2**).¹⁵ Manifestation of fibulin-4 related pathology is dose-dependent, since Fibulin-4^{+R} mice, with a milder 2-fold reduction in fibulin-4 expression, develop no apparent cardiovascular abnormalities.

In **part II** of this thesis we used our fibulin-4 mouse model to study aortic and cardiac pathology, as well the effects of RAS blockade. The pathology of the model resembles many other aneurysm diseases, with increased TGF β -signaling in the aortic wall, accompanied by increased tissue levels of Ang II, a well-known regulator of the TGF β -axis.^{4,16} In **chapter 2** we describe that reduction of fibulin-4 in a dose-dependent manner results in deterioration of the aortic wall, which displays the histological features of cystic media degeneration, including elastin fiber fragmentation, loss of smooth muscle cells, and deposition of ECM in the aortic media. Furthermore,

we observed that the aortic contractile capacity, determined by isometric force measurements, was diminished in Fibulin-4^{R/R} mice. Accordingly, transcriptome analysis showed that a dysregulation of contractile genes associated with this phenotype. The structural and functional alterations were accompanied by upregulation of TGF β -signaling, as identified by genome-scaled network analysis as well as by immunohistochemical staining for phosphorylated Smad2, an intracellular mediator of TGF β . Prenatal treatment with the AT₁ receptor antagonist losartan, to block the Ang II-TGF β -axis, blunted TGF β -signaling in newborn Fibulin-4^{R/R} mice, and prevented elastic fiber fragmentation in the aortic media. Postnatal losartan treatment reduced haemodynamic stress and greatly improved the lifespan of homozygous knockdown fibulin-4 animals, without affecting the aortic vessel wall structure.

In **chapter 3** we investigated the influence of reduced fibulin-4 expression on cardiac pathology, to delineate whether cardiac pathology is a consequence of the arterial disease or whether fibulin-4 is directly involved in cardiac structure and function. Using echocardiography and hemodynamic measurements, we showed that Fibulin-4^{R/R} mice spontaneously develop cardiac hypertrophy, dilation and dysfunction as well as aortic aneurysms. In addition, Fibulin-4^{R/R} cardiomyocytes display reduced force-generating capacity and altered TGF β -signaling. We also evaluated the effects of reduced fibulin-4 expression in human induced pluripotent stem cell-derived cardiomyocytes. shRNA-mediated fibulin-4 knockdown resulted in increased parameters associated with heart impairment, like cardiomyocyte size, and the expression of atrial natriuretic peptide (ANP), connective tissue growth factor (CTGF) and plasminogen activator inhibitor-1 (PAI-1). Cardiac hypertrophy might be influenced by aortic regurgitation in homozygous Fibulin-4^{R/R} mice. Importantly, heterozygous Fibulin-4^{+R} mice show no apparent cardiovascular or valvular abnormalities. When exposing the latter to transverse aortic constriction (TAC), we observed aggravated mortality, left ventricular dysfunction and pathological alterations in gene expression, without changes in valvular function. Taken together, these data suggest that reduced fibulin-4 levels in the heart drive myocardial pathology.

Given the findings in **chapter 2** on postnatal losartan treatment, in **chapter 4** we further explored this treatment in Fibulin-4^{R/R} mice, now also investigating aortic function and pathology. A comparison was made to the renin inhibitor aliskiren and the β -blocker propranolol, a classical TAA drug. Although both types of RAS blockers identically lowered hemodynamic stress, only losartan increased survival, reduced aneurysm size and improved aortic wall distensibility. Losartan (but none of the other drugs) also increased ejection fraction, decreased left ventricle diameter and reduced cardiac TGF β -signaling. None of these drug affected aortic wall morphology. To explain the beneficial effect of losartan compared to aliskiren we reasoned that losartan offers an additional advantage, possibly stimulation of angiotensin II type 2 (AT₂) receptors.

In **chapter 5**, we investigated how fibulin-4 deficiency leads to dysregulation of the TGF β pathway. We observed reduced growth in isolated aortic SMCs from fibulin-4 deficient mice, which could be reversed by treatment with TGF β neutralizing antibodies. Correspondingly, increased TGF β signaling was confirmed on the basis of elevated levels of phosphorylated Smad2. We found not only increased TGF β 1 levels in serum of cells, but also considerably increased TGF β 2 levels. Interestingly, elevated TGF β 2 levels were also detected in plasma from Fibulin-4^{R/R} mice, but not in losartan treated mice.

In **part III** of this thesis we investigated genetic factors involved in aneurysm formation and progression. In **chapter 6** we first focused on the potential mechanisms and targets that have been linked to AAA, comparing genetic RNA expression profiles of abdominal aortic samples from AAA patients with 'best match control' material of patients with aortic occlusive disease (AOD). We showed separation of the samples in distinct AAA and AOD groups, by principal component analysis. In addition, using ingenuity pathway analysis (IPA), we identified immune-related pathways with significantly changed expression in AAA. Interestingly, while expression of canonical TGF β signaling genes was significantly upregulated, bone morphogenetic protein (BMP) signaling was downregulated in AAA. Furthermore, we obtained a list of potential targets related to AAA that may result in biomarkers in future studies.

In **chapter 7**, we optimized the long-range PCR of TAA-associated genes to use the enriched fragments in massive parallel DNA sequencing for complete mutation analysis, including intron, exon and regulatory sequences.

In **part IV** of this thesis we investigated the beneficial effects of (pro)renin receptor blockade with the so-called handle region peptide (HRP) on top of renin inhibition in diabetic nephropathy. We confirmed that aliskiren alone lowered blood pressure and exerted renoprotection, most likely by suppressing plasma and tissue RAS activity. However, HRP, when given on top of aliskiren, did not alter the effects of renin inhibition on blood pressure, RAS activity, or aldosterone, and counteracted the beneficial effects of aliskiren in the kidney.

DISCUSSION

Aortic disease is an important cause of cardiovascular morbidity and mortality. Hence, treatment or surgical intervention is a prerequisite, and in case of aneurysm disease even essential to prevent growth, dissection or rupture. In TAA disease, β -adrenergic receptor blockade is the standard therapy to reduce hemodynamic stress.² Numerous studies showed the importance of the RAS in aneurysm development, and raised the possibility to reduce the increase in TGF β -signaling in the aortic wall of TAA patients by AT₁ receptor blockade. Indeed, given the concept of an AT₁ receptor-TGF β -axis, AT₁ receptor blockade should reduce TGF β -signaling, thereby reducing aneurysm progression and improving aortic wall structure.^{4,5} Theoretically, AT₁ receptor blockade might even outperform a β -blocker for a given degree of blood pressure-lowering. Indeed, initial studies in Marfan syndrome mouse models,¹⁸ together with our fibulin-4 mouse model,¹⁹ and in small patient cohorts,² confirmed this hypothesis. In particular, losartan appeared to reduce TGF β -signaling by targeting its non-canonical pathway component pERK.⁵ Yet, Lacro et al.²⁰ reported losartan and β -receptor blockade with atenolol reduced aneurysm progression equally well in MFS patients. The efficacy of β -adrenoceptor blockade is controversial, and based on small-scale studies.^{17, 21-24} Nevertheless, guidelines recommend β -adrenoceptor blockade to treat aortic dilation in MFS patients.^{25, 26} A randomized trial comparing β -blockade or AT₁ receptor blockade versus placebo is unlikely to be ever performed because of ethical issues. Recent studies showed that timing of AT₁ receptor blockade is of utmost importance, i.e. different ages at the start of treatment (e.g. children/adolescents versus adults) may explain the success (or lack thereof) of RAS blockers in clinical trials.^{20, 27, 28} The underlying mutation is an additional determinant of the success of AT₁ receptor blockade.²⁹

Our animal model suggested that RAS blockade with losartan is superior versus blockade with the renin inhibitor aliskiren. Since both drugs exerted the same degree of RAS blockade and blood pressure-lowering, losartan has an additional feature that aliskiren lacks. This might be AT₂ receptor stimulation. Obviously, further work in alternative models is needed to substantiate this view. Longitudinal microCT measurement is a novel and quick method allowing monitoring of cardiac and aneurysm parameters in mice *in vivo*. Fluorescent mediated tomography (FMT)-CT imaging additionally allows monitoring of cardiac or aortic remodeling. An important advantage of these non-invasive techniques is that animals are their own baseline control, so that fewer animals need to be studied.

The work described in this thesis supports the important contribution of the AT₁ receptor-TGF β -axis in TAA, and revealed the upregulation of immune pathways in AAA. Interestingly, losartan decreased the upregulated TGF β 2 plasma levels in fibulin-4 mice. Future studies should investigate to what degree this exclusively relates to AT₁ receptor blockade, i.e., whether other types of RAS blockers exert identical/better effects. (Pro) renin receptor blockade on top of other RAS blockers may lead to side effects and must be avoided. A detailed knowledge of the various upregulated pathways in AAA may help to design new drugs and new biomarkers in the aneurysm field. Complete genomic mutation analysis of the TAA-linked genes may similarly bring new insight in aneurysm research. It is important to realize that although in ageing humans atherosclerosis plays an important role in aneurysm formation, mice do not normally develop atherosclerosis. The combination of atherosclerosis and aneurysm formation might be mimicked in mice by crossing ApoE knock-out mice with our heterozygous fibulin-4^{+R}, assuming at least that the addition of aortic atherosclerosis on top of a mild ECM defect triggers aneurysm formation. If so, RNA expression analysis of these mice would help to better understand aneurysm disease, and extend the ingenuity pathway analysis data of our AAA patient group.

Our studies in isolated cardiomyocytes and intact hearts of fibulin-4 mice revealed that improper elastogenesis might be a primary cause of cardiac disease. Given the beneficial effects of losartan (but not aliskiren) on the heart of fibulin-4 mice, which potentially involve AT₂ receptor stimulation, other inherited ECM defects in the heart could also benefit from AT₂ receptor stimulation.

REFERENCES

1. Lu H, Rateri DL, Bruemmer D, Cassis LA, Daugherty A. Involvement of the renin-angiotensin system in abdominal and thoracic aortic aneurysms. *Clin Sci* 2012;**123**:531-543.
2. Moltzer E, Essers J, van Esch JHM, Roos-Hesselink JW, Danser AHJ. The role of the renin-angiotensin system in thoracic aortic aneurysms: Clinical implications. *Pharmacol Therapeut* 2011;**131**:50-60.
3. Lu H, Rateri DL, Bruemmer D, Cassis LA, Daugherty A. Involvement of the renin-angiotensin system in abdominal and thoracic aortic aneurysms. *Clin Sci (Lond)* 2012;**123**:531-543.
4. Habashi JP, Judge DP, Holm TM, Cohn RD, Loeys BL, Cooper TK, Myers L, Klein EC, Liu GS, Calvi C, Podowski M, Neptune ER, Halushka MK, Bedja D, Gabrielson K, Rifkin DB, Carta L, Ramirez F, Huso DL, Dietz HC. Losartan, an AT1 antagonist, prevents aortic aneurysm in a mouse model of Marfan syndrome. *Science* 2006;**312**:117-121.
5. Habashi JP, Doyle JJ, Holm TM, Aziz H, Schoenhoff F, Bedja D, Chen YC, Modiri AN, Judge DP, Dietz HC. Angiotensin II Type 2 Receptor Signaling Attenuates Aortic Aneurysm in Mice Through ERK Antagonism. *Science* 2011;**332**:361-365.
6. Isselbacher EM. Thoracic and abdominal aortic aneurysms. *Circulation* 2005;**111**:816-828.
7. Loeys BL, Schwarze U, Holm T, Callewaert BL, Thomas GH, Pannu H, De Backer JF, Oswald GL, Symoens S, Manouvrier S, Roberts AE, Faravelli F, Greco MA, Pyeritz RE, Milewicz DM, Coucke PJ, Cameron DE, Braverman AC, Byers PH, De Paepe AM, Dietz HC. Aneurysm syndromes caused by mutations in the TGF-beta receptor. *New Engl J Med* 2006;**355**:788-798.
8. Mizuguchi T, Collod-Beroud G, Akiyama T, Abifadel M, Harada N, Morisaki T, Allard D, Varret M, Claustres M, Morisaki H, Ihara M, Kinoshita A, Yoshiura K, Junien C, Kajii T, Jondeau G, Ohta T, Kishino T, Furukawa Y, Nakamura Y, Niikawa N, Boileau C, Matsumoto N. Heterozygous TGFBR2 mutations in Marfan syndrome. *Nat Genet* 2004;**36**:855-860.
9. van der Linde D, van de Laar I, Wessels MW, Oldenburg RA, Bekkers JA, Mattace-Raso FU, van den Meiracker AH, Moelker A, Tanghe HL, van Kooten F, Bertoli-Avella AM, Roos-Hesselink JW. Cardiovascular Phenotype of the Recently Discovered Aggressive Aneurysms-Osteoarthritis Syndrome (aos) Caused by Smad3 Mutations. *Circulation* 2011;**124**.
10. Dietz HC, Cutting GR, Pyeritz RE, Maslen CL, Sakai LY, Corson GM, Puffenberger EG, Hamosh A, Nanthakumar EJ, Currustin SM, Stetten G, Meyers DA, Francomano CA. Marfan-Syndrome Caused by a Recurrent Denovo Missense Mutation in the Fibrillin Gene. *Nature* 1991;**352**:337-339.
11. Loeys BL, Chen J, Neptune ER, Judge DP, Podowski M, Holm T, Meyers J, Leitch CC, Katsanis N, Sharifi N, Xu FL, Myers LA, Spevak PJ, Cameron DE, De Backer J, Hellems J, Chen Y, Davis EC, Webb CL, Kress W, Coucke P, Rifkin DB, De Paepe AM, Dietz HC. A syndrome of altered cardiovascular, craniofacial, neurocognitive and skeletal development caused by mutations in TGFBR1 or TGFBR2. *Nat Genet* 2005;**37**:275-281.
12. Huchtagowder V, Sausgruber N, Kim KH, Angle B, Marmorstein LY, Urban Z. Fibulin-4: a novel gene for an autosomal recessive cutis laxa syndrome. *Am J Hum Genet* 2006;**78**:1075-1080.
13. Argraves WS, Greene LM, Cooley MA, Gallagher WM. Fibulins: physiological and disease perspectives. *EMBO Rep* 2003;**4**:1127-1131.
14. Giltay R, Timpl R, Kostka G. Sequence, recombinant expression and tissue localization of two novel extracellular matrix proteins, fibulin-3 and fibulin-4. *Matrix Biol* 1999;**18**:469-480.
15. Hanada K, Vermeij M, Garinis GA, de Waard MC, Kunen MG, Myers L, Maas A, Duncker DJ, Meijers C, Dietz HC, Kanaar R, Essers J. Perturbations of vascular homeostasis and aortic valve abnormalities in fibulin-4 deficient mice. *Circ Res* 2007;**100**:738-746.
16. Sun Y, Zhang JQ, Zhang J, Ramires FJ. Angiotensin II, transforming growth factor-beta1 and repair in the infarcted heart. *J Mol Cell Cardiol* 1998;**30**:1559-1569.
17. Shores J, Berger KR, Murphy EA, Pyeritz RE. Progression of aortic dilatation and the benefit of long-term beta-adrenergic blockade in Marfan's syndrome. *N Engl J Med* 1994;**330**:1335-1341.
18. Huang JB, Yamashiro Y, Papke CL, Ikeda Y, Lin YL, Patel M, Inagami T, Le VP, Wagenseil JE, Yanagisawa H. Angiotensin-Converting Enzyme-Induced Activation of Local Angiotensin Signaling Is Required for Ascending Aortic Aneurysms in Fibulin-4-Deficient Mice. *Sci Transl Med* 2013;**5**.
19. Moltzer E, te Riet L, Swagemakers SMA, van Heijningen PM, Vermeij M, van Veghel R, Bouhuizen AM, van Esch JHM, Lankhorst S, Ramnath NWM, de Waard MC, Duncker DJ, van der Spek PJ, Rouwet EV, Danser AHJ,

- Essers J. Impaired Vascular Contractility and Aortic Wall Degeneration in Fibulin-4 Deficient Mice: Effect of Angiotensin II Type 1 (AT(1)) Receptor Blockade. *PLoS One* 2011;**6**:e23411.
20. Lacro RV, Dietz HC, Sleeper LA, Yetman AT, Bradley TJ, Colan SD, Pearson GD, Selamet Tierney ES, Levine JC, Atz AM, Benson DW, Braverman AC, Chen S, De Backer J, Gelb BD, Grossfeld PD, Klein GL, Lai WW, Liou A, Loeys BL, Markham LW, Olson AK, Paridon SM, Pemberton VL, Pierpont ME, Pyeritz RE, Radojewski E, Roman MJ, Sharkey AM, Stylianou MP, Wechsler SB, Young LT, Mahony L, Pediatric Heart Network I. Atenolol versus losartan in children and young adults with Marfan's syndrome. *N Engl J Med* 2014;**371**:2061-2071.
 21. Rossi-Foulkes R, Roman MJ, Rosen SE, Kramer-Fox R, Ehlers KH, O'Loughlin JE, Davis JG, Devereux RB. Phenotypic features and impact of beta blocker or calcium antagonist therapy on aortic lumen size in the Marfan syndrome. *Am J Cardiol* 1999;**83**:1364-1368.
 22. Ladouceur M, Fermanian C, Lupoglazoff JM, Edouard T, Dulac Y, Acar P, Magnier S, Jondeau G. Effect of beta-blockade on ascending aortic dilatation in children with the Marfan syndrome. *Am J Cardiol* 2007;**99**:406-409.
 23. Selamet Tierney ES, Feingold B, Printz BF, Park SC, Graham D, Kleinman CS, Mahnke CB, Timchak DM, Neches WH, Gersony WM. Beta-blocker therapy does not alter the rate of aortic root dilation in pediatric patients with Marfan syndrome. *J Pediatr* 2007;**150**:77-82.
 24. Gersony DR, McClaughlin MA, Jin Z, Gersony WM. The effect of beta-blocker therapy on clinical outcome in patients with Marfan's syndrome: a meta-analysis. *Int J Cardiol* 2007;**114**:303-308.
 25. Hiratzka LF, Bakris GL, Beckman JA, Bersin RM, Carr VF, Casey DE, Jr., Eagle KA, Hermann LK, Isselbacher EM, Kazerooni EA, Kouchoukos NT, Lytle BW, Milewicz DM, Reich DL, Sen S, Shinn JA, Svensson LG, Williams DM, American College of Cardiology Foundation/American Heart Association Task Force on Practice G, American Association for Thoracic S, American College of R, American Stroke A, Society of Cardiovascular A, Society for Cardiovascular A, Interventions, Society of Interventional R, Society of Thoracic S, Society for Vascular M. 2010 ACCF/AHA/AATS/ACR/ASA/SCA/SCAI/SIR/STS/SVM guidelines for the diagnosis and management of patients with Thoracic Aortic Disease: a report of the American College of Cardiology Foundation/American Heart Association Task Force on Practice Guidelines, American Association for Thoracic Surgery, American College of Radiology, American Stroke Association, Society of Cardiovascular Anesthesiologists, Society for Cardiovascular Angiography and Interventions, Society of Interventional Radiology, Society of Thoracic Surgeons, and Society for Vascular Medicine. *Circulation* 2010;**121**:e266-369.
 26. Baumgartner H, Bonhoeffer P, De Groot NM, de Haan F, Deanfield JE, Galie N, Gatzoulis MA, Gohlke-Baerwolf C, Kaemmerer H, Kilner P, Meijboom F, Mulder BJ, Oechslin E, Oliver JM, Serraf A, Szatmari A, Thaulow E, Vouhe PR, Walma E, Task Force on the Management of Grown-up Congenital Heart Disease of the European Society of C, Association for European Paediatric C, Guidelines ESCCfP. ESC Guidelines for the management of grown-up congenital heart disease (new version 2010). *Eur Heart J* 2010;**31**:2915-2957.
 27. Dietz HC. Potential Phenotype-Genotype Correlation in Marfan Syndrome: When Less is More? *Circ Cardiovasc Genet* 2015;**8**:256-260.
 28. Groenink M, den Hartog AW, Franken R, Radonic T, de Waard V, Timmermans J, Scholte AJ, van den Berg MP, Spijkerboer AM, Marquering HA, Zwinderman AH, Mulder BJ. Losartan reduces aortic dilatation rate in adults with Marfan syndrome: a randomized controlled trial. *Eur Heart J* 2013;**34**:3491-3500.
 29. Franken R, den Hartog AW, Radonic T, Micha D, Maugeri A, van Dijk FS, Meijers-Heijboer HE, Timmermans J, Scholte AJ, van den Berg MP, Groenink M, Mulder BJM, Zwinderman AH, de Waard V, Pals G. Beneficial Outcome of Losartan Therapy Depends on Type of FBN1 Mutation in Marfan Syndrome. *Circ Cardiovasc Gene* 2015;**8**:383-388.

NEDERLANDSE SAMENVATTING

De aorta is de grootste slagader in het menselijk lichaam die zuurstof vervoert. Vernauwing van slagaders (occlusief vaatlijden), zoals optreedt bij aderverkalking (atherosclerose), kan leiden tot een pathofysiologisch beeld dat gevolgen kan hebben voor de patiënt. Daarnaast is bij verwijding van de aorta, aneurysma genoemd, een progressief proces gaande van vaatwand re- en deconstructie wat leidt tot vergroting van de aorta. Meestal hebben patiënten een asymptomatisch ziektebeeld, en worden aorta aneurysmata vrijwel alleen ontdekt in een laat en ernstig stadium. Beide aorta aandoeningen, occlusie en verwijding, dragen bij aan sterfte veroorzaakt door hart- en vaatziekten (cardiovasculaire sterfte). Naast hogere leeftijd en hoge bloeddruk (hypertensie) zijn ze dan ook een belangrijke risicofactor voor cardiovasculaire sterfte. Hoge bloeddruk heeft een belangrijke uitwerking op de aorta, waarbij het renine-angiotensine systeem (RAS) pathologie van de aorta zowel lokaal als via het effect op de bloeddruk beïnvloedt. Steeds meer bewijs ondersteunt de rol van het RAS in aneurysma ontwikkeling, zoals in abdominale aorta aneurysmata (AAA) en thoracale aorta aneurysma (TAA) patiënten. In preklinische studies op atherosclerotische apolipoproteïne-E en LDL-receptor knock-out muizen resulteert infusie van angiotensine (Ang) II, de belangrijkste RAS effector peptide, in het ontstaan van aorta aneurysmata. Deze experimentele muismodellen verschaffen inzicht in de ziekte processen die een rol spelen bij AAA, waarbij de bevindingen in deze modellen laten zien dat het RAS een sleutelrol heeft in aneurysma ontwikkeling. De effecten van het RAS en met name van Ang II op de vaatwand worden bewerkstelligd door activering van Ang II type 1 (AT1) receptoren, waarbij algemeen wordt aangenomen dat AT1 receptoren vaatvernauwing induceren, evenals endotheel dysfunctie, ontstekingsreacties, vaatwand groei, en vaatwand re- en deconstructie. Daarentegen gaan Ang II type 2 (AT2) receptoren deze effecten tegen (**hoofdstuk 1**). Tot slot hebben recente studies een belangrijke rol aangetoond voor de Ang II-*transforming growth factor-β* (TGFβ)-as in aneurysma ontwikkeling.

Wanneer men aneurysma ziektes nader onderzoekt, worden TAA's gekenmerkt door degeneratie van de media (middelste laag) van de aortawand, fragmentatie van elastische vezels, verlies van gladde spiercellen en door ophoping van extracellulaire matrix. Deze aortawand degeneratie is vooral bij jongere patiënten vaak het gevolg van erfelijke bindweefsel-aandoeningen, waarbij TAA's vooral aanwezig zijn in syndromale ziektebeelden. De verantwoordelijke genen zijn grotendeels geïdentificeerd binnen deze patiënten populatie en coderen voornamelijk voor cytoplasmatische, contractiele en extracellulaire matrix eiwitten of voor één van de TGFβ componenten. Een bekende aneurysma ziekte is het Marfan syndroom (MFS), met een mutatie in het extracellulaire matrix eiwit fibrilline-1. Dit is het eerste gen beschreven in de literatuur waarvan bekend is dat het TAA veroorzaakt. Een ander bekend voorbeeld is het Loeys-Dietz syndroom met een mutatie in één van de TGFβ receptor subtypes (zowel TGFβR1 en TGFβR2). Daarnaast leiden mutaties in het gen dat codeert voor SMAD3, een intracellulaire mediator van de TGFβ signaal transductie route, tot TAA's. Toegenomen TGFβ signaal transductie in MFS patiënten, evenals ontregeling van TGFβ signaal transductie tonen het belang van het TGFβ systeem in aneurysma ziekten aan. Hoewel mutaties in verschillende genen aneurysmata veroorzaken, zijn de histologische afwijkingen veelal gelijk, zoals fragmentatie van de elastische lamina in de aortawand en het verdwijnen van de extracellulaire matrix integriteit. Tot slot resulteren mutaties in het extracellulaire matrix eiwit fibuline-4 in TAA. Het fibuline-4 eiwit is lid van de zevenledige familie van extracellulaire matrix eiwitten die een rol spelen bij de vorming van elastische vezels, en het goed functioneren daarvan. Fibulin-4 komt onder andere tot expressie in bloedvaten, hartkleppen, basale membranen en in het hart rondom hartspiercellen. Mutaties in fibuline-4 leiden tot het 'cutis laxa' syndroom bij mensen, dat wordt gekenmerkt door een losse huid en door cardiovasculaire pathologie, zoals vasculaire kronkeligheid en TAA's. Wij hebben in studies laten zien dat een systematische viervoudige verlaging van fibuline-4 expressie (Fibulin-4^{R/R}, R staat voor gereduceerd) in muizen resulteert in pathologie vergelijkbaar met die van fibuline-4 patiënten. Dit betreffen afwijkingen behorend tot het 'cutis laxa' syndroom, zoals aortawand degeneratie, aorta aneurysma, aortaklep afwijkingen, verhoogde TGFβ signaal transductie en verminderde hartfunctie (**hoofdstuk 2**). Het manifesteren van fibuline-4 pathologie is dosis afhankelijk, aangezien Fibulin-4^{+R} muizen met een (mildere) tweevoudige verlaging van

fibulin-4 expressie geen cardiovasculaire pathologie vertonen.

In **deel II** van dit proefschrift onderzochten we de facetten van aorta en hart pathologie in ons fibuline-4 muismodel, alsmede de effecten van RAS blokkade. De pathologie van het fibuline-4 muismodel lijkt veel op andere aneurysma ziekten en wordt gekarakteriseerd door onder andere verhoogde TGF β signaal transductie in de aortawand, vergezeld door verhoogde weefselconcentraties van Ang II, een bekende regulator van de TGF β -as. In **hoofdstuk 2** beschrijven we dat dosis afhankelijke verlaging van fibulin-4 expressie leidt tot verslechtering van de aortawand, histologisch gekenmerkt door media degeneratie, fragmentatie van elastische vezels, het verlies van gladde spiercellen en de ophoping van extracellulaire matrix in de aorta. Verder hebben we door middel van isometrische krachtmetingen aangetoond dat de contractiele capaciteit van de aorta is afgenomen in Fibulin-4^{R/R} muizen. In overeenstemming hiermee heeft transcriptoom analyse aangetoond dat er sprake is van ontregeling van de contractiele genen, hetgeen geassocieerd kan worden met bovenstaande beschreven afwijkingen. De structurele en functionele veranderingen in ons fibuline-4 muismodel worden gekenmerkt door toegenomen activiteit van de TGF β signaal transductie route, hetgeen wij hebben vastgesteld door middel van genoom expressie analyse, alsmede door immunohistochemische kleuring voor het gefosforyleerde SMAD2 eiwit, een intracellulaire mediator van TGF β . Prenatale behandeling met de AT1 receptor antagonist losartan, blokkeert de TGF β signaal transductie route in pasgeboren Fibulin-4^{R/R} muizen waarmee fragmentatie van de elastische vezels in de aortawand voorkomen wordt. Postnatale behandeling van Fibulin-4^{R/R} muizen met losartan vermindert hemodynamische stress in de aorta en verlengt de levensduur van deze muizen, maar geeft geen verbetering van de extracellulaire matrix integriteit van de aortawand.

In **hoofdstuk 3** onderzochten we de invloed van verminderde fibuline-4 expressie op hartafwijkingen. Dit om te onderzoeken of hart pathologie een gevolg is van de aorta afwijking, of dat fibulin-4 zelf van belang is voor een goed functionerend hart zonder structurele afwijkingen. Met behulp van echocardiografie en hemodynamische metingen hebben we aangetoond dat Fibulin-4^{R/R} muizen spontaan hypertrofie, dilatatie en dysfunctie van het hart ontwikkelen en daarbij aorta aneurysmata ontwikkelen. Daarnaast laten we zien dat hartspiercellen van Fibulin-4^{R/R} muizen een verminderde kracht-genererende capaciteit hebben, als ook een verandering in de TGF β signaal transductie route. Bovendien hebben we de effecten onderzocht van verminderde fibulin-4 expressie in humane hartspiercellen, welke door inductie van pluripotente stamcellen waren gegenereerd. shRNA gemedieerde fibulin-4 knockdown in deze hartspiercellen resulteert in verhoging van parameters geassocieerd met hartfalen, zoals hartspiercel grootte (hypertrofie), en de expressie van 'atrial natriuretische peptide' (ANP), 'connective tissue growth factor' (CTGF) en 'plasminogen activator inhibitor-1' (PAI-1). Hypertrofie van het hart zou kunnen worden verergerd door aortaklep insufficiëntie in Fibulin-4^{R/R} muizen. Daarentegen vertonen heterozygote Fibulin-4^{+/R} muizen van nature geen duidelijke cardiovasculaire of aortaklep problemen. Echter, wanneer deze Fibulin-4^{+/R} muizen worden blootgesteld aan een geïnduceerde aorta vernauwing ('trans-aortic constriction', TAC), zien we een verslechterde overleving, evenals linker ventrikel dysfunctie en pathologische veranderingen in de genexpressie van parameters geassocieerd met hartfalen, zonder veranderingen van de hartklep functie zelf. Dit betekent dat aorta klep insufficiëntie niet per se hypertrofie van het hart veroorzaakt in Fibulin-4 muizen. Samenvattend kunnen wij concluderen dat reductie van fibuline-4 expressie in het hart leidt tot hart pathologie en hartfalen.

Afgaande op de bevindingen van de postnatale losartan behandeling uit **hoofdstuk 2** zijn we in **hoofdstuk 4** verder ingegaan op de effecten van losartan behandeling op het functioneren van de aorta en op aorta pathologie in Fibulin-4^{R/R} muizen. Daarbij hebben we een vergelijking gemaakt tussen losartan, de renine remmer aliskiren en de β -blokker propranolol (het gebruikelijk medicijn in de behandeling van TAA's). Hoewel beide RAS blokkers (losartan en aliskiren) gelijkwaardig de bloeddruk verlagen, zien we dat alleen losartan zorgt voor een betere overleving, verminderde aneurysma groei en verbeterde aortawand flexibiliteit. Verder zorgt losartan behandeling, voor een verbeterde ejectiefractie, een verkleining in linker ventrikel diameter, en een verlaging van TGF β signaal transductie in het hart. Desalniettemin zien we dat geen enkel geneesmiddel

postnataal de aortawand morfologie verbetert. Om verschil tussen losartan versus aliskiren te verklaren, moet worden aangenomen dat losartan een extra voordeel biedt, aangezien het zijdelings voor Ang II Type 2 (AT2) receptor stimulatie zorgt.

In **hoofdstuk 5** hebben we onderzocht hoe reductie van fibulin-4 expressie leidt tot ontregeling van de TGF β signaal transductie route. We zien een verminderde groei van gladde spiercellen geïsoleerd uit de aortawand van Fibulin-4^{R/R} muizen. Deze verminderde groei kan worden opgeheven door de behandeling met TGF β neutraliserende antilichamen. Verder wordt een verhoogde TGF β signaal transductie bevestigd op basis van verhoogde aanwezigheid van het gefosforyleerde SMAD2 eiwit. Bovendien hebben we verhoogde TGF β 1 levels in celweek serum gemeten, en ook aanzienlijk verhoogde TGF β 2 levels. Interessant is dat we deze verhoogde levels van TGF β 2 hebben gedetecteerd in het plasma van Fibulin-4^{R/R} muizen, terwijl losartan behandeling deze stijging voorkomt.

In **deel III** van dit proefschrift onderzochten we de genetische factoren betrokken bij de vorming van aneurysmata en de progressie daarvan. In **hoofdstuk 6** hebben we ons gericht op de mogelijke mechanismen en aangrijpingspunten die geassocieerd zijn met AAA ziekte. Hierbij vergeleken we de genetische RNA-expressie profielen van aorta weefsel van AAA patiënten met 'best match control' materiaal van patiënten lijdend aan occlusief vaatlijden van de aorta ('aortic occlusive disease', AOD). Er is een duidelijke scheiding van RNA-expressie profielen in de AAA ten opzichte van de AOD groep aangetoond door middel van een 'principal-component' analyse. Vervolgens hebben we met 'ingenuity pathway analysis' (IPA) meerdere immuun gerelateerde mechanismen geïdentificeerd, die significant verschillen in de AAA ten opzicht van de AOD groep. Een interessante bevinding is dat genen in de TGF β signaal transductie route activiteit verhoogd zijn, terwijl genen in de 'bone morphogenetic protein' (BMP) signaal transductie route activiteit verlaagd zijn. Bovendien hebben we een lijst opgesteld van mogelijke genen, mechanismen en aangrijpingspunten die gerelateerd zijn aan AAA, die kunnen leiden tot potentiële bio-markers voor toekomstige studies. In **hoofdstuk 7** hebben we de 'long range'-PCR geoptimaliseerd om TAA geassocieerde genen te amplificeren, om met deze verrijkte DNA fragmenten door middel van de 'massive parallel DNA sequencing' methode een volledige mutatie sequentie analyse uit te voeren, met daarbij mutatie analyse van intronen, de exonen, en regulerende DNA sequenties.

In **deel IV** van dit proefschrift onderzochten we de additionele effecten van de (pro)renine-receptor blokker 'handle region peptide' (HRP) bovenop renine remming in diabetische nefropathie. We laten zien dat bij gebruik van alleen de renine remmer aliskiren er een bloeddrukverlaging optreedt. Daarnaast tonen wij een beschermend effect voor nier schade, hoogstwaarschijnlijk door onderdrukking van het RAS in zowel bloedplasma en als in de weefsels. Wanneer HRP in combinatie met aliskiren wordt gegeven zien we geen additionele effecten op de bloeddruk, RAS activiteit, of aldosteron levels, en zien we de gunstige effecten van aliskiren in de nier teniet gedaan worden.

Curriculum Vitae

Luuk te Riet werd geboren op 26 februari 1985 te Oldenzaal. In 2003 haalde hij zijn VWO diploma op het Twents Carmel Lyceum te Oldenzaal. Aansluitend volgde hij de studie Biologie aan de Radboud Universiteit Nijmegen met de afstudeerrichting Medische Biologie. Tijdens de bachelor van deze studie liep hij stage op de afdeling Moleculaire Biologie onder de begeleiding van Dr. Jorrit Tjeertes. Het onderzoek richtte zich op de functie van acetylering van het DOC-1 eiwit. Zijn eerste masterstage werd gedaan op de afdeling Kindergeneeskunde en Neurologie onder de begeleiding van Dr. Ilona Bruinsma en Dr. Marcel Verbeek. Dit onderzoek richtte zich op de functie van gesulfateerde glycosaminoglycanen in de ziekte van Alzheimer. Een tweede masterstage werd gedaan op de afdeling Farmacologie en Toxicologie onder de begeleiding van Dr. Kim Wever en Dr. Gerard Rongen. Dit onderzoek richtte zich op het voorkomen van ischemie reperfusie schade. Na het halen van zijn doctoraal begon hij als junior onderzoeker op de afdeling Vasculaire Chirurgie en op de afdeling Inwendige Geneeskunde sectie Farmacologie en Vasculaire Geneeskunde van het Erasmus MC. Onder supervisie van Dr. Jeroen Essers, Dr. Ellen Rouwet, Prof. Dr. Jan Danser en Prof Dr. Hence Verhagen werd het promotieonderzoek uitgevoerd dat in dit proefschrift beschreven is.

List of publications

Bruinsma IB, **te Riet L**, Gevers T, ten Dam GB, van Kuppevelt TH, David G, Küsters B, de Waal RM, Verbeek MM. **Sulfation of heparan sulfate associated with amyloid-beta plaques in patients with Alzheimer's disease.** Acta Neuropathol 2010 ;119:211-220

Moltzer E, **te Riet L**, Swagemakers SM, van Heijningen PM, Vermeij m, van Veghel R, Bouhuizen AM, van Esch JHM, Lankhorst S, Ramnath NWM, de Waard MC, Duncker DJ, van der Spek PJ, Rouwet E, Danser AHJ, Essers J. **Impaired vascular contractility and aortic wall degeneration in fibulin-4 deficient mice: effect of angiotensin II type 1 (AT1) receptor blockade.** PLoS One 2011 ;6:e23411

te Riet L, van den Heuvel M, Peutz-Kootstra CJ, van Esch JHM, van Veghel R, Garrelds IM, Musterd-Bhaggoo U, Bouhuizen AM, Leijten FP, Danser AHJ, Batenburg WW. **Deterioration of kidney function by the (pro) renin receptor blocker handle region peptide in aliskiren-treated diabetic transgenic (mRen2)27 rats.** Am J Physiol Renal Physiol 2014 ;306:F1179-F1189

te Riet L, van Esch JHM, Roks AJM, van den Meiracker AH, Danser AHJ. **Hypertension: Renin-Angiotensin Aldosterone Alterations.** Circ Res 2015 ;116:960-975

van Thiel BS, van der Pluijm I, **te Riet L**, Essers J, Danser AHJ. **The renin-angiotensin system and its involvement in vascular disease.** Eur J Pharmacol 2015 ;763:3-14

Ramnath NW[#], Hawinkels LJ[#], van Heijningen PM, **te Riet L**, Paauwe M, Vermeij M, Danser AHJ, Kanaar R, ten Dijke P, Essers J. **Fibulin-4 deficiency increases TGF- β signaling in isolated aortic smooth muscle cells due to elevated TGF- β 2 levels.** Sci Rep 2015 ;5:16872

te Riet L, van Deel ED, Van Thiel BS, Moltzer E, van Vliet JN, Ridwan R, van Veghel R, van Heijningen PM, Robertus J, Gerralds IM, Vermeij M, van der Pluijm I, Danser AHJ, Essers J. **Angiotensin II Type 1 Receptor Blockade, but not Renin Inhibition, Reduces Aneurysm Progression, and Improves Cardiac Morphology and Function in Aneurysmal Fibulin-4 Mice.** (Journal of Hypertension 2016)

van Deel ED[#], **te Riet L**[#], Moltzer E, van Vliet JN, Robertus J, Boontje N, Fiedler LR, Dekker SO, Maifoshie E, van Heijningen, Vermeij M, van der Pluijm I, Speelman L, Roos-Hesselink JW, Rouwet E, Reinhardt DP, van der Velden J, Danser AHJ, Duncker DJ, Schneider MD, Essers J. **Reduced Fibulin-4 Expression Causes Myocardial Remodelling and Dysfunction.** (Submitted for publication) [#]These authors contributed equally.

van der Pluijm I, van Heijningen PM, Ijpma A, van Vliet JN, Sluiter W, Davis EC, Ringuette LJ, Dekkers, Ghazi S, Que I, Kaijzel EL, **te Riet L**, Gabriels SIC, Mastroberardino PG, van der Linden R, Vermeij M, Demmers JA, Das D, Yanagisawa H, Kanaar R, Essers J. **Fibulin-4 Induced Disintegration of the Extracellular Matrix Causes Changes in Mitochondrial Function and Altered Energy Metabolism.** (Submitted for publication)

PhD Portfolio

Name Ph.D. Student: Luuk te Riet
Erasmus MC Departments: Vascular Surgery & Internal Medicine, division of Pharmacology and Vascular Medicine.
Research School: Cardiovascular Research School (COEUR), Erasmus MC, Rotterdam, The Netherlands.
Promotors: Prof.dr. A.H.J. Danser
Prof.dr. H.J.M. Verhagen.
Copromotors: Dr. J. Essers
Dr. E.V. Rouwet

PhD training

	year
In-depth courses (17.3 ECTS)	
Classical Methods for Data Analysis	2011
COEUR lectures, seminars and courses	2011-2015
Teaching (3.9 ECTS)	
Supervising practical 'Farmacologische beïnvloeding van het autonome zenuwstelsel' 1 st year medical students, Erasmus MC, Rotterdam, The Netherlands	2011-2014
Supervising practical, students Junior Med School, High school, MSc in Molecular Medicine, Erasmus MC, Rotterdam, The Netherlands	2011-2014
Supervising 6 Bachelor and Master students Erasmus MC, Rotterdam, The Netherlands	2011-2014
Symposia and conferences (9.7 ECTS)	
12 th Dutch-German Joint Meeting of the Molecular Cardiology Working Groups, Groningen, Nederland **	2014
Erasmus MC PhD Day, Rotterdam, Nederland	2014
American Heart Association's Scientific Sessions, Dallas TX,	2013

Verenigde Staten **

Gordon Elastin, Elastic Fibers & Microfibrils, Biddeford ME,
Verenigde Staten * ** 2013

ESH 23rd European Meeting on Hypertension & Cardiovascular Protection,
Milaan, Italië * 2013

13th FIGON Dutch Medicines Days,
Lunteren, Nederland * 2011

Jaarlijks congres afd. heeskunde,
Erasmus MC, Rotterdam, Nederland 2011-2014

Jaarlijks congres afd. interne geneeskunde,
Erasmus MC, Antwerpen, België * 2011-2014

* Mondelinge Presentatie, **Poster Presentatie

Total (30.9 ECTS)

Grants

Travel Grant - European Meeting on Hypertension &
Cardiovascular Protection 2013

Dankwoord

Het is zover, ik kan de hand leggen aan het laatste stukje van mijn proefschrift. Met natuurlijk het dankwoord voor iedereen die een bijdrage heeft geleverd aan het tot stand komen van dit proefschrift.

Ten eerste wil ik mijn promotor Jan Danser bedanken. Beste Jan, bedankt voor de goede begeleiding tijdens mijn onderzoek. Het was fijn dat je mijn vragen altijd zeer snel beantwoordde, dit door je zeer georganiseerde en pragmatische aanpak. Verder wil ik je bedanken voor de vrijheid die je me hebt gegeven in mijn promotietraject waardoor ik het onderzoek in mijn eigen richting kon sturen, desondanks was je goed op de hoogte van alles. Hierdoor heb ik me als junior onderzoeker goed kunnen ontwikkelen en heb ik zeer veel geleerd.

Daarnaast wil ik mijn co-promotor Jeroen Essers bedanken. Beste Jeroen, bedankt voor de zeer prettige samenwerking, intensieve begeleiding en jouw onmisbare inzet tijdens mijn onderzoek. Je was nooit op je werkplek aanwezig als ik even langs kwam lopen, maar als je dan wel aanwezig was had je altijd tijd om mijn vragen te beantwoorden. Tijdens mijn promotietraject zijn we samen naar het Gordon Research congres geweest te Biddeford. Na het intensieve wetenschappelijke programma hebben we 's middags en 's avonds de tijd genomen om te ontspannen en om wat van de omgeving te zien, dit was erg gezellig. Ook de kajaktocht zal mij nog lang heugen, waarbij ik kopje onder ging door dwars te gaan liggen in de sterke stroming van de rivier. Zonder jouw vertrouwen en sturing had dit boekje er niet zo goed uitgezien. Ontzettend bedankt.

Mijn tweede promotor Hence Verhagen wil ik natuurlijk ook bedanken. Beste Hence, ondanks dat we weinig contact hebben gehad tijdens mijn promotietraject heb je het wel mogelijk gemaakt. Bedankt hiervoor. Tijdens de contactmomenten die we hadden bracht je veel optimisme over waardoor ik met plezier mijn promotietraject heb kunnen afronden.

Mijn tweede co-promotor Ellen Rouwet. Beste Ellen, bedankt voor jouw enthousiasme, klinische input, en voor jouw inzet betreffende het in goede banen leiden van de weefselcollectie. Hierdoor hebben we een mooi translationeel onderzoekstuk op kunnen zetten.

Ingrid van der Pluijm, beste Ingrid, jij hebt veel tijd gestoken in het begeleiden van mijn promotietraject, bedankt hiervoor. Zonder jouw doortastende en motiverende begeleiding was dit boekje niet tot stand gekomen. Bovendien heeft jouw kritische en praktische blik op de wetenschap ervoor gezorgd dat de zaken net wat sneller en beter op papier werden gezet. Nogmaals dank.

Graag wil ik Prof. dr J.W. Roos-Hesselink, Prof. dr. D.J.G.M. Duncker en Prof. dr. M.C. de Rooter bedanken voor het plaatsnemen in de leescommissie en de beoordeling van mijn proefschrift.

Mijn collegae van de Farmacologie. Beste Wendy, samen hebben we een onderzoeksartikel afgerond, bedankt hiervoor. Verder wil ik Richard, Frank, Usha, Ingrid, Joep, René, Ton, Antoinette en Anton bedanken voor technische en wetenschappelijke ondersteuning bij het tot stand komen van dit boekje. Mijn andere (oud)collegae: Luit, Nils, Ilse, Els, Stijn, Thijs, Sieneke, Manne, Matej, Hisko, Marcel, Xifeng, Koen, Bruno, Birgitte, Stefanie, Lodi, Khatera, Kayi, Paula, Langeza, Katie, Estrellita, Mahdi, David, Charles, Dominique en Arthur wil ik bedanken voor alle gezelligheid en de goede werksfeer. Bovendien wil ik de BD-zuipkeet genootschap in het bijzonder bedanken voor de gezellige borrels in de BD of in één van de omliggende bierlokalen. Beste Lodi, bedankt dat je mij wil bijstaan als paranimf op deze belangrijke dag.

Beste Elza, heel erg bedankt voor jouw prettige samenwerking, jouw technische assistentie, maar natuurlijk heel erg bedankt voor het mogelijk maken van twee mooie hoofdstukken in dit boekje.

De rest van de Fibuline-4 groep: Beste Paula, Nicole, Natasja, Yanto, Bibi en Joyce. Allen bedankt voor de prettige samenwerking, de werkdiscussies en de assistentie bij mijn experimenten. De verdere Ee655 collegae, Nathalie, Charlie en Cecile bedankt voor de prettige werksfeer in het lab en alle anderen van Genetica.

Lambert, Kim en Kim bedankt voor de gezellige en prettige tijd op de 23^e en natuurlijk voor de assistentie bij de muizen echo's en analyse. Marcel en Jan-Lucas; Veel histologie data is verzameld met jullie hulp en kennis, veel dank hiervoor. Koen bedankt voor je klinische input, weefselcollectie en prettige samenwerking. Arne bedankt voor je biostatistiek input en prettige samenwerking. De studies met muizen zouden niet gedaan kunnen worden zonder de ondersteuning vanuit het EDC, iedereen bedankt hiervoor.

Verder wil ik mijn vrienden van het Twents Carmel Lyceum, Thijs, Wouter, Arjan en Ivo bedanken. Bedankt nog voor de fijne en gezellige leeromstandigheden en ontspanningsmomenten, het was een goede tijd. Beste Thijs, veel succes met jouw promotie in Edinburgh, en dank voor je gastvrijheid in Berlijn en in het mooie Schotland. Daarnaast bedankt dat je mij wil bijstaan als paranimf op deze belangrijke dag.

Zonder ontspanning is een promotietraject niet vol te houden. Daarom wil ik Rob, Aniek, Ruud, Nienke, Frank, Miranda, Arjan, Iris, Peter, Chantal, Rob, Nicole, Rick, Anke, Jan en Desiree bedanken voor alle gezelligheid en het helpen relativeren van mijn promotiewerk.

Natuurlijk wil ik mijn (schoon)familie bedanken voor alle steun en interesse in het promoveren. Lieve pap en mam, bedankt voor alles. Joost & Thijs jullie zijn twee top-broers en Barbara & Petra jullie zijn twee topschoonzussen.

Lieve Anne. Samen zijn met jou en eropuit trekken in onze vrije tijd doet mij altijd veel plezier. Graag wil ik met jou de toekomst tegemoet gaan. Ik hou van je!